

SELF-COMPLEXING AND TRANSPORT PROCESSES  
IN AQUEOUS SOLUTIONS OF GROUP IIB METAL  
HALIDES

A thesis submitted to the University of  
Glasgow for the degree of Ph.D.

by

LUTFULLAH

FACULTY OF SCIENCE  
CHEMISTRY DEPARTMENT  
JANUARY, 1977.

ProQuest Number: 13804106

All rights reserved

INFORMATION TO ALL USERS

The quality of this reproduction is dependent upon the quality of the copy submitted.

In the unlikely event that the author did not send a complete manuscript and there are missing pages, these will be noted. Also, if material had to be removed, a note will indicate the deletion.



ProQuest 13804106

Published by ProQuest LLC (2018). Copyright of the Dissertation is held by the Author.

All rights reserved.

This work is protected against unauthorized copying under Title 17, United States Code  
Microform Edition © ProQuest LLC.

ProQuest LLC.  
789 East Eisenhower Parkway  
P.O. Box 1346  
Ann Arbor, MI 48106 – 1346

TO MY PARENTS

## CONTENTS

	Subject	Page
	Acknowledgements .....	3
	Declaration .....	4
	Abstract .....	5
	List of Principal Symbols .....	7
	Introduction .....	10
	References .....	13
Chapter 1	Potentiometric Measurements of	
	Aqueous Zinc Chloride Solutions .....	14
	Introduction .....	15
1.1	Experimental .....	17
1.2	Results and Discussion .....	22
	References .....	41
Chapter 2	Thermodynamic Stability Constants	
	for Self-Complexed Salts in Group	
	IIB Metal Halides .....	43
	Introduction .....	44
2.1	Theoretical .....	46
2.2	Results and Discussion .....	56
	References .....	70
Chapter 3	Relationship between the Transport	
	Properties of Aqueous Cadmium Iodide	
	Solutions and the degree of Self-	
	Complexing in these Solutions .....	72
	Introduction .....	73

CONTENTS (cont'd)

	Subject	Page
3.1	An Irreversible Thermodynamic Treatment of a Self-Complexing System .....	75
3.2	Experimental .....	83
3.3	Results and Discussion .....	90
	References .....	165
Chapter 4	Isotopic-Diffusion of Cadmium in Aqueous Solutions of Cadmium Iodide..	166
	Introduction .....	167
4.1	Influence of Self-Complexing on Isotopic-Diffusion of Cadmium in Aqueous Cadmium Iodide .....	168
4.2	The Measurements of Diffusion .....	181
4.3	Experimental.....	199
4.4	Results and Discussion .....	233
	References .....	256
	Appendix A .....	260
	Appendix B .....	265
	Appendix C .....	283
	Appendix D .....	292

### Acknowledgements

I wish to express my deep sense of gratitude to Dr. Russell Paterson for his continuous guidance and innumerable discussions throughout the course of the present investigations and during the preparation of this thesis.

Thanks are also due to Dr. H.S.Dunsmore for her assistance during the work presented in Chapter 1, and to Dr. P.Rosenberg for his collaboration in preparing the computer programme for the evaluation of stability constants of complexed 2:1 electrolytes.

I am also indebted to the staff of the departmental workshop and to the glassblowers for their untiring efforts in constructing the newly designed multicell unit for the diaphragm-cell diffusion measurements.

Many thanks are also due to several colleagues, in particular to A.Agnew, J.F.Walker, S.Anderson and I.G.Lyle, both for their help during the work and for their pleasant company throughout the period of study.

Finally I must thank Professor G.A.Sim for providing admission to research facilities at the University of Glasgow, the Vice Chancellor of the University of Peshawar for granting the necessary study leave, and the Ministry of Education of the Government of Pakistan for the financial support which enabled me to complete this study.

### Declaration

The work presented in Chapter 1 has been published in the Journal of Chemical Society, Faraday Transactions I (1976, 72, 2, 495) and that described in Chapter 3 has been submitted to the same journal for publication.

### Abstract

Potentiometric measurements on aqueous solutions of zinc chloride have been made in the concentration range  $0.0004 - 1.0 \text{ mol.kg}^{-1}$ . The standard electrode potential of zinc electrode in zinc chloride and the activity coefficients for this salt have been calculated, taking into account incomplete dissociation. Comparison with literature data has been made and reasons for discrepancies are suggested. Existing potentiometric data on aqueous cadmium iodide has been used to obtain refined values of stability constants and concentrations of  $\text{CdI}_x^{2-x}$  ( $x=1,2,3,4$ ) complexes by the relatively new method, reported by Reilly and Stokes in 1970.

It is shown that this method can be used with a fair degree of confidence for heavily complexed systems such as cadmium iodide and cadmium chloride. For salts which are complexed to a lesser degree, the method may lead to dubious results mainly because of computational difficulties. This has been assessed in the light of results obtained for zinc chloride.

The theory of irreversible thermodynamics has been applied to transport processes in aqueous cadmium iodide solutions.

Relations are derived, in terms of phenomenological coefficients, which lead to the prediction of experimentally measurable quantities, transport number, equivalent conductance and salt diffusion coefficients. The/



The analysis has been further extended to include isotopic-diffusion of cadmium ion in cadmium iodide solutions.

The predicted transport parameters are compared with those derived from experimental measurements.

The isotopic-diffusion of cadmium in cadmium iodide has been studied by the diaphragm-cell method. A new type of diaphragm cell magnetic stirring unit capable of accommodating four diffusion cells has been designed and constructed. Its advantages over the previous systems are discussed.

Several computer programs have been written for involved and repetitive calculations.

List of Principal Symbols

$E$	electro-motive force
$E^0$	standard potential of the cell
$\gamma_{\pm}$	mean molal activity coefficients
$m$	molal concentration ( $\text{mol Kg}^{-1}$ )
$R$	gas constant
$T$	absolute temperature
$F$	Faraday's constant
$K_{sp}$	specific conductance
$C$	concentration in mol. $l^{-1}$
$a$	distance of closest approach in Debye-Huckel theory
$\beta_n$	$n$ th thermodynamic stability constant
$J_i$	flow of the $i$ th species
$X_i$	thermodynamic force of the $i$ th species
$\phi$	rate of dissipation of free energy
$L_{ik}$	phenomenological coefficients
$\ell_{ik}$	mobility coefficients of complex species
$j_i$	solvent-fixed flow of the $i$ th complex species
$x_i$	thermodynamic driving force of the complex species
$\tilde{\mu}_i$	electrochemical potential
$Z_i$	valency
$\Lambda$	equivalent conductance
$N$	equivalent concentration
$t_1$	transport number of the cation
$I$	ionic strength

$D_v$	Diffusion coefficient of volume-fixed frame of reference
$r_1, r_2$	stoichiometric coefficients for ionisation
mA	milliampares
$^0\lambda_i$	equivalent conductance at infinite dilution
$R_{ik}$	resistance coefficients
$D_{aa}$	isotopic diffusion coefficient in a binary electrolyte solution
$L_{aa}^T$	direct mobility of the ion in the binary solution
$C_a^T$	total molar concentration of the ion
$a^*$	isotopically labelled species
$a^0$	unlabelled species
$C_a^*$	molar concentration of the isotopically labelled species, $a^*$
$C_a^0$	molar concentration of the unlabelled species, $a^0$
$C_i$	molar concentration of the $i$ th complex species in solution
$c_i^0$	molar concentration of the unlabelled complex species, $i$
$c_i^*$	molar concentration of the labelled complex species, $i$
$\rho_i^*$	specific activity of the labelled ion
$\rho_i^0$	specific activity of the unlabelled ion
$J_a^*$	total flux of labelled cadmium species
$J_a^0$	total flux of unlabelled component

$z_i$	valency of the complex species including sign
$Y_i$	molar activity coefficient
$-d\psi/dx$	gradient of electrical potential
$\ell_{ki},$	
$\ell_{k^*i},$	mobility coefficients of labelled (*) or
$\ell_{k^*i^*},$	unlabelled complex species in solution
$\ell_{ki^*}$	
$\partial C/\partial x$	concentration gradient
$\ell$	length of the diaphragm
$A$	area of the diaphragm
$V_T$	volume of the top compartment in a diaphragm cell
$V_B$	volume of the bottom compartment
$V_D$	volume of the diaphragm
$C_T$	concentration of solution in the top compartment
$C_B$	concentration of bottom solution
$t$	time in seconds
$\beta$	diaphragm cell constant
$\delta$	deviation

I N T R O D U C T I O N

Since the earliest measurements of transport numbers, it has been known that aqueous solutions of cadmium and zinc halides exhibit anomalous transport properties.<sup>1,2,3</sup> Hittorf in 1859 first observed that the transport number of cadmium ion decreased rapidly to zero with increase in concentration and subsequently became negative in more concentrated solutions of cadmium iodide.<sup>4</sup> Such effects have been qualitatively described in terms of complexing. Negatively charged complex ions, for example  $\text{CdI}_3^-$ ,  $\text{CdI}_4^{2-}$  cause cadmium to flow to the anode in a Hittorf experiment. The balance of cathodic and anodic flows of cadmium cause the transport number of cadmium ion to be zero at  $0.28 \text{ mol.l}^{-1}$ .

Other transport properties like equivalent conductance and salt diffusion coefficients for such systems are also abnormally low.

In order to have a clear understanding of these anomalous properties, it is evident that the concentrations of the complex species in solution, believed to be the cause of anomaly, must be known.

In Chapter 1 and 2, therefore, potentiometric data are analysed to obtain stability constants and subsequently the concentrations of individual complex species in aqueous cadmium iodide and zinc chloride systems. Existing literature data for cadmium iodide<sup>5,6</sup> has/

has been used to evaluate refined values for stability constants of  $\text{CdI}_x^{2-x}$  ( $x=1,2,3$ ) complexes.

Chapter 1 mainly deals with the controversy over the standard electrode potential of amalgamated zinc electrode in zinc chloride solutions and the activity coefficients for this salt.<sup>7,8</sup> In Chapter 2 the method of obtaining stability constants devised by Reilly and Stokes<sup>9</sup> is described and its application to complexed 2:1 electrolytes is critically assessed.

The transport properties of solutions of cadmium iodide are dealt with in Chapter 3 and 4. The method is fundamental and based upon the thermodynamics of irreversible processes. It is shown that the properties of a self-complexing electrolyte containing four complexes of the type  $\text{MX}_x^{2-x}$  ( $x=1,2,3,4$ ) may be described in terms of twenty one mobility and coupling coefficients. Only combinations of these coefficients are accessible from experimental study.

For the particular system of aqueous cadmium iodide for which self-complexing is pronounced, a method of predicting transport properties in solution is developed and tested.

In the final Chapter (4) this method of analysis is extended to predict the isotopic diffusion coefficients of cadmium in cadmium iodide solutions and compared with experimental measurements on this system.

References to the introduction

1. Harris, A.C. and Parton, H.N.,  
Trans. Faraday Soc., 1940, 36, 1139.
2. Stokes, R.H. and Levien, B.J.,  
J. Amer. Chem. Soc., 1946, 68, 333.
3. Sahay, J.N., J.Sci. Ind. Research, 1959, 18B, 235.
4. Robinson, R.A. and Stokes, R.H., 'Electrolyte  
Solutions' 2nd Edn., Butterworths, London, 1970.
5. Bates, R.G., J. Amer. Chem. Soc., 1941, 63, 399.
6. Bates, R.G. and Vosburgh, W.C.,  
J. Amer. Chem. Soc., 1938, 60, 137.
7. Robinson, R.A. and Stokes, R.H.,  
Trans. Faraday Soc., 1940, 35, 740.
8. Scatchard, G. and Tefft, R.F.,  
J. Amer. Chem. Soc., 1930, 52, 2272.
9. Reilly, P.J. and Stokes, R.H., Aust. J. Chem.,  
1970, 23, 1397.

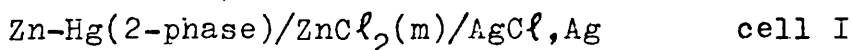


C H A P T E R 1

Potentiometric Measurements of Aqueous  
Zinc Chloride Solutions.

## I N T R O D U C T I O N

In a detailed analysis of the thermodynamic and transport properties of self-complexing salts, mean molal activity coefficients  $\gamma_{\pm}$ , are required for aqueous salt solutions over a wide range of concentration. A literature search revealed that most tabulated activity coefficient data for zinc chloride have been obtained by potentiometric measurements, using the cell



for which

$$E = E^{\circ} - \frac{k}{2} \log 4 m^3 \gamma_{\pm}^3 \quad 1.1$$

with  $m$ , the concentration of salt in  $\text{mol kg}^{-1}$  and  $k = 2.30259 RT/F$ . They were, in consequence, dependent upon the values obtained for the standard potential of the cell,  $E^{\circ} (E^{\circ}_{\text{Ag,AgCl}} - E^{\circ}_{\text{Zn}})$ .

Previous workers <sup>1, 2, 3</sup> have reported that reproducible potentials could not be obtained at concentrations less than  $0.008 \text{ mol kg}^{-1}$ . Horsh <sup>1</sup> reported a precision of  $\pm 2\text{mV}$ , while, in the extrapolation procedure to determine  $E^{\circ}$ , Robinson and Stokes <sup>2/</sup>

Stokes <sup>2</sup> discarded their dilute solution results as inaccurate and confined their analysis to the concentration range 0.01 - 0.2 mol kg<sup>-1</sup>. The value of  $E^0$  obtained by these workers was 984.85 mV (Int.). If dilute solution data ( $\leq 0.008$  mol kg<sup>-1</sup>) were included, the results of both Robinson and Stokes <sup>2</sup> and Scatchard and Tefft,<sup>3</sup> (as calculated in reference 2), would lead to a value of  $E^0$  some 1.4 mV less positive. Such a reduction would lower the calculated values of  $\gamma_{\pm}$  by some 4%. In the absence of precise emf data for dilute solutions, the system was re-investigated.

## 1.1 Experimental

### 1.1.1 Preparation of Stock Solutions of Zinc Chloride

The preparation of stock solutions has presented some practical difficulties,<sup>2, 3</sup> largely because the salt cannot be conveniently purified by recrystallisation. Zinc chloride of high nominal purity was obtained commercially, (Mark p.a.), but all batches examined were found to contain a slight excess of zinc, which precipitated as an insoluble oxy-chloride when a clear concentrated solution was diluted. The preparation of zinc chloride from spectroscopically pure zinc oxide (dried at 900°C) and the stoichiometric quantity of acid (analysed to  $\pm 0.02\%$  by conductivity measurements on diluted stock) was unsuccessful. Stock solutions 2.5 mol. l<sup>-1</sup> were acidic, pH 2.5. An excess of acid of 0.06% would be sufficient to cause this effect. Quantitative addition of zinc oxide to neutralise the excess acidity gave solutions which, although clear, produced a faint cloudy precipitate on extreme dilution. The stoichiometric ratios of Zn:Cl in both the original and treated solutions were 1:2, within the limits of analysis ( $\pm 0.05\%$  for each component). The criterion of precipitation was therefore considered the most sensitive test and, following Robinson and Stokes,<sup>2</sup> small quantities of acid were added to stock solutions until no precipitate was obtained on dilution. Using this /

this method three stock solutions were prepared with concentrations in the range 3.0 - 5.0 mol.  $l^{-1}$ . In each case the stoichiometric ratio of zinc to chloride was 1:2 within the above limits of experimental error. The equivalence and reproducibility of these preparations were tested by conductivity measurements on each batch, in the concentration range 0.3 - 0.7 mol.  $l^{-1}$ . at 25°C. The results were compared graphically and the best-fit curve through the points obtained by a computer programme, given in Appendix A.1. Calculations indicated that the standard deviation of the experimental points from the computer fit was in every case  $\leq 0.05\%$ , which corresponds to the expected uncertainty in the analytical estimation of concentration. The relationship between specific conductivity,  $K_{sp}$ , and concentration,  $C$ , (mol.  $l^{-1}$ ), is given below.

$$K_{sp} = 2.315346 + 171.9464 \times C - 119.1111 \times C^2 + 32.0959 \times C^3$$

(range of validity:  $0.3 \leq C \leq 0.7$ )

### 1.1.2 The Electrodes

Silver-silver chloride electrodes were of the thermal electrolytic type, prepared by the method of Ives and Janz.<sup>5</sup> Bias potentials between electrodes were 0.02 mV or less.

Zinc electrodes consisted of zinc rods (99.999% pure) sealed into pyrex ground-glass cones with Araldite. The electrodes were cleaned with dilute nitric /

nitric acid, washed and immersed in a dilute mercuric chloride solution containing a little nitric acid. A period of thirty minutes was sufficient for amalgamation. The whole process was performed in an oxygen-free atmosphere ( $H_2/N_2$ ). Potentiometric measurements were made in a hydrogen gas atmosphere or in a mixture of hydrogen and nitrogen gases (50:50). Bias potentials of less than 0.005 mV were obtained.

### 1.1.3 The Apparatus

Cylindrical glass cells constructed by cutting and grinding 250 ml. pyrex beakers were used. Teflon tops with 'O'-rings were constructed for these cells. These were drilled with tapered holes corresponding to standard ground-glass joints. Each cell was provided with a gas inlet and outlet (bubbler) together with two pairs of electrodes; Zn/Hg, Ag/AgCl. In this way four separate cell emf measurements could be made and bias potentials monitored. A weight titration addition was used throughout except for dilute solutions, below  $0.01 \text{ mol kg}^{-1}$ , where a separate solution was made for each measurement. All weights were vacuum corrected. Air was eliminated by passing purified, presaturated hydrogen gas through the experimental cell. Three presaturators containing the same solution as in the cell were used and these were maintained at  $25.0 \pm 1.0^\circ\text{C}$ . In titrations sufficient /

sufficient time was allowed after each addition for equilibrium to be attained. When equilibrium was established, all readings agreed to within  $\pm 0.1$  mV for all four possible electrode combinations and remained constant for about 24 hours. For more dilute solutions, below  $10^{-3}$  mol kg<sup>-1</sup>, however, the deviations occasionally reached  $\pm 0.2$  mV. The cells were maintained at  $25.00 \pm 0.01^{\circ}\text{C}$  and emf measurements were made with a Solartron A210 digital voltmeter (sensitivity 10  $\mu\text{V}$  on the one volt range). The constant temperature bath was the same as described in Chapter 3, except that water was used instead of oil as bath liquid.

#### 1.1.4 Analysis of Solutions

Volumetric methods were used. All glassware was calibrated at  $25^{\circ}\text{C}$  ( $\pm 1^{\circ}\text{C}$ ) and duplicate calibrations were reproducible to  $\pm 0.05\%$ . Chloride was estimated by potentiometric titration with silver nitrate. The potentials between two silver electrodes, one in the titration vessel and the other in the burette tip, were measured and the end-point of the titration determined by the linear titration plot method of Gran, refined by McCallum.<sup>6</sup> These routine analyses were reproducible to  $\pm 0.05\%$ . A similar method of analysis, ferrocyanide titration, was used for zinc. In this case platinum electrodes were used and the titrant /

titrant was potassium ferrocyanide solution containing a trace of potassium ferricyanide. The potentials were measured with a Solartron digital voltmeter. Reproducibility was  $\pm 0.05\%$  (as for chloride analysis). Standard zinc solutions for calibration were prepared by dissolving a weighed sample of spectroscopically pure zinc rod in a slight excess of hydrochloric acid. All potentiometric measurements were made at  $25.00 \pm 0.05^{\circ}\text{C}$ .



## 1.2 Results and Discussion

### 1.2.1 Determination of $E^0$ by Classical Methods

The variation of emf for cell I with molality of zinc chloride is shown in columns 1 and 2 of table (1.1). The amalgamated zinc rod was found to be stable and reproducible when used under an atmosphere of hydrogen gas or a 50:50 hydrogen, nitrogen gas mixture, as reported by Clyton and Vosbergh.<sup>15</sup> In contrast to the reported studies on the liquid amalgam electrodes,<sup>2, 3</sup> it was also found to be stable in the dilute solution range  $m \leq 0.008 \text{ mol kg}^{-1}$ .

The stable potentials, obtained in very dilute solutions, allow a rigorous investigation of the theoretical activity expressions for unsymmetrical electrolytes. At concentrations below  $0.01 \text{ mol kg}^{-1}$  there is little possibility of self-complexing of the salt, table (1.2).

An attempt was made to determine the standard potential for the cell,  $E^0$ , by the method of Bates,<sup>8</sup> employed by Robinson and Stokes.<sup>2</sup> The extended Debye-Huckel equation is assumed and a function  $E'_0$  plotted against molal concentration  $m$ , equation (2.2).<sup>2</sup>

$$\begin{aligned} E'_0 &= E + \frac{k}{2} \log \left[ 4m^3 / (1.0 + 0.054m)^3 \right] - \frac{3}{2} k \log \sqrt{3m} / (1.0 + A\sqrt{m}) \\ &= E^0 - 4.5 k Bm. \end{aligned} \quad 1.2$$

where /

where  $k = 2.30259 RT/F$ ;  $\mathcal{S}$  is the limiting Debye-Huckel slope,  $\mathcal{S} = 1.012$  and  $A = 0.3291 \times \mathcal{Q}$  where  $\mathcal{Q}$  is the distance of closest approach of ions in Angstrom units. From equation (1.2) the potential,  $E'_0$ , will be a linear function of  $m$  and extrapolate to the standard potential,  $E^0$ , at infinite dilution, provided  $B$  is a constant, equation (1.1).

As with the data of Robinson and Stokes<sup>2</sup> a linear plot could only be obtained by ignoring data below  $0.008 \text{ mol kg}^{-1}$ . Furthermore no value of  $\mathcal{Q}$  could be obtained which fitted the experimental data over the full range of concentration. In Fig. 1.1 the present data are compared with those of earlier workers<sup>2, 3</sup> (with their emf data corrected to abs. volts) using  $\mathcal{Q} = 5.0 \text{ \AA}$ .<sup>2</sup> The inflection at lower concentrations must be considered to be real and not due to experimental error. There are two possible explanations of this effect. Gronwall, La Mer and Sandved<sup>9</sup> attributed the non-linearity of equation (1.2) to the use of linear approximations in the solution of the Poisson-Boltzmann equation in the traditional Debye-Huckel analysis. The second possibility is that the salt is self-complexed in the concentration range studied by earlier workers, ( $0.01 - 0.20 \text{ mol kg}^{-1}$ ). Hydrolysis can be discounted, since, to have significant effect, it would have to be considerably larger than indicated in the literature.<sup>10, 11, 12</sup>

The theory of La Mer, Gronwall and Grief<sup>4</sup> was applied /

Legend for Fig. 1.1

Extrapolation method of Robinson and Stokes, equation (1.2), in which the distance of closest approach was taken as  $5.0 \text{ \AA}$ .    ●, this work; ○, from ref(2),  $\Delta$ , from ref(3).

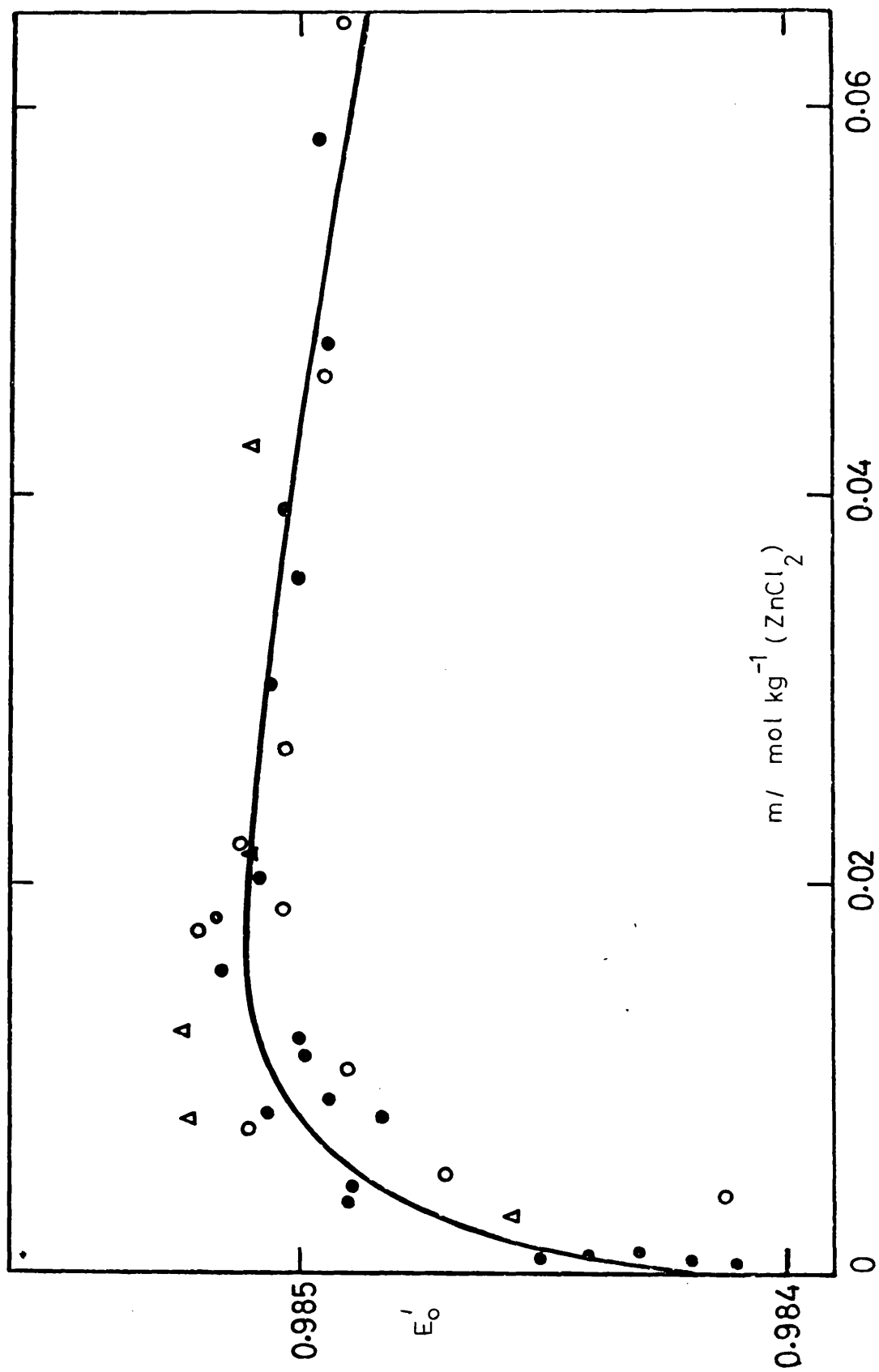


Fig. 1.1

applied to eleven points in the dilute solution range up to  $0.01 \text{ mol kg}^{-1}$ , which is the upper limit of validity for this theory. The values of  $E^0$  obtained for each concentration were calculated from equation (1.1), the activity expression for  $f_{\pm}$  from reference 4 being used. The sole variable in this analysis is  $\bar{a}$ , the distance of closest approach of the ions. Values for the parameter,  $\bar{a}$ , were varied from  $3.5 - 4.5 \text{ \AA}$ . A minimum standard deviation,  $\pm 0.13 \text{ mV}$ , was obtained with  $\bar{a} = 4.05 \text{ \AA}$  and the corresponding  $E^0$  was  $984.20 \text{ mV}$ . A computer program, given in Appendix A.2, was written to perform these calculations. Above  $0.01 \text{ mol kg}^{-1}$  the theory is no longer valid and subsequent analysis has shown that complex formation becomes increasingly significant.

### 1.2.2 Incomplete Dissociation

The effect of incomplete dissociation was studied by the method of Reilly and Stokes<sup>13</sup> described in detail in Chapter 2. The emf of the cell may be expressed in terms of ionic concentrations,

$$E = E^0 - \frac{k}{2} \log [\text{Zn}^{2+}] [\text{Cl}^-]^2 \gamma_{21}^3 \quad 1.3$$

where  $[\text{Zn}^{2+}]$  and  $[\text{Cl}^-]$  are respectively the molalities, ( $\text{mol kg}^{-1}$ ), of uncomplexed zinc and chloride ions and  $\gamma_{21}$ , the activity coefficient of the uncomplexed salt,  $\text{ZnCl}_2$ . If only the first complex is considered, then

$$\beta_1 = \frac{[\text{ZnCl}^+]}{[\text{Zn}^{2+}][\text{Cl}^-]} \cdot \frac{\gamma_{11}^2}{\gamma_{21}^3} \quad 1.4$$

From the mass balance and electroneutrality conditions (neglecting the concentration of free hydrogen and hydroxyl ions), it can be shown that

$$m = [\text{Zn}^{2+}] \left[ 1 + \beta_1 [\text{Cl}^-] \gamma_{21}^3 / \gamma_{11}^2 \right] \quad 1.5$$

$$2m = [\text{Cl}^-] \left[ 1 + \beta_1 [\text{Zn}^{2+}] \gamma_{21}^3 / \gamma_{11}^2 \right] \quad 1.6$$

where  $m$  is the total molality of the salt. The ionic strength is defined,

$$I = 2 [\text{Zn}^{2+}] + m \quad 1.7$$

The activity coefficients  $\gamma_{11}$  and  $\gamma_{21}$  were calculated from the extended Debye-Huckel expressions,

$$\log \gamma_{21} = -1.023 \sqrt{I} / (1.0 + A_{21} \sqrt{I}) + B_{21}I \quad 1.8a$$

$$\log \gamma_{11} = -0.5115 \sqrt{I} / (1.0 + A_{11} \sqrt{I}) + B_{11}I \quad 1.8b$$

where  $A_{21} = g_{21} \times 0.3291$ ,  $A_{11} = g_{11} \times 0.3291$  and  $B_{21}$  and  $B_{11}$  are empirical constants.

From equations (1.3) to (1.8) the value of  $E^0$  and /

and  $\beta_1$  may be obtained by the method of successive approximations. For a chosen value of  $\beta_1$  and starting values of the constants of equations (1.8), a first approximation to  $[\text{Zn}^{2+}]$  for each point may be obtained from equations (1.5) and (1.6). These may be used to evaluate ionic strength and in turn the activity coefficients, which allow a better value of  $[\text{Zn}^{2+}]$  to be calculated. This cyclic calculation was repeated until the value of  $[\text{Zn}^{2+}]$  was constant to within 0.01%. The value for  $[\text{Cl}^-]$  was obtained and  $E^0$  evaluated from equations (1.3) and (1.8a). Values for all the parameters were then optimised to give the most constant value of  $E^0$ . The computer program for optimisation of the unknown parameters is given in Appendix B.1. The results are shown in table (1.2). For the forty two points considered, including six points from the data of Scatchard and Tefft<sup>3</sup> and nine points from the work of Robinson and Stokes,<sup>2</sup> a constant  $E^0$  of 984.28,  $\delta = 0.15$  mV was obtained. Our own data alone gave a value of  $E^0$  of 984.29 with the same standard deviation. Table (1.2) shows that in the range  $4.0 \times 10^{-4} - 4.0 \times 10^{-3}$  mol kg<sup>-1</sup> the salt is completely dissociated and the value of  $E^0$  depends only upon the constants chosen in equation (1.8a). In that range the La Mer<sup>4</sup> theory and extended Debye-Huckel equation, equation (1.8a), are equally valid. As expected in this dilute concentration range, the Debye-Huckel limiting law remains a good approximation and /

and consequently the value of  $E^0$  obtained is insensitive to the values of  $A_{21}$  and  $B_{21}$  chosen in equation (1.8a). Only in the most concentrated solutions do the values chosen for  $\beta_1$  and the Debye-Huckel constants become significant.

In the optimisation procedure standard deviations for  $E^0$  greater than 0.2 mV were considered unacceptable. The data in table (1.2), however, do not give a unique solution for  $\beta_1$ . Sets of Debye-Huckel parameters could be chosen for other values of  $\beta_1$  to give the same precision in  $E^0$  and the same absolute value as shown in table (1.3). The value of  $\beta_1$  equal to 4.5 is, however, preferable because a positive value of  $B_{11}$  is more in keeping with the reported data for fully-dissociated binary electrolytes.

To illustrate that the  $E^0$  value is relatively insensitive to the optimised parameters used, the results have also been calculated according to the Davies equation for activity coefficients, table (1.3). The restriction imposed by the use of this equation prevents optimisation of other than  $\beta_1$  and correspondingly  $E^0$  is obtained with a slightly larger deviation.

The value of  $E^0$  is thus established within close limits by two independent methods.

Ambiguity concerning the value of  $\beta_1$  cannot be resolved without further experimental investigations of /



of mixed electrolyte systems in which more complexing may be obtained at low ionic strengths by the addition of chloride salts. This will be further discussed in Chapter 2.

A list of  $E^0$  values is given in table (1.4), where they are compared with other literature data. In some cases the original measurements were made in International Volts and these have been converted to absolute units. In addition, recalculations from original sources have been made and the standard reduction potential for zinc calculated.

The value of  $E_{Zn}^0$  obtained in this study, -761.90,  $\delta = 0.15$  mV, and those recalculated from the data of Robinson and Stokes<sup>2</sup> and Scatchard and Tefft<sup>3</sup> are in good agreement. It should be noted that in recalculated data it is difficult to take into account the possible differences in preparation of the standard electrodes. Discussion in the literature shows that accepted values for the standard potentials of the halide reversible electrodes may differ by up to  $\pm 0.2$  mV.<sup>18</sup> In this study the latest literature values have been adopted.

It now appears certain that the extrapolation procedure of Robinson and Stokes,<sup>2</sup> Fig. 1.1, equation (1.2), was in error, because zinc chloride is significantly complexed in the concentration range studied (0.01 - 0.13 mol kg<sup>-1</sup>). Stokes and Stokes<sup>16</sup> from their osmotic coefficient measurements on zinc and /

and magnesium halides arrived at the same conclusion. It has been observed in this work that the linearity expected from equation (1.2) may be obtained over a limited concentration range in the presence of complexing if the value of  $\beta$  is increased sufficiently e.g.  $\beta = 5.0 \text{ \AA}$ , Fig. 1.1. Equally the emf data at concentrations below  $0.008 \text{ mol kg}^{-1}$  reported, but rejected, by both Robinson and Stokes<sup>2</sup> and Scatchard and Tefft<sup>3</sup> were more precise than the authors themselves considered, table (1.2). Taken separately, data from these two sources, including the dilute points, give average  $E^0$  values 984.27,  $\delta = 0.11 \text{ mV}$  and 984.29,  $\delta = 0.19 \text{ mV}$  using the optimised parameters of table (1.2) shown in table (1.3). It is interesting to note that these authors obtained  $E^0$  values of 984.85<sup>2</sup> and 984.00<sup>3</sup> mV (Int.) respectively. The former is the usually-accepted value quoted in most standard texts.

### 1.2.3 Mean Molal Activity Coefficients of Aqueous Zinc Chloride at 25°C

Table (1.1) gives the mean molal activity coefficients,  $\gamma_{\pm}$ , calculated for the full range of concentration studied ( $4.0 \times 10^{-4} - 1.0 \text{ mol kg}^{-1}$ ) taking  $E^0$  as 984.28 mV. The activity coefficients,  $\gamma_{\pm}$ , were curve-fitted by a least squares standard computer programme in terms of the square root of concentration /

concentration to the fifth order,

$$\gamma_{\pm} = 1.01685 - 4.90609 \times S + 28.08897 \times S^2 - 115.0959 \\ \times S^3 + 265.8095 \times S^4 - 249.7339 \times S^5 \\ \text{(range of validity } 0.0005 - 0.1 \text{ mol kg}^{-1}) \quad 1.9a$$

$$\gamma_{\pm} = 0.73838 - 1.086186 \times S + 1.30381 \times S^2 - 0.764138 \\ \times S^3 + 0.138333 \times S^4 \\ \text{(range of validity } 0.1 - 1.0 \text{ mol kg}^{-1}) \quad 1.9b$$

where  $S = \sqrt{m}$ .

For comparison, the mean molal activity coefficients at rounded concentrations have been calculated using these equations. The values reported by Robinson and Stokes<sup>20</sup> are some 2% higher than in this work, table (1.5).

Table 1.1

## Mean Molal Activity Coefficients

m (mol kg <sup>-1</sup> )	emf volts	$\gamma_{\pm}$
0.00043035	1.26805	0.9283
0.00061083	1.25550	0.9058
0.00063382	1.25383	0.9116
0.00083190	1.24405	0.8952
0.00098120	1.23792	0.8899
0.003663	1.19131	0.7989
0.004420	1.18471	0.7853
0.008051	1.16399	0.7385
0.008272	1.16330	0.7317
0.008857	1.16085	0.7282
0.01115	1.15311	0.7069
0.01204	1.15055	0.7000
0.01549	1.14230	0.6740
0.01812	1.13710	0.6591
0.02019	1.13345	0.6505
0.03018	1.12030	0.6121
0.03571	1.11480	0.5966
0.03911	1.11190	0.5874
0.04086	1.11088	0.5772
0.04775	1.10540	0.5694
0.05822	1.09910	0.5500
0.06154	1.09770	0.5396
0.07281	1.09190	0.5301
0.08189	1.08805	0.5209
0.08660	1.08650	0.5127
0.10180	1.08110	0.5018
0.10299	1.08078	0.5000
0.15807	1.06680	0.4683
0.16252	1.06595	0.4656
0.16431	1.06550	0.4660
0.19300 /		

Table 1.1 (cont'd)

m	emf	$\gamma_{\pm}$
(mol kg <sup>-1</sup> )	volts	
0.19300	1.06070	0.4493
0.22253	1.05560	0.4448
0.23114	1.05450	0.4407
0.29673	1.04670	0.4213
0.32792	1.04300	0.4186
0.33940	1.04320	0.4090
0.33960	1.04180	0.4170
0.48516	1.03080	0.3883
0.5133	1.02910	0.3836
0.5140	1.02855	0.3886
0.5249	1.02860	0.3800
0.6498	1.02170	0.3671
0.6650	1.02065	0.3686
0.6639	1.02100	0.3659
0.6828	1.02020	0.3633
0.8607	1.01337	0.3441
0.8605	1.01297	0.3477
0.8766	1.01273	0.3435
*1.0310	1.00846	0.3263

\* Robinson and Stokes<sup>2</sup> measurement

Table 1.2

Standard e.m.f. of Cell 1, taking into account incomplete dissociation

 $\beta_1 = 4.5$  ;  $\beta_{21} = 4.5 \text{ \AA}$  ,  $\beta_{11} = 4.0 \text{ \AA}$  ;  $\beta_{21} = 0.3$  ,  $\beta_{11} = 0.055$ 

(m)	(emf)	$[\text{Zn}^{2+}]$	$[\text{Cl}^-]$	$[\text{ZnCl}^+]$	$E^0(\text{volts})$	$E^0 - E^0$ av. cal. (volts)
0.00043035	1.26805	0.00043	0.00086	0.00000	0.98401	0.00027
0.00061083	1.25550	0.00061	0.00122	0.00000	0.98438	-0.00010
0.00063382	1.25383	0.00063	0.00126	0.00000	0.98407	0.00021
0.00083190	1.24405	0.00083	0.00166	0.00000	0.98425	0.00003
0.00098120	1.23792	0.00097	0.00196	0.00001	0.98414	0.00014
*0.002940	1.19869	0.00289	0.00583	0.00005	0.98418	0.00010
0.003663	1.19131	0.00358	0.00725	0.00008	0.98449	-0.00021
0.004420	1.18471	0.00431	0.00873	0.00011	0.98443	-0.00015
**0.005082	1.17968	0.00494	0.01002	0.00014	0.98420	0.00008
**0.007354	1.16735	0.00708	0.01444	0.00027	0.98451	-0.00023
*0.007814	1.16540	0.00751	0.01532	0.00030	0.98461	-0.00033
0.008051	1.16599	0.00773	0.01578	0.00032	0.98421	0.00007
0.008272	1.16330	0.00794	0.01621	0.00034	0.98444	-0.00016
0.008857	1.16085	0.00848	0.01734	0.00038	0.98430	-0.00002
**0.01040	1.15537	0.00990	0.02030	0.00050	0.98421	0.00007
0.01115	1.15311	0.01059	0.02174	0.00057	0.98429	-0.00001
0.01204	1.15055	0.01139	0.02343	0.00065	0.98427	0.00001
*0.01236 /						

Table 1.2 (cont'd)

m	(mol kg <sup>-1</sup> )	(emf)	[Zn <sup>2+</sup> ]	[Cl <sup>-</sup> ]	[ZnCl <sup>+</sup> ]	E <sup>o</sup> (volts)	E <sup>o</sup> -E <sup>o</sup> av. cal. (volts)
*0.01236	1.14989	0.01168	0.02404	0.00068	0.98450	-0.00021	
0.01549	1.14230	0.01448	0.02997	0.00100	0.98438	-0.00010	
**0.01753	1.13823	0.01629	0.03382	0.00124	0.98440	-0.00012	
0.01812	1.13710	0.01680	0.03493	0.00132	0.98436	-0.00008	
**0.01854	1.13621	0.01717	0.03571	0.00137	0.98422	0.00006	
0.02019	1.13345	0.01860	0.03879	0.00159	0.98425	0.00003	
*0.02144	1.13138	0.01908	0.04112	0.00176	0.98415	0.00013	
**0.02201	1.13065	0.02017	0.04218	0.00184	0.98428	0.00000	
**0.02671	1.12424	0.02414	0.05085	0.00257	0.98418	0.00010	
0.03018	1.12030	0.02701	0.05719	0.00317	0.98421	0.00007	
0.03571	1.11480	0.03148	0.06719	0.00423	0.98417	0.00011	
0.03911	1.11190	0.03417	0.07327	0.00494	0.98421	0.00007	
0.04086	1.11088	0.03554	0.07640	0.00533	0.98461	-0.00033	
*0.04242	1.10933	0.03674	0.07916	0.00568	0.98426	0.00002	
**0.04602	1.10658	0.03949	0.08551	0.00653	0.98415	0.00013	
0.04775	1.10540	0.04079	0.08855	0.00696	0.98416	0.00012	
0.05822	1.09910	0.04843	0.10665	0.00979	0.98425	0.00003	
0.06154	1.09770	0.05077	0.11230	0.01077	0.98464	-0.00036	
**0.06439	/						

Table 1.2 (cont'd)

(m)	(mol kg <sup>-1</sup> )	(emf)	[Zn <sup>2+</sup> ]	[Cl <sup>-</sup> ]	[ZnCl <sup>+</sup> ]	E <sup>0</sup> (volts)	E <sup>0</sup> -E <sup>0</sup> av. cal. (volts)
**0.06439		1.09584	0.05274	0.11713	0.01165	0.98424	0.00004
0.07281		1.09190	0.05841	0.13122	0.01439	0.98425	0.00003
0.08189		1.08805	0.06425	0.14614	0.01763	0.98418	0.00010
0.08660		1.08650	0.06718	0.15378	0.01943	0.98443	-0.00015
*0.09048		1.08471	0.06953	0.16001	0.02095	0.98405	0.00023
0.10180		1.08110	0.07611	0.17790	0.02569	0.98422	0.00006
0.10299		1.08078	0.07678	0.17978	0.02622	0.98428	0.00000

Average E<sup>0</sup> = 984.28 mV,  $\delta$  = 0.15 mV\* Scatchard and Tefft<sup>3</sup>\*\* Robinson and Stokes<sup>2</sup>



Table 1.3

Comparison of different parameters used in calculation of  $E^0$  for Cell 1.

	$\beta_1$	$g_{21}$	$B_{21}$	$g_{11}$	$B_{11}$	$E^0$ (mV)	$\delta$ (mV)
(a)	-	4.05	-	-	-	984.20	0.13
(b)	4.50	4.50	0.30	4.00	0.055	984.29	0.15
(c)	2.57	3.70	0.30	3.00	-0.05	984.29	0.15
(d)	1.59	3.04	0.30	3.04	0.15	984.06	0.24

(a) Gronwall, La Mer and Sandved<sup>9</sup> theory

(b, c) Reilly and Stokes<sup>13</sup> method

(d) Davies equation<sup>14</sup>

Table 1.4

Standard Reduction Potentials of Zinc at 25°C

CELL	$E^{\circ}$ (abs.V)	(mV)	$E^{\circ}_{\text{ref.}}$	$E^{\circ}_{\text{Zn}/\text{Zn}^{2+}}$
(a) Zn-Hg(2-phase)/ZnCl <sub>2</sub> (4.0x10 <sup>-4</sup> -1.0x10 <sup>-1</sup> mol kg <sup>-1</sup> )/AgCl, Ag	0.98429 (27)*	0.15	0.22234 <sup>18</sup>	-0.76195
(b) " " " "	0.98420 (11)	0.13	"	-0.76186
(c) Zn-Hg(2-phase)/ZnCl <sub>2</sub> (5.0x10 <sup>-3</sup> -6.0x10 <sup>-2</sup> mol kg <sup>-1</sup> )/AgCl, Ag	0.98427 (9)	0.11	"	-0.76183
(d) Zn-Hg(2-phase)/ZnCl <sub>2</sub> (2.0x10 <sup>-3</sup> -9.0x10 <sup>-2</sup> mol kg <sup>-1</sup> )/AgCl, Ag	0.98429 (6)	0.19	"	-0.76195
(e) Zn-Hg(2-phase)/ZnCl <sub>2</sub> (1.7x10 <sup>-3</sup> -8.0x10 <sup>-2</sup> mol kg <sup>-1</sup> )/Hg <sub>2</sub> Cl <sub>2</sub> , Hg	1.03011 (5)	0.17	0.26813 <sup>19</sup>	-0.76198

(a) This work - Reilly and Stokes method - using parameters of table 3.

(b) This work - Gronwall theory.

(c, d) emf data<sup>2, 3</sup> corrected to abs. volts and optimised for  $E^{\circ}$  using set of parameters of table 1.(e) emf data<sup>17</sup> corrected to abs. volts and optimised for  $E^{\circ}$  using  $\beta_1 = 4.5$ ;  $\beta_{21} = 4.2$ ;  
 $\beta_{11} = 4.0$ ;  $\beta_{21} = 0.3$ ;  $\beta_{11} = 0.055$ \* Figures in brackets represent the number of points used in the calculation of  $E^{\circ}$ .

Table 1.5

Activity Coefficients of Zinc Chloride at  
Rounded Concentrations

m	$\gamma_{\pm}$		
	(a)	(b)	(c)
0.0005	0.9200	0.913	-
0.001	0.8864	0.881	-
0.002	0.8443	0.838	-
0.005	0.7759	0.767	0.789
0.01	0.7161	0.708	0.731
0.02	0.6515	0.642	0.667
0.05	0.5624	0.556	0.570
0.1	0.5025	0.502	0.518
0.2	0.4506	0.448	0.465
0.3	0.4215	0.415	0.435
0.4	0.4018	0.393	0.413
0.5	0.3867	0.376	0.396
0.6	0.3740	0.364	0.382
0.8	0.3517	0.343	0.359
1.0	0.3302	0.325	0.341

(a) This work, eqn (9)

(b) Scatchard and Tefft<sup>3</sup>

(c) Robinson and Stokes<sup>2</sup>

References for Chapter 1

1. Horsch, W.G., J. Amer. Chem. Soc., 1919, 41, 1787
2. Robinson, R.A. and Stokes, R.H., Trans. Faraday Soc., 1940, 35, 740
3. Scatchard, G. and Tefft, R.F., J. Amer. Chem. Soc., 1930, 52, 2272
4. La Mer, V.K., Gronwall, T.H. and Greiff, L.T., J. Phys. Chem., 1931, 35, 2245
5. Ives, D.J.H. and Janz, G.J., 'Reference Electrodes' Academic press (Lon.) 1961
- 6(a) Gran, G., Acta Chem. Scand., 1950, 4, 559  
 (b) Gran, G., Analyst., 1952, 77, 661  
 (c) McCallum, C., Ph.D. Thesis, Glasgow University, 1970
7. Vogel, A.I., 'Quantitative Inorganic Analysis', 3rd Ed., Longmans, London, 1961
8. Bates, R.G., J. Amer. Chem. Soc., 1938, 60, 2983
9. Gronwall, T.H., La Mer, V.K. and Sandved, K., Physik, Z., 1928, 29, 358
10. Perrin, D.D., J. Chem. Soc. 1962, 4500
11. Rokric, B. and Pucar, Z., J. Inorganic and Nucl. Chem., 1971, 33 (2), 445
12. Lilick, L.S. and Varshvaskil, Yu.S., Zhur. Obscheli Khim., 1956, 26, 317  
 (J. Gen. Chem. U.S.S.R., 1956, 26, 337)
13. /

13. Reilly, P.J. and Stokes, R.H., Aust. J. Chem.,  
1970, 23, 1397
14. Davies, C.W., 'Ion Association', Butterworths,  
London, 1962
15. Clyton, W.J. and Vosburgh, W.C., J. Amer. Chem.  
Soc., 1936, 58, 2093
16. Stokes, R.H. and Stokes, J.M., Trans. Faraday  
Soc., 1945, 41, 688
17. Brull, L., Gazz. Chim. ital., 1934, 64, 261
- 18(a) Hetzer, H.R., Robinson, R.A. and Bates, R.G.,  
J. Phys. Chem., 1964, 68, 1929  
(b) Bates, R.G. et al., J. Chem. Phys., 1956, 25,  
361
19. Grzybowski, A.K., J. Phys. Chem., 1958, 62,  
550
20. Robinson, R.A. and Stokes, R.H., 'Electrolyte  
Solutions', 2nd Ed., Butterworths, London,  
1959

C H A P T E R 2

Thermodynamic Stability Constants for  
Self-Complexed Salts in Aqueous Solutions  
of Group IIB Metal Halides.

## I N T R O D U C T I O N

In an irreversible thermodynamic treatment of the transport process in aqueous solutions of self-complexing halides of Group IIB metals, the mobility coefficients  $L_{ik}$ , discussed in greater detail in Chapter 3, can be expressed as combinations of the mobility coefficients of the individual complex species,  $\ell_{ik}$ . The total contribution to the transport parameter,  $L_{ik}$ , will obviously depend upon the intrinsic mobilities of the individual free and complexed ions, their interactions and most important their concentrations in solution.

It is to the concentrations of the individual free and complexed species in aqueous solutions of cadmium chloride, cadmium iodide and zinc chloride that this chapter is directed.

Thermodynamic stability constants for  $\text{CdCl}_x^{2-x}$  and  $\text{CdI}_x^{2-x}$  complexes have been recalculated from the existing literature data<sup>1,2,3</sup>. The method of Reilly and Stokes<sup>1</sup>, originally used for cadmium chloride complexes, has been adopted for the calculation of thermodynamic stability constants and its application to such systems has been critically assessed.

The calculated stability constants for cadmium iodide complexes,  $\text{CdI}_x^{2-x}$ , have been used extensively in Chapters 3 and 4.

The transport properties of aqueous zinc chloride solutions/

solutions, reported to exhibit extensive self-complexing,<sup>4,5</sup> are known from the experimental measurements of Agnew and Paterson<sup>6</sup> carried out in this laboratory. Having established the standard electrode potential for Cell I (Chapter 1) and the activity coefficients for this salt, it was of interest to extend the e.m.f. measurements to include some mixtures of potassium chloride and zinc chloride.

This would provide the necessary data for the determination of stability constants for  $\text{ZnCl}_x^{2-x}$  ( $x=1,2,3,4$ ) complexes and hence the concentrations of individual complex species, required for a more detailed understanding of the anomalous transport parameters of this salt.



## 2.1 Theoretical

### 2.1.1 Self-Complexing in Aqueous Solutions of Group IIB Metal Halides

Although a number of methods<sup>7,8</sup> are available for the study of ionic equilibria in aqueous solutions of metal halides, the potentiometric method is by far the most accurate and widely applicable technique currently in use. It is evident, however, that the thermodynamic stability constants, defined by equations (2.5) to (2.8), can be determined by potentiometric method only if the activity coefficients are either known or are at least held constant. In the latter method, concentrated supporting electrolytes are used to maintain a constant ionic medium. The method has been used extensively by several workers<sup>9,10</sup> for determination of stability constants. Measurements are usually made in the presence of an excess of inert electrolyte, which is assumed not to form complexes with the central metal ion, the ligand or with the complex species themselves. Sodium perchlorate is most frequently used as the bulk electrolyte for such measurements.

It has been reported, however, that together with its other inherent disadvantages,<sup>7,8</sup> Fe(III), Ce(III), Hg(I), Hg(III), Cd(II) and Mg(II) form weak complexes with perchlorate ions.

The method is intrinsically unsuited to this study because the activity coefficients, although held constant by a high ionic strength medium, cannot be evaluated with confidence/

confidence. As a result concentrations of complex species in solution cannot be obtained.

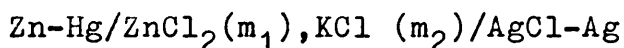
In 1970, Reilly and Stokes<sup>1</sup> reported a new method of calculation of the thermodynamic stability constants for cadmium chloride complexes in aqueous solutions.

The method, in principle, can be used for any similar system such as  $\text{CdI}_2$  and  $\text{ZnCl}_2$  and has the advantage that no constant ionic medium is required during experimental measurements of the e.m.f of the appropriate cell.

This method is described in detail below. Since the mathematical treatment is similar for halides of cadmium and zinc, zinc chloride has been chosen as a typical example.

#### 2.1.2 The Method of Reilly and Stokes<sup>1</sup> for the Calculation of Stability Constants of Complexes in Aqueous Solutions of Group IIB Metal Halides

The method essentially consists in constructing a suitable cell without liquid junction. The potential of the cell is then measured as a function of the concentration of the pure electrolyte and with added ligand for enhanced complexation. The cell used in this work, for the system zinc chloride - potassium chloride was,



Cell I

The e.m.f of the cell is given by,

$$E = E^{\circ} - \frac{RT}{2F} \ln m_1(2m_1+m_2)^2 \gamma_{\pm}^3 \quad 2.1$$

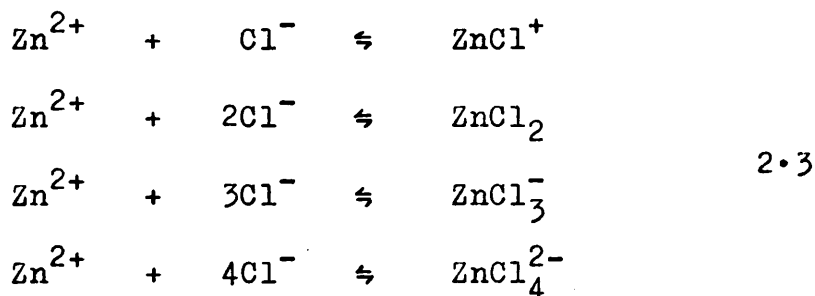
If/

If the molalities of the free zinc and free chloride ions are represented by  $[Zn^{2+}]$  and  $[Cl^-]$  respectively, equation (2.1) may be written as,

$$E = E^0 - RT/2F \ln [Zn^{2+}] [Cl^-]^2 \gamma_{21}^3 \quad 2.2$$

where  $\gamma_{\pm}$ , in equation (2.1), is the stoichiometric activity coefficient of zinc chloride and  $\gamma_{21}$  is the activity coefficient for the non-complexed zinc chloride.  $E^0$  is the standard e.m.f of the cell and R, T and F have their usual meanings.

If the various stages of the complex formation between zinc and chloride ions are represented as:



The thermodynamic stability constants are defined by,

$$\beta_1 = \frac{(ZnCl^+)}{(Zn^{2+})(Cl^-)} \quad 2.4 (a)$$

$$\beta_2 = \frac{(ZnCl_2)}{(Zn^{2+})(Cl^-)^2} \quad 2.4 (b)$$

$$\beta_3 = \frac{(\text{ZnCl}_3^-)}{(\text{Zn}^{2+})(\text{Cl}^-)^3} \quad 2.4 \text{ (c)}$$

$$\beta_4 = \frac{(\text{ZnCl}_4^{2-})}{(\text{Zn}^{2+})(\text{Cl}^-)^4} \quad 2.4 \text{ (d)}$$

The curved brackets in equations (2.4) represent the activities.

The first stability constant,  $\beta_1$ , for example, can be written in terms of concentrations and activity coefficients as follows,

$$\begin{aligned} \beta_1 &= \frac{[\text{ZnCl}^+]}{[\text{Zn}^{2+}] [\text{Cl}^-]} \times \frac{\gamma_+}{\gamma_{++} \cdot \gamma_-} \\ &= \frac{[\text{ZnCl}^+]}{[\text{Zn}^{2+}] [\text{Cl}^-]} \times \frac{\gamma_+}{\gamma_{++} \cdot \gamma_-} \times \frac{\gamma_-}{\gamma_-} \\ &= \frac{[\text{ZnCl}^+]}{[\text{Zn}^{2+}] [\text{Cl}^-]} \times \frac{\gamma_{11}^2}{\gamma_{21}^3} \quad 2.5 \end{aligned}$$

The higher stability constants are given similarly by,

$$\beta_2 = \frac{[\text{ZnCl}_2]}{[\text{Zn}^{2+}] [\text{Cl}^-]^2} \times \gamma_0 / \gamma_{21}^3 \quad 2.6$$

$$\beta_3 = \frac{[\text{ZnCl}_3^-]}{[\text{Zn}^{2+}] [\text{Cl}^-]^3} \times \gamma_1 / \gamma_{21}^3 \quad 2.7$$

$$\beta_4 = \frac{[\text{ZnCl}_4^{2-}]}{[\text{Zn}^{2+}] [\text{Cl}^-]^4} \times \gamma_{12}^3 / \gamma_{21}^3 \gamma_{11}^4 \quad 2.8$$

As has been discussed previously, in Chapter 1, equation (1.5), from the mass balance and electroneutrality conditions (neglecting the small amounts of free hydrogen and hydroxide ions) it can be shown that,

$$m_1 = [\text{Zn}^{2+}] + [\text{ZnCl}^+] + [\text{ZnCl}_2] + [\text{ZnCl}_3^-] \\ + [\text{ZnCl}_4^{2-}] \quad 2.9$$

and

$$2m_1 + m_2 = [\text{Cl}^-] + [\text{ZnCl}^+] + 2[\text{ZnCl}_2] + \\ 3[\text{ZnCl}_3^-] + 4[\text{ZnCl}_4^{2-}] \quad 2.10$$

where  $m_1$  is the total molality of zinc ions and  $(2m_1 + m_2)$  is the amount of total chloride in  $\text{mol.kg}^{-1}$ . By the condition of electroneutrality,

$$2[\text{Zn}^{2+}] + [\text{ZnCl}^+] + m_2 = \\ [\text{Cl}^-] + [\text{ZnCl}_3^-] + 2[\text{ZnCl}_4^{2-}] \quad 2.11$$

and the ionic strength,  $I$ , is defined by

$$I = 0.5 \left[ 4 [\text{Zn}^{2+}] + [\text{ZnCl}^+] + [\text{ZnCl}_3^-] + 4 [\text{ZnCl}_4^{2-}] + [\text{Cl}^-] + m_2 \right] \quad 2.12$$

$m_2$  in equations (2.11) and (2.12) is the concentration of potassium ions in  $\text{mol.kg}^{-1}$ .

For mathematical simplicity, using equations (2.5) to (2.8), we can define new functions  $K_1$ ,  $K_2$ ,  $K_3$  and  $K_4$  as,

$$\beta_1 \cdot \gamma_{21}^3 / \gamma_{11}^2 = \frac{[\text{ZnCl}^+]}{[\text{Zn}^{2+}][\text{Cl}^-]} = K_1 \quad 2.13$$

$$\beta_2 \cdot \gamma_{21}^3 / \gamma_0 = \frac{[\text{ZnCl}_2]}{[\text{Zn}^{2+}][\text{Cl}^-]^2} = K_2 \quad 2.14$$

$$\beta_3 \cdot \gamma_{21}^3 = \frac{[\text{ZnCl}_3^-]}{[\text{Zn}^{2+}][\text{Cl}^-]^3} = K_3 \quad 2.15$$

$$\beta_4 \cdot \frac{\gamma_{21}^3 \gamma_{11}^4}{\gamma_{12}^3} = \frac{[\text{ZnCl}_4^{2-}]}{[\text{Zn}^{2+}][\text{Cl}^-]^4} = K_4 \quad 2.16$$

Equations (2.9) and (2.10) can now be written in terms of the concentrations of zinc and chloride ions as

$$m_1 = [\text{Zn}^{2+}] \cdot \left[ 1 + K_1 [\text{Cl}^-] + K_2 [\text{Cl}^-]^2 + K_3 [\text{Cl}^-]^3 + K_4 [\text{Cl}^-]^4 \right] \quad 2.17$$

$$(2m_1 + m_2) = [\text{Cl}^-] + [\text{Zn}^{2+}] \cdot \left[ K_1 [\text{Cl}^-] + 2K_2 [\text{Cl}^-]^2 + 3K_3 [\text{Cl}^-]^3 + 4K_4 [\text{Cl}^-]^4 \right] \quad 2.18$$

The values of zinc and chloride concentrations are also restricted by equation (2.19), obtained from the combination of equations (2.1) and (2.2).

$$m_1 (2m_1 + m_2)^2 \gamma_{\pm}^3 = [\text{Zn}^{2+}] [\text{Cl}^-]^2 \gamma_{21}^3 \quad 2.19$$

By simple rearrangements and substitutions equations (2.17) and (2.18) can be combined to give a pentic equation of the type given by equation (2.20), in terms of free chloride ions,  $[\text{Cl}^-]$ .

$$a A^5 + b A^4 + c A^3 + d A^2 + e A + f = 0 \quad 2.20$$

where  $A = [\text{Cl}^-]$  and the coefficients are given by

$$a = K_4$$

$$b = K_3 + K_4 (4m_1 - (2m_1 + m_2))$$

$$c = K_2 + K_3 (3m_1 - (2m_1 + m_2))$$

$$d = K_1 + K_2 (2m_1 - (2m_1 + m_2))$$

$$e = 1 + K_1 (m_1 - (2m_1 + m_2)) \quad \text{and}$$

$$f = - (2m_1 + m_2)$$

If the activity coefficients are expressed by extended Debye-Huckel equations, equations (2.21), it is possible to evaluate the values of the four stability constants/

constants from combinations of equations (2.1) to (2.21).

$$\log \gamma_{21} = -1.023 \sqrt{I} / (1 + A_{21} \sqrt{I}) + BI + B'I^2 + B''I^3$$

$$\log \gamma_{11} = -0.5115 \sqrt{I} / (1 + A_{11} \sqrt{I}) + BI + B'I^2 + B''I^3$$

$$\log \gamma_0 = BI + B'I^2 + B''I^3$$

$$\log \gamma_{12} = -1.023 \sqrt{I} / (1 + A_{12} \sqrt{I}) + BI + B'I^2 + B''I^3$$

$$(A_{21} = b \cdot g_{21}, A_{11} = b \cdot g_{11} \text{ and } A_{12} = b \cdot g_{12} ; b = 0.3291)$$

2.21

### 2.1.3 Procedure for Calculation of Stability Constants

This essentially consists in finding out suitable parameters to reproduce the e.m.f or activity coefficients, measured for the system, by an iterative optimisation technique. It should be noted, however, that there are twenty unknown parameters, including the  $E^0$ , in the mathematical analysis given above. The value of the  $E^0$  for the given system must be either accurately known or could be determined independently by the method described in Chapter 1. Fifteen parameters appear in the activity coefficients expressions, equations (2.21), in addition to four stability constants defined by equations (2.5) to (2.8).

Unfortunately, the computer program for the optimisation of these unknown parameters was not available. The authors (Reilly and Stokes) indicated further improvements required in their method of computation.<sup>11</sup>

The computer program, given in Appendix B.1 was therefore written in collaboration with Dr. P. Rosenberg, University of Glasgow. Although for computing efficiency the method has been slightly modified, the basic principle/



principle of calculation is the same as due to Reilly and Stokes.<sup>1</sup>

The method requires initial assumptions about the activity coefficients  $\gamma_{21}$ ,  $\gamma_{11}$ ,  $\gamma_0$ , and  $\gamma_{12}$ . The values initially assigned to these coefficients were those of fully dissociated model electrolytes with similar valency and ionic size characteristics. Activity coefficients for these fully dissociated electrolytes were expressed as a function of the ionic strength, equations (2.21). The values of mean distance of ionic approach,  $\bar{a}$ , and the empirical constants of the Debye-Huckel equations for these electrolytes were evaluated by a least squares technique using the author's own program given in Appendix B.2.

The electrolytes considered and the data obtained will be given in the results and discussion section of this chapter.

Having the parameters of equations (2.21) fixed at their initial values, for each experimental concentration an ionic strength was assumed and the activity coefficients  $\gamma_{21}$ ,  $\gamma_{11}$ ,  $\gamma_0$  and  $\gamma_{12}$  were calculated. These were combined with guessed values of stability constants and a value for the free chloride ion concentration was calculated from equation (2.20). The free zinc ion concentration and the concentrations of the individual complexes were then computed using equations (2.5) to (2.11). A new value of the ionic strength was then calculated from equation (2.12). Activity coefficients were then recalculated, using the new/

new ionic strength, and a new value for chloride ion concentration was obtained. This cyclic calculation was repeated until the value of the ionic strength and the free chloride ion concentration were constant to 0.01%.

Having obtained the free chloride and zinc concentrations a value for the e.m.f was obtained from equation (2.2) and compared to the experimentally measured value. The standard deviation between the calculated and measured e.m.f for all the experimental concentrations was then minimised by optimisation of the four stability constants in a least square sense; utilizing the standard computer subroutines.

The entire procedure was then repeated allowing the optimisation to be performed on the activity coefficient parameters as well as the stability constants for optimum reproduction of the experimental data.

## 2.2            Results and Discussion

### 2.2.1        Test of Computational Methods

Since a new computer program had been written, it was necessary to make a series of investigative calculations.

The experimental data and final values of stability constants and activity coefficient parameters used by Reilly and Stokes were processed. The program reproduced exactly the same deviations between measured and calculated e.m.fs for the cadmium chloride system. Data obtained by Reilly and Stokes and by our own calculation are given in table (2.1).

This first calculation did not test the optimisation capabilities of the program. To this end a new set of stability constants which were significantly different from the literature results were introduced into the program as initial 'guess' values; simulating the normal procedure for dealing with a truly unknown system. Activity coefficient parameters were retained at their reported values, table (2.4).

The optimised values of stability constants obtained from the second calculation are given in table (2.1), together with a new set of deviations between observed and calculated e.m.f of the cell, table (2.1), column II. It can be seen that with the exception of last two points these deviations are equally acceptable to those of Reilly and Stokes. Since/

Table 2.1

Comparison of measured and calculated e.m.f for cadmium chloride.

$m_1$	$2m_1+m_2$	$E_{(meas.)}$ Volts	** Lit.	$E_{(cal.)} -$ I	$E_{(meas.)}$ <sup>†</sup> II
0.0009139	0.0018278	0.83297	-0.01	-0.02	-0.09
0.002229	0.004458	0.80305	0.31	0.30	0.18
0.003458	0.006916	0.78968	-0.08	-0.09	-0.24
0.005294	0.010588	0.77668	0.12	0.11	-0.06
0.010026	0.020052	0.75861	0.02	0.00	-0.17
0.03230	0.06460	0.72752	0.80	0.79	0.67
0.03763	0.07526	0.72490	-0.27	-0.28	-0.38
0.04802	0.09604	0.71936	-0.49	-0.51	-0.57
0.05061	0.10122	0.71771	-0.06	-0.08	-0.14
0.05105	0.10210	0.71719	0.26	0.24	0.18
0.05431	0.10862	0.71569	0.33	0.31	0.26
0.06812	0.13624	0.71098	-0.11	-0.13	-0.15
0.09568	0.19136	0.70385	-0.45	-0.46	-0.43
0.10196	0.20392	0.70235	-0.31	-0.32	-0.29
0.27463	0.54926	0.68274	-0.45	-0.46	-0.35
0.44080	0.88160	0.67440	-0.48	-0.48	-0.42
0.46730	0.93460	0.67343	-0.50	-0.51	-0.45
0.49080	0.98160	0.67276	-0.65	-0.65	-0.60
0.69223	1.38446	0.66722	-0.63	-0.63	-0.66
0.91069	1.82138	0.66276	-0.31	-0.31	-0.43
1.22611	2.45222	0.65825	-0.03	-0.03	-0.26
0.03345	0.56690	0.70431	0.02	0.01	0.08
0.07725	0.65450	0.69362	-0.21	-0.22	-0.16
0.08516	0.67032	0.69170	0.44	0.43	0.48
0.24419	0.98838	0.67792	0.36	0.36	0.34
0.39398	1.28796	0.67181	0.18	0.17	0.09
0.40536	1.31072	0.67155	0.07	0.06	-0.02
0.41550	1.33100	0.67118	0.11	0.11	0.01
0.43104	1.36208	0.67089	-0.08	-0.08	-0.18
0.61551	1.73102	0.66604	0.14	0.14	-0.02

(Continued)

Table 2.1 Continued

$m_1$	$2m_1+m_2$	$E_{(\text{meas.})}$ Volts	$E_{(\text{cal.})}$	$- E_{(\text{meas.})}^*$	
			** Lit.	I	II
0.80974	2.11948	0.66267	0.37	0.28	0.15
1.09022	2.68044	0.65838	0.55	0.55	0.25
0.027023	2.1682	0.70675	1.02	1.02	0.49
0.005248	4.1619	0.73488	-0.46	-0.46	-3.27
0.002448	4.2988	0.74478	-0.20	-0.19	-0.97

\*  $E_{(\text{cal.})} - E_{(\text{meas.})}$  in millivolts.

\*\* Reported data of Reilly and Stokes.<sup>1</sup>

	$\beta_1$	$\beta_2$	$\beta_3$	$\beta_4$
(a) I	$85 \pm 1$	$231 \pm 2$	$122 \pm 1$	$0.053 \pm 0.001$
(b) II	82.3	269.5	73.3	0.032

(a)- Reported values of stability constants<sup>1</sup> and the activity coefficients were used and calculations were carried out with the computer program given in Appendix B.1.

(b)- Values of stability constants obtained when the program was allowed to perform optimisation of stability constants from new 'guess' values. The activity coefficient parameters were fixed at the reported values, given in table (2.4).

Since the sole test of the optimisation procedure depends upon the deviations between calculated and measured e.m.fs, it is important to note that stability constants obtained by this second calculation are somewhat different from those of Reilly and Stokes<sup>1</sup> and outwith their uncertainty limits.

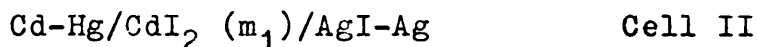
While the limits of uncertainty are smaller than for the similar but less refined calculations, the method of Reilly and Stokes could also produce a range of final results for stability constants. It seems that the method is somewhat dependent upon techniques of numerical analysis available for carrying out optimisation of unknown parameters.

Inclusion of initial guess values for activity coefficient expressions would be expected to modify the final results to some degree, but for cadmium chloride the optimisation of activity terms are of secondary importance. This is even more true for the comparable but more complexed system of aqueous cadmium iodide discussed below.

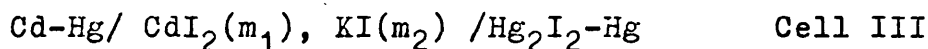
#### 2.2.2      Stability Constants of Cadmium Iodide Complexes in aqueous Solutions.

The primary aim of carrying out this calculation was to obtain refined values for the stability constants of  $\text{CdI}_x^{2-x}$  ( $x=1,2,3,4$ ) complexes suitable for calculation of concentrations of individual complex species in solutions of  $\text{CdI}_2$ , containing no/

no added salt. The e.m.f measurements of the cell,



made by Bates<sup>2</sup> and those of Bates and Vosburgh<sup>3</sup> for the cell,



were used.

Bates<sup>2</sup> and Bates and Vosburgh<sup>3</sup> have shown that the silver-silver iodide electrode behaves abnormally in cadmium iodide solutions. Following these authors, the normal potential of this electrode in cadmium iodide solutions was taken as  $-0.1508 \text{ V}$  and  $E^{\circ}_{\text{Hg}_2\text{I}_2/\text{Hg}}$  equal to  $-0.0405 \text{ V}$ .

To obtain an extended set of experimental data, e.m.f measurements for the mercury-mercurous iodide cell (Cell III) were converted to those for the silver-silver iodide system (Cell II) using the relationship,

$$E_{\text{cell II}} = E_{\text{cell III}} - 0.1103$$

The combined data are given in table (2.2).

The published stability constants of Bates and Vosburgh<sup>3</sup> were used as initial 'guess' values in the computer program together with the activity coefficient parameters obtained by Reilly and Stokes in their study of cadmium chloride. Preliminary calculations showed that the calculation of stability constants/

constants for cadmium iodide was rather insensitive to changes in activity coefficient parameters. The formal similarity between the cadmium iodide and cadmium chloride complex ions made this a suitable initial assumption.

In the first calculation on cadmium iodide the activity coefficient parameters were not optimised. The resulting stability constants are given in table (2.2), where they may be compared with literature values.

The deviations between the measured and calculated e.m.fs are much smaller than for cadmium chloride system and were not improved by further optimisation of activity terms. This effect is due to the very high degree of complexation which reduces the contribution of activity coefficients terms significantly.

The stability constants obtained in these calculations were used to calculate the concentrations of individual complex species in aqueous cadmium iodide, shown in table (3.3) (Chapter 3).

### 2.2.3 Thermodynamic Stability Constants for Complexes in Aqueous Zinc Chloride Solutions

The e.m.f data used in Chapter 1 for a re-investigation of the normal potential of the zinc amalgam electrode were extended by further experiments in which potassium chloride was present in the cell solution.

The /



Table 2.2

Thermodynamic Stability Constants for  $\text{CdI}_x^{2-x}$  ( $x=1,2,3,4$ ) complexes, re-calculated from the e.m.f. measurements of Bates and Bates and Vosburgh. The activity coefficients parameters were fixed at those given in Set 1, table (2.4).

	$m_1$	$2m_1+m_2$	$E_{(\text{meas.})}$	I	$E_{(\text{cal.})}-E_{(\text{meas.})}$	$\gamma_{\pm}$
*	0.001224	0.002448	0.45503	0.002923	-0.00021	0.7026
*	0.003993	0.007986	0.42052	0.007731	0.00016	0.5223
*	0.006407	0.012814	0.40805	0.011208	0.00033	0.4479
*	0.007912	0.015824	0.40293	0.013197	0.00025	0.4150
*	0.01250	0.02500	0.39214	0.018728	0.00052	0.3452
	0.01032	0.02064	0.39700	0.016182	-0.00006	0.3742
	0.01023	0.02046	0.39730	0.016074	-0.00016	0.3755
	0.01023	0.02870	0.39220	0.022104	-0.00017	0.3421
	0.01032	0.03679	0.38970	0.028527	-0.00053	0.3113
	0.01023	0.04125	0.38810	0.032293	0.00017	0.2961
	0.01023	0.05274	0.38720	0.042199	-0.00032	0.2607
	0.01032	0.07357	0.38690	0.061005	-0.00029	0.2096
	0.01023	0.08299	0.38710	0.069964	0.00015	0.1908
	0.02020	0.04040	0.38280	0.026978	0.00008	0.2753
	0.02020	0.04528	0.38130	0.030274	0.00019	0.2645
	0.02020	0.05105	0.38040	0.034398	-0.00013	0.2521
	0.02020	0.05259	0.38000	0.035531	0.00000	0.2488
	0.02020	0.05890	0.37890	0.040313	0.00024	0.2359
	0.02020	0.08882	0.37780	0.065087	0.00029	0.1844

$$\beta_1 = 265.76 \quad (192.31)$$

$$\beta_2 = 1415.5 \quad (8333.3)$$

$$\beta_3 = 1.1147 \times 10^5 \quad (1.0 \times 10^5)$$

$$\beta_4 = 7.7112 \times 10^5 \quad (1.25 \times 10^6)$$

The values in parenthesis are those of Bates and Vosburgh.<sup>3</sup>

\* Bates data.<sup>2</sup>

The experimental techniques were as described in Chapter 1. The total e.m.f data which has been used for the calculation of stability constants are given in table (2.3).

A variety of stability constants have been presented in the literature for this system.<sup>13</sup>

Table (2.3) contains a selection of these results.

To apply the Reilly and Stokes method for calculating stability constants initial 'guess' values are required both for the stability constants and the parameters of equations (2.21).

Activity coefficients data for a number of fully dissociated model electrolytes with the same stoichiometric coefficients as the component electrolytes of the complexed salt were obtained by the method of least squares to conform with the format of equations (2.21). For example sodium chloride data was used as initial model for  $\text{ZnCl}^+, \text{Cl}^-$ . The parameters of the extended Debye-Huckel equations, equations (2.21) are given in table (2.5). The first set of model electrolytes chosen was  $\text{NaCl}$ ,  $\text{CaCl}_2$  and  $\text{Na}_2\text{SO}_4$ . The starting values for the activity coefficients for the neutral complex,  $\text{ZnCl}_2$ , were obtained from the same relation as for cadmium chloride.

Having fixed the activity coefficient parameters at their initial guessed values, the four stability constants were optimised using the literature values as the starting points. In contrast to cadmium/

cadmium chloride and cadmium iodide, very little improvement was achieved, in terms of minimising the sum of squares between the measured and calculated e.m.fs, by this initial optimisation. This, however, signified the importance of activity coefficient terms in dealing with the zinc chloride system.

A total optimisation of the fifteen activity coefficient parameters in one computing run was not possible. For this reason a cycle of calculations was made. In each cycle only four parameters were attacked. Once these had been improved they were held constant and a further four unknown parameters were optimised. The criterion of optimisation was once more the improvement in deviations between measured and calculated e.m.fs.

These calculations show that solely on the basis of agreement between calculated and measured e.m.fs of the zinc chloride cell, a variety of stability constants could be obtained.

The problem of optimisation is made more difficult than for cadmium iodide or cadmium chloride because zinc chloride is complexed to a lesser degree than either of the above examples. The activity coefficient parameters appear to have almost equal weight to the stability constants. The values of the input parameters in the extended Debye-Huckel expressions, equations (2.21), and in particular the chosen values of  $\beta$ , have major effects/

effects upon the set of stability constants. The problem is essentially an extension of that discussed in Chapter 1, where it was shown that by choosing a higher value for  $\beta$ , Robinson and Stokes<sup>12</sup> could totally absorb the effect of the first complex ( $\text{ZnCl}^+$ ) in their extrapolation procedure to obtain  $E_{\text{Zn}}^0$  in a zinc chloride system.

It has become obvious that no unequivocal solution for the stability constant of zinc chloride complexes can be obtained using our present optimisation procedures. Although further sophistication of the method of optimisation is under consideration, in which the more efficient NAG (Nottingham Algorithms Group) subroutines recently made available at the University of Glasgow, are intended to be used it appears that these difficulties are inherent to the zinc chloride system. This observation in no way prejudices its application to more complexed systems where the optimisation of activity expressions constitute a secondary refinement upon the prediction of a series of cell potentials, which are dominated by the relatively large magnitudes of stability constants.

Typical results for zinc chloride system are given in table (2.3). It should be noted, however, that direct comparison of stability constants obtained here with those of literature values is not possible. Most of the results of previous workers tabulated<sup>13</sup> refer to particular ionic strengths or have been obtained with various standard conditions.

Table 2.3

Deviations between measured and calculated e.m.f for zinc chloride.  
The activity coefficient parameters are those given in table (2.4)  
(Set, 2) , obtained by cyclic optimisation procedure.

$m_1$	$2m_1+m_2$	$E_{(meas.)}$	I	$E_{(cal.)}-E_{(meas.)}$	$\gamma_{\pm}$
0.0006108	0.00122166	1.25550	0.001828	-0.00011	0.908
0.0008319	0.0016638	1.24405	0.002488	0.00002	0.895
0.003663	0.007326	1.19131	0.010866	-0.00024	0.804
0.008051	0.016102	1.16399	0.023653	0.00004	0.738
0.008857	0.017714	1.16085	0.025979	-0.00004	0.729
0.01115	0.02230	1.15311	0.032566	-0.00002	0.707
0.03018	0.06036	1.12030	0.085676	0.00011	0.610
0.04086	0.08172	1.11088	0.114454	-0.00026	0.581
0.05104	0.10208	1.10299	0.141276	0.00051	0.560
0.05822	0.11644	1.09910	0.159854	0.00012	0.548
0.06154	0.12308	1.09770	0.168352	-0.00027	0.543
0.07281	0.14562	1.09190	0.196773	0.00011	0.528
0.08660	0.17320	1.08650	0.230679	-0.00009	0.514
0.10299	0.20598	1.08078	0.269776	0.00003	0.499
0.15303	0.30606	1.06790	0.381534	0.00003	0.469
0.15807	0.31614	1.06680	0.392189	0.00011	0.467
0.19300	0.38600	1.06070	0.463226	-0.00027	0.452
0.29603	0.59206	1.04670	0.647649	-0.00004	0.421
0.32173	0.64346	1.04360	0.688692	0.00041	0.416
0.33960	0.67920	1.04180	0.716233	0.00050	0.411
0.51330	1.02660	1.02910	0.949930	0.00039	0.379
0.64980	1.29960	1.02170	1.102622	0.00072	0.360
0.86067	1.72130	1.01340	1.306389	0.00086	0.336
1.0310	2.0620	1.00846	1.453029	0.00063	0.321
0.049135	0.18056	1.09120	0.211927	0.00039	0.528
0.045860	0.31545	1.08020	0.335949	0.00035	0.495
0.083658	0.24687	1.07955	0.293194	-0.00057	0.498

( Continued)

Table 2.3 (Continued)

$m_1$	$2m_1 + m_2$	$E_{\text{(meas.)}}$	$I$	$E_{\text{(cal.)}} - E_{\text{(meas.)}}$	$\gamma_{\pm}$
0.078009	0.38820	1.07137	0.416522	-0.00153	0.477
0.039572	0.57445	1.07050	0.579384	-0.00111	0.467
0.033239	0.83534	1.06618	0.830031	-0.00294	0.452
0.14752	0.36645	1.06330	0.427249	0.00095	0.464
0.13725	0.47901	1.05710	0.515983	0.00187	0.456
0.11435	0.72998	1.05040	0.727744	0.00110	0.444
0.10443	0.83863	1.04860	0.824684	0.00081	0.440
0.30936	0.69679	1.04190	0.722074	0.00055	0.415
0.28651	0.79529	1.03980	0.788589	0.00029	0.415
0.24477	0.97523	1.03750	0.925342	-0.00058	0.415
0.20520	1.14580	1.03690	1.071815	-0.00194	0.416

The values of stability constants obtained are given below.

	a	b	c	d	e
$\beta_1$	3.53	3.1	0.64	2.69	2.7
$\beta_2$	0.072	1.1	3.98	4.07	2.9
$\beta_3$	0.067	0.6	1.41	3.38	0.14
$\beta_4$	0.0102	0.1	-	-	-

a This work.

b Belousov and Alovainikov.<sup>14</sup> (distribution method)

c Sillen and Liljeqvist.<sup>15</sup> (3 molar  $\text{NaClO}_4$ )

d Marcus and Maydan.<sup>16</sup> (anion exchange method).

e Fedorev and Cherikova.<sup>17</sup> (Ionic strength, extrapolation method).

Table 2.4

Empirical constants of the extended Debye-Huckel expressions, equations (2.21).

Set 1<sup>\*</sup>

log	$\frac{a}{a}$	B	B'	B''
$\gamma_{21}$	3.07	0.04014	0.005254	0.001001
$\gamma_{11}$	3.55	-0.05077	0.009006	-0.000799
$\gamma_0$		-0.13540	0.000365	0.000609
$\gamma_{12}$	3.82	-0.06060	0.005441	0.000846

Set 2<sup>\*\*</sup>

$\gamma_{21}$	4.49	0.2165	0.004721	0.000115
$\gamma_{11}$	4.30	0.0535	0.007953	0.000200
$\gamma_0$		-0.08894	0.020080	0.000776
$\gamma_{12}$	4.46	0.17421	0.005006	0.000985

\* Reilly and Stokes data <sup>1</sup>, used for cadmium chloride

\*\* This work, using the computer program given in Appendix B.1. These coefficients were obtained during cyclic optimisation procedure adopted for zinc chloride system.

Table 2.5

Parameters of the extended Debye-Huckel equations, equations (2.21), for the fully dissociated electrolytes, used as initial guesses on the activity coefficients.

Salt	$\alpha$	$B_1$	$B_2$	$B_3$
NaCl	4.42	0.02227	0.0025998	0.00090254
CaCl <sub>2</sub>	4.86	0.04409	0.0036399	0.00012905
MgCl <sub>2</sub>	4.95	-0.06313	-0.0009836	-0.00072298
Na <sub>2</sub> SO <sub>4</sub>	4.04	-0.07220	0.0082490	-0.00041380
Li <sub>2</sub> SO <sub>4</sub>	4.45	0.03776	-0.0090111	0.000541930

The values of these empirical constants were obtained by the method of least squares, using the program given in Appendix B.2, from the data tabulated in ref. (18 ).



References for Chapter 2

1. Reilly, P.J. and Stokes, R.H., Aust. J. Chem., 1970, 23, 1397.
2. Bates, R.G., J. Amer. Chem. Soc., 1941, 63, 399.
3. Bates, R.G. and Vosburgh, W.C., J. Amer. Chem. Soc., 1938, 60, 137.
4. Harris, A.C. and Parton, H.N., Trans. Faraday Soc., 1940, 36, 1139.
5. Irish, D.R., Davies, A.R. and Plane, R.A., J. Chem. Phys., 1969, 50, 2262.
6. Agnew, A. and Paterson, R., in preparation.
7. Rossotti, F.C. and Rossotti, H., 'The Determination of Stability Constants', McGraw-Hill book company, Inc. New York, London, Toronto, 1961.
8. Beck, M.T., 'Chemistry of Complex Equilibria' Van Nostrand Reinhold Company, London, 1970.
9. Biedermann, G. and Sillen, L.G., Arkiv Kemi, 1952, 5, 425.
10. ref. 7 and 8.
11. Private communication.
12. Robinson, R.A. and Stokes, R.H., Trans. Faraday Soc., 1940, 35, 740.
13. Bjerrum, J., Schwarzenbach, G and Sillen, L.G., Eds., 'Stability Constants of Metal-ion Complexes; Chemical Society Special Publication No.17 and 18, London, 1958.

14. Belousov, E.A. and Alovvainikov, AA.,  
Zh. Neorg. Khim., 1975, 20, 5, 1428.  
( Russ. J. Inorg. Chem., 1975, 5, 803.).
15. Sillen, L.G. and Liljeqvist, B.,  
Svensk. Kem. Tidskv., 1944, 56, 85.
16. Marcus, Y and Maydan, D., J. Phys. Chem.,  
1963, 67, 979.
17. Fedorev, V.A., Cherikova, G.E. and Mironov, V.E.,  
Russian. J. of Inorg. Chem. 1970, 15(8), 1082.
18. Robinson, R.A. and Stokes, R.H.,  
'Electrolyte Solutions' 2nd Ed., Butterworths,  
London, 1959.

C H A P T E R 3

Relationship between the transport properties of aqueous cadmium iodide solutions and the degree of self-complexing in these solutions.

## Introduction

Chapter 2 was devoted to the analysis of the stability constants of Group IIB metal halides in aqueous solutions (particularly zinc chloride and cadmium iodide) from which the concentrations of the free and complexed ions may be computed at a given salt concentration.

This present chapter deals with the problem of the transport behaviour of such self-complexed salts.

In any discussion of the transport properties of an ionic solution both the concentrations of the component ions and their mobilities must be known. The basic treatment of such transport process is discussed in terms of irreversible thermodynamic theory.

It is shown in the theoretical section that the binary mobility coefficients of a self-complexed salt can be expressed as summations of the mobility and coupling coefficients of individual ionic components: that is, the free ions themselves and such complexes as exist at any concentration. This analysis can be used to predict firstly the mobility coefficients which characterise the system and then transport properties which are usually measured in the laboratory, equivalent conductance, transport number and salt diffusion coefficient.

The method of calculation is based upon Pikal's analysis,<sup>1</sup> which is, in reality, a re-statement of the classical /

classical theories of Fuoss and Onsager in macroscopic, irreversible thermodynamic terms. As such it retains the inherent limitations of that analysis and is only precise when the electrolyte to which it is applied is at very low concentration.

With this limitation in mind the predictive capabilities of the theory have been applied to the aqueous cadmium iodide system. Cadmium iodide is the most complexed of the halides of the Group IIB metals in dilute solutions. Its transport properties are quite anomalous when compared to dissociated 2:1 electrolytes. In particular, it is characterised by a transport number for cadmium which decreases rapidly with concentration and, at  $0.28 \text{ mol. l}^{-1}$ , becomes zero and subsequently negative.<sup>2</sup> Equivalent conductance and salt diffusion coefficients are also abnormally low.

Earlier, experimental studies by Paterson et al.<sup>3</sup> have provided both measured transport data and the mobilities and coupling coefficients for this system in the concentration range  $0.05 - 0.6 \text{ mol. l}^{-1}$ . There are therefore sufficient data from experimental sources to test any predictive theory. Equally since the theory must be limited to application in the dilute concentration range  $0.0 - 0.05 \text{ mol. l}^{-1}$  cadmium iodide is again the most suitable test system. Zinc chloride, which has also been investigated by Agnew and Paterson,<sup>4</sup> is much less complexed in dilute solutions and shows inversion of the sign of the transport number for zinc only at  $2.0 \text{ mol. l}^{-1}$ .

### 3.1 An Irreversible Thermodynamic Treatment of a Self-Complexing System

The aqueous cadmium iodide system has been treated as a binary electrolyte in which the net flow of cadmium  $J_1$  and iodide  $J_2$  were expressed as functions of their conjugate thermodynamic forces,  $X_1$  and  $X_2$  respectively.<sup>3</sup> These forces are defined as the negative gradients of the electrochemical potentials of these species under the experimental conditions of transport.

From the dissipation function,  $\Phi$ , equation (3.1), linear phenomenological equations may be obtained, equations (3.2).

$$\Phi = J_1 X_1 + J_2 X_2 \geq 0 \quad 3.1$$

(The flows, here are obtained on a solvent-fixed frame of reference)

$$J_1 = L_{11} X_1 + L_{12} X_2 \quad 3.2$$

$$J_2 = L_{21} X_1 + L_{22} X_2$$

These equations show that the flow  $J_1$  is influenced not only by its conjugate force  $X_1$  but also by the non-conjugate force (in this case the thermodynamic force on iodide,  $X_2$ ). The transport properties of any solution are therefore determined by the mobility coefficients  $L_{11}$ ,  $L_{22}$  and  $L_{12} = L_{21}$  of that solution. This /

This latter equality is obtained from the Onsager Reciprocal Relations. These coefficients are functions of concentration and it is only from an examination of the factors which determine their magnitude that a true understanding of the transport phenomena may be obtained.

When the flows,  $J_i$ , and forces,  $X_i$ , are expressed as  $\text{mol cm}^{-2} \text{s}^{-1}$  and  $\text{J mol}^{-1} \text{cm}^{-1}$ , respectively, the units of  $L_{ik}$  are  $\text{mol}^2 \text{cm}^{-1} \text{s}^{-1} \text{J}^{-1}$ .

Although this representation is mathematically rigorous, it provides little insight into the factors which influence transport properties in a self-complexed system such as cadmium iodide. In qualitative terms the observation that the transport number of cadmium may become negative in concentrated solutions ( $\geq 0.3 \text{ mol. l}^{-1}$ ) can only be understood by considering the influence of increasing proportions of negatively charged cadmium complexes  $\text{CdI}_3^-$  and  $\text{CdI}_4^{2-}$  upon the net flow of cadmium in an electrical experiment. The theory presented below therefore deals explicitly with the individual species in solution and the forces upon these species.

Consider an electrolyte containing six solute species,  $i=a,1,2,3,4,b$  in a solvent. Using a solvent-fixed frame of reference, the dissipation function,

$\Phi$ , may be expressed as the sum of the products of the solvent-fixed flows,  $j_i$  and their conjugate forces  $x_i$ , equation (3.3).

$$\Phi = /$$

$$\Phi = j_a x_a + j_1 x_1 + j_2 x_2 + j_3 x_3 + j_4 x_4 + j_b x_b \geq 0 \quad 3.3$$

Under conditions close to equilibrium phenomenological equations may be defined which express the flows  $j_i$  as linear functions of all the forces in the system, equation (3.4).

$$\begin{array}{c|c|cccccc|c}
 j_a & & l_{aa} & l_{a1} & l_{a2} & l_{a3} & l_{a4} & l_{ab} & x_a \\
 j_1 & & l_{1a} & l_{11} & l_{12} & l_{13} & l_{14} & l_{1b} & x_1 \\
 j_2 & & l_{2a} & l_{21} & l_{22} & l_{23} & l_{24} & l_{2b} & x_2 \\
 j_3 & = & l_{3a} & l_{31} & l_{32} & l_{33} & l_{34} & l_{3b} & x_3 \\
 j_4 & & l_{4a} & l_{41} & l_{42} & l_{43} & l_{44} & l_{4b} & x_4 \\
 j_b & & l_{ba} & l_{b1} & l_{b2} & l_{b3} & l_{b4} & l_{bb} & x_b
 \end{array}$$

3.4

The direct mobility coefficients,  $l_{ii}$ , express the contribution of the conjugate force,  $x_i$ , upon the flow  $j_i$  (as  $l_{ii} x_i$ ). However, all the remaining (non-conjugate) forces also influence the flow of species  $i$  by coupling. The terms  $l_{ik} x_k$  therefore represent the contribution to  $j_i$  of a force on species  $k$ .

Since /



Since by the Onsager reciprocal relations  $\ell_{ik} = \ell_{ki}$ , the system is described by 21 mobility coefficients.

If this system represents a self-complexed electrolyte, as for example cadmium iodide, then certain additional limiting conditions apply. The six species a, 1, 2, 3, 4 and b are identified as  $\text{Cd}^{2+}$ ,  $\text{CdI}^+$ ,  $\text{CdI}_2$ ,  $\text{CdI}_3^-$ ,  $\text{CdI}_4^{2-}$  and  $\text{I}^-$ , respectively.

A basic postulate of irreversible thermodynamics is that, even in a system in which there are gradients of free energy, there may be chosen a volume element in which local equilibrium may be assumed. The restriction to the lower volume limit for such a postulate is that the element, although small on a macroscopic scale, should contain sufficient molecules to define a local temperature, pressure or chemical potential without undue statistical fluctuations. This condition is known to be obeyed when the macroscopic gradients of chemical potential are small and the true system as a whole is close to equilibrium. Applying this postulate to the self-complexing system then local equilibrium between the complexed species must be assumed, equation (3.5).

$$\bar{\mu}_i = \bar{\mu}_a + i \bar{\mu}_b \quad (i=1,2,3,4) \quad 3.5$$

In equation (3.5)  $\bar{\mu}_i$  represents the electro-chemical potential of the species i. (Since for the neutral species 2,  $\text{CdI}_2$  there is no charge, chemical and electrochemical /

electrochemical potentials become identical).

Since the forces,  $x_i$ , of equation (3.4) are the local gradients of chemical potential ( $-d\bar{\mu}_i/dx$ ), from equation (3.5) a series of force relationships are obtained, equation (3.6).

$$x_i = x_a + i x_b \quad \text{where } i=1,2,3,4 \quad 3.6$$

If the total flow of cadmium and iodide are defined as  $J_1$  and  $J_2$  as in equation (3.1) and (3.2) then:

$$J_1 = j_a + j_1 + j_2 + j_3 + j_4 = \sum_{i=a}^4 j_i \quad 3.7$$

and

$$J_2 = j_1 + 2j_2 + 3j_3 + 4j_4 + j_b = \sum_{i=1}^4 i j_i + j_b \quad 3.8$$

Substituting equations (3.6), (3.7) and (3.8) into the phenomenological equations, equation (3.4), the binary representation corresponding to equation (3.2) is obtained where:

$$J_1 = L_{11} x_a + L_{12} x_b \quad 3.9$$

$$J_2 = L_{21} x_a + L_{22} x_b$$

In equation (3.2), the thermodynamic forces on free cadmium and iodide ions are defined as  $X_1$  and  $X_2$ , identified /

identified as  $x_a$  and  $x_b$  in equation (3.9). Equations (3.2) and (3.9) are thus identical and the binary coefficients may be expressed as summations of the mobility coefficients of the complexes in the solution, equations (3.10) to (3.12).

$$\begin{aligned}
 L_{11} = & \ell_{aa} + \ell_{a1} + \ell_{a2} + \ell_{a3} + \ell_{a4} \\
 & + \ell_{1a} + \ell_{11} + \ell_{12} + \ell_{13} + \ell_{14} \\
 & + \ell_{2a} + \ell_{21} + \ell_{22} + \ell_{23} + \ell_{24} \\
 & + \ell_{3a} + \ell_{31} + \ell_{32} + \ell_{33} + \ell_{34} \\
 & + \ell_{4a} + \ell_{41} + \ell_{42} + \ell_{43} + \ell_{44}
 \end{aligned} \tag{3.10}$$

$$\begin{aligned}
 L_{12} = L_{21} = & \ell_{a1} + 2\ell_{a2} + 3\ell_{a3} + 4\ell_{a4} + \ell_{ab} \\
 & + \ell_{11} + 2\ell_{12} + 3\ell_{13} + 4\ell_{14} + \ell_{1b} \\
 & + \ell_{21} + 2\ell_{22} + 3\ell_{23} + 4\ell_{24} + \ell_{2b} \\
 & + \ell_{31} + 2\ell_{32} + 3\ell_{33} + 4\ell_{34} + \ell_{3b} \\
 & + \ell_{41} + 2\ell_{42} + 3\ell_{43} + 4\ell_{44} + \ell_{4b}
 \end{aligned} \tag{3.11}$$

and /

$$\begin{aligned}
\text{and } L_{22} = & \ell_{11} + 2\ell_{12} + 3\ell_{13} + 4\ell_{14} + \ell_{1b} \\
& + 2\ell_{21} + 4\ell_{22} + 6\ell_{23} + 8\ell_{24} + 2\ell_{2b} \\
& + 3\ell_{31} + 6\ell_{32} + 9\ell_{33} + 12\ell_{34} + 3\ell_{3b} \quad 3.12 \\
& + 4\ell_{41} + 8\ell_{42} + 12\ell_{43} + 16\ell_{44} + 4\ell_{4b} \\
& + \ell_{b1} + 2\ell_{b2} + 3\ell_{b3} + 4\ell_{b4} + \ell_{bb}
\end{aligned}$$

In these equations the coefficients  $\ell_{ik} = \ell_{ki}$  by the Onsager reciprocal relations.

The values of  $L_{11}$ ,  $L_{22}$  and  $L_{12}$  obtained experimentally are complicated functions of  $\ell_{ik}$  coefficients. In the absence of complexing, equations (3.10), (3.11) and (3.12) would become  $L_{11} = \ell_{aa}$ ,  $L_{12} = L_{21} = \ell_{ab}$  and  $L_{22} = \ell_{bb}$ . The experimentally measurable transport properties, equivalent conductance,  $\Lambda$ , transport number of cation,  $t_1$ , and 'volume-fixed' salt diffusion coefficient,  $D_v$  for a given electrolyte are related to the mobility coefficients by the relations:<sup>5</sup>

$$\Lambda = (\alpha \cdot 10^3 F^2) / N \quad 3.13$$

$$t_1 = (z_1^2 L_{11} + z_1 z_2 L_{21}) / \alpha \quad 3.14$$

$$D_v = /$$

$$D_v = \frac{10^3 R T r}{C} (1 + d \ln \gamma / d \ln m)$$

$$\left[ \frac{|z_1 z_2|}{r_1 r_2} (L_{11} L_{22} - L_{12} L_{21}) / \alpha \right]$$

3.15

$$\text{where } \alpha = (z_1^2 L_{11} + z_2^2 L_{22} + z_1 z_2 (L_{12} + L_{21}))$$

In equations (3.13) to (3.15) the dimensions of  $\Lambda$  and  $D_v$  are  $\text{cm}^2 \text{ ohm}^{-1} \text{ equiv.}^{-1}$  and  $\text{cm}^2 \text{ s}^{-1}$  respectively. Molar, molal and normal concentrations of the salt are denoted by  $C$ ,  $m$  and  $N$ , respectively. The stoichiometric coefficients for the salt are  $r_1$  and  $r_2$  for cation and anion respectively and  $r = r_1 + r_2$ . In the 'Activity term' of equation (3.15),  $\gamma$  is the mean molal activity coefficient of the salt.

It is now obvious that the binary coefficients  $L_{ik}$  can be represented as summations of the mobility and coupling coefficients defined on the basis of a prior knowledge of the complex species and their mobilities in a complexed electrolyte solution.

In principle therefore, any theoretical method of evaluation of the  $\ell_{ik}$  coefficients of equation (3.4) would allow prediction of the measured transport data using equations (3.10) to (3.15).

### 3.2 Experimental

#### 3.2.1 Measurement of Conductivity

Conductivity measurements were made in the dilute solution range 0.001 - 0.1 mol.  $l^{-1}$  of cadmium iodide. The design of the cell used was similar to that of Jones and Bollinger.<sup>6</sup> A schematic diagram of the cell is given in Fig. 3.1. The bulbs incorporated in the filling tubes facilitated rinsing and filling the cell.

The electrodes consisted of 16 mm platinum disks connected to platinum wires sealed into the glass side tubes. The side tubes were filled with mercury. Electrical contact with the conductance bridge was then made with short pieces of thick copper wires dipping into mercury.

#### 3.2.2 Platinisation of Electrodes

The effect of polarisation was minimised by platinising the electrodes by the method recommended by Jones and Bradshaw.<sup>7</sup> The platinising solution was 0.025 molar hydrochloric acid containing 0.3 % platinic chloride and 0.025 % lead acetate. A current of 10 mA  $cm^{-2}$  supplied by a Solartron P.S.U. AS 1413 constant current source was used. The polarity of the electrodes was reversed every ten seconds by an electronic switching device. The cell, after platinisation of the electrodes, was thoroughly washed with /

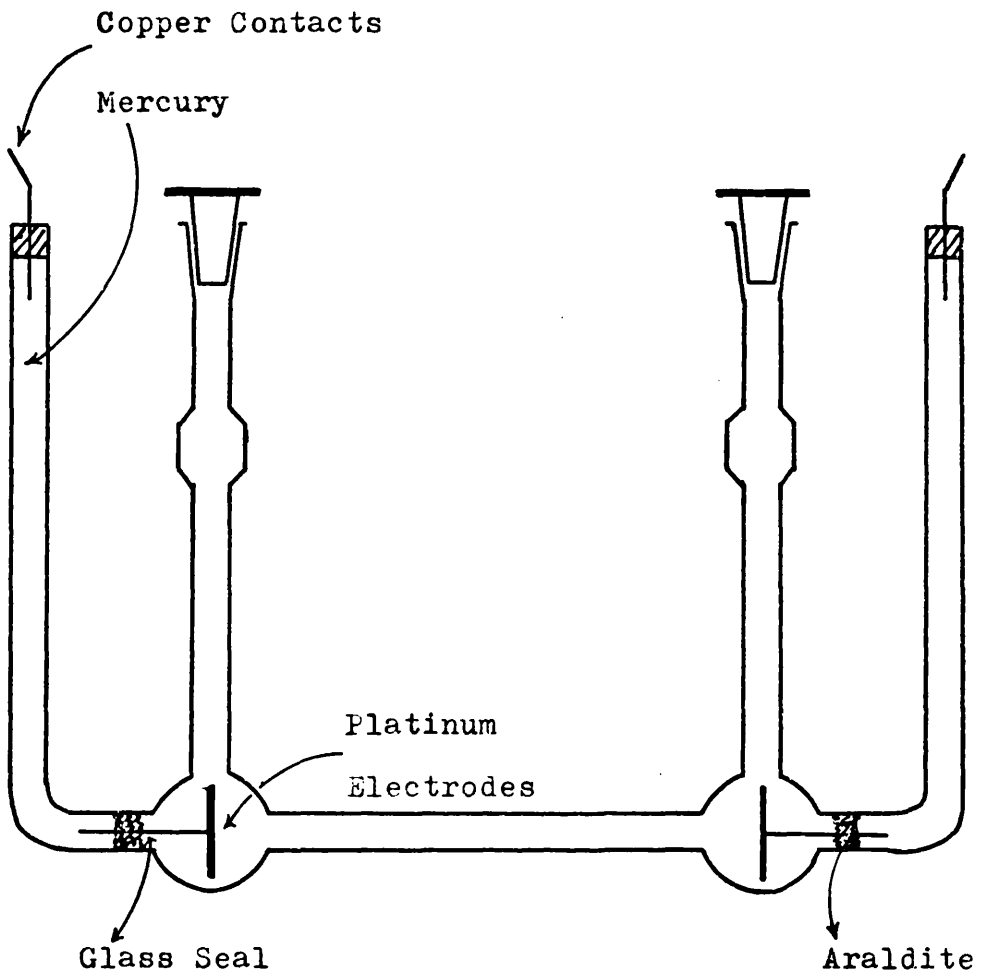


Fig. 3.1— Conductivity Cell

with distilled water and was always stored filled with it.

### 3.2.3 Constant Temperature Bath

A light mineral oil bath was used for temperature control. The bath was fitted with a toluene-mercury coiled glass thermoregulator, connected with an electronic relay and a 40 watt electric bulb as a source of heat in the bath. Cooling was achieved with controlled circulation of cold water through a coiled copper tubing immersed in the oil. The bath oil was vigorously stirred with a paddle stirrer attached to an electric motor. The bath was installed in a room maintained at  $25^{\circ} \pm 1^{\circ}\text{C}$  and by adjusting the heating, cooling and stirring rates, the bath temperature was maintained at  $25^{\circ}\text{C}$  with temperature fluctuations less than  $\pm 0.003^{\circ}\text{C}$ . Temperature was recorded with an E.Mil Standard Thermometer, model K14047, calibrated to N.P.L. standards.

### 3.2.4 The Conductance Bridge

Conductance measurements were made using a Wyne-Kerr digital autobalance precision bridge, type B-331. The bridge had a special 'lead eliminator' circuit which eliminated errors in resistance caused by the use of connecting leads. Measurements were made at a frequency of 1591.55 Hz.

### 3.2.5 /



### 3.2.5 Calibration of the Conductivity Cells

The two cells in use were calibrated with 0.01, 0.1 and 1.0 demal solutions of potassium chloride by the method due to Jones and Bradshaw.<sup>7</sup> Potassium chloride used for preparation of calibrating solutions was recrystallised twice from distilled water, dried at 130°C and stored over silica gell in a vacuum desiccator. The weights required for preparation of the standard solutions, with the corresponding specific conductances, are given in table (3.1). All weights were corrected for buoyancy of air.

Cell I with a cell constant of 35.801 was used for measurements of conductivity of dilute solutions (less than 0.1 mol. l<sup>-1</sup>) and was calibrated with 0.01 and 0.1 demal solutions of potassium chloride. Cell II (cell constant, 87.265) was calibrated with 0.1 and 1.0 demal solutions of potassium chloride and was used for solutions above 0.1 mol. l<sup>-1</sup> (zinc chloride analysis, Chapter 2). The cell constants were periodically checked and remained constant within 0.1%.

### 3.2.6 Measurements of Conductivity of Cadmium Iodide Solutions

Analar cadmium iodide supplied by Hopkin and Williams Ltd., England, was used for preparation of the stock solution. Conductivity water was prepared from water, distilled in an all Pyrex glass apparatus, by first boiling and degassing with a suction pump and /

Table 3.1

Weights of potassium chloride in vacuo and the specific conductances required for calibration of the conductance cell.

conc.	Wt. of KCl	Wt. of Sol.	$K_{sp}$ (ohm <sup>-1</sup> cm <sup>-1</sup> )
1.00 D	7.11352	100 g	0.000342
0.10 D	0.741913	100 g	0.012856
0.01 D	0.0745263	100 g	0.0014087

and then saturating with purified nitrogen. The stock solution was standardised with EDTA by a similar method as described in Chapter 2, for zinc chloride analysis. Further dilutions were made by weight-dilution technique. The apparatus shown in Fig. 3.2 was used for purification of nitrogen and direct transfer of solution to the conductivity cell under the pressure of nitrogen. The cell was flushed several times with a few ml of solution before final filling was accomplished. It was placed in the oil bath to equilibrate to temperature for about half an hour. Readings were then taken every five minutes until no change in successive readings was observed. The specific conductance,  $K_{sp}$ , was then calculated from the relation:

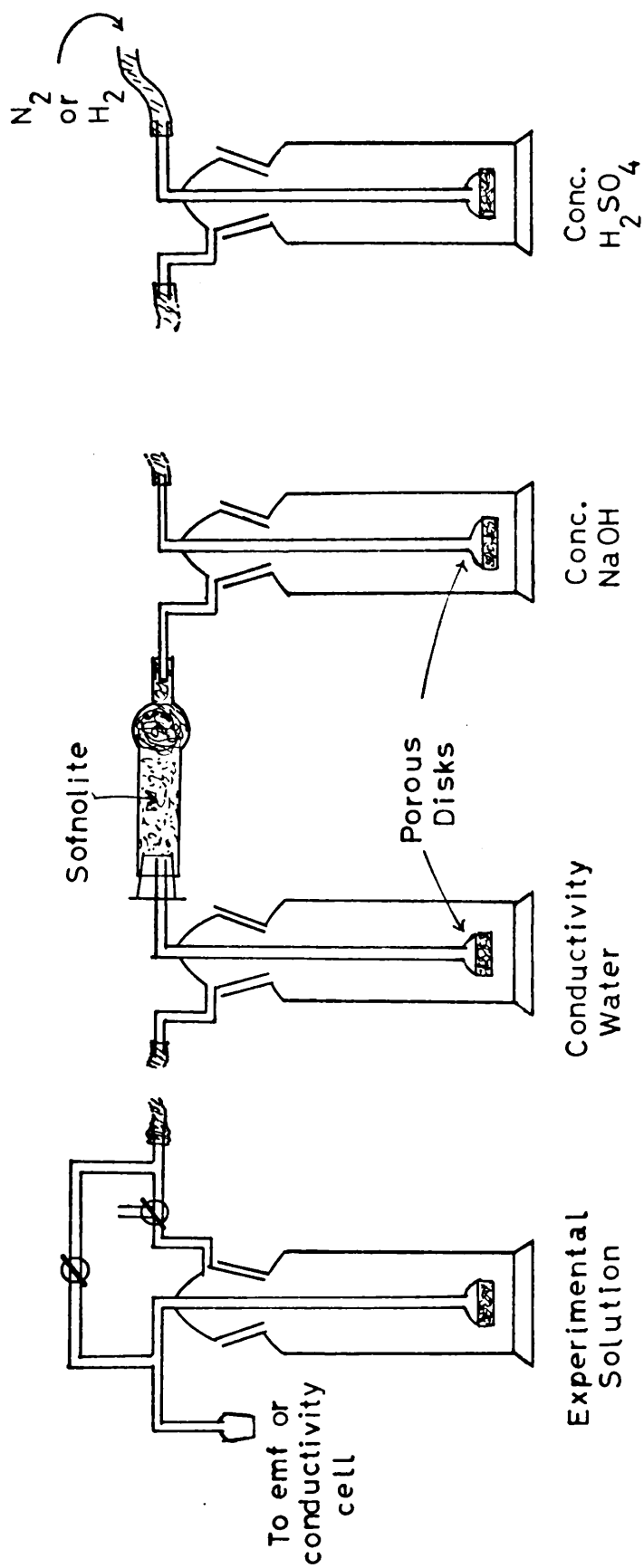
$$K_{sp} = k/R$$

where  $k$  is the cell constant and  $R$  the measured resistance. The equivalent conductance,  $\Lambda$ , was calculated from:

$$\Lambda = 1000 K_{sp} / N$$

$N$ , being the concentration in equivalents per litre.

Fig. 3.2  
Degassing and cell filling apparatus



### 3.3 Results and Discussion

The results of conductance measurements in the concentration range 0.001 - 0.1 mol. l<sup>-1</sup> are given in table (3.2).

In Section 3.1 of this chapter it was shown that the binary coefficients  $L_{ik}$ , for cadmium iodide system, may be expressed as summations of mobility and coupling coefficients,  $\ell_{ik}$ , of the individual complex species, equations (3.10), (3.11) and (3.12). From a prior knowledge of the stability constants for cadmium iodide, Chapter 2, the concentrations of the individual complex species present in solution may be obtained. Using these constants an attempt was made to evaluate the  $\ell_{ik}$  coefficients via Pikal theory.<sup>1</sup> This would allow prediction of all the transport properties of aqueous cadmium iodide, including the equivalent conductance, which might then be compared with the experimental data for this system.

#### 3.3.1 Application of Pikal's Theory to a Self-Complexing System

Pikal<sup>1</sup> has used the classical transport theories of Fuoss and Onsager to obtain expressions for mobility coefficients and has shown clearly the dependence of these coefficients upon the concentrations of the ionic species present in solution and their mobilities at infinite dilution. The treatment is not confined to simple binary electrolytes, which are completely dissociated /

dissociated in solution, and so may be used to evaluate the  $\ell_{ik}$  coefficients of equations (3.10) to (3.12). The expressions for  $\ell_{ik}$  in terms of ionic conductances at infinite dilution are given below.

$$10^{12} \frac{\ell_{ii}}{C_i} = 0.10740 \frac{{}^0\lambda_i}{|Z_i|} -$$

$$0.10740 \left[ \frac{({}^0\lambda_i)^2 / Z_i^2}{\sum_i \mu_i {}^0\lambda_i / |Z_i|} (1 - \mu_i) A_{ii} + \frac{B_0}{2} Z_i^2 \mu_i \right] I^{\frac{1}{2}} \quad (i=k) \quad 3.16$$

and

$$10^{12} \frac{\ell_{ik}}{\sqrt{C_i C_k}} = 0.1074 \sqrt{\mu_i \mu_k} \times$$

$$\left[ \frac{({}^0\lambda_i / |Z_i|)({}^0\lambda_k / |Z_k|)}{\sum_i \mu_i {}^0\lambda_i / |Z_i|} A_{ik} - B_0 / 2 (Z_i Z_k) \right] I^{\frac{1}{2}} \quad (i \neq k) \quad 3.17$$

The ionic strength fraction,  $\mu_i$ , is defined as  $\mu_i = C_i Z_i^2 / 2I$ , where  $I$  is the true ionic strength and  $C_i$  and  $Z_i$  are the concentration and charge, respectively, of the species,  $i$ , present in solution. The term involving  $A_{ik}$  is due to the relaxation effect, with  $A_{ik} = 0.22962 |Z_i Z_k|$  (after substitution of the numerical values for the appropriate constants).

The electrophoretic effect is given by the term associated/

associated with  $B_0$ , where  $B_0/2 = 30.2475$ .

Pikal's own calculations have shown that these expressions, equations (3.16) and (3.17), adequately estimate the direct mobility coefficients  $L_{11}$  and  $L_{22}$  of dissociated 1:1 electrolytes and give a rather better estimate of the interionic coupling coefficients  $L_{12}$  above the concentration limits for the validity of the limiting theory of Fuoss-Onsager.

In applying the Pikal representation to the present problem of cadmium iodide system, the aims were not to achieve quantitative prediction of the binary coefficients  $L_{11}$ ,  $L_{22}$  and  $L_{12}$  but to find out whether this method of analysis would faithfully reproduce the abnormal concentration dependence of these parameters and the measured transport number, conductance and diffusion characteristics.

In the Fuoss-Onsager theory and consequently in Pikal's analysis there is no satisfactory method for estimating the direct mobility coefficients  $\ell_{22}$  (for the neutral complex,  $\text{CdI}_2$ ) or the associated coupling coefficients,  $\ell_{2k}$ . This analysis therefore omits these terms.

### 3.3.2 Optimisation of the Values of Equivalent Conductance at Infinite Dilution, $\lambda_i^0$ , for the Complex Species present in aqueous Cadmium Iodide Solutions

From equations (3.16) and (3.17), it is obvious that /

that a complete mathematical analysis would require a knowledge of the concentrations of the individual complex species,  $i$ , present in solution and their ionic conductance at infinite dilution,  ${}^0\lambda_i$ .

Earlier analysis of potentiometric data for cadmium iodide (Chapter 2) provided the refined values of stability constants for the complexes between cadmium and iodide.

A computer subroutine was written to generate the concentrations of free  $\text{Cd}^{2+}$ ,  $\text{I}^-$  and the complex species,  $\text{CdI}^+$ ,  $\text{CdI}_2$ ,  $\text{CdI}_3^-$  and  $\text{CdI}_4^{2-}$  in the required concentration range ( $0.001 - 0.1 \text{ mol. l}^{-1}$ ) by the method of Reilly and Stokes<sup>9</sup> described in Chapter 2; utilizing the four stability constants and the given activity coefficient parameters, Appendix C, Subroutine PATHAN. The remaining problem, however, was to estimate the ionic conductances at infinite dilution for all the ionic entities present in solution. The values of  $53.5^8$  for  ${}^0\lambda_{\text{Cd}^{2+}}$  and  $76.8^2$  for  ${}^0\lambda_{\text{I}^-}$  are well known, but those of  $\text{CdI}^+$ ,  $\text{CdI}_3^-$  and  $\text{CdI}_4^{2-}$  must be estimated by an optimisation procedure. This was accomplished as follows.

For the chosen experimental concentrations in the range  $0.001 - 0.01 \text{ mol. l}^{-1}$ , the concentrations of the individual complex species were calculated by subroutine PATHAN. These were inserted into equations (3.16) and (3.17) with  ${}^0\lambda_{\text{Cd}^{2+}}$  and  ${}^0\lambda_{\text{I}^-}$  fixed at 53.5 and 76.8 respectively, with guessed values for the /



the ionic conductances,  ${}^0\lambda_i$ , of the remaining three complexes,  $\text{CdI}^+$ ,  $\text{CdI}_3^-$  and  $\text{CdI}_4^{2-}$ . The calculated  $\ell_{ik}$  coefficients from equations (3.16) and (3.17) were used to obtain the binary mobility coefficients  $L_{11}$ ,  $L_{12}$  and  $L_{22}$  from equations (3.10) to (3.12). These binary coefficients have been shown to be related to the equivalent conductance,  $\bar{\Lambda}$ , by equation (3.13) reproduced below.

$$\bar{\Lambda} = \left[ (z_1^2 L_{11} + z_2^2 L_{22} + z_1 z_2 L_{12}) F^2 10^3 \right] / N$$

3.13

Equation (3.13) thus allowed calculation of a value for the equivalent conductance,  $\bar{\Lambda}$ , for the given concentration. A standard NAG subroutine (EØ4FAF, Nottingham Algorithms Group, Document No. 329, 1972) was then used to minimise the sum of squares of the deviations between the calculated and the experimentally measured equivalent conductance, over the concentration range 0.001 - 0.01 mol.  $\text{l}^{-1}$ , by adjusting the unknown parameters,  ${}^0\lambda_{\text{CdI}^+}$ ,  ${}^0\lambda_{\text{CdI}_3^-}$  and  ${}^0\lambda_{\text{CdI}_4^{2-}}$ .

The method of optimisation is thus solely based upon the conductance of dilute solutions, precise experimental measurements of which are easily made.

Furthermore, the terms in  $\ell_{22}$  and  $\ell_{2k}$  cancel in the expansion of the expression for the equivalent conductance in terms of ionic coefficients,  $\ell_{ik}$ , equations /

equations (3.10) to (3.13). This means that the neutral complex species,  $\text{CdI}_2$ , does not contribute in any way to the electrical conductance. (This is an assumption which is often made in electrochemistry, but has not been proved by mathematical analysis.) For our purpose, however, this method is probably suitable since the optimised  $^0\lambda_i$  are in no way influenced by the omission of  $\ell_{2k}$  terms due to the lack of theory regarding the coupling and mobility coefficients of a neutral species in an ionic medium.

The complete computer program, incorporating the subroutines PATHAN and EØ4FAF is given in Appendix C. The program is capable of calculating the equivalent conductance, transport number and diffusion coefficient, for the given concentrations, after evaluating the  $\ell_{ik}$  coefficients and the binary mobility coefficients,  $L_{ik}$ , by optimising the values of  $^0\lambda_i$  for the five ionic species involved or for any arbitrarily fixed values of  $^0\lambda_i$ . The transport number and diffusion coefficients being calculated from equations (3.14) and (3.15), respectively.

Before discussing the results of optimisation of the ionic conductances at infinite dilution for the complex species present, a mention will be given to the concentrations of these species and their relative proportion in solution. In table (3.3) are listed the values of concentrations of free  $\text{Cd}^{2+}$ , free /

free  $I^-$  and the four complex species  $CdI^+$ ,  $CdI_2$ ,  $CdI_3^-$  and  $CdI_4^{2-}$ , over the concentration range  $0.001 - 0.5 \text{ mol. l}^{-1}$ . In Figs. 3.3 and 3.4 the distribution of the free and complexed ions are shown as a function of the total cadmium and total iodide respectively. Figures 3.3 and 3.4 immediately reveal the fact that the dominant species is the  $CdI^+$  over almost the entire range of concentration. At  $0.01 \text{ molar}$  a maximum of  $60\%$  of the total cadmium is present as  $CdI^+$ , only thereafter do the concentrations of the higher complexes become significant.

In the optimisation procedure it was found that the experimental values of equivalent conductance could be reproduced, within  $0.5\%$ , only if  $^0\lambda_{Cd^{2+}}$  was also allowed to 'float' up to  $57.8$  compared to the literature value of  $53.5^8$ . Otherwise, to attain this degree of accuracy, the computer subroutine assigns unrealistic values to  $^0\lambda_{CdI_3^-}$  (low,  $-22$ ) and  $^0\lambda_{CdI_4^{2-}}$  (high,  $\sim 150$ ).

The reason is most probably due to the limiting validity of Pikal theory and the relatively lower proportion of the complex species  $CdI_3^-$  and  $CdI_4^{2-}$  compared to  $CdI^+$  in the concentration range  $0.001 - 0.01 \text{ mol. l}^{-1}$ , Figs. 3.3 and 3.4.

The value of  $^0\lambda_{CdI^+}$  obtained ( $33.51$ ), however, was found to be rather insensitive to the guessed values for  $^0\lambda_{CdI_3^-}$  and  $^0\lambda_{CdI_4^{2-}}$ . This reflects the secondary contribution of these higher complexes in /

in such dilute solutions.

With the above mentioned limitations in mind, constrained optimisation was performed in which  ${}^0\lambda_{\text{Cd}^{2+}}$  and  ${}^0\lambda_{\text{I}^-}$  were fixed at their literature values of 53.5 and 76.84, respectively, and the values of  ${}^0\lambda_{\text{CdI}^+}$ ,  ${}^0\lambda_{\text{CdI}_3^-}$  and  ${}^0\lambda_{\text{CdI}_4^{2-}}$  were allowed to float within chemically acceptable limits. In consequence, the values of measured equivalent conductance could only be reproduced to 2-3%. The optimised values of  ${}^0\lambda_i$  are given in table (3.4).

The value of 33.51 obtained for the ionic conductance at infinite dilution of the complex species  $\text{CdI}^+$  appears to be lower than for the common uni-valent cations ( $\text{Ag}^+$ ,  $\text{Cs}^+$ ,  $\text{Rb}^+$ ,  $\text{K}^+$ ,  $\text{Na}^+$  etc.) but is close to  $\text{Li}^+$  ion (38.68)<sup>2</sup>. It may be worth mentioning here that a value as low as 22.0 for  ${}^0\lambda_{\text{CdI}^+}$  has been suggested by McBain, Van Rysselberge and Squance<sup>10</sup> in 1931.

The equivalent conductance at infinite dilution for the complex species  $\text{CdI}_3^-$  and  $\text{CdI}_4^{2-}$  are, however, similar to those of  $\text{IO}_3^-$  and  $\text{CO}_3^{2-}$  (40.5 and 69.3 respectively)<sup>2</sup>.

### 3.3.3 Calculation of the $L_{ik}$ Coefficients and Prediction of the Transport Properties in dilute solutions of Cadmium Iodide

The irreversible thermodynamic mobility and coupling coefficients,  $L_{ik}$  for aqueous cadmium iodide, in /

in the concentration range 0.05 - 0.6 mol. l<sup>-1</sup>, are available from the experimental transport data of Paterson, Anderson and Anderson.<sup>3</sup> In Figs. 3.5 (a, b and c), these coefficients,  $L_{11}/N$ ,  $L_{12}/N$  and  $L_{22}/N$  are reproduced as a function of the square root of concentration,  $N$ . The values of the intrinsic mobilities,  $L_{11}/N$  and  $L_{22}/N$  at infinite dilution, were calculated from equation (3.18) given below.

$$\frac{L_{ii}}{N} = \frac{{}^0\lambda_i}{|z_i|^2 10^3 F} \quad i = 1, 2 \quad 3.18$$

$$N \rightarrow 0$$

Where  ${}^0\lambda_i$  is the limiting ionic conductance of cadmium ion (53.5)<sup>8</sup> or iodide ion (76.84)<sup>2</sup>. The infinite dilution value of the coupling coefficient,  $L_{12}/N$  is known to be zero, as for any other electrolyte system.

From Fig. 3.5(c) it appears that in the region of discontinuity between experimental and infinite dilution value,  $L_{22}/N$  will pass through a minimum at a concentration below 0.05 mol. l<sup>-1</sup> and there is a possibility that  $L_{11}/N$  might behave similarly, Fig. 3.5(a). Experimental evidence in support of these assumptions is not available due to the lack of reliable data in dilute solutions, in particular, those for the salt diffusion coefficients and transport number. /

number. An attempt was therefore made to investigate these minima by theoretical evaluation of the mobility and coupling coefficients,  $L_{ik}$ , in the concentration range  $0.003 - 0.06 \text{ mol. l}^{-1}$ . The method of calculations described in the previous section was used once again, except that the values of  $^0\lambda_i$  for the three complex species  $\text{CdI}^+$ ,  $\text{CdI}_3^-$  and  $\text{CdI}_4^{2-}$  were now held constant at their optimised values, table (3.4).

The results of these calculations are given in table (3.5) where the predicted transport properties, equivalent conductance, transport number and salt diffusion coefficients are also listed, up to an increased concentration of  $0.1 \text{ mol. l}^{-1}$ .

The calculated binary mobility coefficients are shown graphically in Fig. 3.5 (a, b and c), together with the experimental values of  $L_{11}/N$ ,  $L_{12}/N$  and  $L_{22}/N$ . These figures show pronounced minima in both  $L_{11}/N$  and  $L_{22}/N$  which could only be implied previously. It must be stressed, however, that the calculated binary coefficients,  $L_{ik}$ , are subject to increasing inaccuracies, as concentration is increased, due to the intrinsic limitations of Pikal theory. Nevertheless, these predicted coefficients and the derived estimates of measurable transport data, shown in Figs. 3.6 (a, b and c), are remarkably good.

### 3.3.4 Effect of Variations of $^0\lambda_i$ , from their Optimised Values, upon Predicted Transport Properties and Binary Mobility Coefficients

Having illustrated the predictive capability of the theory in solutions far above the concentrations used for estimation of  $^0\lambda_i$  values (Section 3.3.2) it was of interest to investigate the effects of arbitrary variations from the optimised values of  $^0\lambda_{\text{CdI}^+}$ ,  $^0\lambda_{\text{CdI}_3^-}$  and  $^0\lambda_{\text{CdI}_4^{2-}}$  upon the calculated transport properties and binary mobility coefficients.

In preliminary calculations it was found that the transport parameters and, in particular  $L_{11}$ , were sensitive to relatively small variations, of the order of two units of conductance, in  $^0\lambda_{\text{CdI}^+}$ . Such small variations in  $^0\lambda_i$  for the complex species  $\text{CdI}_3^-$  and  $\text{CdI}_4^{2-}$ , however, were found to have little effect upon the transport properties.

A scheme of calculations was therefore adopted, in which the value of  $^0\lambda_i$  for a given species,  $i$ , was raised and lowered by suitable units, while all others were fixed at their optimised values. The exact values used are given in table (3.4). The calculated transport properties and  $L_{ik}$  coefficients, using the six sets of  $^0\lambda_i$  values (table (3.4), sets 2-7), are given in tables (3.6) to (3.8). The relative sensitivity of the  $L_{ik}$  coefficients, equivalent conductance, cationic transport number and the salt diffusion coefficient to changes in  $^0\lambda_i$  is shown in /

in Figs. 3.7 (a,b,c) to 3.12 (a,b,c). In these figures the experimental values of transport number <sup>3</sup>, <sup>11</sup> salt diffusion coefficients <sup>3</sup> and the derived  $L_{ik}$  coefficients <sup>3</sup> have been retained for the purpose of comparison. The experimental values of the equivalent conductance, are those measured in this work.

Figures 3.7 (b,c) indicate that the parameters  $L_{12}/N$ ,  $L_{22}/N$  and the equivalent conductance,  $\Lambda$ , Fig. 3.8(a), are relatively insensitive to variations in  $^0\lambda_{\text{CdI}^+}$  (table (3.4), sets 2 and 3). The intrinsic mobility for cadmium,  $L_{11}/N$ , is however, most sensitive to even such small variations in  $^0\lambda_{\text{CdI}^+}$  Fig. 3.7(a). In consequence, measurable transport data (transport number and diffusion coefficient) are also subject to large variations, Figs. 3.8 (b,c). In addition, it may be observed that although the higher value of  $^0\lambda_{\text{CdI}^+}$  (35.0) gives a better agreement with the experimental transport number, Fig. 3.8(b) the lower value (30.0) is more favourable for the salt diffusion predictions, Fig. 3.8(c). The optimised value of  $^0\lambda_{\text{CdI}^+}$  (33.51) provides, as would be expected, a compromise between the two limits.

The optimised values of  $^0\lambda_{\text{CdI}_3^-}$  and  $^0\lambda_{\text{CdI}_4^{2-}}$  were 39.70 and 68.67, respectively, and to test the sensitivity of calculations upon variations in these parameters  $^0\lambda_{\text{CdI}_3^-}$  was varied by approximately  $\pm 10$  units /



units and  ${}^0\lambda_{\text{CdI}_4^{2-}}$  by  $\pm 20$  units. The exact values are given in table 3.4 (sets, 4-7). The results of these calculations are given in table (3.7) to (3.8) and are shown graphically in Figs. (3.9) to (3.12). In the most dilute solutions where neither complex is present to significant proportions the calculated transport parameters are insensitive to such variations in  ${}^0\lambda_{\text{CdI}_3^-}$  and  ${}^0\lambda_{\text{CdI}_4^{2-}}$ . They therefore affect the transport predictions only in the higher concentration range above  $0.01 \text{ mol. l}^{-1}$ . Once more the essential validity of the optimised values of  ${}^0\lambda_{\text{CdI}_3^-}$  and  ${}^0\lambda_{\text{CdI}_4^{2-}}$  is obvious. It is noted, however, that lower values of the conductances for these species raise the transport number,  $t_1$ . This is the reverse of the observation for  ${}^0\lambda_{\text{CdI}^+}$ . This effect is obvious, since larger mobilities of the two negatively charged cadmium containing species will increase the anodic migration of cadmium. However, in diffusion where both positive and negative complex species flow concurrently an increase in either  ${}^0\lambda_{\text{CdI}_3^-}$  or  ${}^0\lambda_{\text{CdI}_4^{2-}}$  will increase the overall mobility of the salt and hence increase diffusion coefficient.

### 3.3.5 Percentage Contribution of the $\ell_{ik}$ Coefficients to the Binary Mobility Coefficients, $L_{11}$ , $L_{12}$ and $L_{22}$

It may be recalled that in section (3.3.2) the component /

component coefficients,  $\ell_{ik}$ , which define the binary mobility coefficients,  $L_{ik}$ , were calculated as a necessary step in the assessment of the optimisation procedure for predicting the cadmium iodide transport properties. The complete matrices of the  $\ell_{ik}$  coefficients, calculated over the concentration range 0.003 - 0.06 mol. l<sup>-1</sup>, are given in table (3.9). From this table it is obvious that certain cross coefficients are positive and other negative in sign. From the basic theory of irreversible thermodynamics the direct coefficients,  $\ell_{ii}$ , must always be positive, since a force,  $x_i$ , on a species,  $i$ , will cause a flow  $j_i$  always in the direction of  $x_i$ . Equally since the dissipation function,  $\Phi$ , equation (3.1), must always be positive or zero the additional condition  $\ell_{ii} \cdot \ell_{kk} \geq (\ell_{ik})^2$  is obtained. This allows that the cross coefficients may be positive or negative.

An examination of Pikal's equation for  $\ell_{ik}$  ( $i \neq k$ ), equation (3.17), shows that when ions of the type  $i$  and  $k$  have opposite signs,  $\ell_{ik}$  is positive but  $\ell_{ik}$  is negative if the two ions have like signs. This is caused by the dominant electrophoretic term which is either positive or negative depending upon the sign of the term  $-(B_0/2) Z_i Z_k$ . In a dissociated binary electrolyte, the ions  $i$  and  $k$  have opposite charges and the coefficient,  $\ell_{ik}$ , will always be positive.<sup>12,13</sup> In a complexed system, however, the sign of the coefficient, /

coefficient,  $\ell_{ik}$ , will always depend whether the complexes have similar or opposite charges, table (3.9). At infinite dilution cadmium iodide is completely dissociated and the direct coefficients  $L_{11}$  and  $L_{22}$  are identical to the ionic coefficients,  $\ell_{aa}$  and  $\ell_{bb}$  respectively, while the coupling coefficient  $L_{12}$  is zero, because there can be no coupling between ionic species at infinite dilution. At concentrations where complexing becomes significant (Fig. 3.3) the direct mobility terms  $L_{ii}$  will include  $\ell_{11}$ ,  $\ell_{33}$  and  $\ell_{44}$  (in addition to  $\ell_{aa}$  and  $\ell_{bb}$ ), and non-zero coupling coefficients between various combinations of the ionic species will also be taken into account. The magnitudes of all are determined by the concentrations and mobilities of the ionic species according to equations (3.16) and (3.17).

Since the binary mobility coefficients,  $L_{ik}$ , are strongly dependent upon concentration, the percentage contributions of  $\ell_{ik}$  to  $L_{11}$ ,  $L_{12}$  and  $L_{22}$  were calculated over the range 0.003 - 0.06 mol.  $l^{-1}$  of cadmium iodide. These percentage contributions are given in tables (3.10) to (3.12) and are also displayed in Figs. 3.13 to 3.15. To facilitate discussion and graphical representation the positive and negative  $\ell_{ik}$  coupling coefficients have been tabulated and displayed as  $\Sigma \ell_{+-}$  and  $\Sigma (\ell_{++} + \ell_{--})$  respectively; this is largely because of the number and in some cases the small magnitude of the coefficients involved.

$L_{11}$  , contributions :-

The percentage contributions of the component mobility coefficients,  $\ell_{ik}$  , to  $L_{11}$  are shown in Fig. 3.13. At the most dilute concentration for which calculations have been made the sole significant complex is  $\text{CdI}^+$  (46%) and its direct mobility,  $\ell_{11}$  ; amounts to 59% of  $L_{11}$  while contribution due to cadmium ion itself ( $\ell_{aa}$ ) is reduced to 44%, table (3.10). The higher complexes  $\text{CdI}_3^-$  and  $\text{CdI}_4^{2-}$  are present to a trace level and contribute no more than 0.5% ( $\ell_{33} + \ell_{44}$ ). The positive coupling coefficients,  $\sum \ell_{+-}$  (equal to  $2(\ell_{3a} + \ell_{aa} + \ell_{31} + \ell_{41})$ ) involve only coupling between  $\text{Cd}^{2+}$  (or  $\text{CdI}^+$ ) with the higher negatively charged complex species,  $\text{CdI}_3^-$  and  $\text{CdI}_4^{2-}$ . As these higher complexes have negligible small concentrations,  $\sum \ell_{+-}$  amounts only to 0.05%. What is, however, most interesting is that because  $\text{CdI}^+$  is the major complex, the coupling coefficient between this species and free cadmium ion,  $\ell_{a1}$  , is negative and contributes -3.7% to the total  $L_{11}$  . (The potentially negative term  $\ell_{43}$  is zero at this concentration.)

Thus in dilute solutions the direct mobility coefficient,  $L_{11}$  , is determined almost entirely by  $\ell_{aa}$  ,  $\ell_{11}$  and  $\ell_{a1}$  .

As concentration is increased, complexing becomes more pronounced and, as can be seen from Fig. 3.13,  $\ell_{aa}$  , the direct mobility coefficient, decreases continuously /

continuously over the range of concentration as free  $\text{Cd}^{2+}$  ions are removed by formation of the higher complexes.

The major contributor to  $L_{11}$ , however, still remains,  $\ell_{11}$ , the direct mobility coefficient for the complex species  $\text{CdI}^+$ . At 0.01 molar it contributes a maximum of 76% and even at highest concentration (0.06 mol.  $\text{l}^{-1}$ ) 59% of the total  $L_{11}$  is due to this coefficient, table (3.10).

The direct mobility coefficients for the complex species  $\text{CdI}_3^-$  and  $\text{CdI}_4^{2-}$  increase from zero and it is seen that  $\ell_{33}$  makes a larger contribution to  $L_{11}$  than  $\ell_{44}$ . This is a concentration effect since  $^0\lambda_{\text{CdI}_3^-}$  is smaller than  $^0\lambda_{\text{CdI}_4^{2-}}$ .

The negative coupling coefficients  $\sum(\ell_{+-} + \ell_{--})$  are still largely due to  $\ell_{a1}$  which alone amounts to -7% at 0.06 mol.  $\text{l}^{-1}$ . The remainder -0.8% is due to coupling between  $\text{CdI}_3^-$  and  $\text{CdI}_4^{2-}$ ,  $\ell_{34}$ .

Positive coupling coefficients at the highest concentration calculated now contribute 14% of the total  $L_{11}$ , made up almost equally by contributions from  $\ell_{a3}$ ,  $\ell_{a4}$ ,  $\ell_{13}$  and  $\ell_{14}$ . In consequence, over the whole range of concentration, the value of  $L_{11}$  is largely dependent upon the summation of direct ionic coefficients ( $\ell_{aa}$ ,  $\ell_{11}$ ,  $\ell_{33}$  and  $\ell_{44}$ ) and the cross or coupling coefficient contributions amount to between -6% and +6% of the total, depending upon the degree of complexation.

$L_{12}$  , contributions :-

As has been noted above, the binary mobility coefficient  $L_{12}$  is zero at infinite dilution. The formulation of  $L_{12}$  as a summation of ionic coupling coefficients, equation (3.11), shows that in a complexed system the direct coefficients  $\ell_{11}$  ,  $3\ell_{33}$  and  $4\ell_{44}$  contribute. This is, of course, quite unlike the situation in a dissociated electrolyte. If cadmium iodide were completely dissociated  $L_{12}$  would equal  $\ell_{ab}$  . It is observed that the positive interionic coupling terms ( $\sum \ell_{+-}$ ) are much larger than the negative ( $\sum (\ell_{++} + \ell_{--})$ ) . Together they amount to some 14-18% of the total over the concentration range, table (3.11). The coefficient  $\ell_{ab}$  which is 14% of  $L_{12}$  at 0.003 molar reduces to 3% at 0.06 mol.  $l^{-1}$ . The major contribution to  $L_{12}$  is once more  $\ell_{11}$  which is maximum at 0.003 mol.  $l^{-1}$  (83%) and decreases thereafter, Fig. 3.14. The direct coefficients for the higher complexes  $\ell_{33}$  and  $\ell_{44}$  make little contribution in dilute solutions but at the highest concentrations both are significant, especially the  $\ell_{33}$  contribution, which, at 0.06 mol.  $l^{-1}$ , amounts to 37% and is larger than that of  $\ell_{11}$  (33%) or  $\ell_{44}$  (12%), table (3.11).

The observed values of  $L_{12}$  for complexed electrolytes are found to be exceptionally large when compared with fully dissociated salts.<sup>3</sup> What becomes obvious from this analysis is that this abnormally large /

large  $L_{12}$  is due to the contributions of the direct mobilities  $\ell_{11}$ ,  $3\ell_{33}$  and  $4\ell_{44}$  to what in binary terms would be interpreted as a cross-coefficient dealing with coupling between ions, only.

$L_{22}$ , contributions :-

Table (3.12) lists the percentage contributions of  $\ell_{ik}$  to  $L_{22}$ , a graphical representation of which are displayed in Fig. 3.15. At infinite dilution the coefficient  $L_{22}$  equals  $\ell_{1b}$  and, at the lowest concentration for which calculations have been made (0.003 mol.  $l^{-1}$ )  $\ell_{bb}$  is still the major contributor to  $L_{22}$  amounting to 87%, table (3.12). Only 12% is due to the mobility of the dominant complex  $CdI^+$  ( $\ell_{11}$ ). Interionic coupling,  $\sum \ell_{+-}$ , makes up the remaining 1% and is due almost entirely to coupling between iodide and  $CdI^+$  ( $\ell_{b1}$ ). As concentration is increased,  $\ell_{bb}$  decreases due to removal of free iodide from solution, Fig. 3.15. The mobility of the  $CdI^+$  species remains almost constant, but shows a small maximum (16%) at 0.01 molar. The emergence of  $CdI_3^-$  and  $CdI_4^{2-}$  complexes is reflected in the increasingly important contributions of  $\ell_{33}$  and  $\ell_{44}$ . Once more the percentage contribution of  $\ell_{33}$  is larger than  $\ell_{44}$ . This is observed in spite of the lower ionic conductance of  $CdI_3^-$  compared to  $CdI_4^{2-}$  and the lower factor for  $\ell_{33}$  in the summation which evaluates  $L_{22}$  ( $9\ell_{33}$  compared to  $16\ell_{44}$ ), equation (3.12). The larger contribution of  $\ell_{33}$  is thus solely /

solely due to its larger concentration in solution. Even at the highest concentrations coupling coefficients are of little significance, amounting in total to no more than 3%, with the positive contribution,  $\sum \ell_{+-}$ , (equal to  $(6\ell_{31} + 8\ell_{41} + 2\ell_{b1})$ ) amounting to 7% of the total compared to  $\sum(\ell_{++} + \ell_{--})$  which contributes -4% to  $L_{22}$ .

What emerges most forcibly from these analyses are the very large contributions of the direct mobility coefficients of the ions to  $L_{11}$ ,  $L_{22}$  and even to  $L_{12}$ , which is formally a purely interionic coupling coefficient.

Cross coefficients, being both positive ( $\sum \ell_{+-}$ ) and negative ( $\sum(\ell_{++} + \ell_{--})$ ) partially cancel, for both the direct binary coefficients,  $L_{11}$  and  $L_{22}$ . Only in the case of  $L_{12}$  do they make a significant and, in this case, positive contribution.

Although aqueous cadmium iodide is a most complicated system, it is worth noting that the percentage contributions of  $\text{Cd}^{2+}$ ,  $\text{CdI}^+$ ,  $\text{CdI}_3^-$  and  $\text{CdI}_4^{2-}$  to the total cadmium in the system are very similar to the percentage contributions of the corresponding mobilities  $\ell_{aa}$ ,  $\ell_{11}$ ,  $\ell_{33}$  and  $\ell_{44}$ , to  $L_{11}$  at each concentration, Figs. 3.3 and 3.13. A similar situation is observed in the comparison of percentage concentrations of iodide species and mobility contributions to  $L_{22}$ , Figs. 3.4 and 3.15. These similarities reflect the concentration dependence of  $\ell_{ii}$  upon  $C_i$  and the secondary /



secondary importance of mobilities of the ions. Secondary but obviously not unimportant since the theory is semi-quantitative only for mobilities selected within rather narrow ranges. It has always been observed that  $\ell_{ii}/C_i$  is a less variable function than  $\ell_{ii}$  or  $C_i$  independently. This is obvious in conductance and diffusion expressions, equations (3.13) and (3.15), where  $\ell_{ii}/C_i$  are defined. What is interesting is that the basic proportionality between  $\ell_{ii}$  and  $C_i$  is retained in this complexed system, calculated by Pikal expressions.

In conclusion, the methods and theory developed here have been proved to be viable for the prediction of transport in complexed ionic systems.

The basic limitations of the Onsager-Fuoss Limiting Law theory, obviously restrict the application to relatively dilute solutions. It is interesting, however, that meaningful predictions have now been made up to a concentration of 0.05 molar, far above the normally acceptable range for that theory.

The direct mobility and coupling coefficients for the neutral complex,  $\text{CdI}_2$ , have been omitted, because there is no satisfactory theory by which they may be estimated. It is probable, however, that they will make a relatively small contribution to the binary mobility coefficients and it has been shown that they do not appear in the expression for conductance. Most probably all  $\ell_{2k}$  ( $k = 0, 1, 3, 4$ ) will /

will be positive, and their magnitudes will depend upon  $C_2$  the concentration of  $\text{CdI}_2$  in solution. This latter never amounts to more than 5% of the total cadmium species present. Furthermore it is a reasonable assumption that the coupling coefficient between a neutral species ( $\text{CdI}_2$ ) and an ion will be many times smaller than the corresponding interionic coupling coefficient. These considerations seem to indicate that the effect of neglect of  $\text{CdI}_2$  in these analyses will be small and most probably within the uncertainties of the basic Pikal theory.

Table 3.2

Experimental equivalent conductance  
data for aqueous cadmium iodide at  
25°C.

Concentration (mol.l <sup>-1</sup> )	Conductance (cm <sup>2</sup> ohm <sup>-1</sup> equiv. <sup>-1</sup> )
0.001026	100.62
0.002023	90.79
0.003160	83.35
0.005012	74.81
0.008503	65.60
0.01135	60.23
0.03063	43.30
0.05501	35.10
0.10845	27.36

Definations of Symbols and Units for Tables (3.3)  
to (3.12).

The salt concentrations  $C$ ,  $m$  and  $N$  represent molarity, molality and normality respectively. (The molar concentration of water is designated  $C_0$ .)  $\Lambda$ ,  $t_1$  and  $D_v$  have their usual significance and the 'Activity term' which appears in equation (3.15) is the function  $(1 + d \ln \gamma / d \ln m)$ . The mobility coefficients  $L_{11}$ ,  $L_{12}$  and  $L_{22}$  are defined by the phenomenological equations (equations (3.2)) and, in inverse form, the corresponding resistance coefficients  $R_{11}$ ,  $R_{12}$  and  $R_{22}$  are obtained by matrix inversion. Additional resistance coefficients relating to solvent, 0, interactions,  $R_{i0}$  ( $i=1,2$ ) and  $R_{00}$ , are obtained from the identity:<sup>12</sup>

$$\sum_i C_i R_{ik} = 0 \quad (i \text{ and } k = 0,1,2)$$

The dimensions of  $R_{ik}$  are  $J \text{ cm s mol}^{-2}$ , the inverse of  $L_{ik}$ .

Most of these tables are reproduced from computer printouts and the format is as in FORTRAN IV computer programming language. The exponent is expressed as  $D \pm x$ , where  $x$  is the power of ten. For example  $1.36909D-12$  may be read as  $1.36909 \times 10^{-12}$ .

Table 3.3

Concentrations of individual species at various  
bulk salt concentrations, C.

C	$\text{Cd}^{2+}$	$\text{CdI}^+$	$\text{CdI}_2$	$\text{CdI}_3^-$	$\text{CdI}_4^{2-}$	$\text{I}^-$
0.001	7.289268D-04	2.685493D-04	2.217659D-06	3.021282D-07	4.034742D-09	1.726093D-03
0.003	1.591759D-03	1.369741D-03	2.807270D-05	1.005324D-05	3.739996D-07	4.542458D-03
0.005	2.177685D-03	2.692107D-03	8.213894D-05	4.526518D-05	2.680242D-06	5.998423D-03
0.010	3.197444D-03	6.166577D-03	3.106032D-04	2.977753D-04	3.236546D-05	1.219571D-02
0.020	4.615485D-03	1.264455D-02	9.699620D-04	1.504954D-03	2.823135D-04	1.979531D-02
0.030	5.816936D-03	1.836603D-02	1.704071D-03	3.330744D-03	8.226517D-04	2.500547D-02
0.040	6.971493D-03	2.358271D-02	2.435971D-03	5.473936D-03	1.609501D-03	2.881656D-02
0.050	8.126850D-03	2.847512D-02	3.148005D-03	7.774359D-03	2.540650D-03	3.176103D-02
0.060	9.298953D-03	3.314796D-02	3.837559D-03	1.015518D-02	3.726691D-03	3.413234D-02
0.070	1.049405D-02	3.766360D-02	4.505890D-03	1.257490D-02	4.991171D-03	3.610300D-02
0.080	1.171459D-02	4.206126D-02	5.156919D-03	1.501030D-02	6.359957D-03	3.778116D-02
0.090	1.296161D-02	4.636671D-02	5.789086D-03	1.744768D-02	7.819599D-03	3.923317D-02
0.100	1.423436D-02	5.059838D-02	6.406259D-03	1.987916D-02	9.358221D-03	4.052243D-02
0.200	2.821425D-02	9.065384D-02	1.203073D-02	4.334451D-02	2.771330D-02	4.858555D-02
0.300	4.385644D-02	1.288567D-01	1.714252D-02	6.520517D-02	4.942700D-02	5.309085D-02
0.400	6.047529D-02	1.665307D-01	2.208285D-02	8.582702D-02	7.318593D-02	5.623085D-02
0.500	7.759805D-02	2.043144D-01	2.702170D-02	1.055225D-01	9.836882D-02	5.862237D-02

Table 3.4

The values of  ${}^0\lambda_i$  used for calculation of the irreversible thermodynamic mobility coefficients,  $L_{11}$ ,  $L_{12}$  and  $L_{22}$  and predicted transport properties of aqueous cadmium iodide in the concentration range 0.003 - 0.1 mol.  $l^{-1}$  are given below. Those marked with an asterisk were obtained by the optimisation procedure from the conductance measurements in the dilute solutions (0.001 - 0.01 mol.  $l^{-1}$ ).

${}^0\lambda_i$	$cd^{++}$	$cdI^+$	$cdI_2$	$cdI_3^-$	$cdI_4^{2-}$	$I^-$
1	53.50	33.51*	-	39.70*	68.67*	76.84
2	"	30.00	-	"	"	"
3	"	35.00	-	"	"	"
4	"	33.51*	-	30.00	"	"
5	"	"	-	50.00	"	"
6	"	"	-	39.70*	50.00	"
7	"	"	-	"	100.00	"

Table 3.5

Predicted transport properties of aqueous cadmium iodide from equations (3.10) to (3.17), using optimised values of equivalent conductance for complexed species. (Set 1, table (3.4)).

C	m	N	$\Lambda$	$t_1$	$D_v \cdot 10^5$	Act. term.
0.00300	0.00301	0.00600	80.05	0.4119	1.0918	0.7308
0.00500	0.00501	0.01000	71.41	0.4175	1.0701	0.6886
0.01000	0.01003	0.02000	59.65	0.4172	0.9895	0.5959
0.02000	0.02008	0.04000	47.29	0.3881	0.9114	0.4949
0.03000	0.03014	0.06000	39.62	0.3492	0.8801	0.4427
0.04000	0.04021	0.08000	34.03	0.3106	0.8633	0.4112
0.05000	0.05030	0.10000	29.62	0.2752	0.8528	0.3907
0.06000	0.06040	0.12000	25.94	0.2429	0.8459	0.3767
0.07000	0.07051	0.14000	22.75	0.2133	0.8416	0.3668
0.08000	0.08063	0.16000	19.92	0.1859	0.8391	0.3598
0.09000	0.09077	0.18000	17.34	0.1598	0.8380	0.3547
0.10000	0.10093	0.20000	14.96	0.1343	0.8380	0.3511

(continued)

Table 3.5

(continued)

$L_{11}/N$	$L_{12}/N$	$L_{22}/N$	$N \cdot R_{11}$	$N \cdot R_{12}$	$N \cdot R_{22}$	$N$
1.369090-12	9.674950-13	6.991560-12	8.095790	-1.120300	1.585320	0.0060
1.378950-12	1.157010-12	6.781530-12	8.463500	-1.443980	1.720950	0.0100
1.395160-12	1.453940-12	6.641950-12	9.285980	-2.032720	1.950550	0.0200
1.429360-12	1.873000-12	6.853650-12	1.089930	-2.978610	2.273090	0.0400
1.466410-12	2.189930-12	7.149500-12	1.256870	-3.849860	2.577930	0.0600
1.499670-12	2.431620-12	7.382920-12	1.431030	-4.713190	2.906800	0.0800
1.527570-12	2.617500-12	7.540540-12	1.615570	-5.608010	3.272840	0.1000
1.550780-12	2.763230-12	7.635520-12	1.815600	-6.570500	3.687480	0.1200
1.570210-12	2.879770-12	7.681930-12	2.038130	-7.640480	4.165990	0.1400
1.586470-12	2.974130-12	7.689910-12	2.292500	-8.866440	4.729570	0.1600
1.600290-12	3.051770-12	7.668450-12	2.592050	-1.031540	5.409210	0.1800
1.612140-12	3.116420-12	7.623930-12	2.956390	-1.208480	6.251520	0.2000

$C_{0R10}$	$C_{0R20}$	$C_{0R00}/N$	$R_{10}$	$R_{20}$	$R_{00}/N$	$C_0$
-2.927590	-1.025170	4.497270	-5.289810	-1.852370	8.126040	55.3440
-2.787770	-9.989640	4.323490	-5.037050	-1.804960	7.811830	55.3454
-2.610270	-9.341890	4.047420	-4.717880	-1.688480	7.315420	55.3272
-2.471030	-7.837810	3.652130	-4.469150	-1.417560	6.605310	55.2908
-2.434500	-6.530000	3.384800	-4.405980	-1.181810	6.125840	55.2544
-2.441940	-5.502070	3.207610	-4.422360	-9.964260	5.808990	55.2180
-2.469820	-4.688320	3.087520	-4.475810	-8.496180	5.595210	55.1815
-2.507490	-4.022290	3.002940	-4.547080	-7.294020	5.445530	55.1450
-2.550180	-3.457540	2.941190	-4.627570	-6.274060	5.337090	55.1085
-2.596080	-2.963500	2.895110	-4.713990	-5.381140	5.256960	55.0719
-2.644830	-2.514970	2.859820	-4.805700	-4.569740	5.196350	55.0353
-2.697170	-2.091430	2.832310	-4.904070	-3.802690	5.149780	54.9986



Table 3.6 (a)

Predicted transport properties of aqueous cadmium iodide from equations (3.10) to (3.17) with lowered  $\lambda_{CdI^+}$ , retaining optimised values for all other species. (Set 2, table (3.4)).

C	m	N	$\Lambda$	$t_1$	$D_V \cdot 10^5$	Act. term.
0.00300	0.00301	0.00600	79.24	0.3961	1.0326	0.7308
0.00500	0.00501	0.01000	70.45	0.3966	1.0047	0.6886
0.01000	0.01003	0.02000	58.56	0.3886	0.9245	0.5959
0.02000	0.02008	0.04000	46.18	0.3507	0.8536	0.4949
0.03000	0.03014	0.06000	38.55	0.3050	0.8275	0.4427
0.04000	0.04021	0.08000	33.00	0.2601	0.8138	0.4112
0.05000	0.05030	0.10000	28.62	0.2180	0.8052	0.3907
0.06000	0.06040	0.12000	24.97	0.1785	0.7995	0.3767
0.07000	0.07051	0.14000	21.81	0.1408	0.7960	0.3668
0.08000	0.08063	0.16000	19.00	0.1037	0.7938	0.3598
0.09000	0.09077	0.18000	16.44	0.0659	0.7928	0.3547
0.10000	0.10093	0.20000	14.08	0.0256	0.7926	0.3511

(Continued)

Table 3.6 (a) Continued.

$L_{11}/N$	$L_{12}/N$	$L_{22}/N$	$N \cdot R_{11}$	$N \cdot R_{12}$	$N \cdot R_{22}$	$N$
1.283770-12	8.821380-13	6.904430-12	8.539240 11	-1.091010 11	1.587740 11	0.0060
1.278540-12	1.056440-12	6.678380-12	8.997500 11	-1.423290 11	1.722520 11	0.0100
1.280520-12	1.338770-12	6.522830-12	9.942880 11	-2.040710 11	1.951920 11	0.0200
1.312140-12	1.754600-12	6.729430-12	1.170060 12	-3.050750 11	2.281450 11	0.0400
1.353010-12	2.074710-12	7.026870-12	1.350540 12	-3.987520 11	2.600440 11	0.0600
1.390480-12	2.320020-12	7.262390-12	1.540040 12	-4.919770 11	2.948610 11	0.0800
1.422070-12	2.509020-12	7.421660-12	1.742620 12	-5.891240 11	3.339040 11	0.1000
1.448380-12	2.657330-12	7.517780-12	1.964300 12	-6.943270 11	3.784440 11	0.1200
1.470430-12	2.775970-12	7.564880-12	2.213510 12	-8.122560 11	4.302510 11	0.1400
1.488920-12	2.872060-12	7.573240-12	2.501720 12	-9.487440 11	4.918430 11	0.1600
1.504640-12	2.951130-12	7.551900-12	2.845750 12	-1.112060 12	5.669870 11	0.1800
1.518150-12	3.016970-12	7.507290-12	3.271080 12	-1.314560 12	6.614890 11	0.2000

$C_0 R_{10}$	$C_0 R_{20}$	$C_0 R_{00}/N$	$R_{10}$	$R_{20}$	$R_{00}/N$	$C_0$
-3.178610 11	-1.042230 11	4.754880 09	-5.743370 09	-1.883190 09	8.591490 07	55.3440
-3.075460 11	-1.010870 11	4.604900 09	-5.556850 09	-1.826470 09	8.320300 07	55.3454
-2.930730 11	-9.315650 10	4.332280 09	-5.297080 09	-1.683740 09	7.830290 07	55.3272
-2.799540 11	-7.560740 10	3.899090 09	-5.063290 09	-1.367450 09	7.051970 07	55.2908
-2.765170 11	-6.066790 10	3.600190 09	-5.004430 09	-1.097970 09	6.515660 07	55.2544
-2.780450 11	-4.887240 10	3.402780 09	-5.035400 09	-8.850820 08	6.162450 07	55.2180
-2.821860 11	-3.934260 10	3.269860 09	-5.113780 09	-7.129670 08	5.925640 07	55.1815
-2.878240 11	-3.128000 10	3.176930 09	-5.219400 09	-5.672320 08	5.761050 07	55.1450
-2.944970 11	-2.412280 10	3.109710 09	-5.343950 09	-4.377330 08	5.642880 07	55.1085
-3.021140 11	-1.747100 10	3.060140 09	-5.485800 09	-3.172410 08	5.556630 07	55.0719
-3.108150 11	-1.095680 10	3.022870 09	-5.647570 09	-1.990880 08	5.492610 07	55.0353
-3.209830 11	-4.209540 09	2.994640 09	-5.836210 09	-7.653910 07	5.444940 07	54.9986

Table 3.6 (b)

Predicted transport properties of aqueous cadmium iodide from equations (3.10) to (3.17) with raised  $\lambda_{\text{CdI}^+}$ , retaining optimised values for all other species. (Set 3, table (3.4)).

C	m	N	$\bar{\Lambda}$	$t_1$	$D_v \cdot 10^5$	Act. term.
0.00300	0.00301	0.00600	80.40	0.4185	1.1164	0.7308
0.00500	0.00501	0.01000	71.81	0.4261	1.0972	0.6886
0.01000	0.01003	0.02000	60.11	0.4289	1.0163	0.5959
0.02000	0.02008	0.04000	47.76	0.4034	0.9350	0.4949
0.03000	0.03014	0.06000	40.07	0.3671	0.9015	0.4427
0.04000	0.04021	0.08000	34.47	0.3310	0.8834	0.4112
0.05000	0.05030	0.10000	30.04	0.2981	0.8719	0.3907
0.06000	0.06040	0.12000	26.34	0.2686	0.8645	0.3767
0.07000	0.07051	0.14000	23.15	0.2421	0.8597	0.3668
0.08000	0.08063	0.16000	20.30	0.2183	0.8570	0.3598
0.09000	0.09077	0.18000	17.72	0.1965	0.8558	0.3547
0.10000	0.10093	0.20000	15.33	0.1763	0.8557	0.3511

(Continued)

Table 3.6. (b) Continued.

$L_{11}/N$	$L_{12}/N$	$L_{22}/N$	$N \cdot R_{11}$	$N \cdot R_{12}$	$N \cdot R_{22}$	$N$
1.405110-12	1.003530-12	7.028330-12	7.925030	-1.131560	1.584380	0.0060
1.421320-12	1.199460-12	6.825050-12	8.260870	-1.451800	1.720340	0.0100
1.443530-12	1.502530-12	6.692180-12	9.040060	-2.029670	1.949980	0.0200
1.478790-12	1.922930-12	6.905980-12	1.060040	-2.951610	2.269880	0.0400
1.514210-12	2.238470-12	7.201090-12	1.221930	-3.798390	2.569420	0.0600
1.545680-12	2.478610-12	7.433590-12	1.390390	-4.636040	2.891060	0.0800
1.572010-12	2.663150-12	7.590470-12	1.568320	-5.502520	3.248030	0.1000
1.593880-12	2.807780-12	7.684930-12	1.760490	-6.432160	3.651310	0.1200
1.612180-12	2.923410-12	7.730990-12	1.973460	-7.462460	4.115360	0.1400
1.627500-12	3.017010-12	7.738780-12	2.215840	-8.638580	4.660000	0.1600
1.640490-12	3.094020-12	7.717240-12	2.499830	-1.002240	5.314020	0.1800
1.651630-12	3.158140-12	7.672710-12	2.843190	-1.170280	6.120270	0.2000

$C_0 R_{10}$	$C_0 R_{20}$	$C_0 R_{00}/N$	$R_{10}$	$R_{20}$	$R_{00}/N$	$C_0$
-2.830950	-1.018600	4.398090	-5.115190	-1.840490	7.946820	55.3440
-2.678640	-9.944360	4.216710	-4.839860	-1.796780	7.618900	55.3454
-2.490360	-9.351470	3.940790	-4.501150	-1.690210	7.122690	55.3272
-2.348590	-7.940720	3.560020	-4.247690	-1.436170	6.438710	55.2908
-2.311260	-6.702190	3.304440	-4.182940	-1.212970	5.980400	55.2544
-2.315910	-5.730410	3.134640	-4.194120	-1.037780	5.677210	55.2180
-2.339070	-4.967690	3.019670	-4.238860	-9.002440	5.472260	55.1815
-2.370300	-4.352320	2.938400	-4.298300	-7.892510	5.328500	55.1450
-2.404830	-3.841290	2.879950	-4.363820	-6.970410	5.224150	55.1085
-2.440600	-3.407090	2.834500	-4.431670	-6.186620	5.146900	55.0719
-2.476750	-3.028150	2.800360	-4.500290	-5.502200	5.088310	55.0353
-2.513160	-2.688840	2.773640	-4.569510	-4.888920	5.043120	54.9986

Table 3.7 (a)

Predicted transport properties of aqueous cadmium iodide from equations (3.10) to (3.17) with lowered  $\lambda_{\text{CdI}_3^-}^0$ , retaining optimised values for all other species. (Set 4, table (3.4)).

C	m	N	$\bar{\Lambda}$	$t_1$	$D_v \cdot 10^5$	Act.term.
0.00300	0.00301	0.00600	80.04	0.4124	1.0891	0.7308
0.00500	0.00501	0.01000	71.36	0.4189	1.0632	0.6886
0.01000	0.01003	0.02000	59.51	0.4229	0.9699	0.5959
0.02000	0.02008	0.04000	46.92	0.4060	0.8711	0.4949
0.03000	0.03014	0.06000	39.08	0.3801	0.8285	0.4427
0.04000	0.04021	0.08000	33.36	0.3543	0.8060	0.4112
0.05000	0.05030	0.10000	28.85	0.3314	0.7924	0.3907
0.06000	0.06040	0.12000	25.09	0.3120	0.7840	0.3767
0.07000	0.07051	0.14000	21.85	0.2960	0.7789	0.3668
0.08000	0.08063	0.16000	18.98	0.2838	0.7761	0.3598
0.09000	0.09077	0.18000	16.36	0.2753	0.7748	0.3547
0.10000	0.10093	0.20000	13.95	0.2710	0.7748	0.3511

(Continued)

Table 3.7 (a) Continued

$L_{11}/N$	$L_{12}/N$	$L_{22}/N$	$N \cdot R_{11}$	$N \cdot R_{12}$	$N \cdot R_{22}$	$N$
1.367370-12	9.623490-13	6.976120-12	8.099710 11	-1.117350 11	1.587600 11	0.0060
1.374300-12	1.143160-12	6.739960-12	8.471660 11	-1.436870 11	1.727390 11	0.0100
1.379930-12	1.408580-12	6.505850-12	9.302720 11	-2.014130 11	1.973160 11	0.0200
1.391010-12	1.759050-12	6.511570-12	1.091920 12	-2.949740 11	2.332570 11	0.0400
1.409940-12	2.022380-12	6.646490-12	1.258540 12	-3.829460 11	2.669770 11	0.0600
1.430140-12	2.225630-12	6.764430-12	1.432930 12	-4.714620 11	3.029520 11	0.0800
1.448630-12	2.383910-12	6.839130-12	1.618980 12	-5.643290 11	3.429250 11	0.1000
1.464890-12	2.509380-12	6.873160-12	1.822450 12	-6.653760 11	3.884220 11	0.1200
1.479080-12	2.610720-12	6.873760-12	2.051290 12	-7.791010 11	4.413910 11	0.1400
1.491320-12	2.693470-12	6.846680-12	2.316340 12	-9.112430 11	5.045370 11	0.1600
1.502000-12	2.762110-12	6.797980-12	2.633530 12	-1.070040 12	5.818730 11	0.1800
1.511380-12	2.819710-12	6.732020-12	3.027150 12	-1.267920 12	6.796120 11	0.2000

$C_0 R_{10}$	$C_0 R_{20}$	$C_0 R_{00}/N$	$R_{10}$	$R_{20}$	$R_{00}/N$	$C_0$
-2.932510 11	-1.028920 11	4.508490 09	-5.298690 09	-1.859140 09	8.146300 07	55.3440
-2.798960 11	-1.004960 11	4.351660 09	-5.057260 09	-1.823030 09	7.862730 07	55.3454
-2.637230 11	-9.660920 10	4.129440 09	-4.766600 09	-1.746140 09	7.463680 07	55.3272
-2.509880 11	-8.577050 10	3.820970 09	-4.539420 09	-1.551260 09	6.910670 07	55.2908
-2.463240 11	-7.550440 10	3.595480 09	-4.457990 09	-1.366490 09	6.507140 07	55.2544
-2.450050 11	-6.722090 10	3.435900 09	-4.437040 09	-1.217370 09	6.222420 07	55.2180
-2.451630 11	-6.076100 10	3.322530 09	-4.442850 09	-1.101110 09	6.021100 07	55.1815
-2.458500 11	-5.573390 10	3.239800 09	-4.458240 09	-1.010680 09	5.875060 07	55.1450
-2.465440 11	-5.184090 10	3.177600 09	-4.473800 09	-9.407070 08	5.766090 07	55.1085
-2.469260 11	-4.891580 10	3.130070 09	-4.463710 09	-8.882170 08	5.683610 07	55.0719
-2.467270 11	-4.685390 10	3.092880 09	-4.483070 09	-8.513440 08	5.619820 07	55.0353
-2.456530 11	-4.565220 10	3.063320 09	-4.466520 09	-8.300610 08	5.569820 07	54.9986

Table 3.7 (b)

Predicted transport properties of aqueous cadmium iodide from equations (3.10) to (3.17) with raised  $\lambda_{\text{CdI}_3^-}$ , retaining optimised values for all other species. (Set 5, table (3.4)).

C	m	N	$\Lambda$	$t_1$	$D_v \cdot 10^5$	Act. term.
0.00300	0.00301	0.00600	80.07	0.4114	1.0946	0.7308
0.00500	0.00501	0.01000	71.45	0.4160	1.0774	0.6886
0.01000	0.01003	0.02000	59.81	0.4113	1.0100	0.5959
0.02000	0.02008	0.04000	47.68	0.3698	0.9528	0.4949
0.03000	0.03014	0.06000	40.19	0.3178	0.9325	0.4427
0.04000	0.04021	0.08000	34.74	0.2670	0.9208	0.4112
0.05000	0.05030	0.10000	30.42	0.2198	0.9124	0.3907
0.06000	0.06040	0.12000	26.81	0.1759	0.9063	0.3767
0.07000	0.07051	0.14000	23.68	0.1344	0.9019	0.3668
0.08000	0.08063	0.16000	20.89	0.0941	0.8988	0.3598
0.09000	0.09077	0.18000	18.35	0.0537	0.8969	0.3547
0.10000	0.10093	0.20000	15.99	0.0116	0.8958	0.3511

(Continued)

Table 3.7 (b) Continued.

$L_{11}/N$	$L_{12}/N$	$L_{22}/N$	$N \cdot R_{11}$	$N \cdot R_{12}$	$N \cdot R_{22}$	$N$
1.370910-12	9.729140-13	7.007810-12	8.091680 11	-1.123390 11	1.582940 11	0.0060
1.383830-12	1.171580-12	6.825230-12	8.455050 11	-1.451350 11	1.714280 11	0.0100
1.411130-12	1.501480-12	6.784630-12	9.269150 11	-2.051320 11	1.927890 11	0.0200
1.469430-12	1.992070-12	7.211090-12	1.088000 12	-3.005620 11	2.217060 11	0.0400
1.525270-12	2.364570-12	7.673810-12	1.255230 12	-3.867800 11	2.494940 11	0.0600
1.571980-12	2.645880-12	8.026220-12	1.429060 12	-4.710960 11	2.798900 11	0.0800
1.609510-12	2.859970-12	8.263610-12	1.612130 12	-5.576090 11	3.138060 11	0.1000
1.639740-12	3.026220-12	8.425320-12	1.809050 12	-6.497760 11	3.520770 11	0.1200
1.664410-12	3.157980-12	8.517570-12	2.026100 12	-7.511950 11	3.959180 11	0.1400
1.684650-12	3.263800-12	8.560180-12	2.271480 12	-8.660640 11	4.470310 11	0.1600
1.701520-12	3.350170-12	8.565180-12	2.556660 12	-1.000010 12	5.078920 11	0.1800
1.715730-12	3.421530-12	8.541070-12	2.897940 12	-1.160910 12	5.821380 11	0.2000

$C_{0R10}$	$C_{0R20}$	$C_{0R00}/N$	$R_{10}$	$R_{20}$	$R_{00}/N$	$C_0$
-2.922450 11	-1.021250 11	4.485530 09	-5.280520 09	-1.845270 09	8.104820 07	55.3440
-2.776180 11	-9.886090 10	4.294300 09	-5.016100 09	-1.786250 09	7.759100 07	55.3454
-2.583250 11	-9.022290 10	3.965240 09	-4.669050 09	-1.630710 09	7.166890 07	55.3272
-2.434390 11	-7.142480 10	3.493240 09	-4.402880 09	-1.291800 09	6.317940 07	55.2908
-2.408350 11	-5.610390 10	3.194700 09	-4.358650 09	-1.015370 09	5.781790 07	55.2544
-2.434350 11	-4.434250 10	3.007350 09	-4.408610 09	-8.030430 08	5.446320 07	55.2180
-2.484580 11	-3.500190 10	2.885590 09	-4.502560 09	-6.343050 08	5.229260 07	55.1815
-2.547470 11	-2.718940 10	2.802840 09	-4.619580 09	-4.930530 08	5.082680 07	55.1450
-2.618520 11	-2.032000 10	2.744520 09	-4.751580 09	-3.687270 08	4.980210 07	55.1085
-2.696770 11	-1.399830 10	2.702590 09	-4.896820 09	-2.541830 08	4.907390 07	55.0719
-2.783220 11	-7.889380 09	2.671930 09	-5.057160 09	-1.4233510 08	4.854940 07	55.0353
-2.880620 11	-1.684310 09	2.649440 09	-5.237630 09	-3.062460 07	4.817290 07	54.9986



Table 3.8 (a)

Predicted transport properties of aqueous cadmium iodide from equations (3.10) to (3.17) with lowered  $\lambda_{\text{CdI}_4^{2-}}$ , retaining optimised values for all other species. (Set 6, table (3.4)).

C	m	N	$\Lambda$	$t_1$	$D_v \cdot 10^5$	Act. term.
0.00300	0.00301	0.00600	80.05	0.4119	1.0917	0.7308
0.00500	0.00501	0.01000	71.40	0.4177	1.0696	0.6886
0.01000	0.01003	0.02000	59.60	0.4185	0.9869	0.5959
0.02000	0.02008	0.04000	47.06	0.3948	0.9023	0.4949
0.03000	0.03014	0.06000	39.18	0.3640	0.8652	0.4427
0.04000	0.04021	0.08000	33.40	0.3349	0.8441	0.4112
0.05000	0.05030	0.10000	28.82	0.3097	0.8303	0.3907
0.06000	0.06040	0.12000	25.00	0.2885	0.8210	0.3767
0.07000	0.07051	0.14000	21.69	0.2711	0.8148	0.3668
0.08000	0.08063	0.16000	18.76	0.2575	0.8107	0.3598
0.09000	0.09077	0.18000	16.10	0.2476	0.8082	0.3547
0.10000	0.10093	0.20000	13.65	0.2417	0.8071	0.3511

(Continued)

Table 3.8 (a) Continued.

$L_{11}/N$	$L_{12}/N$	$L_{22}/N$	$N \cdot R_{11}$	$N \cdot R_{12}$	$N \cdot R_{22}$	$N$
1.369030-12	9.672600-13	6.990620-12	8.095870 11	-1.120190 11	1.585480 11	0.0060
1.378690-12	1.156010-12	6.777560-12	8.463730 11	-1.443610 11	1.721690 11	0.0100
1.393620-12	1.447990-12	6.618440-12	9.286560 11	-2.031720 11	1.955430 11	0.0200
1.422560-12	1.847550-12	6.753580-12	1.090230 12	-2.982500 11	2.296610 11	0.0400
1.453420-12	2.141080-12	6.958530-12	1.258440 12	-3.872130 11	2.628510 11	0.0600
1.480600-12	2.360600-12	7.106920-12	1.435730 12	-4.768840 11	2.991070 11	0.0800
1.502960-12	2.526730-12	7.189930-12	1.626020 12	-5.714290 11	3.398990 11	0.1000
1.521190-12	2.655130-12	7.220460-12	1.835420 12	-6.749270 11	3.866820 11	0.1200
1.536140-12	2.756400-12	7.211040-12	2.072480 12	-7.921980 11	4.414920 11	0.1400
1.548380-12	2.837310-12	7.170760-12	2.348980 12	-9.294420 11	5.072150 11	0.1600
1.558540-12	2.903000-12	7.107180-12	2.682570 12	-1.095720 12	5.882630 11	0.1800
1.567050-12	2.956960-12	7.025680-12	3.100530 12	-1.304950 12	6.915600 11	0.2000

$C_{0R10}$	$C_{0R20}$	$C_{0R00}/N$	$R_{10}$	$R_{20}$	$R_{00}/N$	$C_0$
-2.927750 11	-1.025390 11	4.497800 09	-5.290090 09	-1.852750 09	8.126990 07	55.3440
-2.788250 11	-9.998800 10	4.325580 09	-5.037920 09	-1.806620 09	7.815610 07	55.3454
-2.611560 11	-9.395710 10	4.058310 09	-4.720210 09	-1.698210 09	7.335120 07	55.3272
-2.468660 11	-8.053550 10	3.689010 09	-4.464860 09	-1.456580 09	6.672010 07	55.2908
-2.420090 11	-6.924430 10	3.443140 09	-4.379910 09	-1.253190 09	6.231430 07	55.2544
-2.409790 11	-6.066530 10	3.280720 09	-4.364140 09	-1.098650 09	5.941400 07	55.2180
-2.415840 11	-5.418430 10	3.170920 09	-4.377990 09	-9.819290 08	5.746350 07	55.1815
-2.427840 11	-4.921800 10	3.093040 09	-4.402650 09	-8.925190 08	5.610370 07	55.1450
-2.440400 11	-4.539270 10	3.037880 09	-4.428360 09	-8.236980 08	5.512540 07	55.1085
-2.450500 11	-4.249420 10	2.996430 09	-4.449640 09	-7.716140 08	5.440950 07	55.0719
-2.455620 11	-4.040030 10	2.965030 09	-4.461910 09	-7.340800 08	5.387520 07	55.0353
-2.453180 11	-3.908590 10	2.940690 09	-4.460440 09	-7.106720 08	5.347210 07	54.9986

Table 3.8 (b)

Predicted transport properties of aqueous cadmium iodide from equations (3.10) to (3.17) with raised  $\lambda_{\text{CdI}_4^{2-}}$ , retaining optimised values of all other species. (Set 7, table (3.4)).

C	m	N	$\Lambda$	$t_1$	$D_v \cdot 10^5$	Act.term.
0.00300	0.00301	0.00600	80.06	0.4118	1.0920	0.7308
0.00500	0.00501	0.01000	71.42	0.4172	1.0709	0.6886
0.01000	0.01003	0.02000	59.74	0.4152	0.9937	0.5959
0.02000	0.02008	0.04000	47.65	0.3780	0.9252	0.4949
0.03000	0.03014	0.06000	40.29	0.3274	0.9022	0.4427
0.04000	0.04021	0.08000	34.98	0.2762	0.8911	0.4112
0.05000	0.05030	0.10000	30.80	0.2275	0.8842	0.3907
0.06000	0.06040	0.12000	27.32	0.1818	0.8799	0.3767
0.07000	0.07051	0.14000	24.29	0.1382	0.8773	0.3668
0.08000	0.08063	0.16000	21.59	0.0960	0.8759	0.3598
0.09000	0.09077	0.18000	19.12	0.0537	0.8755	0.3547
0.10000	0.10093	0.20000	16.83	0.0099	0.8758	0.3511

(Continued)

Table 3.8 (b) Continued.

$L_{11}/N$	$L_{12}/N$	$L_{22}/N$	$N \cdot R_{11}$	$N \cdot R_{12}$	$N \cdot R_{22}$	$N$
1.369190-12	9.678750-13	6.993060-12	8.095650 11	-1.120480 11	1.585070 11	0.0060
1.379360-12	1.158610-12	6.787860-12	8.463130 11	-1.444560 11	1.719790 11	0.0100
1.397590-12	1.463270-12	6.676790-12	9.285020 11	-2.034270 11	1.942970 11	0.0200
1.439680-12	1.912110-12	7.007210-12	1.089430 12	-2.972820 11	2.238320 11	0.0400
1.486180-12	2.263930-12	7.438300-12	1.254510 12	-3.818240 11	2.506520 11	0.0600
1.528410-12	2.538070-12	7.795670-12	1.424330 12	-4.637230 11	2.792520 11	0.0800
1.564350-12	2.752330-12	8.060030-12	1.601320 12	-5.468190 11	3.107960 11	0.1000
1.594640-12	2.922580-12	8.245610-12	1.789670 12	-6.343320 11	3.461090 11	0.1200
1.620350-12	3.060360-12	8.369170-12	1.994940 12	-7.294920 11	3.862400 11	0.1400
1.642190-12	3.173120-12	8.442700-12	2.224210 12	-8.359530 11	4.326320 11	0.1600
1.660980-12	3.266840-12	8.477430-12	2.487080 12	-9.584140 11	4.872920 11	0.1800
1.677320-12	3.345650-12	8.481330-12	2.796800 12	-1.103260 12	5.531120 11	0.2000

$C_{0R10}$	$C_{0R20}$	$C_{0R00}/N$	$R_{10}$	$R_{20}$	$R_{00}/N$	$C_0$
-2.927350 11	-1.024830 11	4.496430 09	-5.289360 09	-1.851740 09	8.124510 07	55.3440
-2.787000 11	-9.975080 10	4.320160 09	-5.035660 09	-1.802330 09	7.805820 07	55.3454
-2.608240 11	-9.258340 10	4.030480 09	-4.714200 09	-1.673380 09	7.284810 07	55.3272
-2.474350 11	-7.519090 10	3.597490 09	-4.475140 09	-1.359920 09	6.506480 07	55.2908
-2.454300 11	-5.973980 10	3.302080 09	-4.441810 09	-1.081180 09	5.976140 07	55.2544
-2.484400 11	-4.739100 10	3.107880 09	-4.499250 09	-8.582520 08	5.628370 07	55.2180
-2.538430 11	-3.738690 10	2.977600 09	-4.600140 09	-6.775260 08	5.396000 07	55.1815
-2.605040 11	-2.694340 10	2.886850 09	-4.723980 09	-5.248610 08	5.235020 07	55.1450
-2.679780 11	-2.149430 10	2.821410 09	-4.862740 09	-3.900360 08	5.119730 07	55.1085
-2.761540 11	-1.465540 10	2.773330 09	-5.014420 09	-2.661130 08	5.035830 07	55.0719
-2.851240 11	-8.085470 09	2.737290 09	-5.180750 09	-1.469140 08	4.973700 07	55.0353
-2.951410 11	-1.481280 09	2.710100 09	-5.366330 09	-2.693300 07	4.927580 07	54.9986

Table 3.9

The component coefficients,  $\ell_{ik}$ , constituting  $L_{11}$ ,  $L_{12}$  and  $L_{22}$ , tabulated according to the 6x6 matrix of equation (3.4), for each salt concentration, N.

N	$\ell_{ik} \times 10^{12}$					
0.006	3.6407D-03	-1.5394D-04	0.0	1.5590D-06	2.2731D-07	8.0277D-04
	-1.5394D-04	4.8339D-03	0.0	3.4804D-07	5.0529D-08	1.8377D-04
	0.0	0.0	0.0	0.0	0.0	0.0
	1.5590D-06	3.4804D-07	0.0	4.2199D-05	-2.4144D-10	-4.6929D-07
	2.2731D-07	5.0529D-08	0.0	-2.4144D-10	1.3049D-06	-7.9432D-08
	8.0277D-04	1.8377D-04	0.0	-4.6929D-07	-7.9432D-08	3.6348D-02
0.01	4.8064D-03	-3.3870D-04	0.0	7.8181D-06	1.8148D-06	1.3753D-03
	-3.3870D-04	9.4364D-03	0.0	2.5062D-06	5.7931D-07	4.5195D-04
	0.0	0.0	0.0	0.0	0.0	0.0
	7.8181D-06	2.5062D-06	0.0	1.8937D-04	-6.3865D-09	-2.6991D-06
	1.8148D-06	5.7931D-07	0.0	-6.3865D-09	9.2402D-06	-7.2439D-07
	1.3753D-03	4.5195D-04	0.0	-2.6991D-06	-7.2439D-07	5.5625D-02
0.02	6.7163D-03	-8.7338D-04	0.0	5.7588D-05	2.4546D-05	2.6788D-03
	-8.7338D-04	2.1341D-02	0.0	2.8785D-05	1.2218D-05	1.3724D-03
	0.0	0.0	0.0	0.0	0.0	0.0
	5.7588D-05	2.8785D-05	0.0	1.2382D-03	-3.8973D-07	-2.4049D-05
	2.4546D-05	1.2218D-05	0.0	-3.8973D-07	1.0921D-04	-1.1802D-05
	2.6788D-03	1.3724D-03	0.0	-2.4049D-05	-1.1802D-05	9.5840D-02
0.04	9.1381D-03	-1.9842D-03	0.0	3.2285D-04	2.3748D-04	4.8249D-03
	-1.9842D-03	4.3001D-02	0.0	2.2926D-04	1.6793D-04	3.5118D-03
	0.0	0.0	0.0	0.0	0.0	0.0
	3.2285D-04	2.2926D-04	0.0	6.1981D-03	-1.3182D-05	-1.5098D-04
	2.3748D-04	1.6793D-04	0.0	-1.3182D-05	9.1722D-04	-1.2798D-04
	4.8249D-03	3.5118D-03	0.0	-1.5098D-04	-1.2798D-04	1.5319D-01

(Continued)

Table 3.9 Continued.

N	$\ell_{ik} \times 10^{12}$			
0.06	1.0961D-02	-3.0947D-03	7.7202D-04	7.4748D-04
	-3.0947D-03	6.1672D-02	6.3220D-04	6.0950D-04
	0.0	0.0	0.0	0.0
	7.7202D-04	6.3220D-04	1.3598D-02	-7.2272D-05
	7.4748D-04	6.0950D-04	-7.2272D-05	2.5648D-03
0.08	6.5986D-03	5.5400D-03	-3.5398D-04	-3.9688D-04
	1.2521D-02	-4.2286D-03	1.3601D-03	1.5670D-03
	-4.2286D-03	7.8375D-02	1.1941D-03	1.3698D-03
	0.0	0.0	0.0	0.0
	1.3601D-03	1.1941D-03	2.2167D-02	-2.0578D-04
0.10	1.5670D-03	1.3698D-03	-2.0578D-04	4.7972D-03
	8.1706D-03	7.3570D-03	-5.8401D-04	-7.8378D-04
	1.3907D-02	-5.4062D-03	2.0602D-03	2.6889D-03
	-5.4062D-03	9.3790D-02	1.8748D-03	2.4363D-03
	0.0	0.0	0.0	0.0
0.12	2.0602D-03	1.8748D-03	3.1242D-02	-4.2616D-04
	2.6889D-03	2.4363D-03	-4.2616D-04	7.3630D-03
	9.6269D-03	8.9875D-03	-8.1439D-04	-1.2458D-03
	1.5147D-02	-6.6378D-03	2.8577D-03	4.1061D-03
	-6.6378D-03	1.0830D-01	2.6474D-03	3.7871D-03
0.14	0.0	0.0	0.0	0.0
	2.8577D-03	2.6474D-03	4.0515D-02	-7.3629D-04
	4.1061D-03	3.7871D-03	-7.3629D-04	1.0080D-02
	1.1010D-02	1.0467D-02	-1.0342D-03	-1.7520D-03
0.16				

Table 3.10

Percentage Contributions of  $\ell_{ik}$  to  $L_{11}$ , using  
 Optimised  ${}^0\lambda_i$  (set 1, table 3.4))

N	$\ell_{aa}$	$\ell_{11}$	$\ell_{33}$	$\ell_{44}$	$\sum \ell_{+-}$	$\sum (\ell_{++} + \ell_{--})$
0.006	44.32	58.845	0.514	0.016	0.054	-3.748
0.01	34.856	68.432	1.373	0.067	0.184	-4.912
0.02	24.07	76.481	4.438	0.391	0.882	-6.262
0.04	15.983	75.210	10.841	1.604	3.350	-6.986
0.06	12.458	70.094	15.456	2.915	6.278	-7.198
0.08	10.436	65.327	18.477	3.999	9.154	-7.394
0.10	9.104	61.398	20.452	4.820	11.862	-7.636
0.12	8.140	68.198	21.771	5.416	14.400	-7.926

Table 3.11

Percentage Contributions of  $\ell_{ik}$  to  $L_{12}$ , using  
Optimised  ${}^0\lambda_i$  (set 1, table (3.4))

N	$\ell_{11}$	$2\ell_{22}$	$3\ell_{33}$	$4\ell_{44}$	$\Sigma \ell_{+-}$	$\Sigma(\ell_{++} + \ell_{--})$
0.006	83.271	-	2.181	0.090	17.12	-2.661
0.01	81.558	-	4.910	0.319	16.17	-2.956
0.02	73.390	-	12.775	1.502	15.469	-3.137
0.04	57.395	-	24.819	4.897	16.033	-3.144
0.06	46.936	-	31.048	7.808	17.52	-3.311
0.08	40.290	-	34.186	9.864	19.277	-3.617
0.10	35.832	-	35.808	11.252	21.101	-3.991
0.12	32.662	-	36.656	12.159	22.918	-4.396



Table 3.12

Percentage Contributions of  $\ell_{ik}$  to  $L_{22}$  , using  
Optimised  ${}^0\lambda_i$  (set 1, table(3.4) )

N	$\ell_{11}$	$9\ell_{33}$	$16\ell_{44}$	$\ell_{bb}$	$\Sigma\ell_{+-}$	$\Sigma(\ell_{++}+\ell_{--})$
0.006	11.523	0.905	0.050	86.648	0.880	-0.008
0.01	13.915	2.513	0.218	82.025	1.360	-0.032
0.02	16.065	8.389	1.315	72.147	2.270	-0.188
0.04	15.685	20.348	5.353	55.879	3.554	-0.820
0.06	14.377	28.530	9.566	44.563	4.602	-1.640
0.08	13.270	33.778	12.996	36.888	5.562	-2.492
0.10	12.438	37.289	15.623	31.515	6.460	-3.326
0.12	11.820	39.796	17.601	27.593	7.324	-4.136

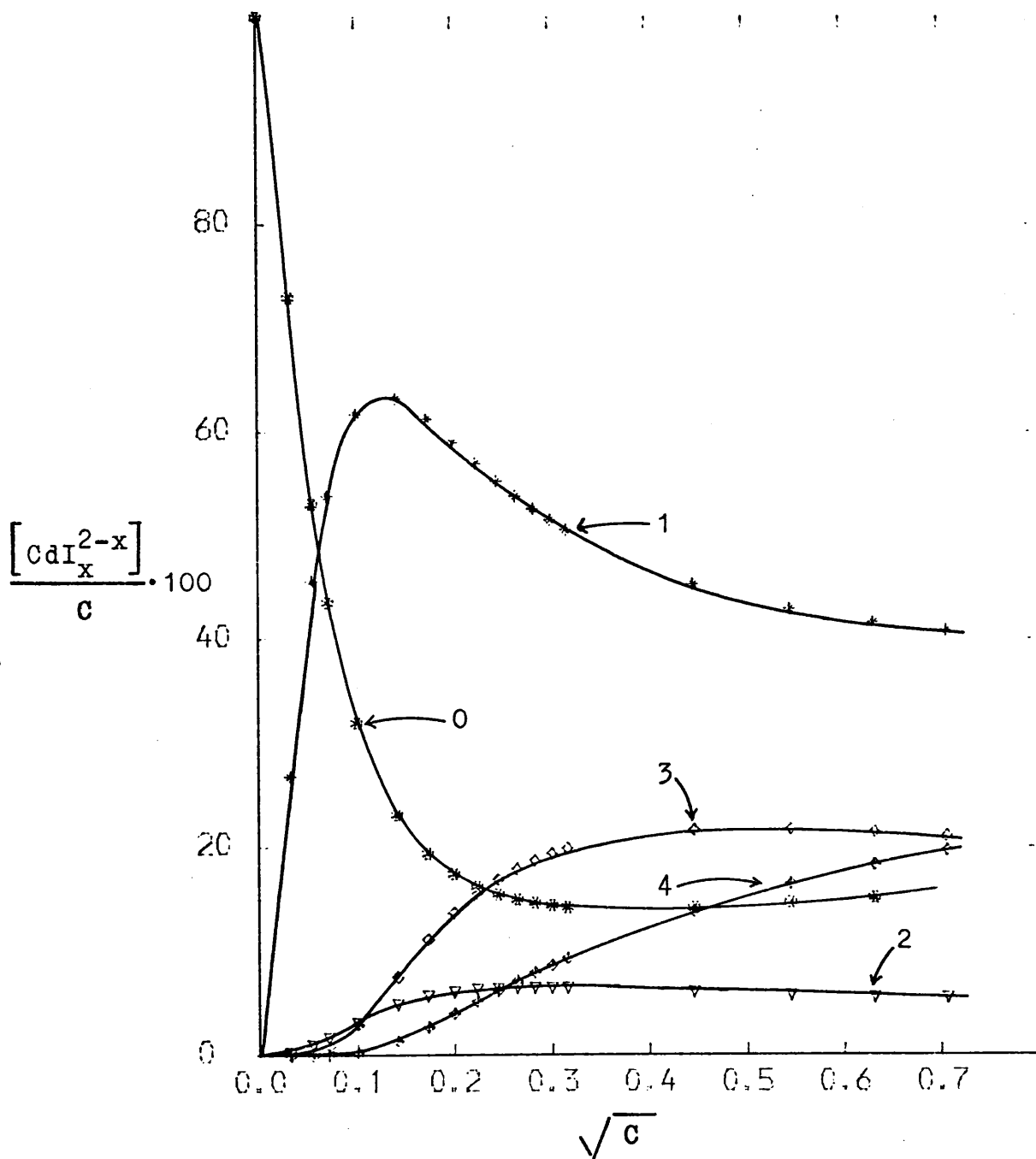


Fig. 3.3 — Percentage distribution of free and complexed cadmium as a function of total concentration of cadmium,  $C$ . ( $x=0,1,2,3,4$ )

0,  $Cd^{2+}$ ; 1,  $CdI^+$ ; 2,  $CdI_2$ ; 3,  $CdI_3^-$ ; 4,  $CdI_4^{2-}$ .

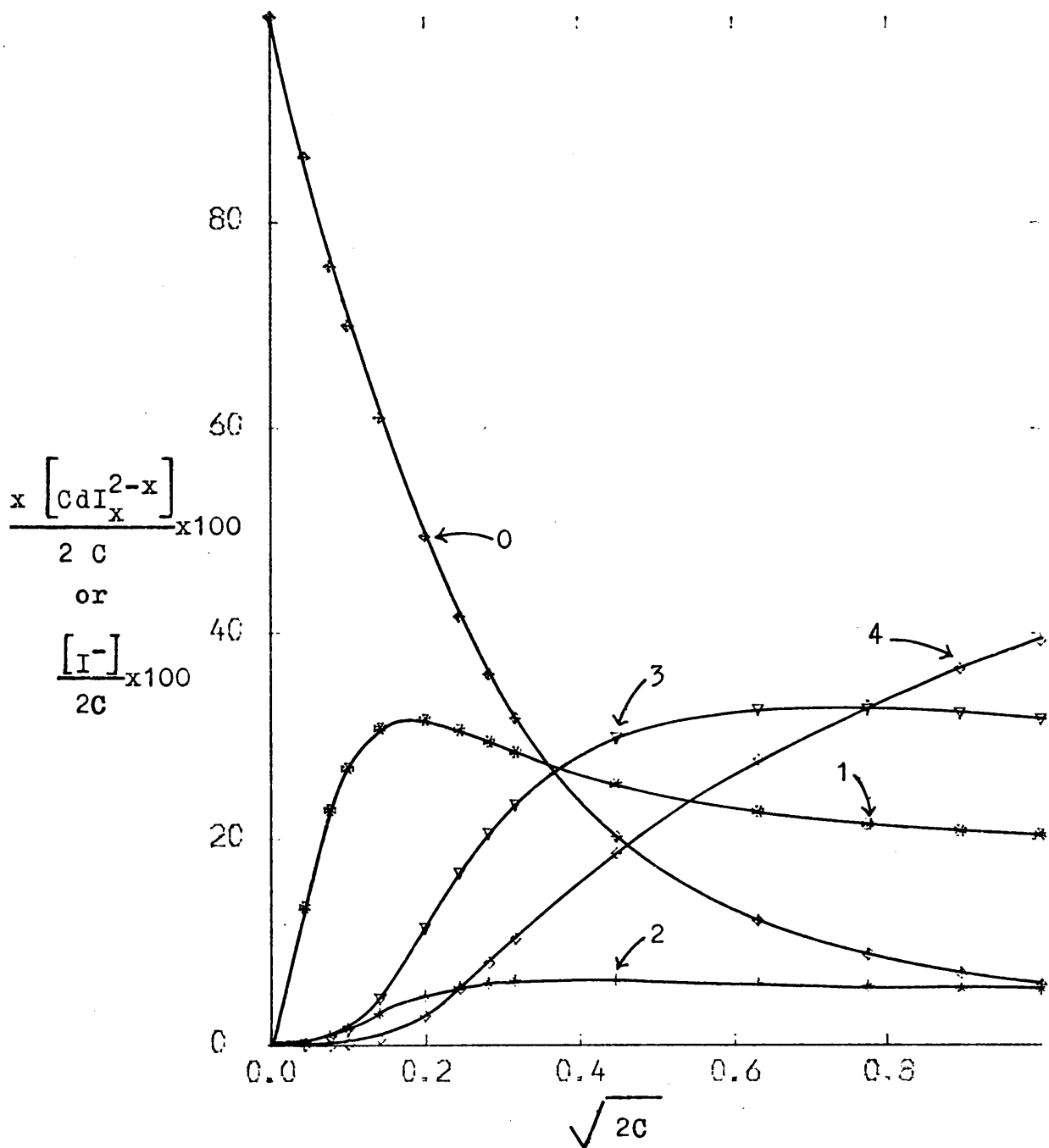


Fig. 3.4— Percentage distribution of free and complexed iodide as a function of total concentration of iodide,  $2C$ . ( $x=1,2,3,4$ ):  
 0,  $\text{I}^-$ ; 1,  $\text{CdI}^+$ ; 2,  $\text{CdI}_2$ ; 3,  $\text{CdI}_3^-$ ; 4,  $\text{CdI}_4^{2-}$ .

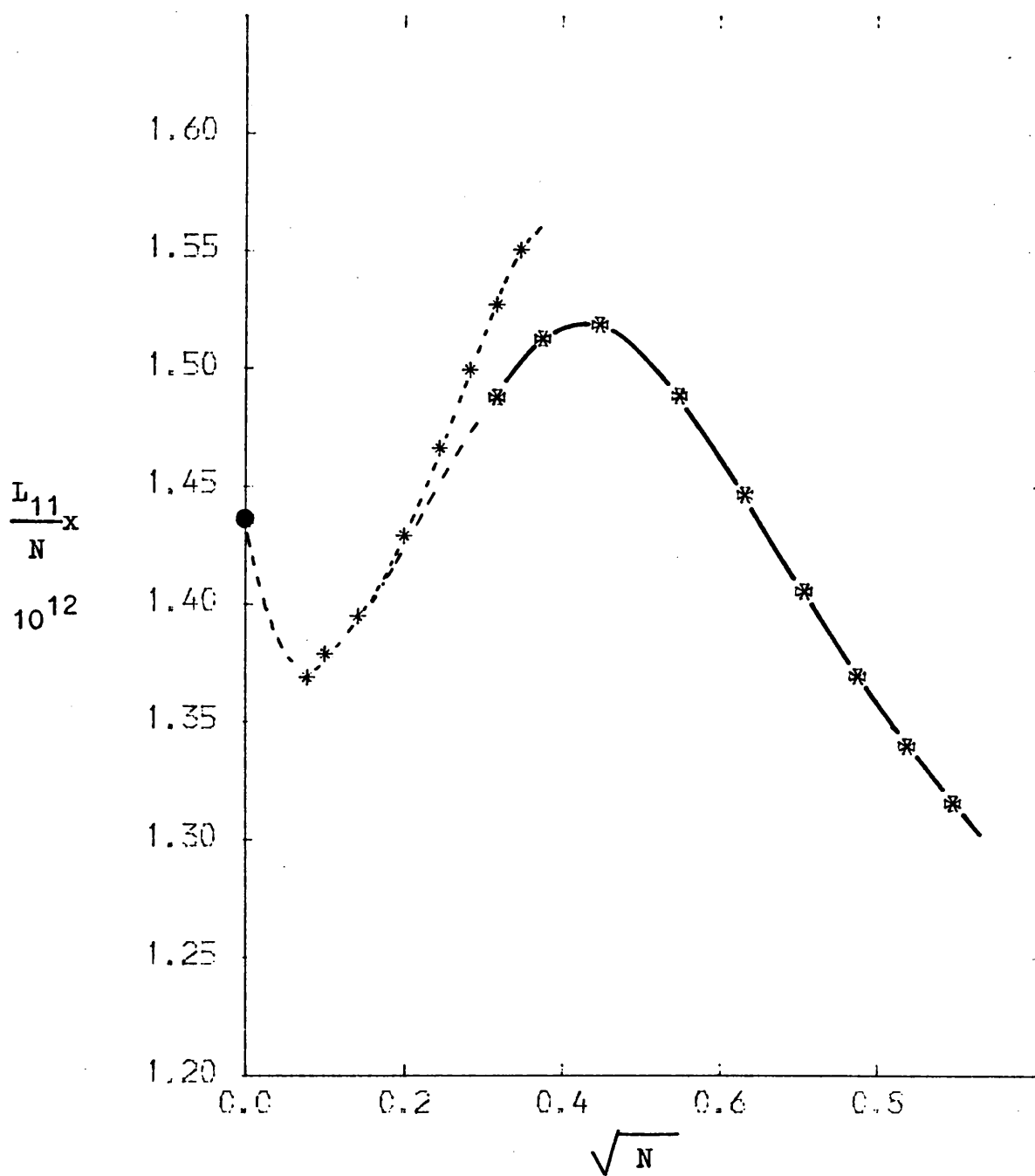


Fig. 3.5 (a).  $L_{11}/N$ . \*, experimental<sup>3</sup>;  
 \*, predicted, using optimised values of  ${}^0\lambda_1$ ;  
 ●, limiting value.

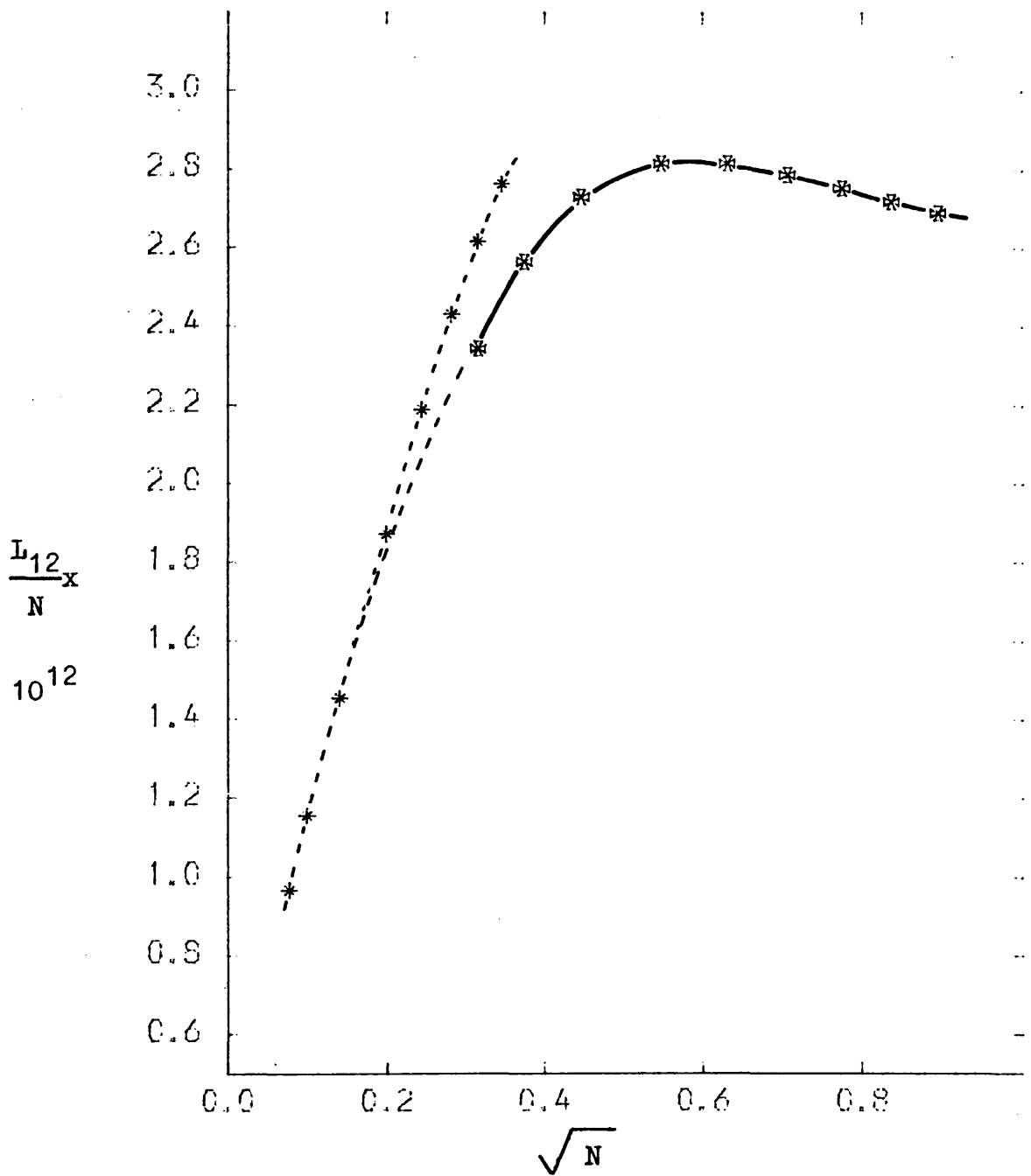


Fig. 3.5 (b).  $L_{12}/N$  . \* , experimental<sup>3</sup>;  
 \* , predicted, using optimised values of  $^0\lambda_i$  .

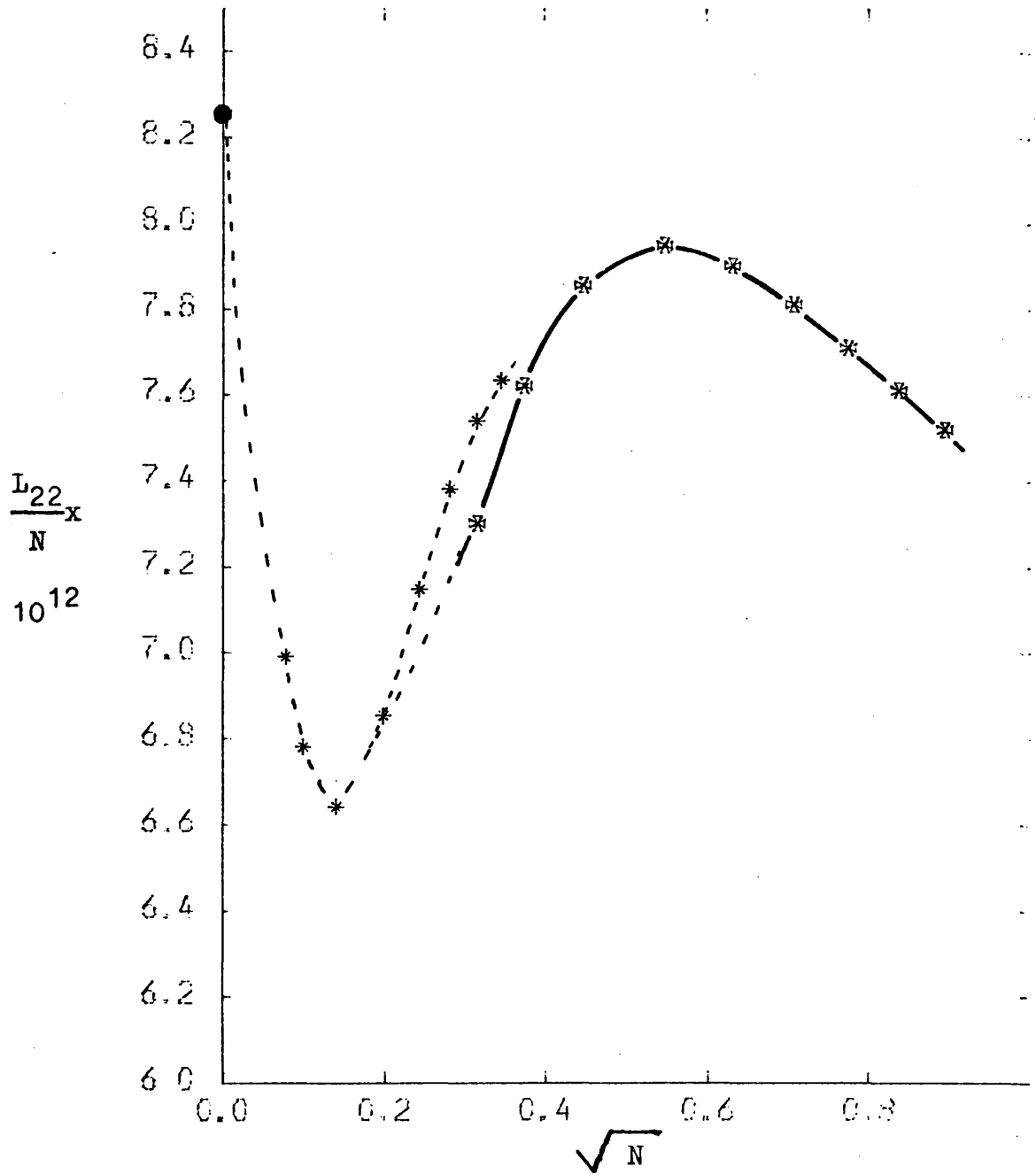


Fig. 3.5 (c).  $L_{22}/N$ . \*, experimental<sup>3</sup>;  
 \*, predicted, using optimised values of  ${}^0\lambda_i$ ;  
 •, limiting value.

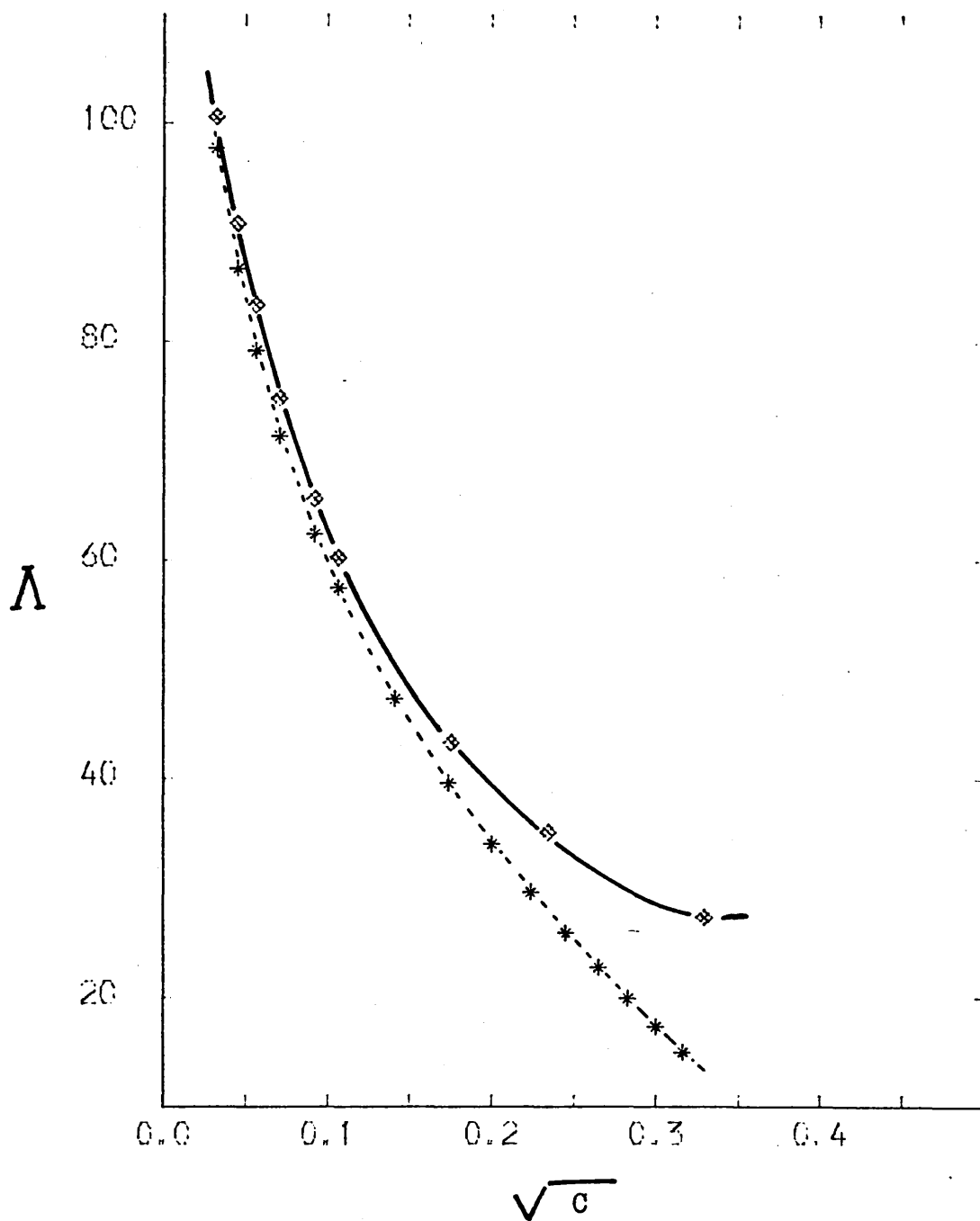


Fig. 3.6 (a)

Equivalent conductance,  $\Lambda$ , for  $\text{CdI}_2$  at  $25^\circ\text{C}$ .

◇, experimental, this work;

\*, predicted, using optimised values of  ${}^0\lambda_i$ .

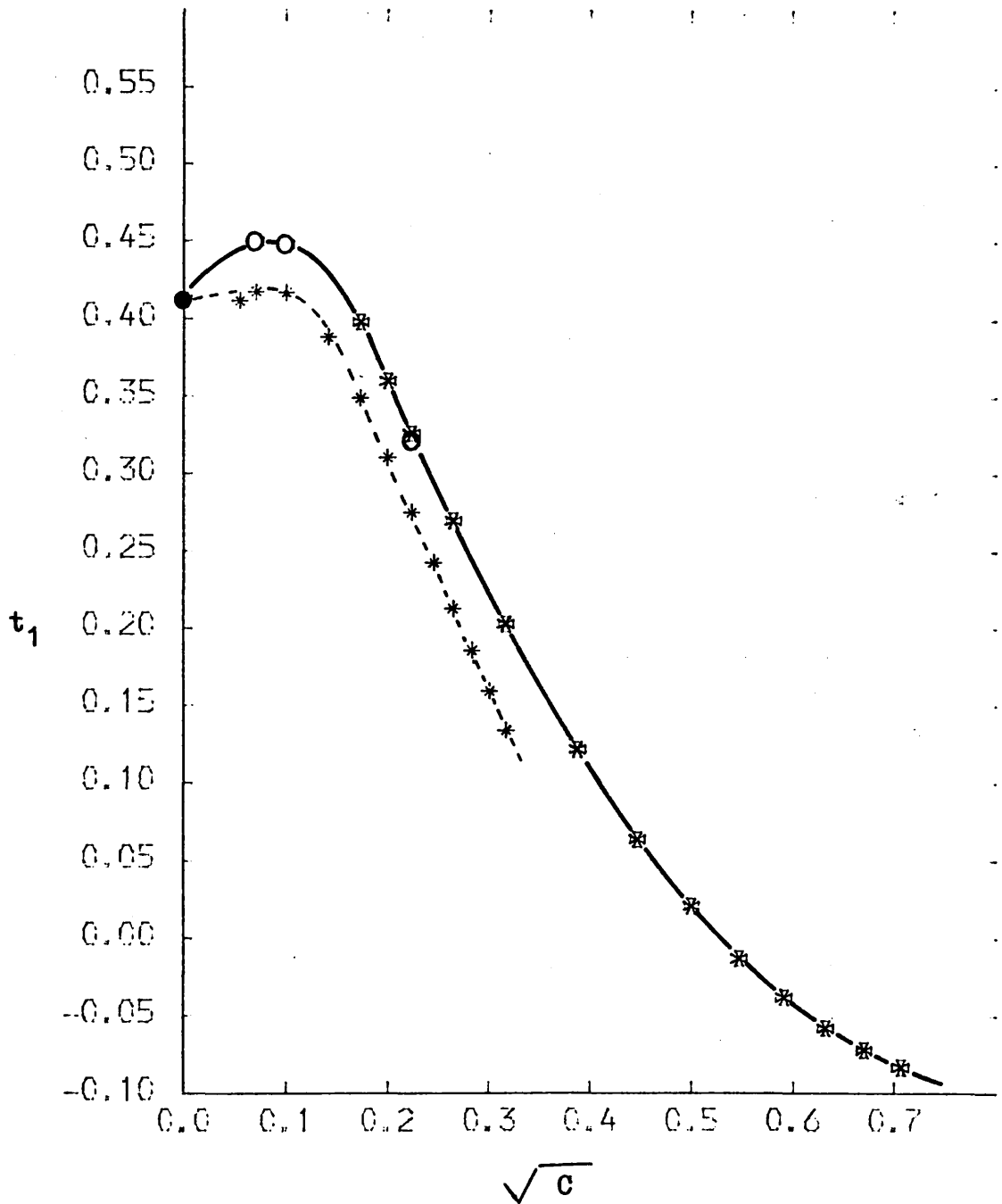


Fig. 3.6 (b)

Cadmium iodide, cationic transport number,  $t_1$ .

\* , from ref.(3); O , from ref. (11);

\* , predicted, using optimised values of  $^0\lambda_i$  ;

● , infinite dilution value.



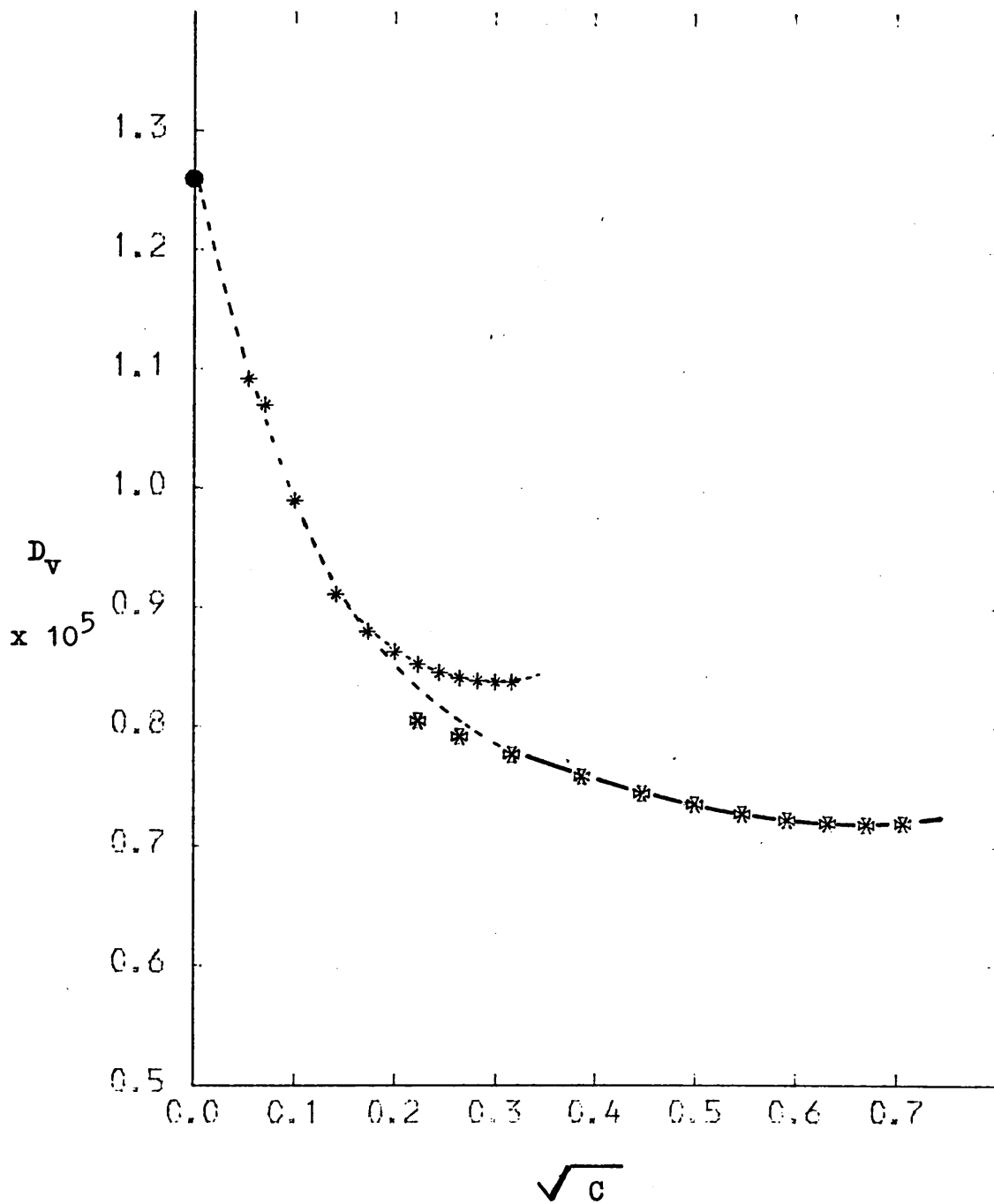


Fig. 3.6 (c)

Salt diffusion coefficient of cadmium iodide.

\* , Paterson et al.<sup>3</sup> ;

\* , predicted, using optimised values of  ${}^0\lambda_i$  ;

● , limiting value.

General Description of the Graphical Representation  
of the Transport Properties of aqueous Cadmium Iodide,  
shown in Figs. 3.7 (a,b,c) to 3.12 (a,b,c)

The sensitivity of transport parameters to deviations from the optimised values of  ${}^0\lambda_i$  is shown in Figs. 3.7 to 3.12, as follows:

Figs. 3.7 and 3.8	variations in	${}^0\lambda_{\text{CdI}^+}$ ,
Figs. 3.9 and 3.10	" "	${}^0\lambda_{\text{CdI}_3^-}$ ,
and Figs. 3.11 and 3.12	" "	${}^0\lambda_{\text{CdI}_4^{2-}}$ .

Positive deviations in  ${}^0\lambda_i$  are represented by  $\Delta$  and negative by  $\nabla$ . (The values of  ${}^0\lambda_i$  chosen are those given in table (3.4).)

For comparison optimised and experimental data, from Figs. 3.5 and 3.6, are also included.

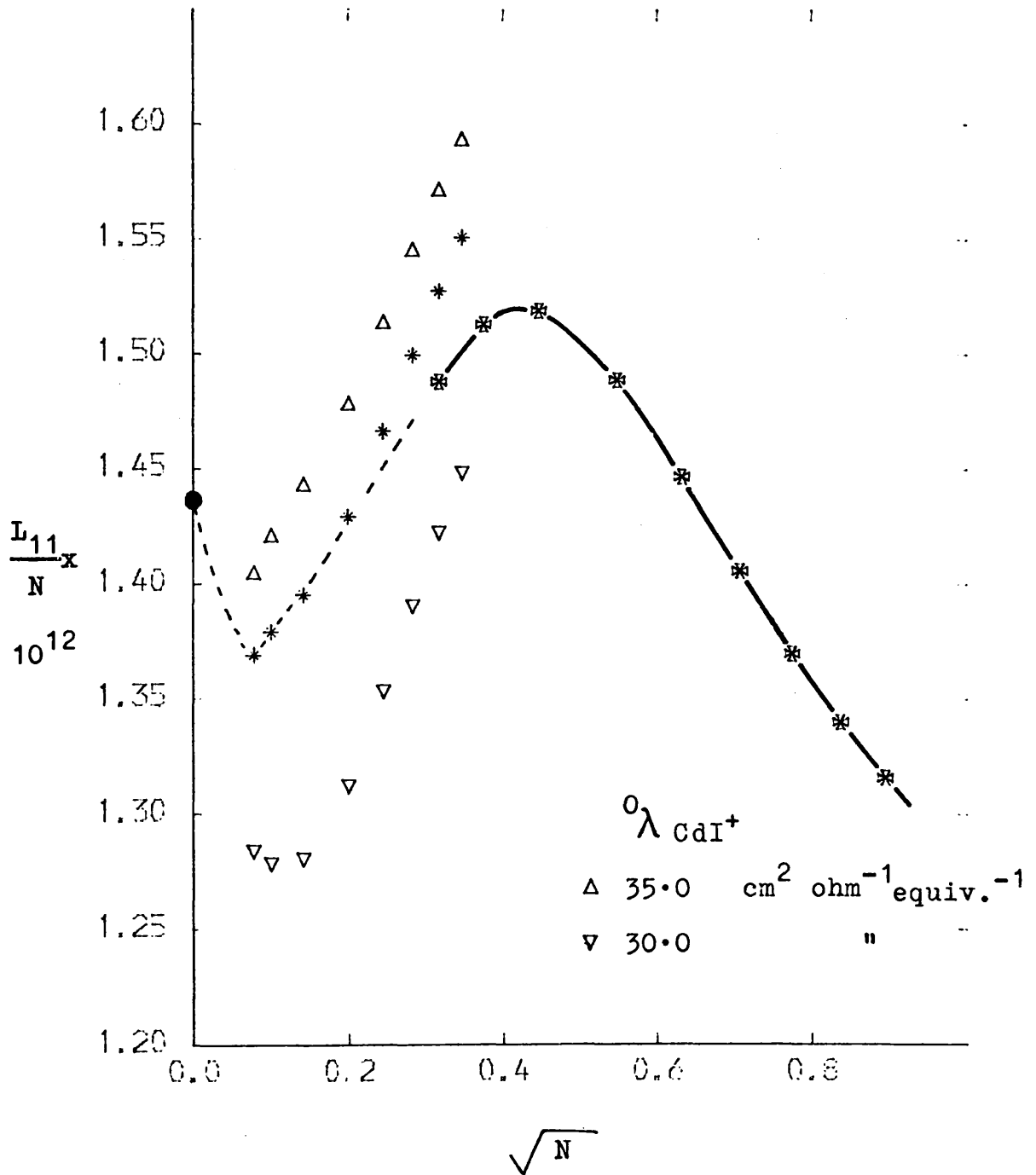


Fig. 3.7 (a)

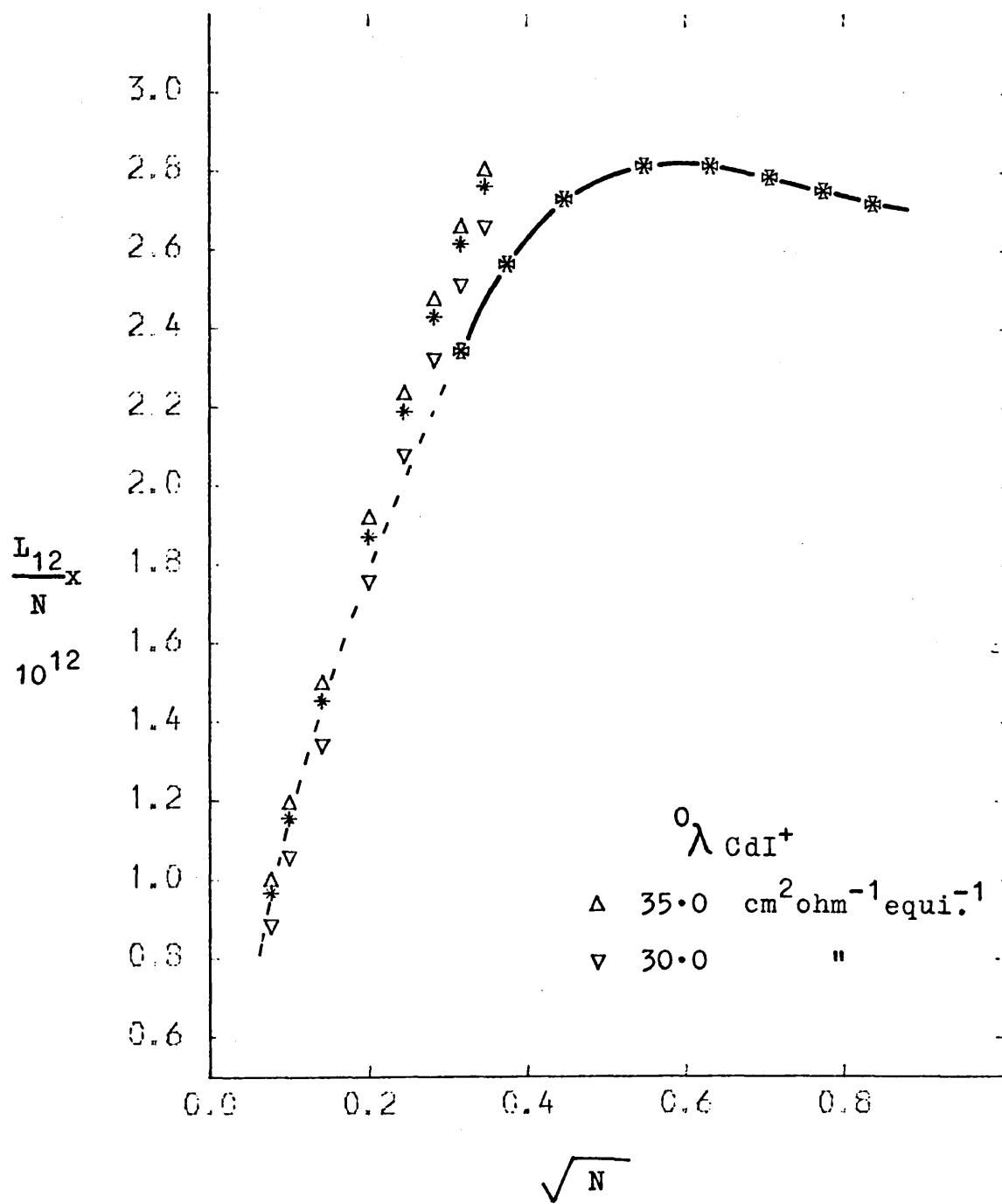


Fig. 3.7 (b)

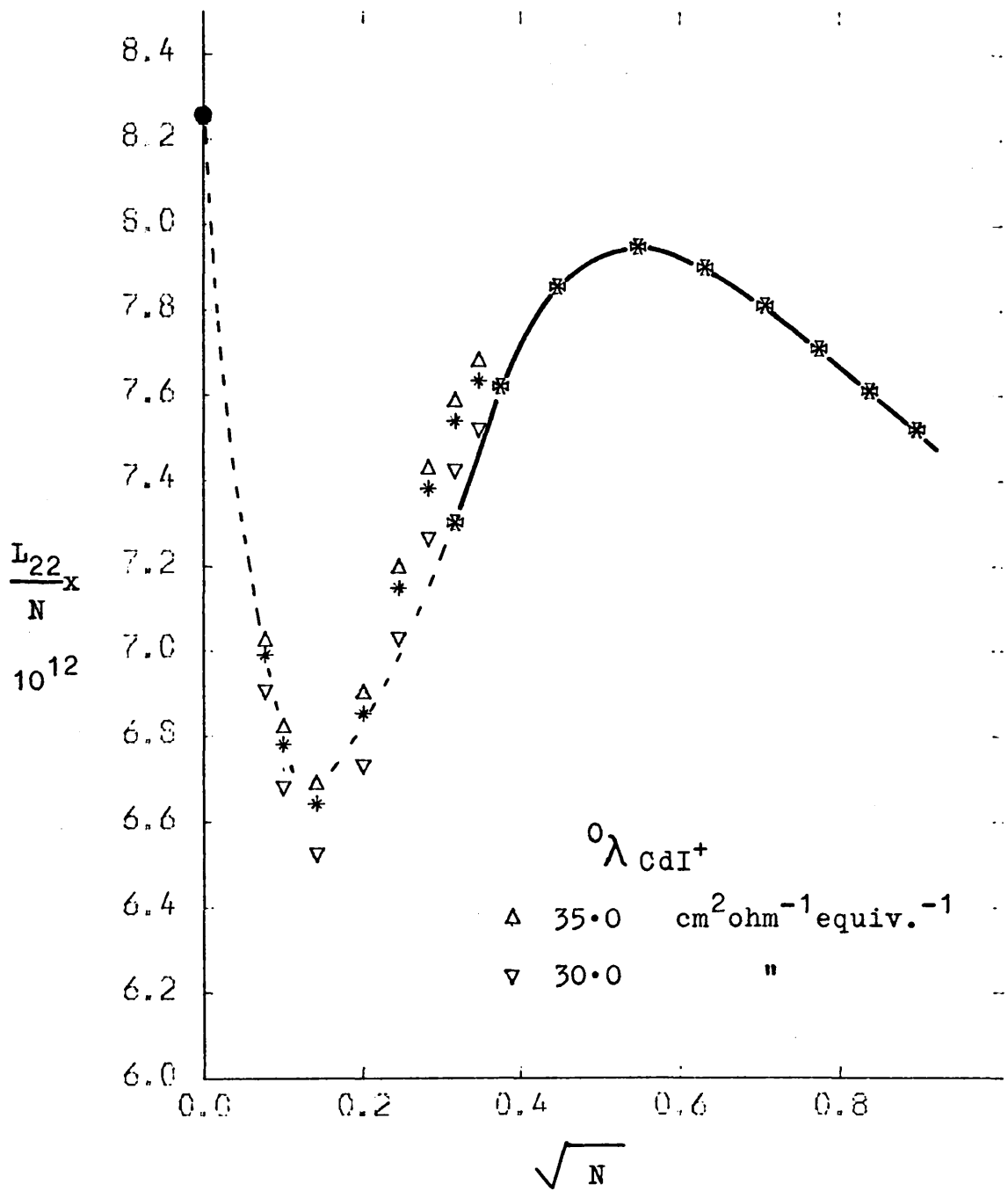


Fig. 3.7 (c)

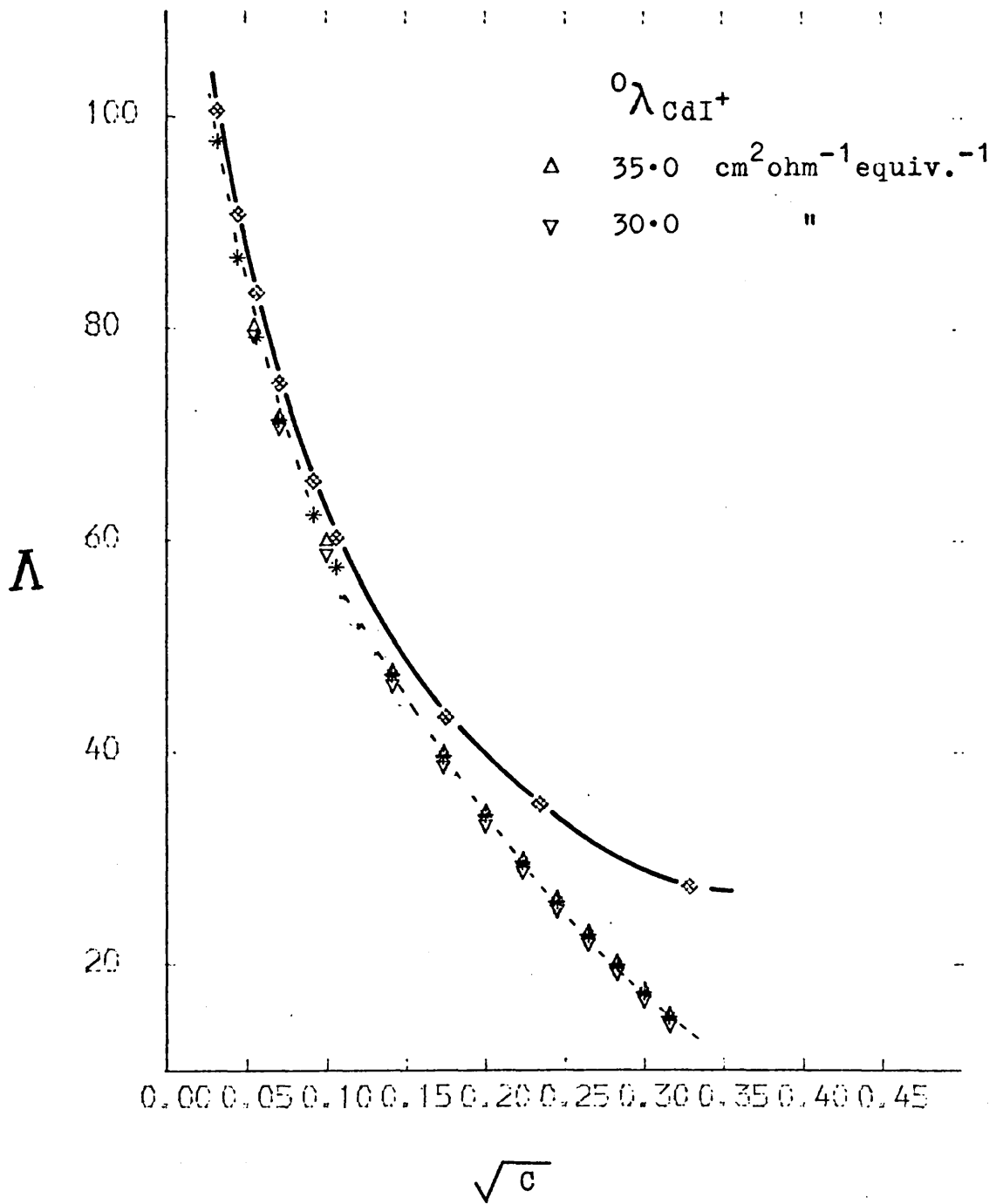


Fig. 3.8 (a)

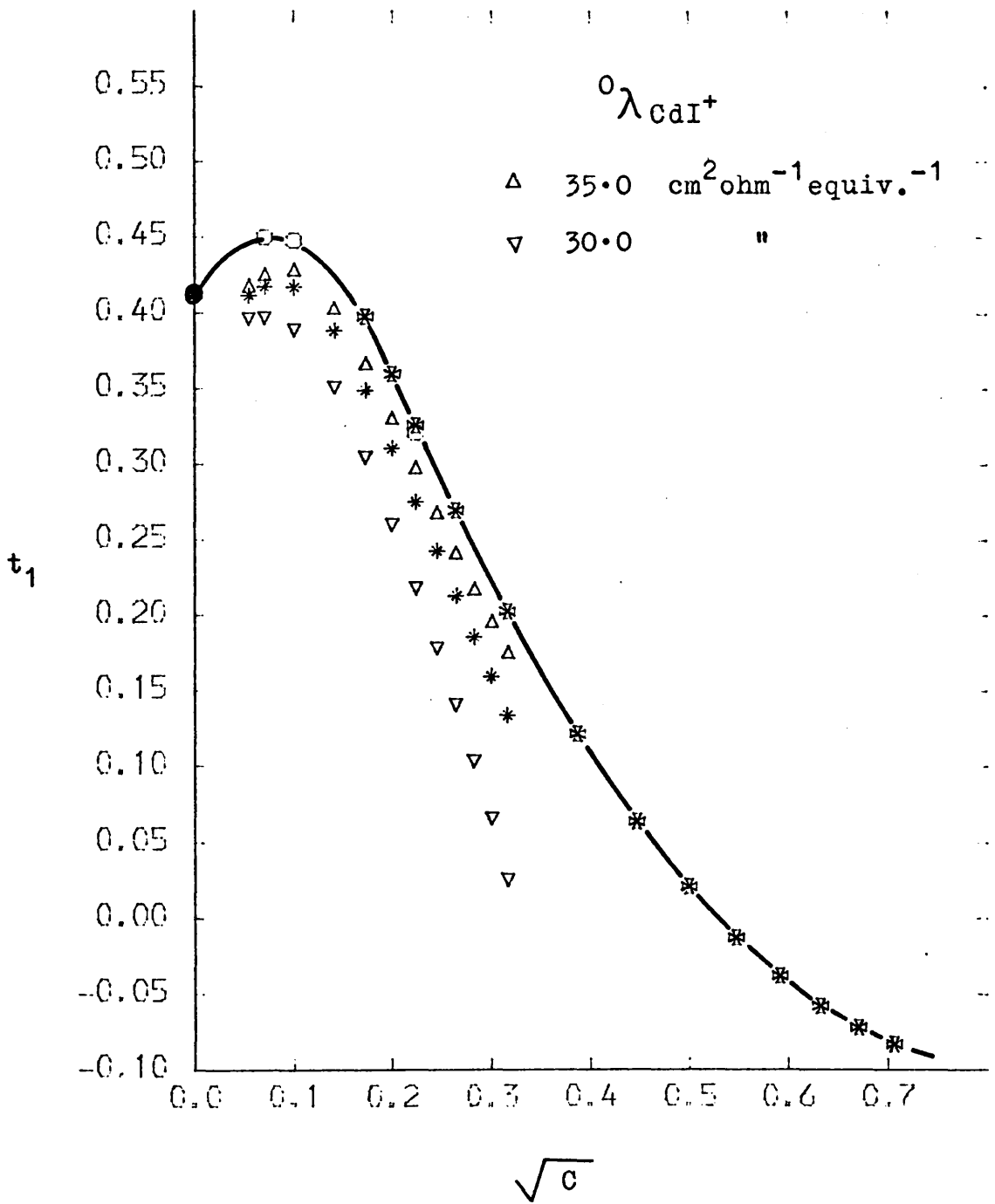


Fig. 3.8 (b)

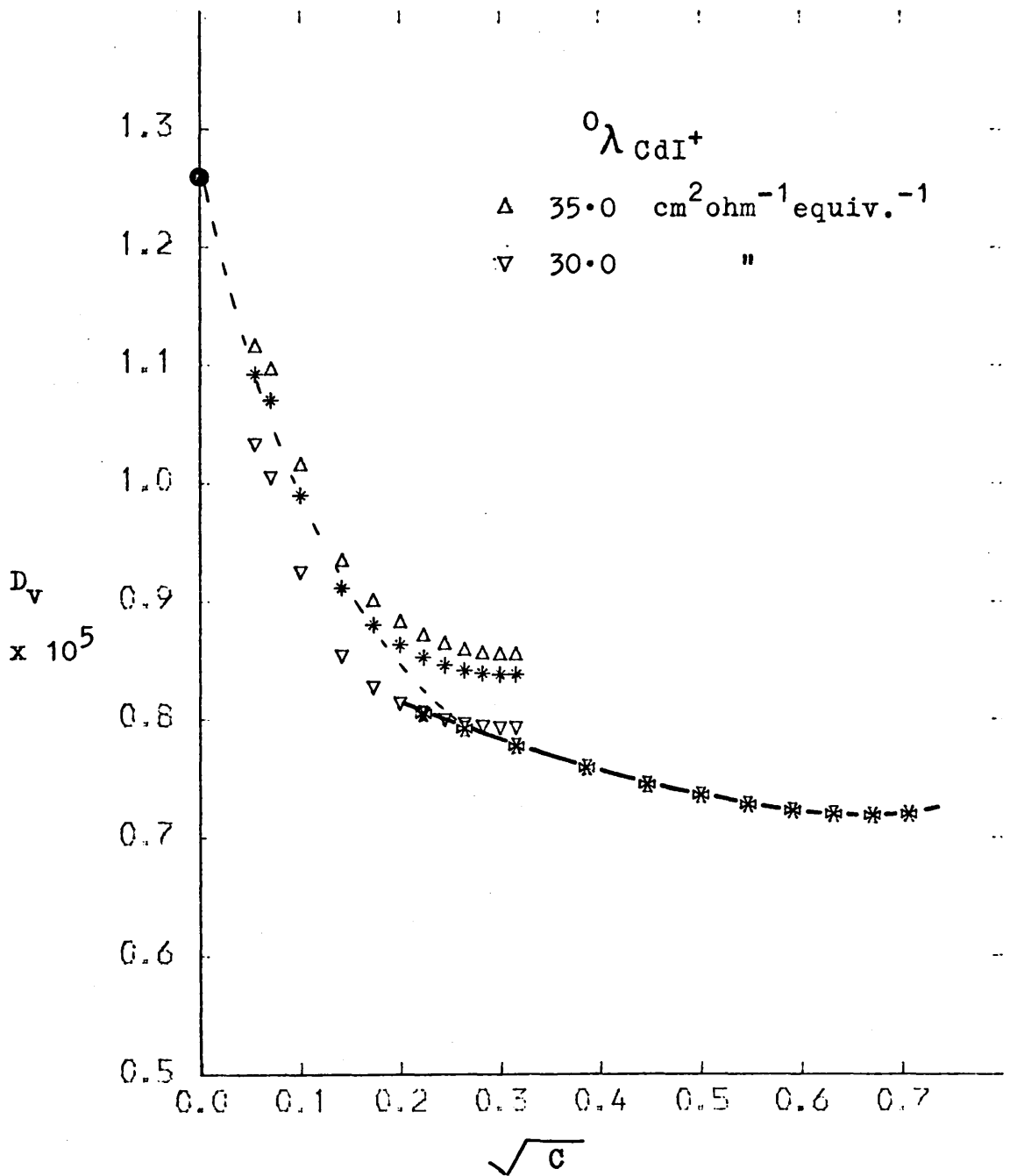


Fig. 3.8 (c)



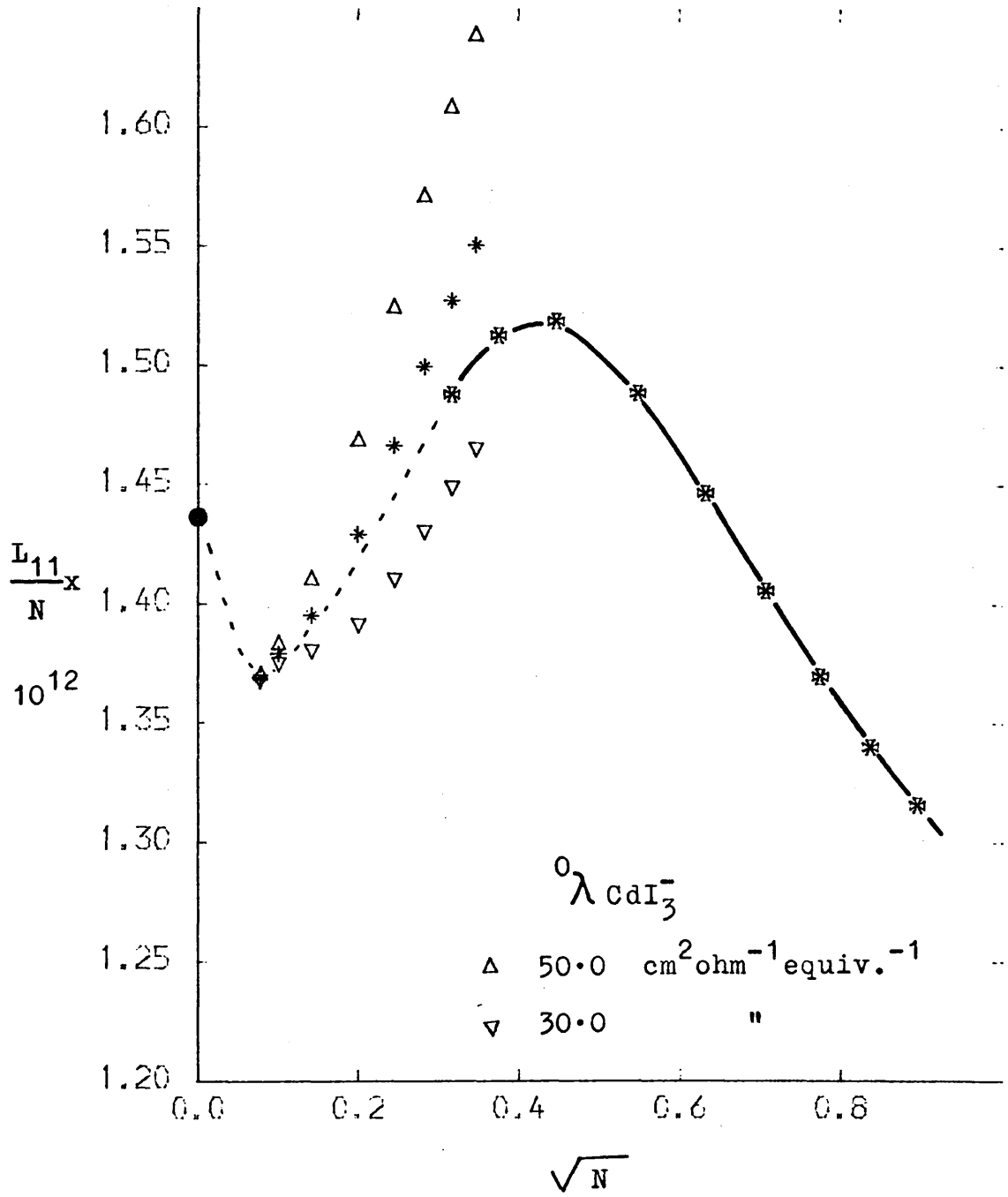


Fig. 3.9. (a)

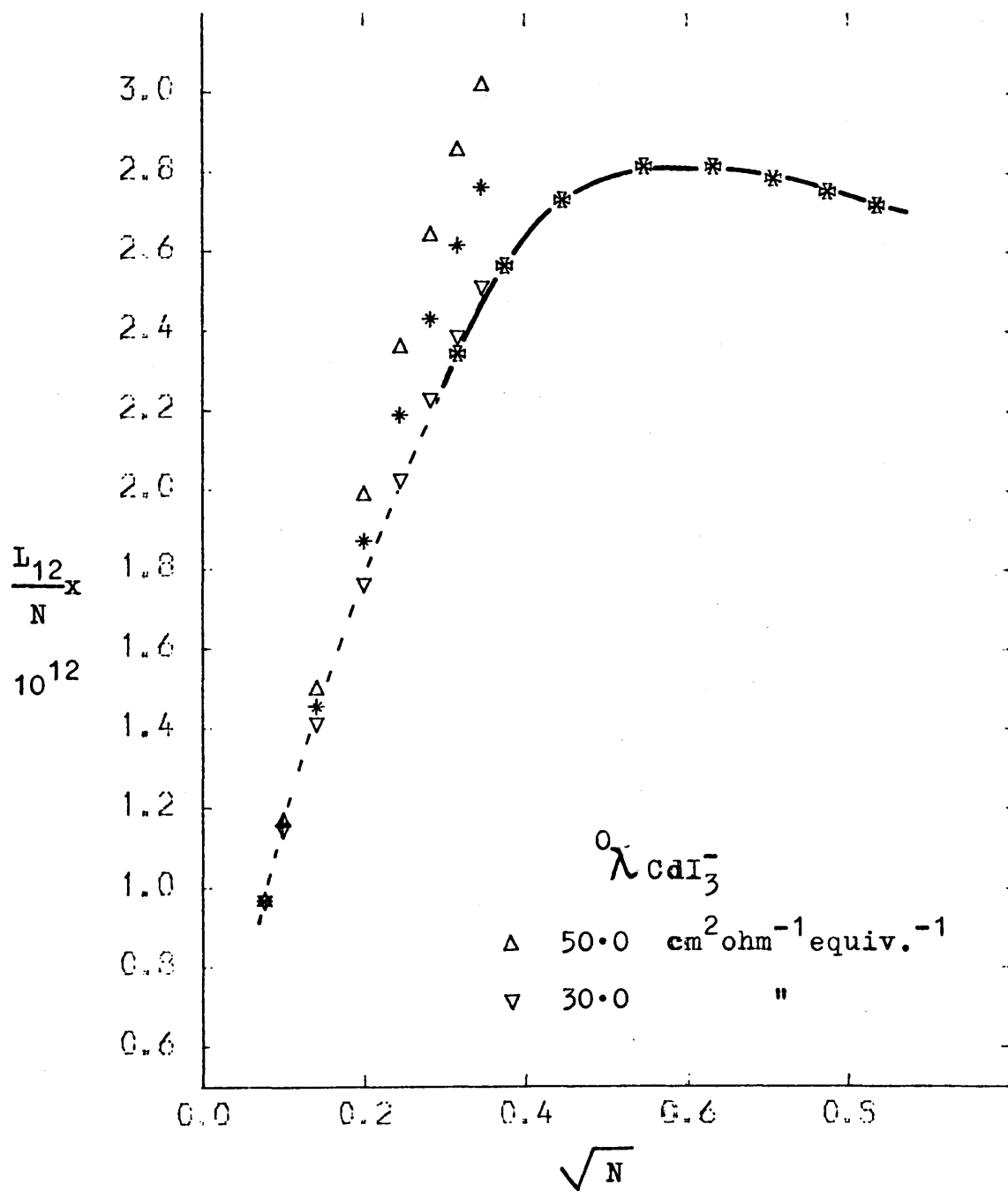


Fig. 3.9 (b)

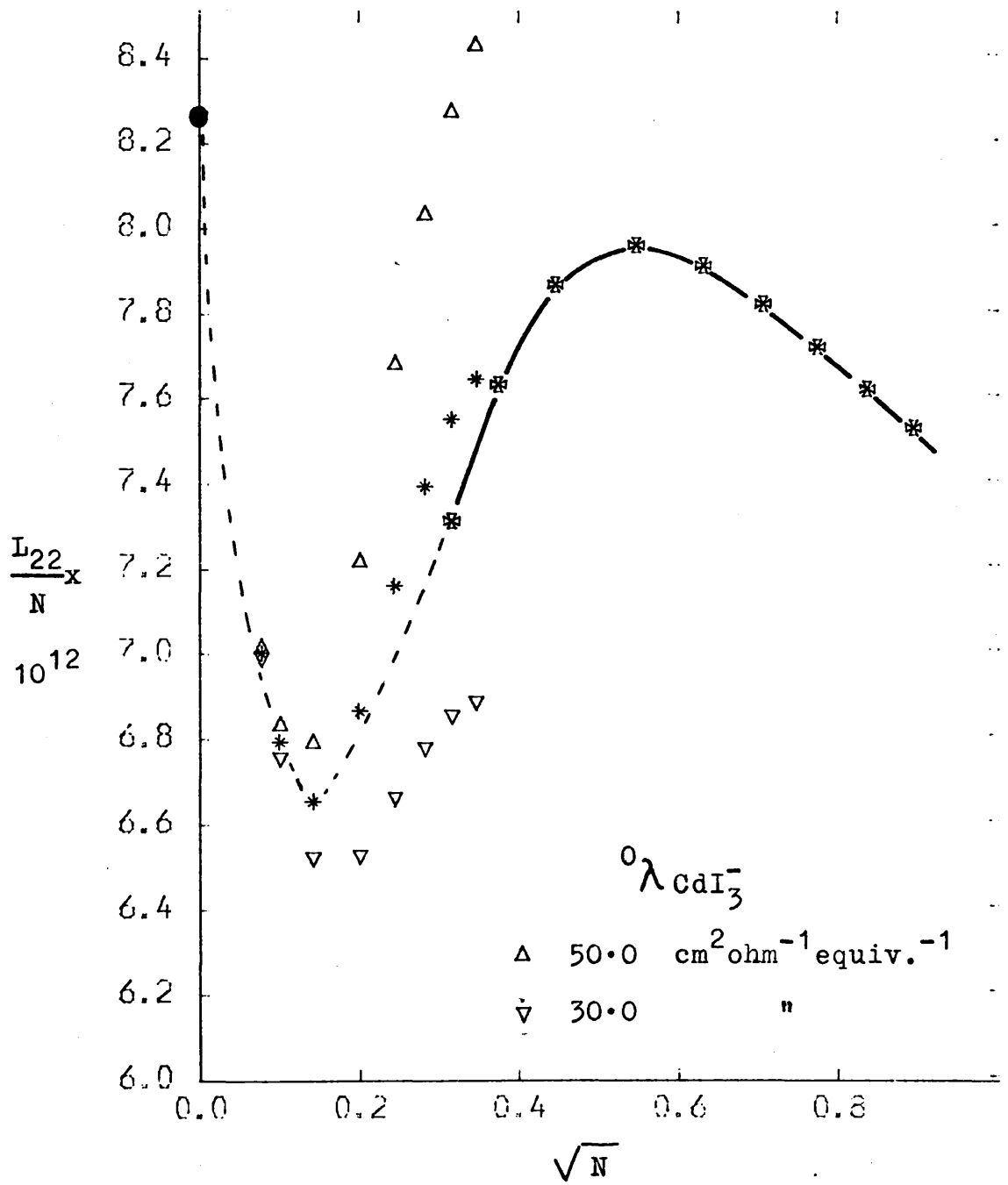


Fig. 3.9 (c)

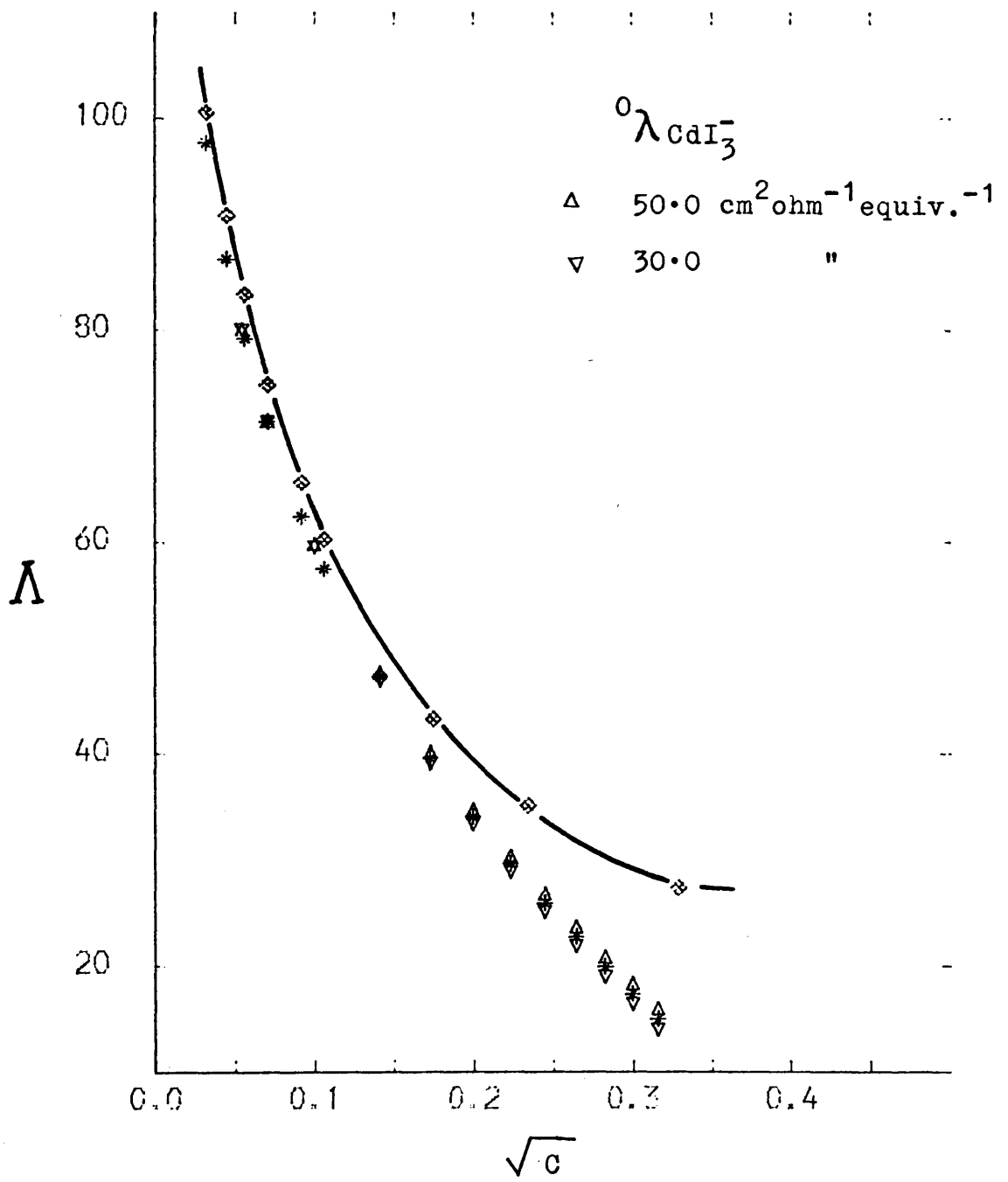


Fig. 3.10 (a)

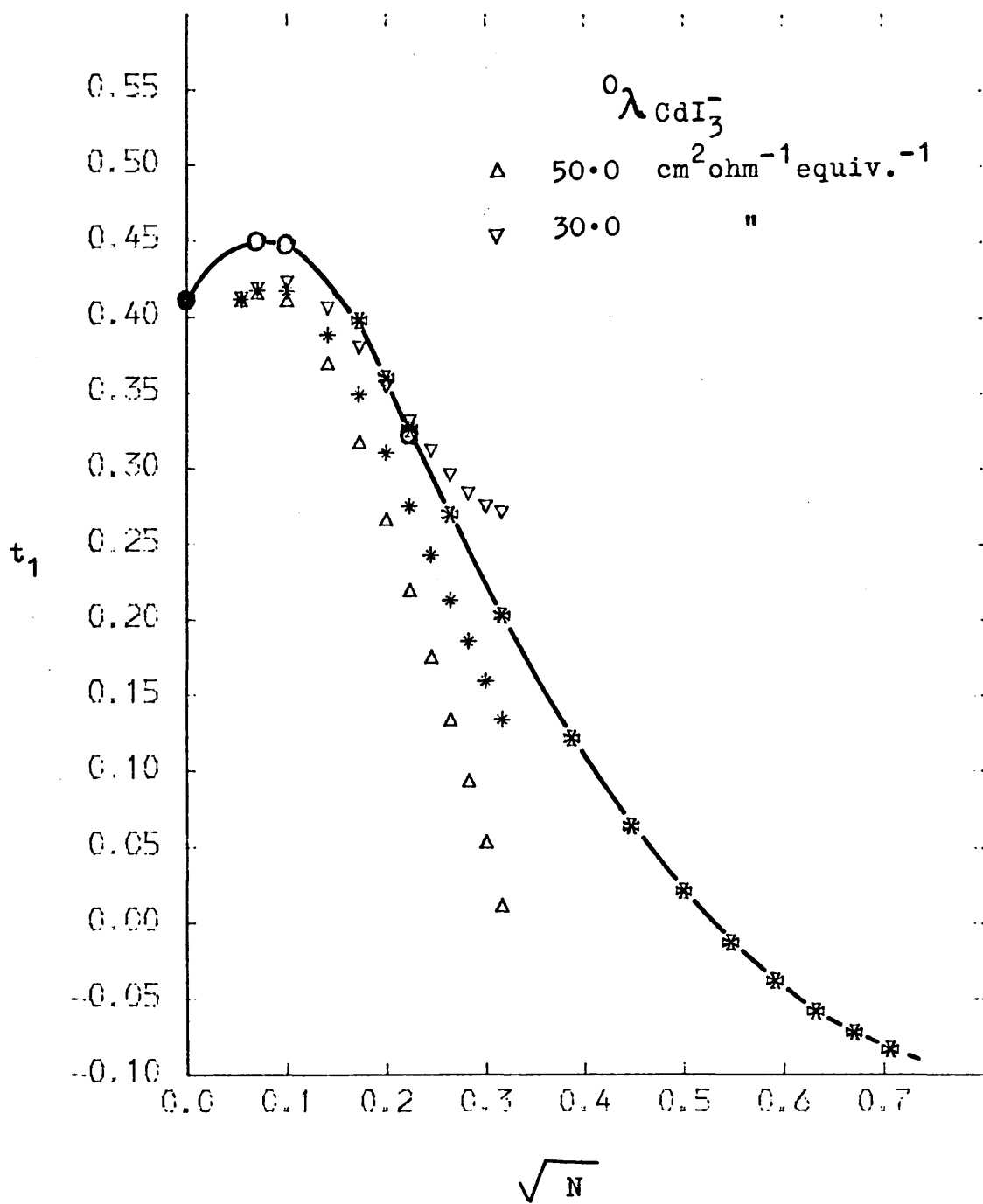


Fig. 3.10 (b)

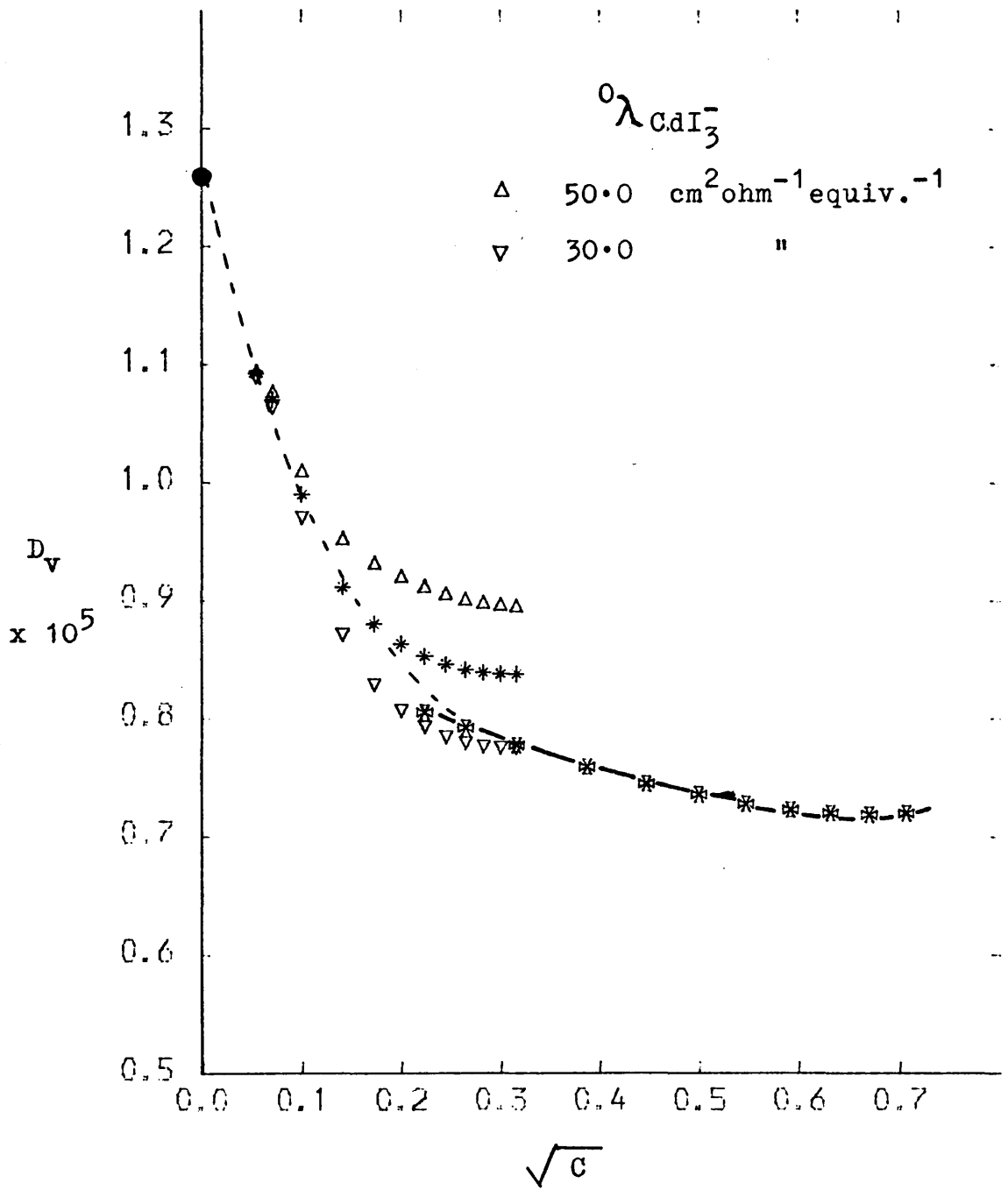


Fig. 3.10 (c)

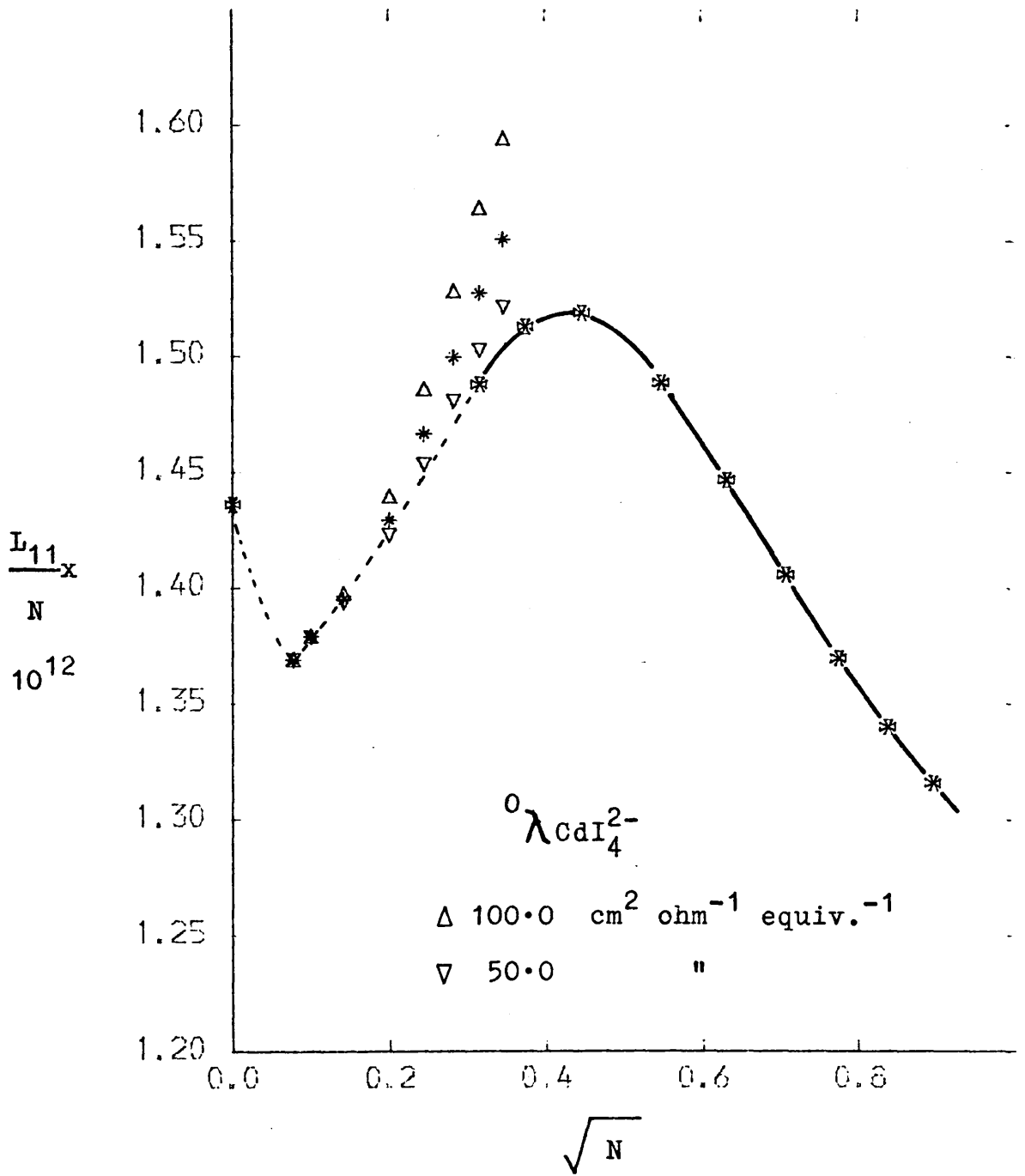


Fig. 3.11 (a)

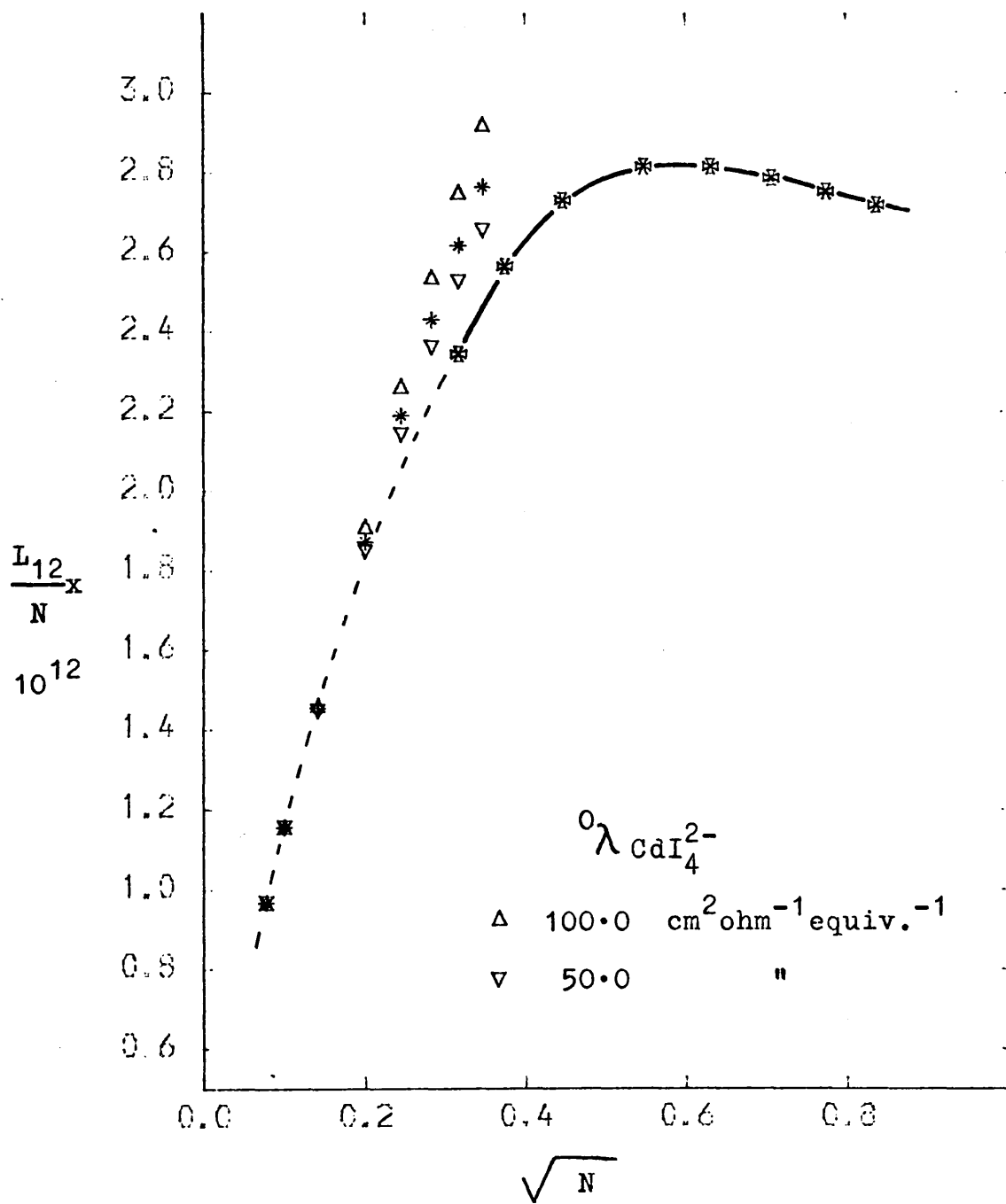


Fig. 3.11(b)



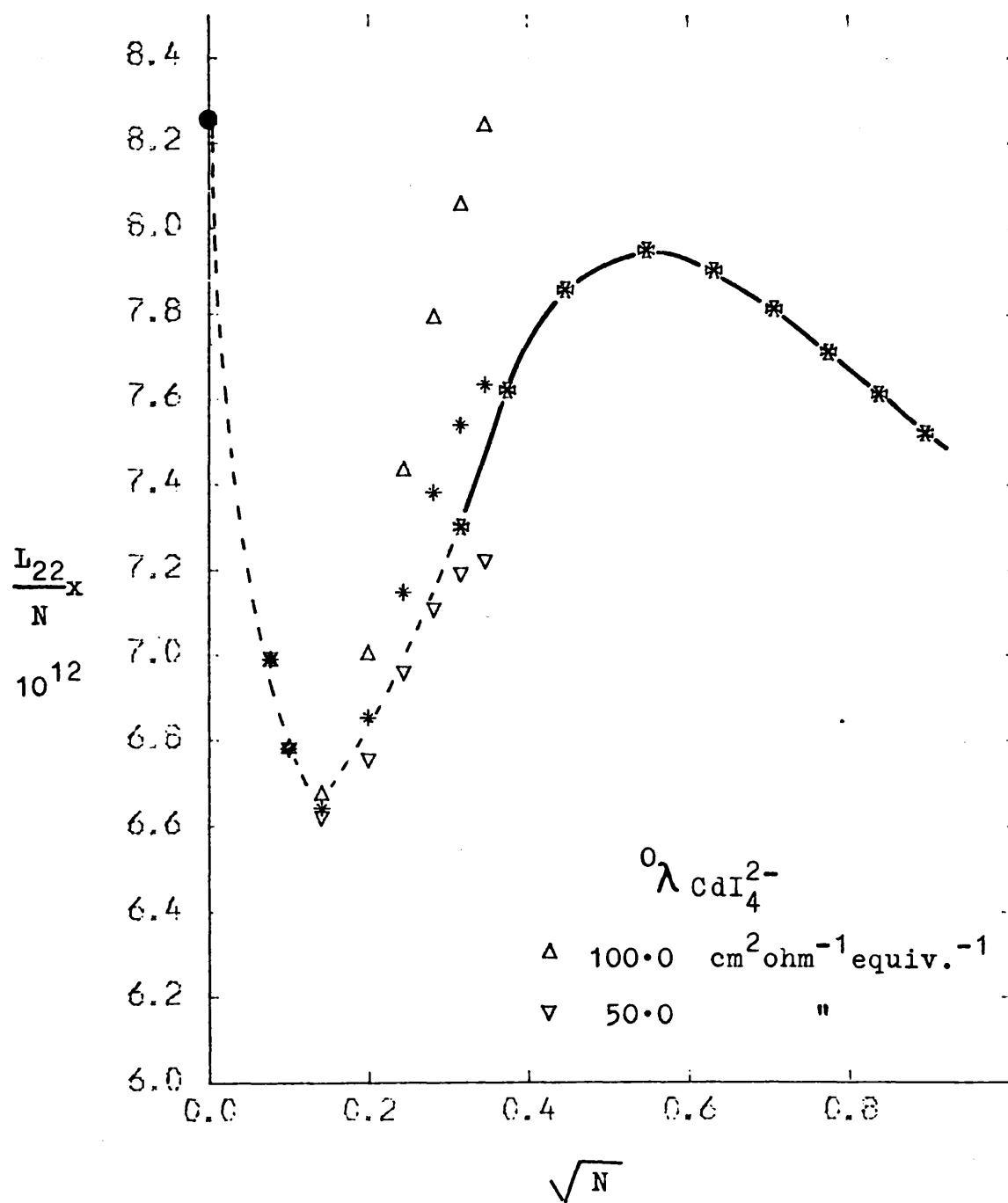


Fig. 3.11 (c)

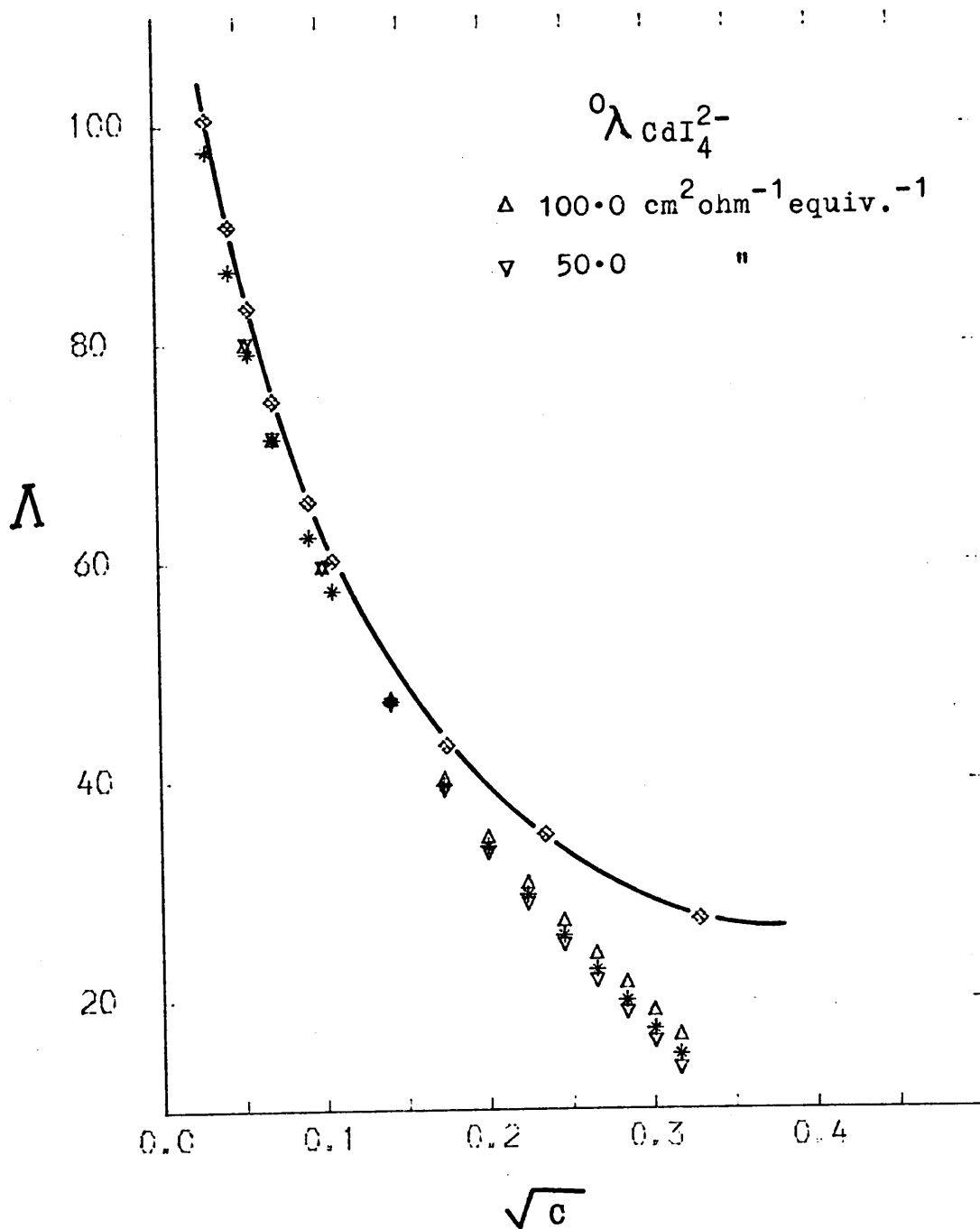


Fig. 3.12 (a)

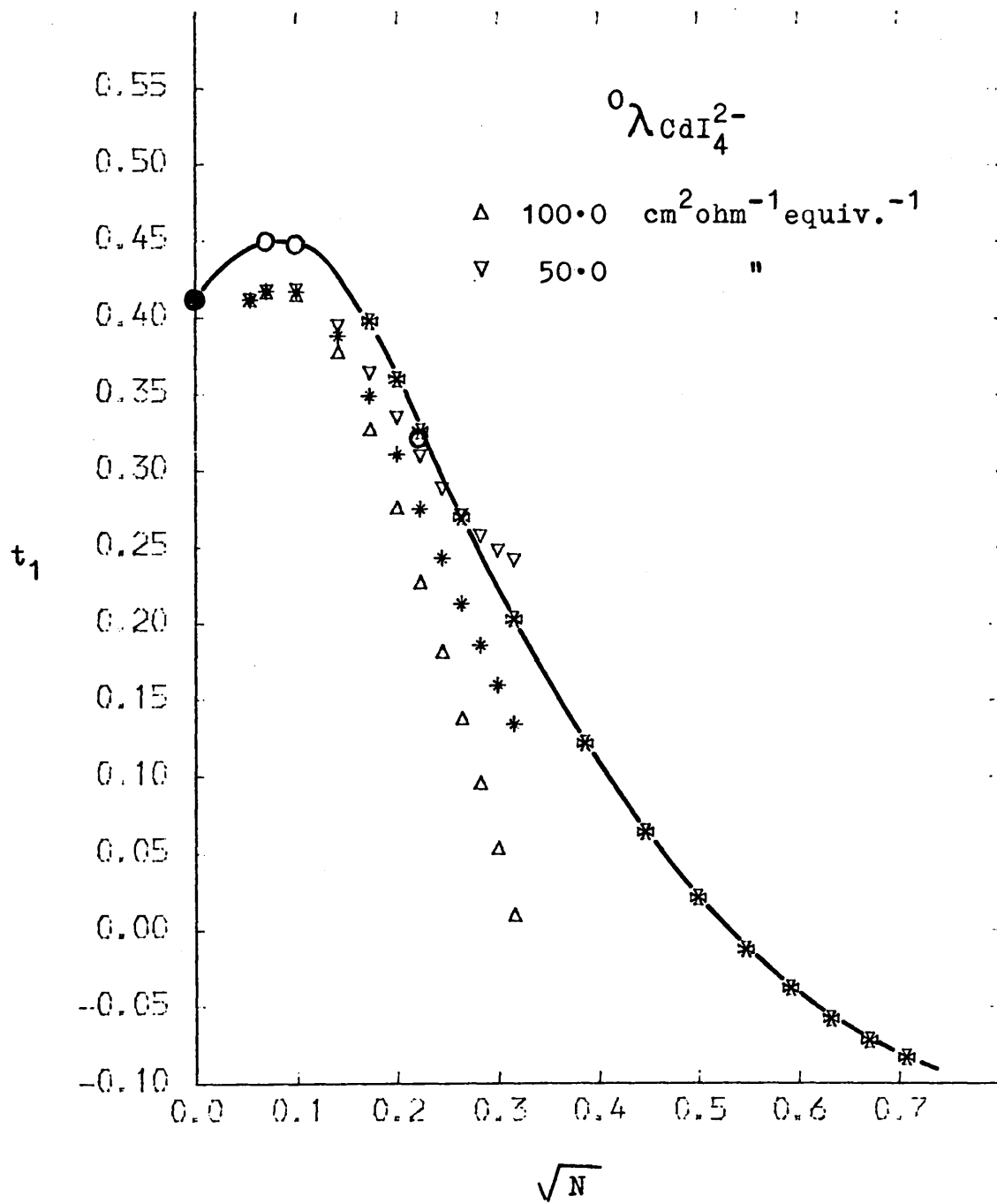


Fig. 3.12 (b)

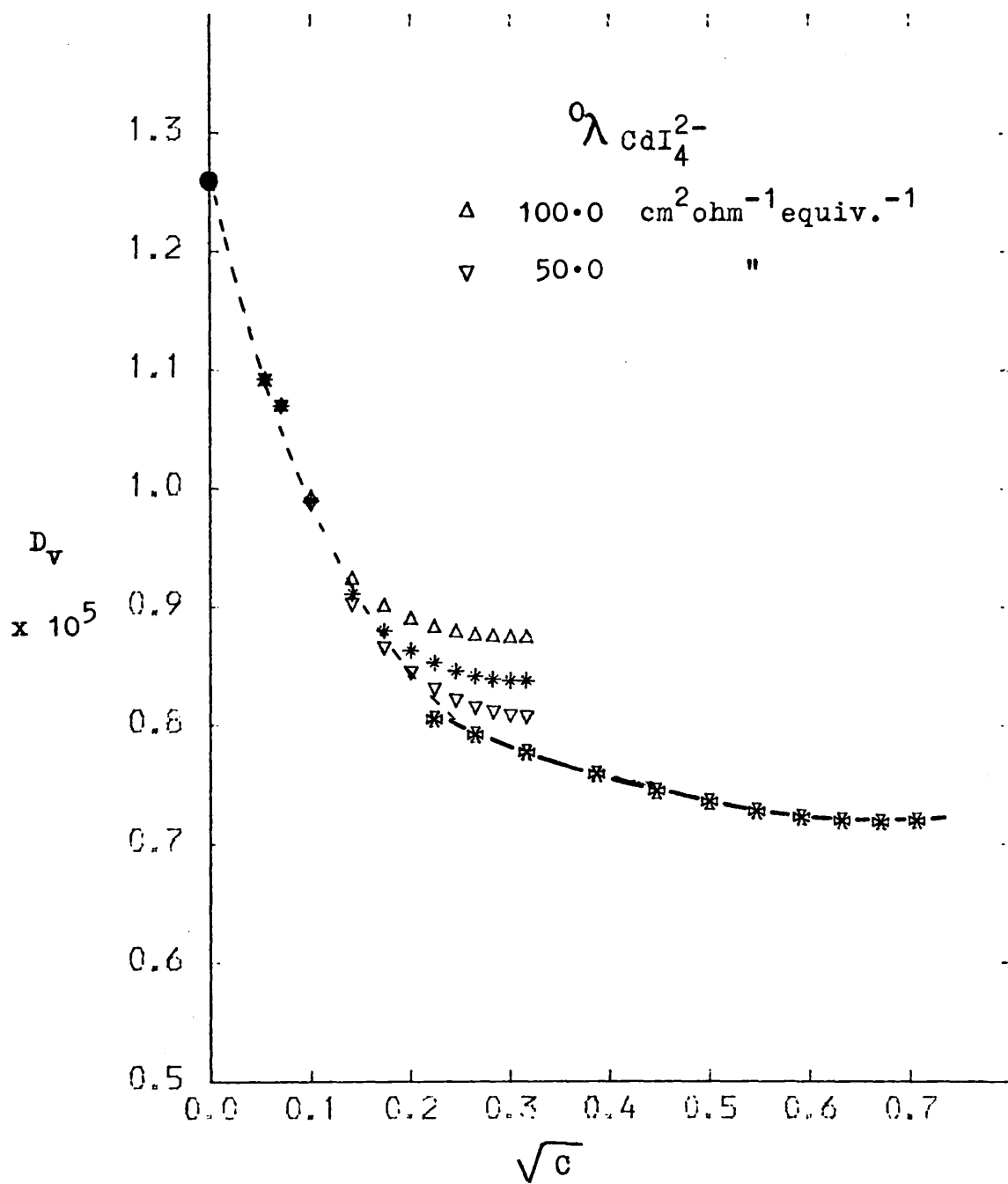


Fig. 3.12 (c)

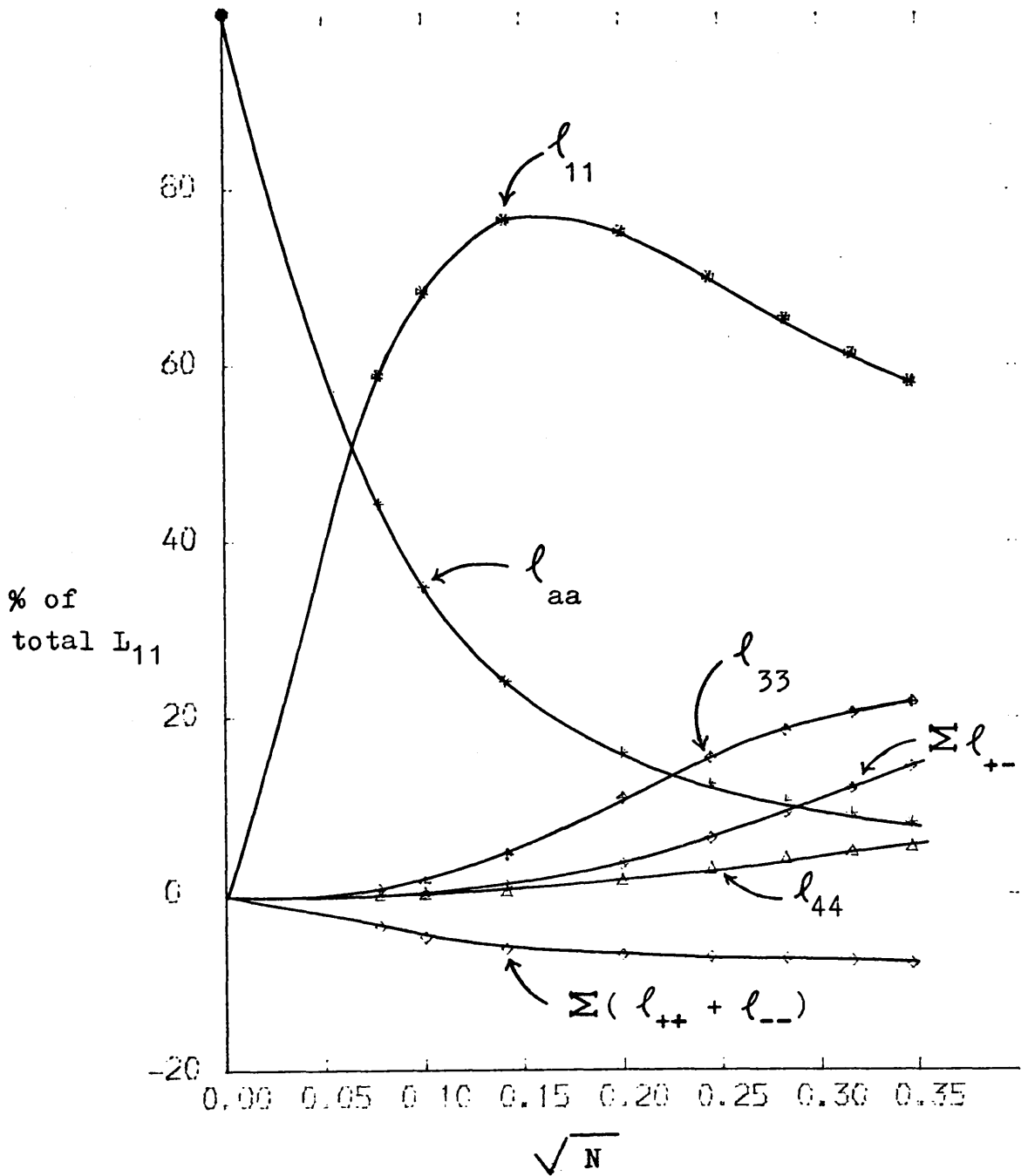


Fig. 3.13 — Percentage contributions of  $l_{ik}$  to  $L_{11}$ , using optimised values of  ${}^0\lambda_i$  (Set 1, table (3.4)).

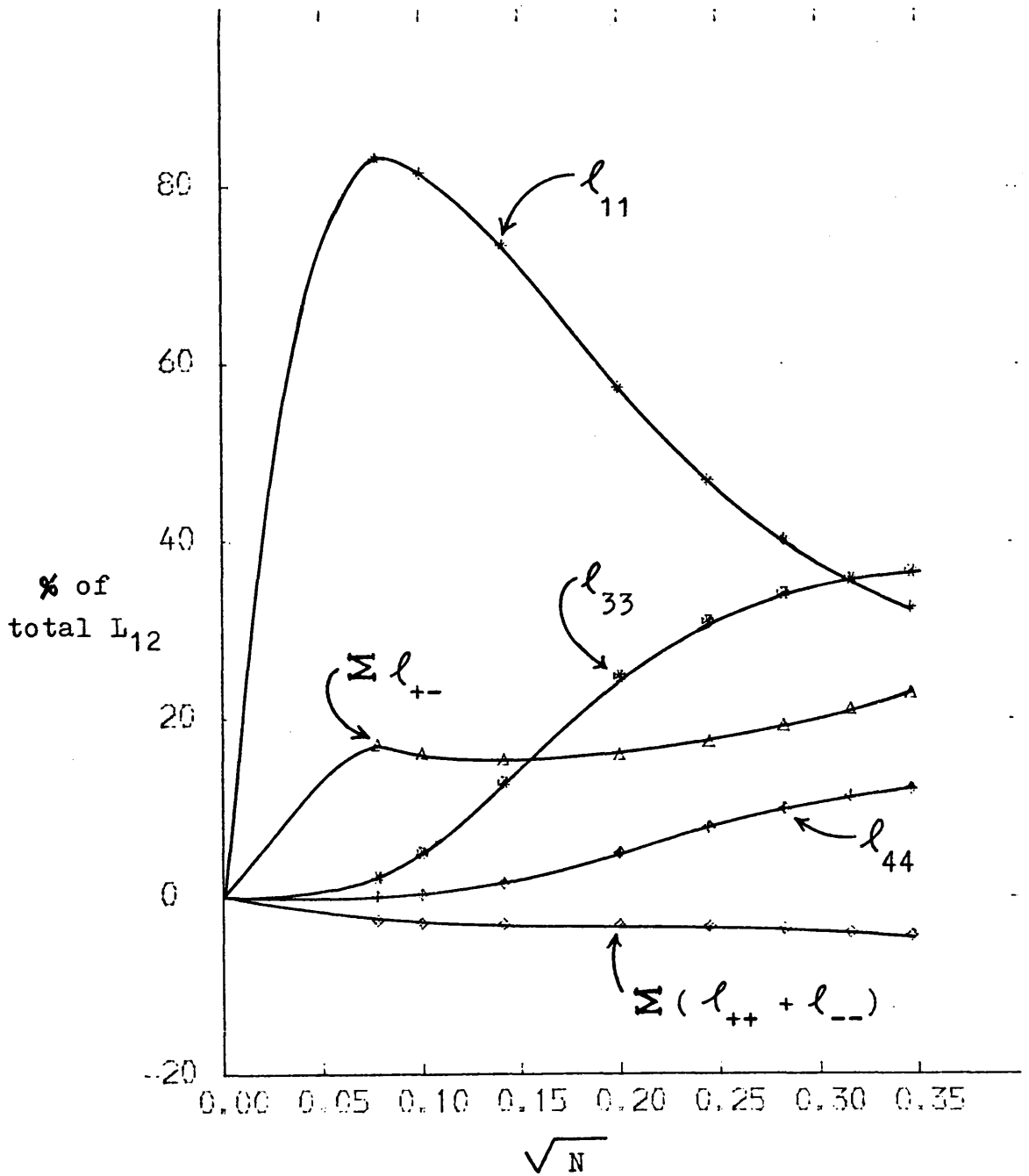


Fig. 3.14 — Percentage contributions of  $l_{ik}$  to  $L_{12}$ , using optimised values of  ${}^0\lambda_i$  (Set 1, table (3.4)).

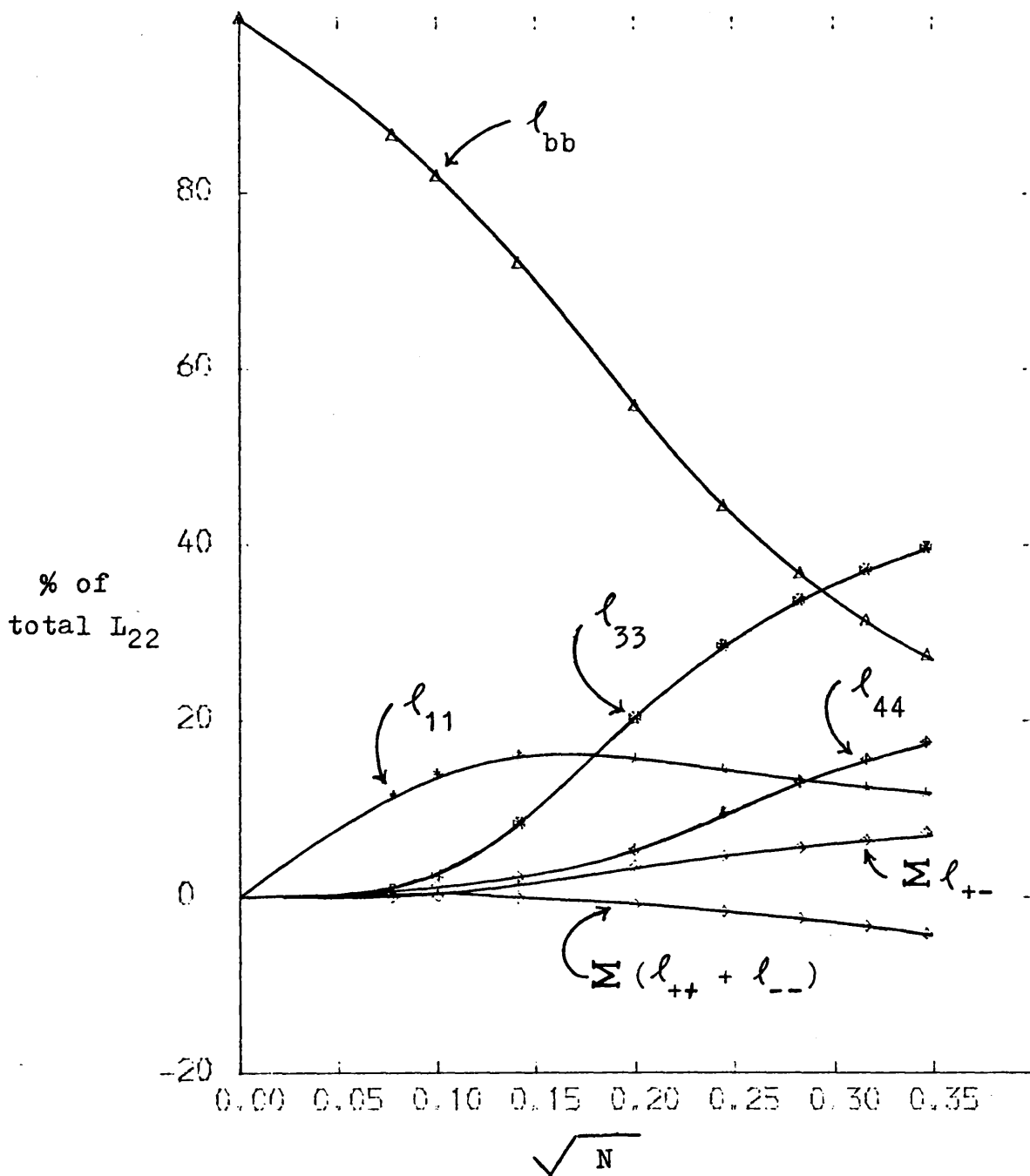


Fig. 3.15 — Percentage contributions of  $l_{ik}$  to  $L_{22}$ , using optimised values of  ${}^0\lambda_i$  (Set 1, table (3.4)).

References for Chapter 3

1. Pikal, M.J., J. Phys. Chem., 1971, 75, 3124.
2. Robinson, R.A. and Stokes, R.H., ' Electrolyte Solutions ', 2nd Edn., Butterworths, London, 1970.
3. Paterson, R., Anderson, J. and Anderson, S., J. Chem. Soc., Farad. Trans. I., in preparation.
4. Paterson, R. and Agnew, A., *ibid.*, in preparation.
5. Miller, D.G., J. Phys. Chem., 1966, 70, 2639.
6. Jones, G. and Bollinger, G.M., J. Amer. Chem. Soc., 1931, 53, 411.
7. Jones, G. and Bradshaw, B.C., *ibid.*, 1933, 55, 1780.
8. Matheson, R.A., J. Phys. Chem., 1962, 66, 439.
9. Reilly, P.J. and Stokes, R.H., Austral. J. Chem., 1970, 23, 1397.
10. McBain, J.W., van Rysselberghe, P.J. and Squance, W.A., J. Phys. Chem., 1931, 35, 999.
11. Sahay, J.N., J. Sci. Ind. Research (India), 1959, 18B, 235.
12. Onsager, L., Ann. N.Y. Acad. Sci., 1945, 46, 247.



C H A P T E R 4

Isotopic-Diffusion of Cadmium in  
Aqueous Solutions of Cadmium Iodide.

## Introduction

The mathematical treatment given in Chapter 3 has been extended to include predictions of isotopic-diffusion coefficients.

Experimental measurements of isotopic-diffusion coefficients for  $^{115}\text{Cd}^{2+}$  in aqueous cadmium iodide have been made in the concentration range  $0.1 - 0.6 \text{ mol.l}^{-1}$ , by the diaphragm-cell method.

A new type of diaphragm-cell and magnetic stirring unit, capable of accommodating four diffusion cells, has been designed and constructed. Its use and advantages over the previous systems are discussed.

Isotopic-diffusion coefficients obtained from experiments are compared with those predicted from the theory and reasons for discrepancies suggested.

#### 4.1 Influence of Self-Complexing on Isotopic Diffusion of Cadmium in aqueous Cadmium Iodide

In earlier discussions upon isotopic diffusion in electrolyte solutions, Anderson and Paterson<sup>1</sup> have shown that the diffusion coefficient  $D_{aa}$  of the ion  $a$  can be represented by equation (4.1),

$$D_{aa} = RT \left( L_{aa}^T / C_a^T - C_a^T L_{aa}^* / C_{a^0} C_{a^*} \right) \quad 4.1$$

The first term, within the brackets, is the direct mobility of the ion in the binary solution ( $L_{aa}^T$ ) divided by the total concentration of the ion  $C_a^T$ . The second term represents the contribution from coupling between labelled species  $a^*$  and the unlabelled remainder  $a^0$ ; concentrations  $C_{a^*}$  and  $C_{a^0}$  respectively. The isotope-isotope coupling coefficient function,  $C_a^T L_{aa}^* / C_{a^0} C_{a^*}$ , was obtained from experimental measurement of the diffusion coefficient, and a prior knowledge of the direct mobility coefficient  $L_{aa}^T$  of the unlabelled solution. For the alkali metal chlorides these isotope-isotope terms were shown to be of negative sign and so contribute positively to  $D_{aa}$ . They had the general characteristics of interionic coupling coefficients and their magnitude could be evaluated from the classical theories of Fuoss and Onsager.

Isotopic diffusion coefficients for cadmium in cadmium iodide solutions have been measured in this study. /

study. They show most unusual variations with increasing concentration of cadmium iodide. Undoubtedly this anomalous behaviour may be ascribed to the extensive self-complexing which occurs in these solutions, Chapter 3. The present theory was developed to obtain an explicit expression for  $D_{aa}$ , the diffusion coefficient of cadmium, in which complex-to-complex species interactions were identified and subsequently evaluated (or at least approximated) by numerical expressions.

Before developing an expression for isotopic diffusion in terms of the complex species present it is necessary to define the nomenclature and symbols.

The complexes  $(CdI_x)^{2-x}$  are identified by the value of  $x$ , thus  $CdI_4^{2-}$  will be species 4. The free aqueous ions  $Cd^{2+}$  and  $I^-$  will be denoted by  $a$  and  $b$  respectively. In any solution of cadmium iodide the total concentration of cadmium,  $C_a^T$ , and iodide,  $C_b^T$  will be given by equations (4.2) and (4.3):

$$C_a^T = C_a + C_1 + C_2 + C_3 + C_4 \quad 4.2$$

and

$$C_b^T = C_1 + 2C_2 + 3C_3 + 4C_4 + C_b \quad 4.3$$

(From the stoichiometry of the salt  $C_b^T = 2C_a^T$ .)

When a proportion of the normal unlabelled cadmium is removed from solution and replaced by an equal amount /

amount of isotopically labelled cadmium, the total concentrations of all species will remain unaltered, but each will now contain both labelled and unlabelled components. For any species  $i$  ( $i = a, 1, 2, 3, 4$ ), the total concentration,  $C_i$ , will be the sum of concentrations  $c_i^0$  and  $c_i^*$ ; those of unlabelled and labelled respectively, equation (4.4).

$$C_i = c_i^0 + c_i^* \quad i = a, 1, 2, 3, 4, \quad 4.4$$

The specific activity of the labelled and unlabelled cadmium in each solution species are defined by  $\rho_i^*$  and  $\rho_i^0$  respectively, equation (4.5).

$$\rho_i^* = c_i^* / C_i \quad \text{and} \quad \rho_i^0 = c_i^0 / C_i \quad 4.5$$

$$i = a, 1, 2, 3, 4$$

(From equation (4.4)  $\rho_i^* + \rho_i^0 = 1$  .)

A fundamental assumption will now be made. It will be assumed that the labelled isotope is chemically identical to the normal bulk isotopic mixture of cadmium in the unlabelled solution. In consequence there can be no isotopic enrichment of labelled species in any one of the complexes. This is a widely held assumption in diffusion studies and essentially equates isotopic diffusion as being equivalent to self-diffusion. In the present context it requires that the specific activities,  $\rho_i^*$ , for all species involving cadmium are equal /

equal and so the subscript i will be dropped in all further discussion. Similarly  $\rho_i^0$  becomes  $\rho^0$ .

The total concentration of labelled cadmium,  $C_a^*$  is therefore related to total cadmium,  $C_a^T$  by equation (4.6).

$$C_a^* = \sum_{i=a}^4 c_i^* = \rho^* C_a^T \quad 4.6$$

The total contribution of unlabelled cadmium,  $C_a^0$ , is given by an expression analogous to equation (4.6).

A similar scheme for defining fluxes is required.  $J_a^T$ ,  $J_b^T$  are the sums of the molar fluxes of all cadmium and all iodide species in solution respectively, equations (4.7) and (4.8).

$$J_a^T = J_a + J_1 + J_2 + J_3 + J_4 \quad 4.7$$

and

$$J_b^T = J_b + J_1 + 2J_2 + 3J_3 + 4J_4 \quad 4.8$$

When a proportion of the cadmium is labelled the total flux of any species will remain unaltered (by the assumption of the chemical identity of isotopes) but will now be the sum of labelled  $j_i^*$  and unlabelled,  $j_i^0$  fluxes, equation (4.9).

$$J_i = j_i^0 + j_i^* \quad 4.9$$

The total flux of labelled cadmium species,  $J_a^*$ , is the only /

only flux to be measured experimentally thus:

$$J_a^* = \sum_{i=a}^4 J_i^* \quad 4.10$$

and in any experiment

$$J_a^T = J_a^* + J_a^0 \quad 4.11$$

where  $J_a^0$  is the net flux of the unlabelled component.

It is now necessary to define forces. For a species  $i$ , the thermodynamic driving force which causes a directed flow is  $(-\text{grad } \tilde{\mu}_i)$ ; the negative gradient of the electro-chemical potential of that species at any point in the non-equilibrium system and will be represented as  $X_i$ , equation (4.12).

$$\begin{aligned} X_i &= -\text{grad } \tilde{\mu}_i \\ &= -RT \, d\ln C_i / dx - RT \, d\ln y_i / dx + Z_i F(-d\psi / dx) \end{aligned} \quad 4.12$$

where  $Z_i$  is the valency, including sign of the species  $i$ , and  $y_i$  the molar activity coefficient. When the species is neutral, the valency is zero and the force is simply the negative gradient of chemical potential.

When labelled and unlabelled species  $i$  are introduced with forces  $x_i^0$  and  $x_i^*$ , respectively then<sup>2</sup>:

$$x_i^* = -\text{grad } \tilde{\mu}_i^* = -RT \, d\ln C_i^* / dx - RT \, d\ln y_i^* / dx + Z_i F(-d\psi / dx) \quad 4.13$$

For /

For unlabelled species the expression for  $x_i^0$  is formally identical, except that the concentration and activity coefficient  $c_i^0$  and  $y_i^0$  replace those of the labelled species in equation (4.13). Since the labelled and unlabelled species may be assumed to have activity coefficients <sup>those of</sup> which are equal to one another and to the total species in any local volume element and since  $dC_i = dc_i^0 + dc_i^*$ , from equation (4.4), then from equations (4.12) and (4.13),

$$C_i X_i = c_i^0 x_i^0 + c_i^* x_i^* .$$

or

$$X_i = \rho^0 x_i^0 + \rho^* x_i^* \quad 4.14$$

Under the special conditions of isotopic diffusion, in which no bulk gradients of chemical potential exist and the sole source of non-equilibrium is due to isotopic gradients,  $X_i = 0$  and so, from equation (4.14)

$$c_i^0 x_i^0 = - c_i^* x_i^* \quad 4.15$$

$$\text{or } \rho^0 x_i^0 = - \rho^* x_i^*$$

Equally there are no gradients of activity coefficients or of electrical potential ( $\psi$ ) and so the forces  $x_i^0$  and  $x_i^*$  are simple functions of concentration gradients, equation (4.16).

$$x_i^g = -(RT/c_i^g) (-dc_i^g/dx) \quad \text{superscript } g = 0 \text{ or } * \quad 4.16$$



#### 4.1.1 Irreversible Thermodynamic Approach

In Chapter 3, the binary coefficients of cadmium iodide were expanded in terms of mobility and coupling coefficients of the uncomplexed and complexed species present in the solution. For any species  $k$ , linear phenomenological equations were written, equation (4.17).

$$J_k = \sum_{i=a}^4 L_{ki} X_i + L_{kb} X_b \quad k = a, 1, 2, 3, 4 \quad 4.17$$

Equation (4.17) deals with any experimental conditions likely to be obtained in normal studies and it is assumed here and in all subsequent discussion that the Onsager Reciprocal Relations (O.R.R.) are obtained and so  $L_{ki} = L_{ik}$ . It is also assumed that the experimental conditions to which equation (4.17) refers were again obtained with the same solution in which now labelled isotope was present, then from equation (4.9)

$$J_k = j_k^0 + j_k^*$$

The sum of the flows of labelled and unlabelled isotopic species,  $k$ , are equal to the net flow,  $J_k$ . The phenomenological equations for isotopic flows will be represented by a symmetrical  $12 \times 12$  matrix of mobility coefficients, since each of the six flows and six forces of equation (4.17) are now subdivided into two components. The phenomenological equations of the isotopic system are given by equations (4.18), (4.19) and /

and (4.20).

$$j_k^0 = \sum_{i=a}^4 ( \ell_{ki} x_i^0 + \ell_{ki}^* x_i^* ) + \ell_{kb} x_b \quad 4.18$$

$$k = a, 1, 2, 3, 4$$

$$j_k^* = \sum_{i=a}^4 ( \ell_{k^*i} x_i^0 + \ell_{k^*i}^* x_i^* ) + \ell_{k^*b} x_b \quad 4.19$$

$$k = a, 1, 2, 3, 4$$

$$j_b = \sum_{i=a}^4 ( \ell_{bi} x_i^0 + \ell_{bi}^* x_i^* ) + \ell_{bb} x_b \quad 4.20$$

From equations (4.9), (4.18) and (4.19),

$$J_k = \sum_{i=a}^4 \left( ( \ell_{ki} + \ell_{k^*i} ) x_i^0 + ( \ell_{ki}^* + \ell_{k^*i}^* ) x_i^* \right) + ( \ell_{kb} + \ell_{k^*b} ) x_b \quad 4.21$$

or,

$$J_k = \sum_{i=a}^4 \left\{ \left( \frac{\ell_{ki} + \ell_{k^*i}}{\rho^0} \right) \rho^0 x_i^0 + \left( \frac{\ell_{ki}^* + \ell_{k^*i}^*}{\rho^*} \right) \rho^* x_i^* \right\} + ( \ell_{kb} + \ell_{k^*b} ) x_b \quad 4.22$$

Comparing terms in equations (4.17) and (4.22), having noted that  $L_{ki} X_i = L_{ki} \rho^0 x_i^0 + L_{ki} \rho_i^* x_i^*$  from equation (4.14) then,

$$\begin{aligned} L_{ki} &= ( \ell_{ki} + \ell_{k^*i} ) / \rho^0 \\ &= ( \ell_{ki}^* + \ell_{k^*i}^* ) / \rho^* \end{aligned} \quad 4.23$$

$i$  and  $k = a, 1, 2, 3, 4$

$$\text{and } L_{kb} = ( \ell_{kb} + \ell_{k^*b} ) \quad k = a, 1, 2, 3, 4 \quad 4.24$$

Since the forces on iodide,  $x_b$  and  $X_b$ , are identical under conditions when only cadmium species are labelled, from equations (4.14), (4.17) and (4.20)

$$L_{bb} = \ell_{bb} \quad 4.25$$

and

$$L_{bi} = \ell_{bi} / \rho^0 = \ell_{bi^*} / \rho^* \quad i = a, 1, 2, 3, 4 \quad 4.26$$

From equations (4.24) and (4.26), using the Onsager reciprocal relations,

$$L_{kb} = \ell_{kb} / \rho^0 = \ell_{k^*b} / \rho^* \quad 4.27$$

Equations (4.23), (4.25) and (4.27) establish specific relationship between the mobility coefficients of equation (4.17) those of the isotopic matrix, equations (4.18), (4.19) and (4.20).

We must now formulate expressions for the total flow of labelled cadmium  $J_a^*$ , equation (4.10) under the more restricted conditions of isotopic diffusion, in which no bulk chemical potential gradient exists and so /

so all  $X_i$  and  $J_i$  are zero in equation (4.17).

Under these conditions  $x_b$  the force on iodide ion is zero and hence from equations (4.10), (4.18) and (4.19),

$$J_a^* = \sum_{k=a}^4 \sum_{i=a}^4 \left( \frac{l_{ki}^*}{\rho^0} (\rho^0 x_i^0) + \frac{l_{ki}^{**}}{\rho^*} (\rho^* x_i^*) \right)$$

since from equation (4.14),  $\rho^* x_i^* = -\rho^0 x_i^0$  when  $X_i = 0$ ,

$$J_a^* = \sum_{k=a}^4 \sum_{i=a}^4 \left( \frac{l_{k^* i^*}}{\rho^*} - \frac{l_{k^* i}}{\rho^0} \right) \rho^* x_i^*$$

and from equation (4.23)

$$J_a^* = \sum_{k=a}^4 \sum_{i=a}^4 \left[ L_{ki} - \left( l_{ki}^* / \rho^* + l_{k^* i} / \rho^0 \right) \right] \rho^* x_i^* \quad 4.28$$

From the analysis of the concentrations of complexes to the binary coefficients (Chapter 3),

$$\sum_{k=a}^4 \sum_{i=a}^4 (L_{ki}) = L_{aa}^T \quad 4.29$$

where  $L_{aa}^T$  is the direct mobility coefficient of cadmium in the binary solution for which the phenomenological equations are:

$$J_a^T = L_{aa}^T X_a + L_{ab}^T X_b$$

and /

and

$$J_b^T = L_{ba}^T X_a + L_{bb}^T X_b$$

Recalling the isotope-isotope terms in equation (4.28), expansion of the summation shows that, when the Onsager reciprocal relations are assumed, equation (4.30) is obtained.

$$\begin{aligned} & \sum_{k=a}^4 \sum_{i=a}^4 \left( \ell_{ki}^* / \rho^* + \ell_{k^*i} / \rho^0 \right) \\ &= \sum_{k=a}^4 \sum_{i=a}^4 \left( \ell_{ki}^* / \rho^0 \rho^* \right) \end{aligned} \quad 4.30$$

From equations (4.28) to (4.30)

$$J_a^* = RT \left[ L_{aa}^T - \sum_{k=a}^4 \sum_{i=a}^4 \left( \ell_{ki}^* / \rho^0 \rho^* \right) \right] (-d\rho^*/dx) \quad 4.31$$

When  $C_a^T$ , total cadmium concentration, is constant at all points in the solution (as it must be for isotopic diffusion) then from equation (4.6) :

$$d\rho^* = 1/C_a^T \cdot dC_a^* / dx \quad 4.32$$

and equation (4.31) becomes

$$J_a^* = RT \left[ \frac{L_{aa}^T}{C_a^T} - \frac{1}{C_a^T} \sum_{k=a}^4 \sum_{i=a}^4 \left( \frac{\ell_{ki}^*}{\rho^0 \rho^*} \right) \right] (-dC_a^* / dx) \quad 4.33$$

Equation (4.33), therefore, has the form of Fick's Law, (section 4.2),

$$J_a^* = D_{aa} \left( - dC_a^* / dx \right) \quad 4.34$$

The flow  $J_a^*$  is that measured by experiment and thus  $D_{aa}$  is the isotopic diffusion coefficient obtained from such experiments. Comparison of equations (4.33) and (4.34) gives :-

$$D_{aa} = RT \left( L_{aa}^T / C_a^T - 1 / C_a^T \sum_{k=a}^4 \sum_{i=a}^4 ( \ell_{ki}^* / \rho^0 \rho^* ) \right) \quad 4.35$$

Equations (4.35) and (4.1) reveal that expressions for isotopic diffusion coefficients in a complex or a simple dissociated electrolyte have identical form.

It may be noted that from equation (4.5) the term  $C_a^T L_{aa}^* / (C_a^0 C_a^*)$  in equation (4.1) is equal to  $(1/C_a^T)(L_{aa}^* / \rho^0 \rho^*)$  making the similarity of equations (4.35) and (4.1) more obvious. The isotope-isotope coupling term, which is a function of a single coupling coefficient  $L_{aa}^*$  in equation (4.1), is now replaced by a summation of coupling coefficients which include all possible interactions between labelled and unlabelled forms of the cadmium containing species in the complexed solution.

In equation (4.1) the isotope-isotope coupling term is bi-ionic, that between two simple ions of equal charge. In such cases  $L_{aa}^*$  is negative and the coupling /

coupling term in equation (4.1) makes a positive contribution to  $D_{aa}$ . Coupling coefficients between ions of opposite charge, are typically positive. The situation may therefore arise that isotope-isotope coupling may occur between cadmium containing species of opposite charge (for example,  $\ell_{a4}^*$ , between  $\text{Cd}^{2+}$  and  $\text{CdI}_4^{2-}$ ) making the summation term in equation (4.35) more positive (and therefore less negative) than for non complexed electrolytes.

Experimental evaluation of the isotope-isotope term shows that much of the anomalous behaviour of cadmium ion diffusion is due to isotope-isotope coupling. In the discussion section methods of predicting these contributions are discussed, section 4.4.

## 4.2 The Measurement of Diffusion Coefficients

A number of ingenious methods<sup>3-5</sup> are available for the study of the fundamental irreversible process of diffusion in electrolyte solutions. In most cases for salt-diffusion and for isotopic-diffusion experiments, the techniques are essentially similar. Isotopic-diffusion, however, is characterized by the fact that the diffusing species is present in negligible quantity in the bulk of electrolyte of much higher concentration. The physical properties of the system such as electrical conductance, density, refractive index etc., are thus unchanged by the addition of the isotope. Perhaps, the only example is the study of 'self-diffusion' of water,<sup>43</sup> using  $D_2O$ , in which case substantial quantities of isotopic species have been used. In general, experimental methods which make use of the physical properties, mostly optical methods, for obvious reasons, are not utilized in isotopic-diffusion measurements.

The primary interest, however, lies in the determination of the coefficient of diffusion,  $D$ , defined by an experimental flow equation:

$$J = - D \partial C / \partial x \quad 4.36$$

where the flux,  $J$ , is the amount of material crossing unit area of a plane perpendicular to the direction of flow in unit time and  $\partial C / \partial x$  is the concentration gradient /



gradient in the positive x-direction. Experimental methods based directly on equation (4.36) usually embody the assumption of a linear gradient of concentration. This assumption is sometimes described as a 'steady state'.

The diaphragm cell method,<sup>5-8</sup> essentially a 'steady state' method was adapted for the study of isotopic-diffusion in this work.

A detailed description of this method and the ancillary apparatus will be given in section 4.3. The alternative methods, in which concentration changes are regarded as a function of both time and distance, are briefly mentioned below. Here the determination of the diffusion coefficients depend on the solution of a second-order partial differential flow equation:

$$\partial C / \partial x = \partial / \partial x D ( \partial C / \partial x ) \quad 4.37$$

with suitable boundary conditions. Further details for these methods can be found in several excellent reviews available on the subject.<sup>4, 7, 9</sup> Equations (4.36) and (4.37) are often referred to as Fick's first and second laws of diffusion.

#### 4.2.1 Optical Methods

Almost exclusively used for salt-diffusion measurements, these methods employ free diffusion from /

from an initially sharp boundary formed between two solutions of different concentration in an effectively infinite column of solution. The non-uniformity of the refractive index, as the diffusion proceeds, provides the basis for the determination of concentration gradient with the help of suitable optical arrangements. Of the various methods in use, the one which has yielded the most precise results and has received a widespread application is the Goüy Interference Method.<sup>10</sup> In this method, monochromatic light from a horizontal slit is passed through a vertical cell in which a concentration gradient exists. The interference fringes containing a finite number of lines are photographically monitored. The method has been theoretically further developed by Gosting and Onsager,<sup>11</sup> Culsen et al,<sup>12</sup> Kegeles and Gosting<sup>13</sup> and Longworth.<sup>14</sup> It is capable of producing absolute values for integral diffusion coefficients to an accuracy of 0.1 - 0.2%, but is unsuitable for dilute solutions. The Rayleigh Interferometric Method,<sup>15, 16</sup> instead, has been used to study both free and restricted diffusion over a wide range of concentration. The basic principles of the Rayleigh's method are the same as for the Goüy's method except that the monochromatic light from a point source is split into two beams. One beam is passed through a cell containing a concentration gradient and the other, passed through a medium of constant refractive index. A band of interference fringes obtained by recombination of the two beams, provides a direct measure of the /

of the refractive index gradient. This method is also very accurate and gives directly differential diffusion coefficients. It is therefore preferred sometimes over the Goüy method.

#### 4.2.2 The Harned Conductimetric Method<sup>17, 18</sup>

This method for the study of restricted diffusion was developed by Harned and co-workers for dilute solutions. The method basically consists of measurement of changes in the electrical conductance of a solution as a function of time in a diffusing system. The method is very accurate but by virtue of its great experimental care and problems with suitable electrode systems for the measurement of the conductivity, its application is limited to very dilute solutions.

Absolute measurements of diffusion coefficients made with optical methods and conductimetric method provide the basis for all the relative methods.

#### 4.2.3 The Porous Frit Method<sup>19</sup>

The procedure involved in this method of studying diffusion consists essentially of soaking a porous disk in the solution of interest and then suspending the disk in a bath of pure solvent. The rate of diffusion of solute from the frit is then monitored by measuring the apparent weight of the suspended disk at various times. The technique originally used for salt-diffusion by Wall, Grieger and Childers<sup>19</sup> has been /

been adapted for the study of isotopic-diffusion by several investigators, notably, Nelson,<sup>20</sup> Marcinkowsky and co-workers.<sup>21</sup>

In the case of isotopic-diffusion, the counting rate of the frit measured over a period of diffusing time reveals a value for the diffusion coefficient. The method is relative and requires suitable calibration system of known diffusion coefficients. It is comparatively cheap and quick but yields values of diffusion coefficients accurate only to a few per cent.

#### 4.2.4 The Capillary Method<sup>22, 23</sup>

The open-ended capillary method, often referred to simply as capillary method, was developed specifically for isotopic-diffusion by Anderson and Saddington<sup>22</sup> in 1949. A general description of the method is given by Wang<sup>24</sup> and Robinson and Stokes.<sup>5</sup> In this method a uniform capillary of known length is filled with an isotopically labelled solution and immersed in a much larger reservoir containing inactive solvent. The coefficient of diffusion is then obtained by measurement of the amount of labelled material in the capillary after certain time, utilizing equation (4.37) with suitable boundary conditions. In theory, the method is an absolute one, but in practice some form of calibration has been found necessary. This method has been extensively used for isotopic-diffusion studies of electrolytes, but the agreement between different workers /

workers has often been poor. Mills and co-workers<sup>25, 26</sup> have attributed this discrepancy to the convectional disturbances at the junction of the capillary mouth and the outer bath solution. Two separate sources of errors have been recognized. The immersion effect occurs when a capillary is lowered into the bath solution for the first time. A loss of 0.5 to 2% of the contents of the capillary may occur during this operation. This effect can be minimized by suitable precautions.<sup>27</sup> The other effect arises from the mode of stirring of the outer bath solution. This turbulence could cause sweeping-strokes across the mouth of the capillary. One of the boundary conditions in application of equation (4.37) to the capillary method can be described as  $C = 0$  for  $x > \ell$ , where  $\ell$  is the length of the capillary. The above action is thus equivalent to reducing the effective length of the diffusing column. It has therefore been termed the  $\Delta\ell$  effect by Wang<sup>28</sup> and gives rise to high results. Mills,<sup>27</sup> however, has overcome this difficulty by careful design of the apparatus. Subsequent studies of the  $\Delta\ell$  effect have been made by Berne and Bergren.<sup>29</sup> Other errors in this method can arise from traces of radioactive material not properly removed from the fine capillaries and the difficulties in preparation of reproducible counting samples. Mills<sup>30</sup> and independently Thomas<sup>31</sup> suggested continuous monitoring of radioactivity by enclosing the capillary in a scintillation counter.

Measurements /

Measurements made by this method indicate that precision of the order of 0.2% could be achieved with capillary method.

Radioactive counting facilities for the present studies were kindly extended by the department of Physiology, University of Glasgow. Under the circumstances it was considered desirable to adapt the diaphragm cell method in this work. It also offered an opportunity to modify the technique to suit the requirements of a practicing diffusion experimentalist.

#### 4.2.5 The Diaphragm Cell Method<sup>5, 6, 8</sup>

Since the development of this technique for the measurements of diffusion coefficients by Northrop and Anson<sup>32</sup> in 1928, a number of attempts have been made to improve the method in various ways. All variations are similar in at least one respect: a concentration gradient is set up between two solutions of different concentration in a porous disk which separates the solution compartments. The process of diffusion is thus confined to the pores of the sintered diaphragm, thereby reducing greatly thermal and mechanical convections. There are, however, some inherent problems associated with confining diffusion process to a sinter of this kind. The method is relative since the effective diaphragm pore area and length can not be determined in an absolute manner. The general practice is to determine the cell constant with a system of known differential diffusion coefficients. Aqueous KCl at /

at 25°C, for which precise and reliable data are available, is usually used as the reference standard. Since it is impossible to analyse the solution within the diaphragm, the diffusion coefficient must be obtained from measurement of material passing through its boundaries. In consequence, it is essential to maintain a uniform concentration on either side of the diaphragm right up to the entrance of the pores. The effective diameter of the pores in the diaphragm must be such that gross streaming through the diaphragm and surface transport along the walls of the pores is avoided. A variety of diaphragm cells have been used to fulfil these requirements. Different types of homogenizing techniques, including the earliest density-stirring<sup>32</sup> and the use of glass spheres rotating<sup>33</sup> on the diaphragm surface, have been used both to avoid the formation of stagnant layers adjacent to the diaphragm and ensure uniformity of the contents of the solution compartments. The problem of surface transport on the diaphragm has also been investigated with experiments carried out in Pyrex glass, stainless steel, and platinum sinters.<sup>6</sup> The surface effects, however, have been attributed to the formation of a double layer due to adsorption of ions rather than the material of the sinter. These effects which result in enhanced diffusion, have been found undetectable at concentrations above 0.05 mol dm<sup>-3</sup>. The diaphragm cell method is therefore /

therefore not suitable for measurements in electrolyte solutions at concentrations less than about  $0.05 \text{ mol dm}^{-3}$ .

The experimental technique adapted for the study of diffusion by diaphragm cell method, at present, is primarily due to Stokes.<sup>5, 8</sup> The Stoke-type of diaphragm cell has been used most widely in the past two decades. Its essential features, modifications by other workers and major changes being brought in the course of the present investigation will be discussed in section 4.3 of this Chapter.

#### 4.2.6 Theoretical Principles of the Diaphragm Cell Method<sup>5, 6</sup>

As mentioned previously, the diaphragm cell method is essentially a steady-state method and measurement of the flux,  $J$ , and the concentration gradient  $\partial C / \partial x$  gives the diffusion coefficient,  $D$ , from equation (4.36). The quantity  $J$  and  $D$  being measured on the cell-fixed frame of reference. In actual practice, however, a true linear gradient of concentration will rarely be present in a diaphragm cell since the concentrations on either side of the diaphragm are changing, although at a relatively slow rate. A 'pseudo' steady-state is therefore assumed to be present and if the flux,  $J$ , is considered to be uniform across the diaphragm at any instant then an effective diffusion coefficient also defined by  $D$  can be treated mathematically as if it were the proportionally /



proportionally constant of a linear gradient of concentration.

A diagrammatic representation of the diaphragm cell is given in Fig. 4.1. The volumes of the compartments and the diaphragm are indicated in the figure.

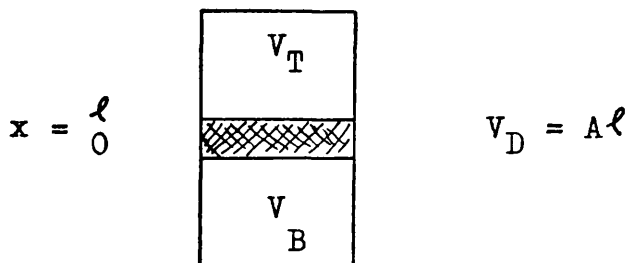


Figure 4.1

If the concentrations in the top and bottom compartments at the commencement of the experiment ( $t = 0$ ) are denoted by  ${}^0C_T$  and  ${}^0C_B$  and after time,  $t$ , by  $C_T$  and  $C_B$ , the changes in the concentrations in the appropriate compartments of the cell while the diffusion is proceeding are given by :

$$dC_T / dt = J(t) A / V_T \quad 4.38a$$

$$dC_B / dt = - J(t) A / V_B \quad 4.38b$$

where  $J(t)$ , the flux of solute, is a function of time. Combination of equations (4.38) gives

$$d(C_B - C_T) / dt = - J(t) A (1/V_B + 1/V_T) \quad 4.39$$

If /

If the diffusion coefficient is assumed to be independent of concentration the flux,  $J(t)$ , is given by Fick's law equation (4.36)

$$J(t) = (C_B - C_T) / \ell \cdot D \quad 4.40$$

so that equation (4.39) becomes :

$$- d \ln(C_B - C_T) / dt = D A / \ell (1/V_B + 1/V_T) \quad 4.41$$

and this after integration may be written as

$$\ln \left[ (C_B - C_T) / (C_B - C_T)_0 \right] = - D t \beta \quad 4.42$$

where  $\beta$ , the cell constant, is given by

$$\beta = A / \ell (1/V_B + 1/V_T) \quad 4.43$$

Equation (4.42) is, however, strictly applicable to systems where  $D$  is independent of concentration, such as self-diffusion. For concentration dependent systems the above equations have been modified by Gordon<sup>7</sup> and Robinson and Stokes<sup>5</sup> and then further theoretical treatment has been given by Barnes.<sup>6, 34</sup> Equation (4.40) for such systems can be written as :

$$J(t) = (C_B - C_T) / \ell \cdot D' \quad 4.44$$

where /

where  $D'$  is the averaged value of the diffusion coefficient over the concentration range  $C_T$  to  $C_B$  during time  $t$ , hence

$$D' = 1 / (C_B - C_T) \int_{C_T}^{C_B} D(C) dC \quad 4.45a$$

$$= -1 / (C_B - C_T) \int_{x=0}^{x=l} D(C) \left( \partial C / \partial x \right) dx \quad 4.45b$$

$D(C)$  is the differential diffusion coefficient at concentration  $C$ . From equations (4.44) and (4.39)

$$- d \ln (C_B - C_T) / dt = A / \ell \left( 1/V_B + 1/V_T \right) D' \quad 4.46a$$

Upon integration this gives :

$$\ln \left[ ({}^0C_B - {}^0C_T) / (C_B - C_T) \right] = A / \ell \left( 1/V_B + 1/V_T \right) \int_0^t D' dt \quad 4.46b$$

It is customary to define an integral diffusion coefficient :

$$\bar{D} = (1 / t) \int_0^t D' dt \quad 4.47$$

Equation (4.20) thus becomes:

$$\bar{D} = \frac{1}{\beta t} \ln \left[ \frac{{}^0C_B - {}^0C_T}{C_B - C_T} \right] \quad 4.48$$

Thus /

Thus from measurements of the concentrations in the top and bottom compartments at the beginning and end of a diffusion run over a period of time  $t$  the diaphragm cell integral diffusion coefficient  $\bar{D}$  may be determined.

#### 4.2.7 Calculation of $D$ from $\bar{D}$

The usually complex concentration- and time-averaged integral diffusion coefficient obtained from the diaphragm cell measurements is very often converted to the more fundamental differential diffusion coefficient,  $D$ , defined by Fick's first law. However, where the concentration gradients are absent, as in isotopic-diffusion,  $\bar{D}$  and  $D$  are identical. For the calculation of  $\bar{D}$  for calibration experiments the method of Gordon<sup>7</sup> and Robinson and Stokes<sup>5</sup> is commonly used. Gordon showed that a negligible error is introduced if  $\bar{D}$  is redefined by :

$$\bar{D} = \left( 1 / (c'_B - c'_T) \right) \int_{c'_T}^{c'_B} D \, dc \quad 4.49$$

where

$$c'_B = ({}^0c_B + c_B) / 2 \quad 4.50a$$

$$c'_T = ({}^0c_T + {}^0c_T) / 2 \quad 4.50b$$

Stokes then defined a diffusion coefficient  $\bar{D}^0(c)$  by

$$\bar{D}^0(c) /$$

$$\bar{D}^0(C) = 1 / C \int_0^C D \, dC \quad 4.51$$

Combination of equations (4.49) and (4.51) gives

$$\bar{D} = 1/(C'_B - C'_T) \left( C'_B \bar{D}^0(C'_B) - C'_T \bar{D}^0(C'_T) \right) \quad 4.52a$$

Multiplying and dividing equation (4.26) by  $(C'_B - C'_T)/C'_B$  and defining  $C'_T/C'_B$  by  $C''$  the resulting equation is

$$\bar{D} = \left[ \bar{D}^0(C'_B) - C'' \bar{D}^0(C'_T) \right] / (1 - C'') \quad 4.52b$$

If reliable data for  $D$  over the required concentration range are available, values of  $\bar{D}^0(C)$  can be obtained by suitable integration for a calibration system.

The values of  $\bar{D}$  for use in equation (4.48) are then obtained from equations (4.52).

#### 4.2.8 Barnes Theoretical Treatment of the Diaphragm Cell<sup>6, 34</sup>

Barnes has shown that since a true steady-state condition in the diaphragm does not exist, a rigorous mathematical solution to the equation of the diaphragm cell should not, therefore, contain the assumption that a linear gradient is continuously present. By assuming  $D$  to be independent of concentration a general solution to Fick's second law,  $\partial C / \partial t = \partial / \partial x (D \partial C / \partial x)$ , giving the variation of concentration with time, has been obtained for two different initial conditions of the /

the diaphragm. This treatment has been further extended by Mills, Woolf and Watts<sup>35</sup> to include a third initial condition. The three cases of interest are usually called, 'solvent-filled diaphragm', 'gradient-filled diaphragm' and 'solution-filled diaphragm'. A diagrammatic representation of the concentration profiles in the diaphragm at the initiation of diffusion is given in Fig. 4.2

On the assumption that  $D$  is independent of concentration, and that  $V_B$  and  $V_T$  are virtually identical so that the ratio  $V_D / V_T = \lambda$  is so small that the terms in  $\lambda^2$  and higher powers are small compared to unity; within these limitations, Barnes has used the boundary conditions of the diaphragm cell:

$$C_D(x,t) = {}^0C_D \quad \text{when } t = 0 \text{ and } 0 \leq x \leq \ell \quad 4.53a$$

$$C_D(0,t) = C_B(t) ; \quad C_D(\ell,t) = C_T(t) \quad \text{when } t > 0 ; \quad 4.53b$$

$$\text{and } \partial C_B / \partial t = D/V_B (\partial C_D / \partial x)_{x=0} ; \quad \partial C_T / \partial t = -D/V_T (\partial C_D / \partial x)_{x=\ell} \\ \text{when } t > 0 \quad 4.53c$$

to obtain the equations for  $C_B$  and  $C_T$  for the first two cases.

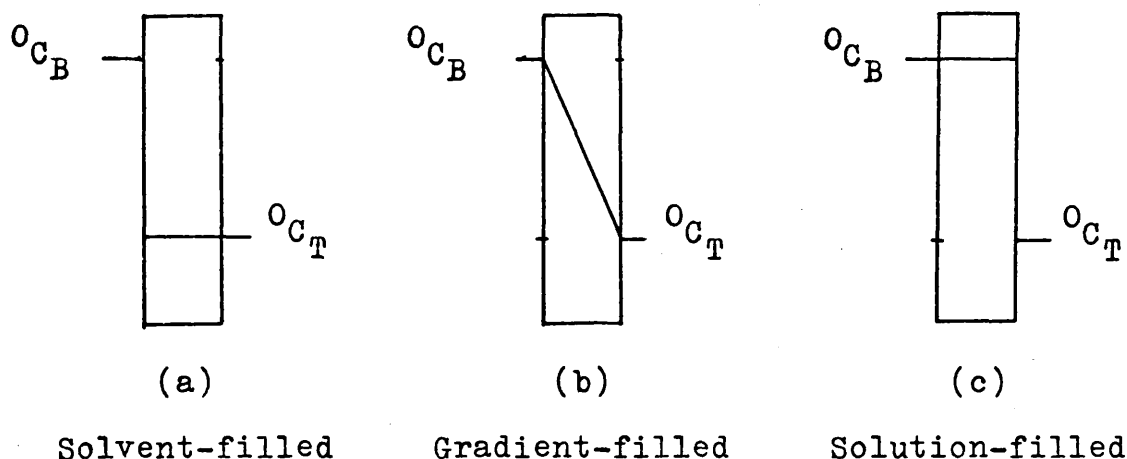


Figure 4.2

4.2.8a Case 1. Solvent-filled Diaphragm The diaphragm and top compartment are filled with pure solvent ( $^0C_T = 0$ ) and the bottom compartment has solution of concentration  $^0C_B$  at the beginning of the experiment (Fig. 4.2 (a)). The equation for this initial condition is given by

$$\ln \left[ \left( ^0C_B / (C_B - C_T) \right) (1 - \lambda/6) \right] = A/\ell (1/V_B + 1/V_T)(1 - \lambda/6) Dt$$

$$= \beta' \bar{D}t \quad 4.54$$

Since the concentration in the top compartment  $^0C_T$  is zero, the initial concentration in the bottom compartment  $^0C_B$  can be readily obtained from the mass-balance equation:

$$^0C_B = C_B (V_B + \frac{1}{2} V_D)/V_B + C_T (V_T + \frac{1}{2} V_D)/V_B \quad 4.55$$

4.2.8b /

4.2.8b Case 2. Gradient-filled Diaphragm In this case prior to beginning a diffusion experiment, a pre-diffusion period is used to establish a concentration gradient across the diaphragm. The top compartment is then rinsed and finally filled with pure solvent. The time at which the final rinsing is completed is normally taken as zero time for the diffusion run. The equation for this case takes the form :

$$\ln \left[ \frac{{}^0C_B}{(C_B - C_T)} \right] = A/\ell (1/V_B + 1/V_T)(1 - \lambda/6) Dt$$

$$= \beta' D t \quad 4.56a$$

and  ${}^0C_B$  is given by

$${}^0C_B = C_B + C_T (V_T + \frac{1}{2}V_D)/(V_B + \frac{1}{2}V_D) \quad 4.56b$$

4.2.8c Case 3. Solution-filled Diaphragm This initial condition for the diaphragm has been included by Mills, Woolf and Watts.<sup>35</sup> It is essentially the reverse of case 1. The bottom compartment and the diaphragm are filled with solution of concentration  ${}^0C_B$  and the top compartment with pure solvent. The equation for the diaphragm is the same as for case 1. In this case  ${}^0C_T$  is calculated from the mass-balance equation :

$${}^0C_T = C_B (V_B + \frac{1}{2}V_D)/V_T + C_T (V_T + \frac{1}{2}V_D)/V_T - {}^0C_B (V_B + V_D)/V_T$$

4.57



A comparison of equations (4.48) and (4.54) reveals that Barnes' mathematical treatment has lead to the inclusion of  $(1 - \lambda/6)$  in the logarithmic term and also

$$\beta (1 - \lambda/6) = \beta'$$

A general theoretical and experimental study of the three types of distributions has been made in 1967 by Mills, Woolf and Watts.<sup>35</sup>

### 4.3 Experimental

#### 4.3.1 The Stokes-Type of Diaphragm Cell<sup>8</sup> and its Modifications

The cell is shown in Fig. 4.3. A sintered disk of porosity No. 4 (2-10 micron pore size) divides the main body of the cell into two nearly equal compartments of approximately 40 - 50 ml capacity. Standard taper ground glass joints are usually sealed to the ends of the cell which can be fitted with suitable plugs.

Mechanical stirring is effected by soft-iron wires enclosed into drawn-out Pyrex glass tubing slightly shorter than the diameter of the disk. The weights of the stirrers are so adjusted that the upper one just sinks and the lower barely floats immediately above and below the diaphragm. A U-shaped permanent magnet, mounted coaxially with the cell, is then rotated around the cell with a motor and belt or a direct drive mechanism.

Several variations of the Stokes method have been used. Nielsen, Adamson and Cobble<sup>36</sup> have used a cell in which the magnets were kept stationary and the body of the cell was rotated with suitable bearings. In another type of cell reported by Lewis,<sup>37</sup> a ring of eight soft-iron cored solenoids have been used to rotate special magnetic stainless steel stirrers. The solenoids are energized, in sequence, with a low voltage d.c source to set up a rotating magnetic field round the cell. A maximum stirring speed of 150 r.p.m. has been /

been achieved. This type of system which seemed, at first glance, to avoid the use of unweildy magnet assembly, has been discarded by later workers<sup>6</sup> on the grounds of heat generated by the magnetic coils during prolonged operations. The original worker has reported the use of seven cells in a single unit, with an obvious number of fifty six coils connected in parallel. Although all the cells have been independently water jacketed the heat associated with the windings of the electromagnets in close vicinity of the diaphragm does not seem to be adequately exchanged with the thermostat bath. A multicell unit has also been reported by Dullien and Shemilt.<sup>38</sup> The body of each cell was enclosed in a brass sleeve with perforations to aid circulation of bath liquid. The cells were kept in position inside the sleeves with pieces of cork. The assembly was mounted on a brass support and a rather complicated gear-mechanism, with a central shaft attached to a motor, was then used to rotate pairs of magnets around each cell.

In general, the conventional rotating assembly or its slightly modified form by Mills and Woolf<sup>6</sup> is preferred over the above variants.

From the viewpoint of the practicing experimentalist, however, the Stokes-type of magnetic stirrers and the associated driving mechanism have a few disadvantages. These are summarised below:

a) /

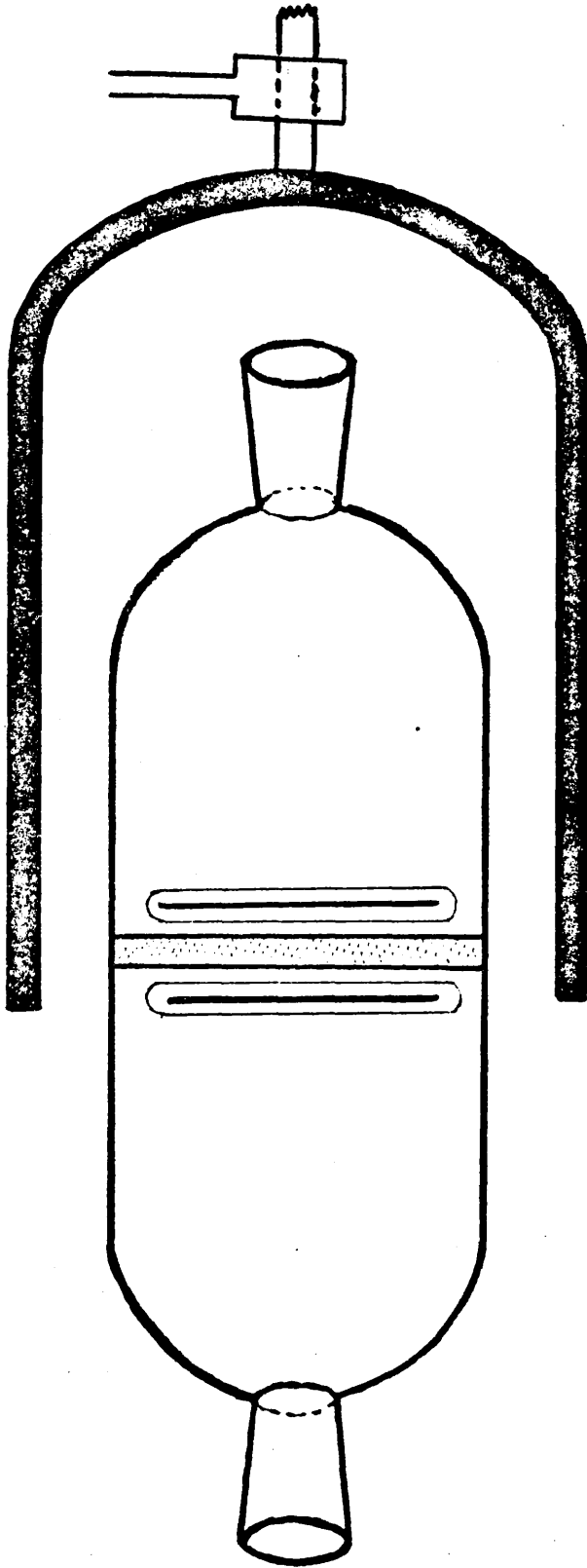


Fig. 4.3 The Stokes type of Diaphragm Cell

a) The diaphragm wearing by action of the stirrers makes it necessary to calibrate the cells periodically, very often after two or three experiments only. Janz and Mayer<sup>39</sup> have avoided this by using a graph of  $A/\ell$ , characteristic of the diaphragm only, as a function of the working life of the cell. While, in their work in this laboratory, Jalota and Paterson<sup>40</sup> overcame this difficulty by adjusting the magnets such that the stirrers rotated 2-3mm away from the surface of the diaphragm. No significant change in the final results, because of this modification, has been reported by the latter authors.

b) Since the weights and densities of the stirrers are involved, several sets of sinking and floating stirrers, for top and bottom compartments respectively, may be required for a given solvent system when wide concentration ranges are being studied.

c) The unwieldiness of the magnet assembly does not permit the use of more than one diaphragm cell in an averagely sized bath. Apart from the space requirements, this causes unnecessary delay in the study of a process for which already an individual experiment may require more than 3 days.

For the above mentioned reasons, the design of the stirrers and their driving mechanism was reconsidered and an extremely simple and new type of method was devised in this work.

The /

The simplicity of the new method of magnetic stirring lies in the fact that no motor and belt or metal gearing system is involved in rotating the magnets around the cell.

Two bar magnets were mounted on a small Perspex impeller, enclosed in an outer casing around the body of the cell. The impeller was then rotated by a jet of water pumped from the thermostat bath itself. The entire rotating device thus occupies a mere 5 cm space around the sinter of the cell. Inside the cell, the Stokes-type of stirrers were also changed to four-bladed propellers, one in each compartment. The propellers were attached to the side walls of the cell and positioned in the centre at a distance of 2-3 mm from the diaphragm. Such type of stirrers would not scratch the surface of the diaphragm and will also rotate in a wide range of solvent systems and concentrations.

A unit capable of accommodating four such cells was constructed. A detailed description of the unit is given below.

#### 4.3.2 The Diaphragm Cell and the Magnetic Stirrers

Pyrex glass standard filter tube with sintered disk (Porosity No. 4) sealed in center waist (no. 3790/68 Jobling Pyrex Ltd., London) was used for the construction of the cell body.

The stirrer for the top compartment was constructed by enclosing a soft-iron wire in a medium walled Pyrex tubing and attaching two side arms at right angles to it. /

it. The side arms consisted of thick walled capillary tubing. The lengths of the arms of the resulting four-bladed propeller were slightly shorter than the diameter of the diaphragm. A central shaft of glass rod was then sealed to the propeller, perpendicular to the junction of the blades. This was passed through a collar and its end melted into a small solid sphere, which rested on the flanged end of the collar. The collar was then sealed to the side wall of the cell with a length of glass rod, such that the propeller is 2-3 mm away from the surface of the disk and is positioned exactly in the centre of the cell.

The stirrer in the bottom compartment of the cell was similar in all respects to the one in the top compartment except that the end of the collar closer to the diaphragm was flanged and a solid sphere on the central shaft adjacent to the junction of the blades provided the seat of rotation for the bottom stirrer.

The action of the stirrers in both compartments was tested to ensure smooth rotation. The ends of the filter tube were terminated into B-19 standard taper ground glass joints. The cell assembly was then thoroughly annealed and tested for pinholes under vacuum.

An exploded diagram of the cell and magnetic stirrers is shown in Fig. 4.4.

#### 4.3.3 The Plugs for the Cell Ends

The top plug, shown in Fig. 4.5 a, was constructed from /

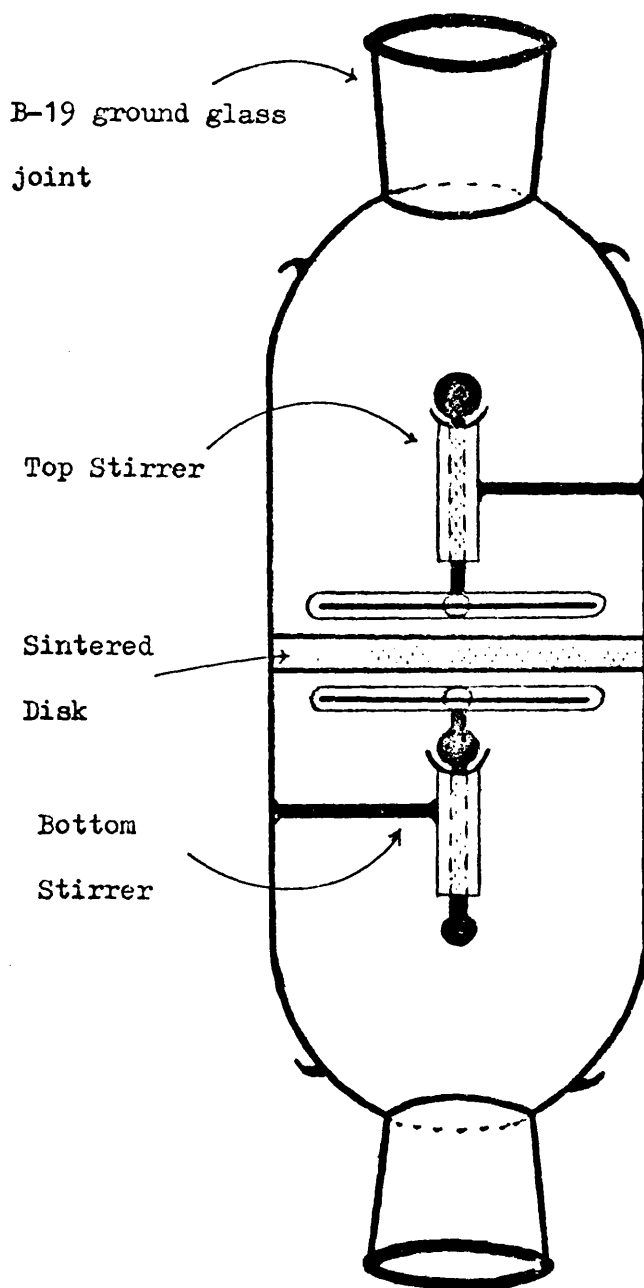
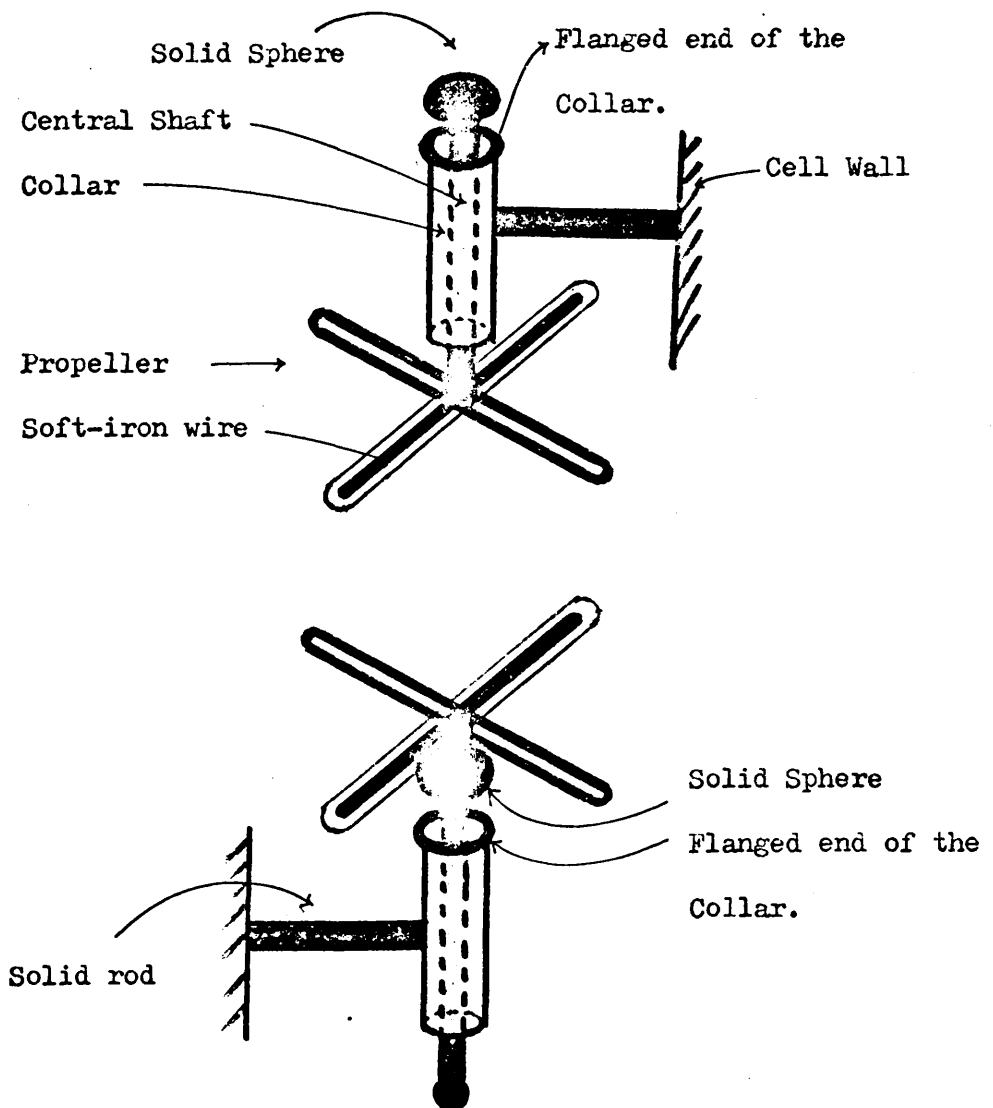


Fig. 4.4 (a)— The Diaphragm Cell used in this work.





**Fig. 4.4 (b)—** Enlarged view of the top and bottom stirrers attached to the side wall of the cell.

Legend for Figure 4.5

- a -           Top Plug
  - A.   Capillary bore B-19 inner joint
  - B.   B-7 ground glass joint
  - C.   B-7 stopper ending into a fine capillary
  
- b -           Bottom Plug
  - A.   Glass impregnated teflon body
  - B.   Stainless Steel valve
  - C.   Brass adjusting knob
  - D.   Brass holding knobs
  - E.   Side holes
  - F.   Plugs for the side holes E
  - G.   Rubber 'o'-rings

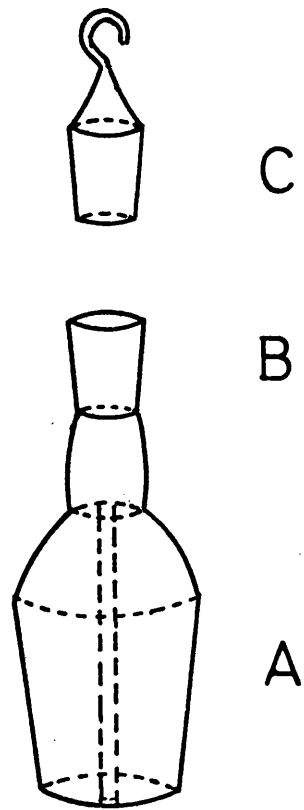


Fig. 4.5a Top Plug

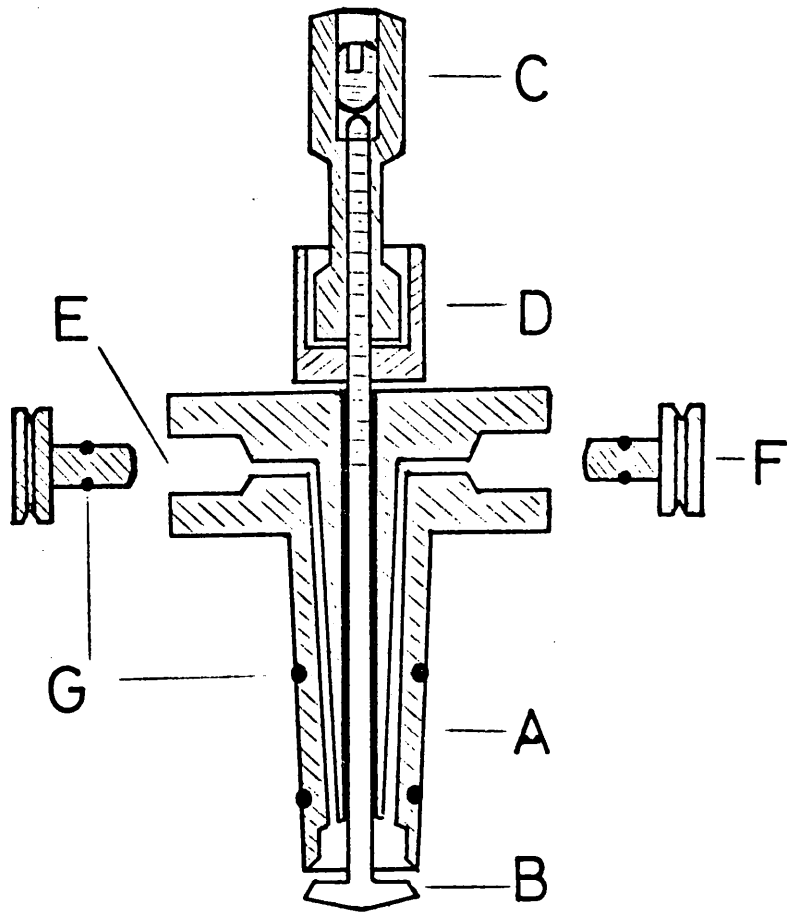
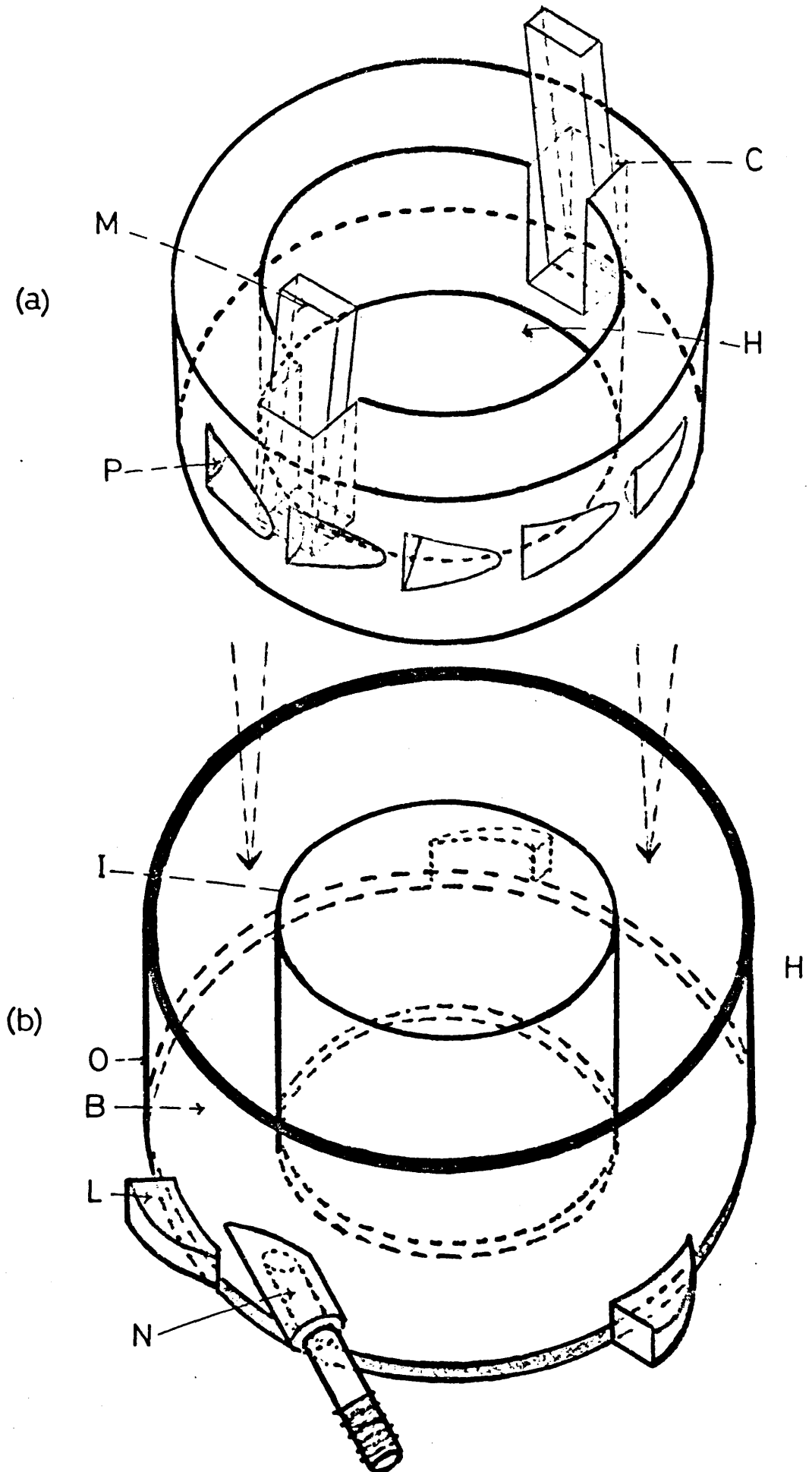


Fig. 4.5 b      Bottom Plug

Legend for Figure 4.6

- (a) -       The impeller
- C   Cuts made into the body of the impeller  
      for magnets
  - H   Central hole
  - M   Magnets
  - P   Paddle drillings around the periphery
- (b) -       Casing for the impeller
- B   Base, filled with 3 mm thick pool of  
      mercury
  - I   Inner wall
  - L   Lugs for mounting the casing on the  
      tray
  - N   Nozzle for the water jet
  - O   Outer wall
  - H   Hole for the body of the cell



from a simple capillary bore B-19 inner joint, broadening into a tube of 0.5 cm inner diameter, cut to a length of 1 cm. A B-7 ground glass joint was attached to the end of this tube. The design of the bottom plug, constructed from glass impregnated teflon, was similar to that reported by Albright and Mills.<sup>41</sup> A diagrammatic representation of the bottom plug is shown in Fig. 4.5 b.

#### 4.3.4 The Rotating Magnet Assembly

A piece of Perspex, 2.5 cm in length, was cut off from a solid rod of 9.5 cm outer diameter. The resulting disk-shaped impeller was bored through to provide a hole of 5.2 cm diameter in the centre. A standard  $\frac{3}{8}$ " (9.5mm) drilling rod was then used to machine twelve tangential paddle drillings around the periphery, to a point 5 mm in from the circumference. Two cuts, facing the central hole and opposite to each other, were made on the top edge of the impeller. These cuts, 2 cm deep and 1.3 cm square, provided access for the magnets. A pair of 'Eclipse' bar magnets (James Neill, Sheffield Limited, England) were wrapped in plastic tape for protection against rust and simply push-fitted in the proper positions. A diagram of the impeller, viewed from an angle, is shown in Fig. 4.6.

The casing for the impeller consisted of an outer wall, an inner wall and a base. The walls were made by cutting standard 3 mm Perspex tubes of 10 cm and 5 cm outer diameters respectively, to a length of 3.5 cm. A 3mm thick circular disk of diameter equal to /

to the outer diameter of the outer wall provided the base. A central hole equal to the inner diameter of the inner wall tubing was drilled through the base. Prior to sealing the walls of the casing to the base, the surface of the inner wall was accurately machined, such that when the impeller is slipped into the casing it provided an axis of rotation for the latter. The gap between the outer wall of the casing and the periphery of the impeller was of the order of 1.5 mm. A 6 mm hole in the side wall of the casing, in line with the paddle drillings of the impeller, was fitted with a 3 cm long nozzle. The end of the nozzle was threaded to accept rubber tubing. A diagram of the casing is shown in Fig. 4.6. The three lugs shown at the base of the casing were used to fix the entire assembly on a common tray in the centre of the thermostat bath. The casing was filled to a depth of 3 mm with mercury to provide a frictionless surface at the bottom of the impeller. Four such magnetic rotating devices were mounted on the common tray made from  $\frac{1}{2}$ " thick sheet of Perspex. Two rectangular bars were glued to the under-surface of the tray for increased stability, Fig. 4.7 (O). The tray was perforated with a number of  $\frac{1}{2}$  cm holes to aid circulation of the bath liquid. Four holes, matching the central holes in the impeller casings were drilled through the tray, allowing the cells to be mounted in position. The tray was supported by four adjustable legs in the thermostat /



Legend for Figure 4.7

- A Perspex Tank
- B Central Tray
- C Cell Holder (Brass)
- D Adjustable Legs for Tray B
- E Cooling Coil
- F Paddle Stirrer
- G Mercury-Toluene Thermoregulator
- H Water Circulation Pump
- I Rubber tubing
- J Pressure Distributer
- K Pressure Regulator
- L Brackets for mounting the Impeller Casing
- M Perforations for Circulation of Water
- N A Typical Cell Assembly
- O Perspex Support Bars

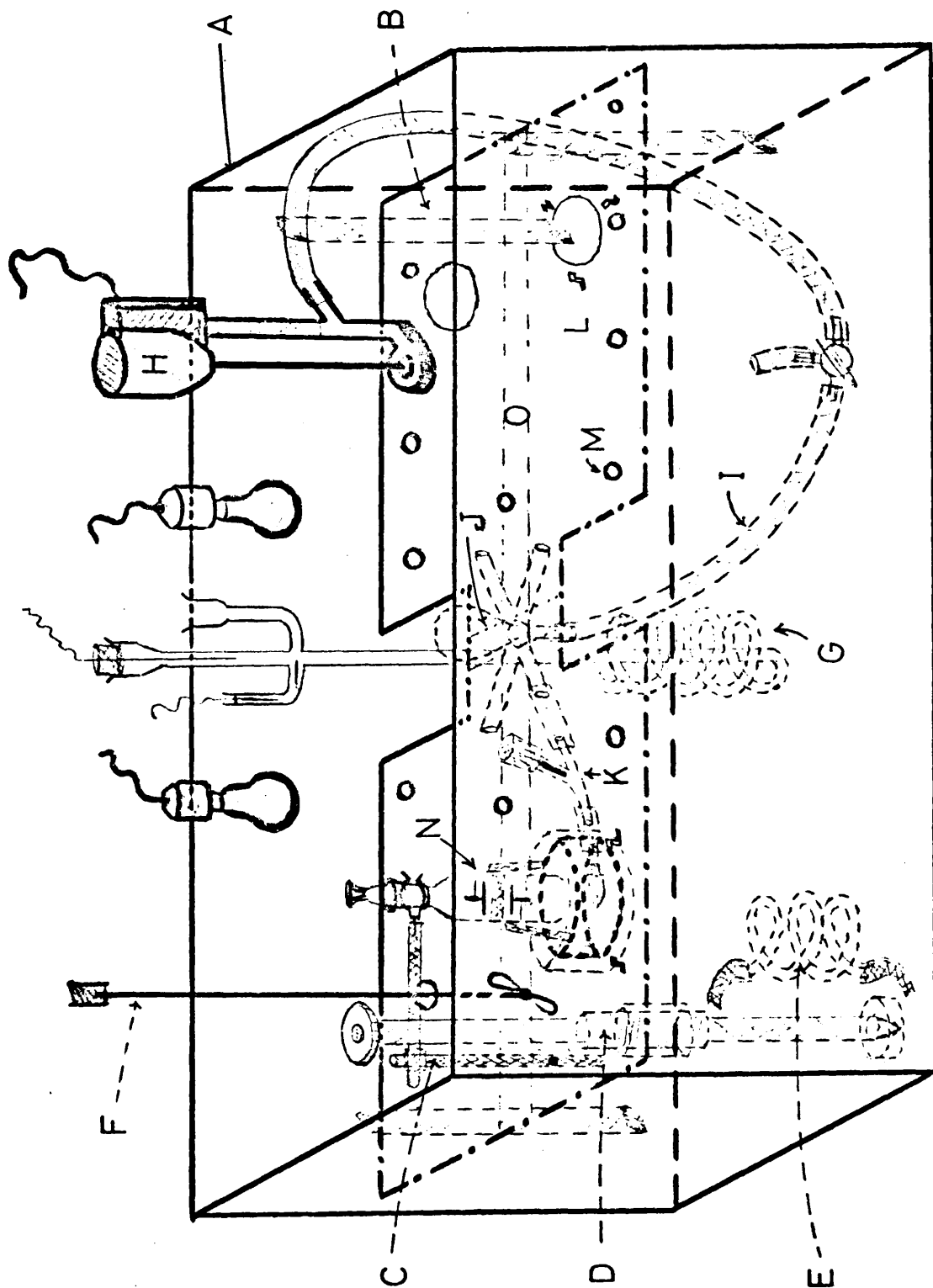


Fig. 4.7- Multicell Unit for diffusion coefficient measurements

thermostat bath. These allowed the tray to be set perfectly horizontal at the required level in the tank. The details of constructions are illustrated in Fig. 4.7. A typical cell assembly with magnet driving device is shown in the figure. The cell holder (Fig. 4.7 C) consisted of a brass rod with a plastic coated terry clip screwed to its tip. The brass rod was then attached with a right angled aluminium screw-bracket to a main support rod which was mounted vertically on the Perspex tray. After initial adjustments, the cell and its attached rod can be removed from between the magnets, for manipulation, and brought back to the same reproducible position.

#### 4.3.5 Water Circulation Pump

A laboratory thermostat-water pump unit (Shandon, Gallenkamp, Ltd., London) was used for driving the four impellers. The thermostat of the unit was disconnected and its heater removed, making use of the immersion pump only. A pressure distributor, shown in Fig. 4.7 J, was constructed from a 100 ml Pyrex round bottom flask by attaching four short side tubes to its stem, near the bulb. The stem of the pressure distributor was then passed through a hole in the middle of the tray and connected with the outlet of the pump with rubber tubing. The four side-outlets from the distributor were then connected to the appropriate nozzles of the magnet driving assemblies, via TF 2/18 'Rotaflo' /

'Rotaflo' pressure regulators, with small pieces of rubber tubing. The speed of any particular impeller can thus be altered by regulating the pressure of the water jet. The minimum speed of stirring obtainable in each cell was found limited by a thresh-hold starting pressure to about 10 r.p.m., but a maximum stirring speed of 100 r.p.m. can be easily achieved with this type of system. Above this speed, however, the combined action of the impeller and the jet of water tends to force out mercury from the impeller-casing.

#### 4.3.6 Constant Temperature Bath

A conventional toluene-mercury glass coiled thermoregulator in conjunction with an electronic relay mechanism (Type 42, Gallenkamp, Ltd., London) was used to maintain a temperature of  $25 \pm 0.01^{\circ}\text{C}$  in a water bath. The bath was heated by two 150 watt bulbs and cooled by tap water cooling coils immersed in the tank. Although the contents of the bath are well stirred by the water circulation pump, a paddle stirrer attached to a continuous duty motor, was also used to ensure thorough mixing. Evaporation from the top of the tank was reduced by covering the surface of the bath with polystyrene pellets. The thermostat tank was installed in a fume cupboard in the 'radiation-room'. The exhaust fan of the fume cupboard was set to a medium draught to avoid temperature fluctuations in the thermostat. A photograph of the entire unit is /

is displayed on p.219 . The use of Perspex for the construction of the tank had the advantage of being transparent and rust proof. The action of the stirrers and the alignment of the cells can be easily seen. Since water in the bath is constantly used for driving the magnet rotating assemblies, any rust or other material may obstruct the inlet nozzle of an impeller, thereby reducing the speed of stirring in the cell. Accordingly, water in the tank was changed before every diffusion run. Growth of algae was limited by the addition of a little sodium benzoate to the bath. The use of a filter in the circulation pump was considered, but this had the adverse effect of reducing the pressure of the pump and was therefore discarded. A totally water submersible pump fitted with its own filter was also tried, but was rejected because of the heat generated by the body of the pump inside the thermostat bath.

#### 4.3.7 Determination of the Volumes of the Cell Compartments

The cell was first cleaned with hot nitric acid, repeatedly washed with distilled water, inverting the cell at regular intervals, and dried with acetone. The volumes of the cell compartments  $V_T$  and  $V_B$  were then determined by weight calibration with carbon tetrachloride. The density of carbon tetrachloride at the temperature of calibration ( $25^{\circ}\text{C}$ ) was calculated from /

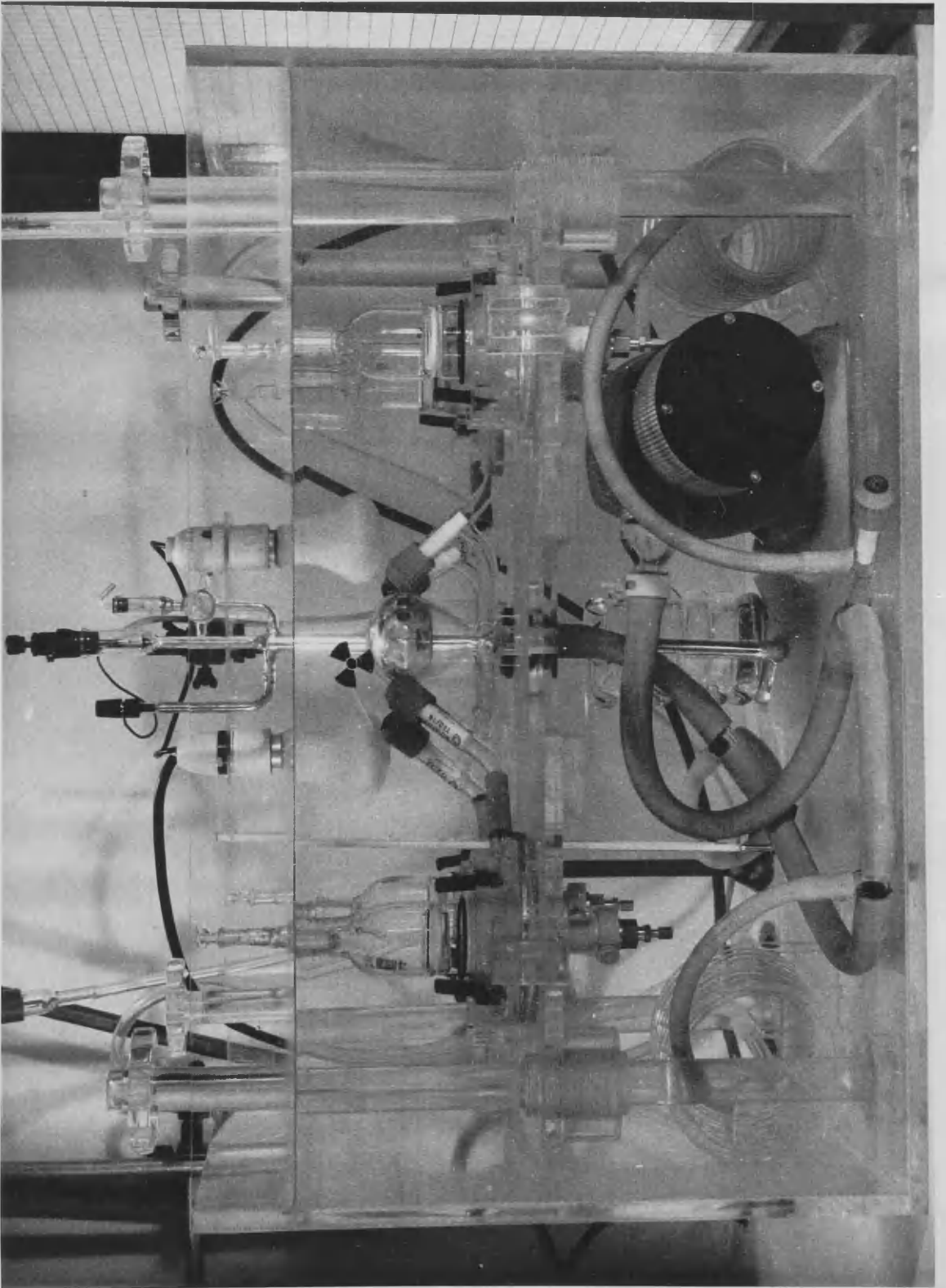


Plate 1. Photograph of the apparatus used for diaphragm-cell diffusion measurements.

from the equation :<sup>42</sup>

$$d_t = 1.63255 - 1.911 \cdot 10^{-3} \cdot t - 0.690 \cdot 10^{-6} \cdot t^2$$

The volume of the diaphragm,  $V_D$ , was determined independently by reweighing, after dropwise addition of  $CCl_4$  with a pasteur pipette to the sintered disk, an otherwise dry cell, held horizontally; the capillary action of the pores draws in  $CCl_4$  to fill the diaphragm.

The average results of duplicate determination of the volumes of the cell compartments, for the four cells used, are listed in table 4.1.

#### 4.3.8 Filling of the Cell for Diffusion Run

The 'vacuum thump' method<sup>39</sup> was used for the cell filling. All the solutions were defibred by passing through a millipore filter and degassed, just prior to cell filling. The bottom compartment of the cell and approximately one-half of the top compartment was filled with the appropriate solution. The top compartment was then evacuated until the solution boiled. The vacuum was suddenly released, allowing the atmospheric pressure to force the solution in the diaphragm pores. The procedure was repeated several times; the cell was reversed in position at intervals to ensure complete filling of the diaphragm. The bottom compartment was then completely filled and the bottom plug, shown in Fig. 4.5 b, was inserted with valve B open /

open to avoid trapping air bubbles. A thin layer of high vacuum quality grease (Apiezon) was applied to the o-rings of the plug. B was then closed by holding knob C and rotating knob D. The internal chamber in the body A was then cleaned and dried by passing water, acetone and air through the side holes E. The holes were then closed with the stoppers F and a thin layer of parafilm was wrapped around the plug assembly for protection against tank water. The plug was maintained firmly seated with rubber bands across the small 'ears' on the diaphragm cell. The filling of the top compartment was then completed and the top plug, shown in Fig. 4.5 a, was inserted after lubricating with a light coat of 'Apiezon' grease and enclosing it in a teflon sleeve.

#### 4.3.9 Calibration of the Diaphragm Cell

Aqueous 0.5 molar potassium chloride, diffusing into pure water, was used for cell calibration. The 'gradient-filled method' (case 2, section 4.2.8b) was adapted for calibration experiments. The cell was filled with distilled water by the filling procedure described in the previous section. Water in the bottom compartment was then replaced by approximately 0.5 molar potassium chloride solution using the special side-hole pipette arrangement shown in Fig. 4.8. The bottom plug was then inserted and the cell clamped into the thermostat bath, properly positioned and aligned /



aligned between the magnet rotating assembly.

A flask of degassed distilled water, fitted with the assembly for washing the top compartment of the diaphragm cell (Fig. 4.8) was also placed in the thermostat to equilibrate to temperature.

Diffusion in the cell was then allowed to proceed for a period of approximately 2 hours to establish a gradient. This prediffusion time,  $t_g$ , was estimated from Gordon's approximation<sup>7</sup>:

$$D t_g / \ell^2 = 1.2$$

It has been shown, however, that Gordon's prediffusion time may be considerably longer than that required for attainment of a 'steady-state', but varying the length of prediffusion period within reasonable limits will cause no significant error in the experimental results.<sup>6</sup> The period of 2 hours was therefore considered suitable both for establishment of a gradient and to bring the cell to temperature equilibrium. At the end of the prediffusion time, the top plug was carefully removed and the top compartment emptied with one of the special pipettes without displacing the cell from its position. The compartment was then filled with thermostated distilled water, directly transferred from the flask, by applying a mild pressure (Fig. 4.8 a). This rinsing procedure of emptying and filling the cell with distilled water was repeated four /

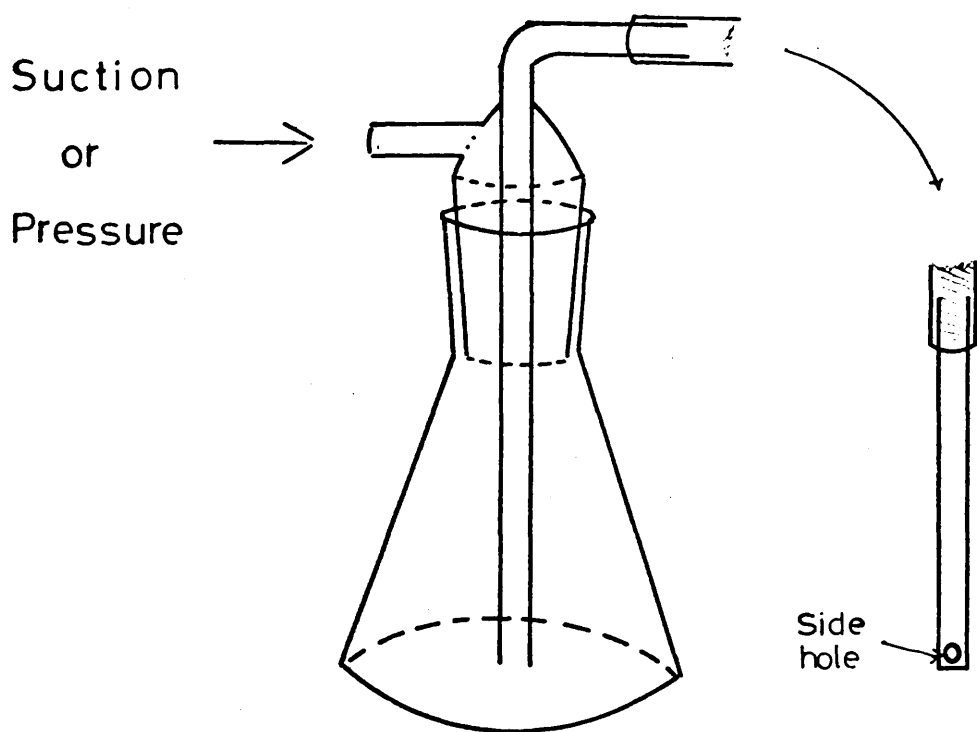


Fig. 4.8

Horizontal Flow Pipette Assembly

four to five times. At the final filling the time was recorded with a stopwatch, the top plug firmly seated and the volume of the top compartment made up to the mark. The experiment was then allowed to proceed for 46 to 48 hours.

At the end of a diffusion run, the top solution was transferred to a 50 ml stoppered flask with the side-hole pipette and kept for analysis. The cell was quickly removed from the thermostat, externally dried, then inverted and the valve of the bottom plug released. A slight pressure was then applied through one of the side holes in this plug, forcing a few ml of solution through the diaphragm and effectively quenching the diffusion process. The time was recorded and about 15 seconds added to compensate for the time loss in the latter operation. The bottom solution was then pipetted out in similar way to the top solution.

#### 4.3.10 Analyses of Potassium Chloride solutions and Calculation of the Cell Constant

Since accurate conductance data for potassium chloride solutions are available from measurements of Shedlovsky and Chambers<sup>43</sup> and Stokes and Stokes,<sup>44</sup> the concentrations  $C_T$  and  $C_B$  were determined from conductimetric analysis of weight-diluted samples of top and bottom solutions, by successive approximations. The values of equivalent conductance,  $\Lambda$ , were curve fitted /

fitted against the corresponding concentrations,  $C$ , by equation (4.58):

$$\Lambda_n = -2.17402 - 0.060649 C_n - 0.0015556 C_n^2 + 0.00032534 C_n^3$$

where  $C_n = \ln(C/d)$  and  $\Lambda_n = \ln(\Lambda d/1000)$

range of validity (0.01-0.1 mol.  $l^{-1}$ )

$$(\delta = \pm 0.00012) \quad 4.58$$

The density,  $d$ , being given by -

$$d = 0.9970874 + 0.04712739 (C/d) + 0.000445855 (C/d)^2$$

range of validity (0.01-0.6 mol.  $l^{-1}$ ) 4.59

$W_1$  gram of each solution of concentration  $C_1$  mol.  $l^{-1}$  and density  $d_1$  gm  $ml^{-1}$  were diluted with distilled water to give a concentration  $C_2$  (less than 0.1 mol.  $l^{-1}$ ) of total weight  $W$  and density  $d_2$ . The concentration of the original solution is then given by:

$$C_1 = (C_2/d_2)(W/W_1) d_1 \quad 4.60$$

The specific conductance,  $K_{sp}$ , equation (4.61), of the diluted solution was measured by the method described earlier.

$$K_{sp} /$$

$$K_{sp} = C_2 \Lambda / 1000 \quad 4.61$$

$$\text{thus } K_{sp} / 10^{-3} \Lambda d_2 = (C_2/d_2) \quad 4.62$$

An estimate was made of  $(C_2/d_2)$  for the solution whose specific conductance was measured. For this guess a value of  $10^{-3} \Lambda d_2$  was calculated from equation (4.58). From the measured specific conductance a first approximation of  $(C_2/d_2)$  was obtained from equation (4.62). This value of  $(C_2/d_2)$  was then used to repeat the iterations until a consistency of 0.02% was achieved. The original concentration of potassium chloride,  $C_1$ , was then calculated from equation (4.60), using equation (4.59). Having calculated the final concentrations  $C_T$  and  $C_B$  by this iterative method, the initial concentration  ${}^0C_B$  of the bottom solution was calculated from equation (4.56b). The cell constant,  $\beta$ , was then computed from the expressions (4.56), using the method described in section 4.2.7.  $\bar{D}$  values for use in equation (4.56a) were calculated from Robinson and Stokes data of  $\bar{D}^0(C)$  for potassium chloride in the concentration range 0.0 to 1.0 mol.  $l^{-1}$ .

A computer program, given in Appendix D.1, was written to perform the iterations and calculate the cell constant. The values of  $\bar{D}^0(C)$  were curve fitted against the corresponding concentrations by the method of least squares into polynomials of the type: /

type:

$$\bar{D}^0(c) = a_0 + \sum_{i=1}^n a_i c^i \quad 4.63$$

The coefficients of the polynomials, listed in table 4.1 are incorporated in the computer program.

Table 4.1

Coefficients of equation (4.63).

C (mol.l <sup>-1</sup> )	a <sub>0</sub>	a <sub>1</sub>	a <sub>2</sub>	a <sub>3</sub>
0.0 - 0.01	1.9834	-10.4036	978.602	-39220.0
0.01 - 0.1	1.9590	- 2.4101	27.3377	-118.482
0.1 - 0.5	1.90175	- 0.36375	0.8250	-0.6250
0.5 - 1.0	1.84273	0.000360167	0.018694	-0.0021745

#### 4.3.11 Preparation of Isotopically Labelled <sup>115</sup>CdI<sub>2</sub>.

Radioactive cadmium chloride (<sup>115m</sup>CdCl<sub>2</sub>), in 0.1 molar hydrochloric acid, was obtained from the Radiochemical Centre, Amersham, England.

Although, experimental cadmium iodide solutions were spiked with injections of 0.01 - 0.05 ml, the presence of HCl in the commercially available labelled cadmium chloride would cause a reduction of ca. 2 - 3 units in the pH of the diffusing solutions. The addition of excess chloride ions to the system was also considered undesirable. Accordingly, labelled cadmium iodide (<sup>115</sup>CdI<sub>2</sub>) was obtained from cadmium chloride by micro-electrolysis in the cell/

the cell shown in Fig. 4.9. The two compartments of the electrolysis cell, constructed from Pyrex glass, were separated by a small sintered disk of porosity no. 4. Each half of the cell had approximately one ml capacity and carried an electrode consisting of 3mm square of platinum foil, spot-welded to a platinum wire. The wire was passed through a 4cm long glass capillary tube which was sealed at both ends, leaving a centimeter length of bare wire at the top for electrical contact. The electrodes were cleaned by heating to redness for a short while in a flame, washing in dilute nitric acid and rinsing thoroughly with distilled water.

A relatively thick layer of cadmium metal was then electrodeposited on both electrodes from a 0.1 molar cadmium chloride solution, acidified with hydrochloric acid. A little hydrazine dihydrochloride was added to the electrolysing solution as an anodic depolariser. The electrolysis was continued for 3-4 hours, using a current of 3 mA from a constant current power supply. (Solartron P.S.U. AS 1413).

After both the electrodes had been coated with cadmium deposits, in a separate experiment, the cathodic compartment was injected with ~0.2 ml of radioactive cadmium<sup>115</sup>chloride. The electrolysis was continued for further 2-3 hours, checking the radioactivity of the electrode and the solution in the cathodic compartment, at regular intervals, with a Geiger-Müller counter. When maximum activity was transferred to the electrode, the/

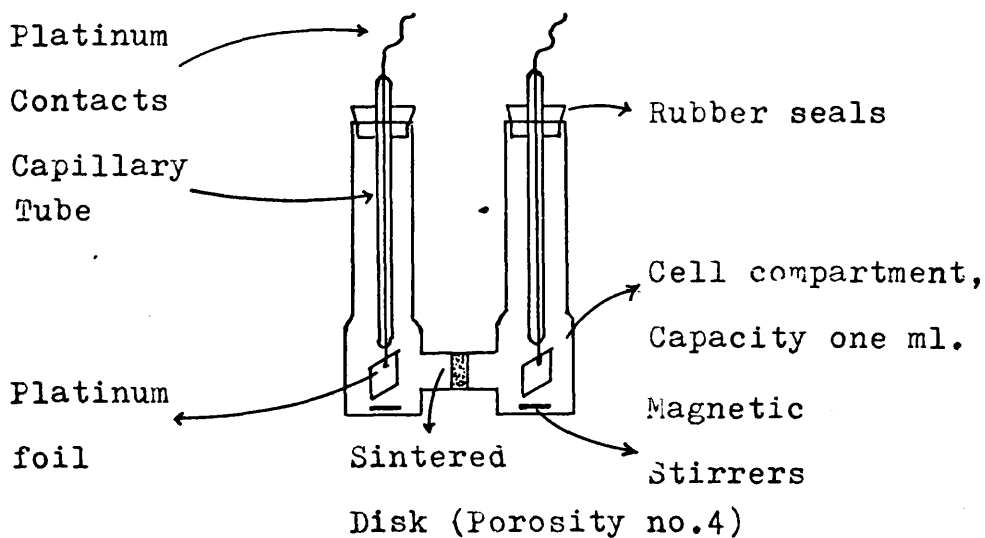


Fig. 4.9 - The electrolysis cell  
used for preparation of  
radioactive cadmium iodide.



the electrolysis was stopped. The solution in the cell compartments was replaced by 0.1 molar cadmium iodide, the polarity of the electrodes was reversed and the electrolysis of cadmium iodide solution carried out for a period of half hour. Sufficient activity is transferred to cadmium iodide during this time to provide samples for a diffusion run. (The pre-deposits of cadmium on both electrodes prevent the liberation of iodine during electrolysis of cadmium iodide solutions.).

The electrode was always kept coated with active cadmium and 0.5 ml radioactive cadmium iodide was prepared prior to every diffusion run.

An estimated 60-70% efficiency of electrolysis could be achieved by this method.

#### 4.3.12 Isotopic-Diffusion Experiments.

The 'Solvent-Filled' method described in section (4.2.8a) was adopted for isotopic-diffusion studies.  $^{22}\text{Na}^+$ , in 0.1 molar sodium chloride, was obtained from the Radiochemical Centre, Amersham, England. Sodium chloride, used for  $^{22}\text{Na}^+$  diffusion experiments, was recrystallised twice from distilled water, dried at  $130^\circ\text{C}$  and stored over silica gell in a vacuum desiccator.

Analar cadmium iodide, supplied by Hopkin and Williams Ltd., England, was used without further purification.

The cell filling procedure was the same as described in section (4.3.8) and injections of appropriate isotope/

isotope were made into the top compartment of the cell, using a Hamilton syringe fitted with Chaney adaptor.

Diffusion run was allowed to proceed for ca. 72-80 hours and 0.1 to 0.2 ml samples from both compartments were analysed using a model 3390 Packard Tri-Carb liquid scintillation spectrometer provided with an automatic sample changer and print-out device. Samples were added to 10ml aliquots of a dioxane-based liquid scintillator contained in special plastic vials. The scintillator had the composition,

40-50 gm	Naphtalene
4-6 gm	PPO
0.1-0.3 gm	Dimethyle POPOP
20 ml	Ethylene glycol
and 100 ml	Ethenol

per litre of 1-4 dioxane. The solvent, 1-4 dioxane, was purified by refluxing with 10 gm ferrous sulphate and 10 gm sodium metabisulphate per litre for one hour. The liquid was decanted and the dioxane distilled out collecting the fraction boiling between 101° and 102°C.

If this precaution was not taken, sever colour quenching was observed in  $\text{CdI}_2$  solutions reducing the counting efficiency by as much as 80-90%. Consequently, counting samples for cadmium iodide solutions were made in freshly prepared phosphor made in freshly distilled 1-4 dioxane.

Counting errors were reduced by diluting samples from the 'Hot' compartment to give approximately the same/

same rate of counting as the samples from the 'Cold' compartment.

The volume of radioactive samples in each analysis was adjusted such to give a rate of the order of  $10^5$ - $10^6$  cpm to minimise statistical errors.

Triplicate and quadruplicate samples of the same solution were analysed and a counting efficiency of 0.3-0.5 % was achieved.

#### 4.4 Results and Discussion

##### 4.4.1 Results of Calibration Experiments

The dimensions of the four cells, used for isotopic diffusion studies, are given in table (4.2).

The speeds of stirring usually chosen, in the Stokes type of diaphragm cell, are in the range 50-60 r.p.m. Since a modified method of stirring was used in this work, the effect of varying the stirring rate in the cell was studied by calibrating the cell with potassium chloride at three different speeds, table (4.3).

Table 4.3

Calibration results for the cell constant,  $\beta$ , at three different speeds.

r.p.m	$\beta$ (Cell no.III)	$\beta / \beta_{60}$
30	0.43202	0.99059
60	0.43612	1.00000
85	0.43576	0.99917

From this table, it is obvious that  $\beta$  is constant from 30-85 r.p.m. The pressure of the jet of water, for the four magnet driving devices, was therefore adjusted to obtain a stirring speed of  $60 \pm 3$  r.p.m in each cell and all subsequent measurements were made at this speed.

The cell constants, determined by the method described in section (4.3.9) are given in table (4.4). Duplicate determinations agreed to within 0.1 %.

It should be noted, however, that the more convenient method the 'Solvent-Filled Method' (Section (4.3.8).) was used / for

Table 4.2

Dimensions of the diaphragm cells used in this work.

Description		Cell No.			
		I	II	III	IV
* Volume of top compartment					
	$V_T$	56.73	53.37	50.04	58.58
* Volume of bottom compartment					
	$V_B$	55.03	54.96	54.84	53.69
* Volume of the diaphragm					
	$V_D$	1.512	1.400	1.279	1.595
$(V_T + \frac{1}{2}V_D)/(V_B + \frac{1}{2}V_D)$	$V$	1.0306	0.972	0.913	1.0898
$2V_D/(V_T + V_B)$		0.02706	0.02585	0.02439	0.02841
$(1 - \lambda/6)$		0.99549	0.99569	0.99594	0.99526
Diameter of the diaphragm					
	(mm)	40	40	40	40
Thickness of the diaphragm					
	(mm)	3	3	3	3
Length of the stirrers					
	(mm)	36	36	36	36

\*  $\delta V_T = \delta V_B = \sim 0.015$  ml;  $\delta V_D = 0.003$  ml.

Table 4.4

Results of a typical calibration run with potassium chloride

Description	Cell-I	Cell-II	Cell-III	Cell-IV
Time, t (seconds)	172131.0	172104.0	169900.0	173374.0
*Wt.(Top)	15.5524	16.9670	15.9755	15.7643
Wt. after dilution	48.1236	44.5607	43.9182	41.8984
K <sub>sp</sub> (Top)	0.0075641	0.0092004	0.0080771	0.0089810
Wt. (Bottom)	8.3659	7.7827	7.3214	11.1557
Wt. after dilution	36.6839	37.9709	47.7871	40.7936
K <sub>sp</sub> (Bottom)	0.0081706	0.0076742	0.0056981	0.0098289
V	1.0306	0.9720	0.9130	1.0898
Guess value ( <sup>0</sup> C <sub>B</sub> )	0.05	0.05	0.05	0.05
<sup>0</sup> C <sub>T</sub>	0.0	0.0	0.0	0.0
<sup>0</sup> C <sub>B</sub>	0.456952	0.465430	0.434141	0.476045
C <sub>T</sub>	0.177525	0.185019	0.168858	0.182542
C <sub>B</sub>	0.273924	0.285592	0.279889	0.277257
( <sup>0</sup> C <sub>B</sub> +C <sub>B</sub> )/2	0.365438	0.375511	0.357015	0.376651
( <sup>0</sup> C <sub>T</sub> +C <sub>T</sub> )/2	0.088762	0.092510	0.084429	0.091271
( <sup>0</sup> C <sub>B</sub> )/(C <sub>B</sub> -C <sub>T</sub> )	4.740171	4.627797	3.910088	5.026053
$\bar{D} \cdot \beta$	0.904005	0.890206	0.802566	0.931301
$\bar{D}$	1.839154	1.839305	1.839155	1.839335
** Cell constant, $\beta$	0.49131	0.48443	0.43638	0.50632
Deviation	±0.0002	±0.00044	±0.00026	±0.0006

\* Wt. is the weight of solution in grams, after vacuum corrections, taken from the top or bottom compartment.

\*\* Averaged values of duplicate determinations.

for the isotopic diffusion measurements of  $^{115}\text{Cd}^{2+}$  in cadmium iodide solutions. Although the error involved in neglecting the differences in the equations for the two procedures is of the order of 0.3% , proper corrections for the  $(1-\lambda/6)$  terms of equation (4.54) were applied and the 'Solvent-Filled' method was tested by studying the diffusion of  $^{22}\text{Na}^{+}$  ion in 0.1, 0.4 and 1.0 molar sodium chloride solutions. The results of these calibration experiments are given in table (4.5), where it can be seen that the two results are within the error limits of the two sets of measurements.

Table 4.5

Results of isotopic diffusion of  $^{22}\text{Na}^{+}$   
in sodium chloride solutions.

Concentration ( C, mol.l <sup>-1</sup> )	Diffusion coefficients ( D x 10 <sup>-5</sup> cm <sup>2</sup> s <sup>-1</sup> )	
	I	II
0.1	1.330	
0.4	1.279	1.283 (1.278)*
1.0	1.199	1.234

I This work (Experimental uncertainty  $\pm$  0.5%)

II Mills et al.<sup>9,23</sup> ( " " " " )

\* Mills, Woolf and Watts<sup>35</sup> measurement; the  
'Solvent-Filled Method' was used.

#### 4.4.2 Isotopic Diffusion Coefficients for Cadmium in Aqueous Cadmium Iodide

The results of diffusion experiments are given in table (4.6) and Fig. 4.10. The variation of  $D_{aa}$  with increasing concentration of the salt is remarkably complex and must be regarded as quite anomalous when compared with literature data for ionic isotopic diffusion coefficients for dissociated electrolytes. In Fig. 4.10 sodium ion diffusion coefficients<sup>9</sup> are given as a function of sodium chloride concentration for comparison.

Before discussing the fluctuations in  $D_{aa}$ , it is noteworthy that all experimental values are lower than the infinite dilution value,  $D_{aa}^0$  ( $7.12 \times 10^{-6} \text{ cm}^2 \text{ s}^{-1}$ ), calculated from the limiting equation given below.

$$D_{aa}^0 = RT^0 \lambda_a / |Z_a| F^2 \quad 4.64$$

(In this equation the equivalent conductance of the cadmium ion at infinite dilution,  $\lambda_a^0$ , was taken as  $53.5 \text{ cm}^2 \text{ ohm}^{-1} \text{ equiv.}^{-1}$ , from the conductance measurements of Matheson<sup>44</sup>.)

Olsztajin, Turq and Chemla,<sup>45</sup> in their studies of the diffusion of  $^{115}\text{Cd}^{2+}$  in increasingly concentrated potassium chloride, have observed a similar increase in  $D_{aa}$ , above the infinite dilution value. The diffusion coefficient increased smoothly with increasing concentration of the supporting electrolyte. These authors tentatively/



Table 4.6

Isotopic diffusion coefficients of  $^{115}\text{Cd}^{2+}$  in cadmium iodide solutions together with mobilities and isotope-isotope coupling terms, defined by equation (4.1).

$C_a^T \times 10^3$ mol.cm <sup>3</sup>	$D_{aa} \times 10^6$ cm <sup>2</sup> s <sup>-1</sup>	$D_{aa}/RT$ x 10 <sup>9</sup>	$L_{aa}^T/C_a^T$ x 10 <sup>9</sup>	$-(L_{aa}^*/\rho\rho^*)/C_a^T$ x 10 <sup>9</sup>
0.0	7.122	2.8730	2.8730	0.0000
0.10	7.860	3.1708	3.0370	0.1338
0.15	*7.436	2.9997	2.9788	0.0209
0.20	7.422	2.9941	2.8940	0.1001
0.30	*7.898	3.1861	2.7390	0.4471
0.40	8.114	3.2732	2.6318	0.6414
0.50	7.884	3.1804	2.5706	0.6098
0.60	*7.164	2.8904	2.6478	0.3426

The experimental uncertainty in  $D_{aa}$  is  $\pm 0.5\%$  and in  $L_{aa}^T/C_a^T$  estimated to be  $\pm 1.0\%$  thus the isotope-isotope coupling term, in the final column, is uncertain to  $\pm 0.04 \times 10^{-9}$  units.

The dimensions of  $L_{aa}^T$  and  $L_{aa}^*$  are mol<sup>2</sup> cm<sup>-1</sup> s<sup>-1</sup> J<sup>-1</sup>.

\* Averaged values of  $D_{aa}$  from duplicate determinations within 0.5%.

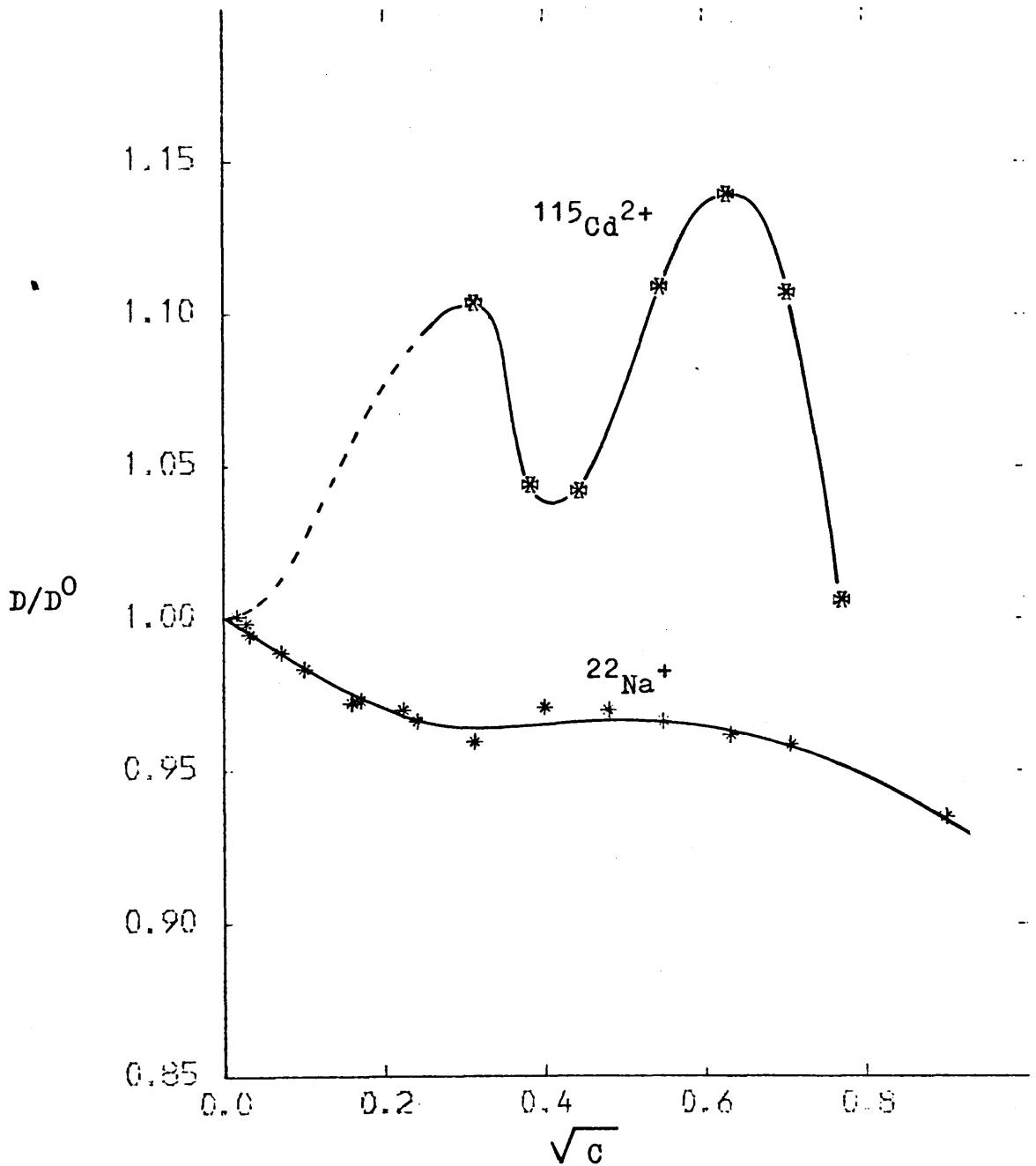


Fig. 4.10— Comparison of isotopic diffusion coefficients of cadmium with those of sodium<sup>9</sup> as a function of the square root of concentration.

tentatively ascribed the effect to the increased concentration of the solvent structure breaking complex,  $\text{CdCl}_4^{2-}$  in these solutions.

The variations in cadmium diffusion coefficients as a function<sup>of</sup> cadmium iodide concentration is obviously too complicated to be ascribed to the effect of a single ion complex. In the range 0.1 to 0.6 molar,  $D_{aa}$  passes through a minimum at 0.2 molar, rises to a maximum at 0.4 molar and falls once more to the value at 0.6 molar. In the range from infinite dilution to 0.1 molar, no experimental data are available, but it is obvious from Fig. 4.10 that  $D_{aa}$  must pass through a maximum between 0.1 mol.l<sup>-1</sup> (the lowest measured value) and the infinite dilution value,  $D_{aa}^0$ , equals  $7.12 \times 10^{-6} \text{ cm}^2 \text{ s}^{-1}$ , from equation (4.64).

To explain these effects a predictive calculation has been made, using the irreversible thermodynamic analysis given in section (4.1.1).

#### 4.4.3 Calculation of the Isotope-Isotope Coupling Terms

In section (4.1) of this chapter, it was shown that the isotopic diffusion coefficient,  $D_{aa}$ , of cadmium in cadmium iodide may be represented by equation (4.1) reproduced below.

$$D_{aa} = RT (L_{aa}^T / C_a^T - 1 / C_a^T \cdot (L_{aa}^* / \rho \rho^*)) \quad 4.1$$

The second term in equation (4.1), the isotope-isotope coupling term, was equated to a summation of coupling coefficients/

coefficients between all labelled and unlabelled cadmium containing species in this complexed system, equation (4.35). In very dilute solutions, where complexing is negligible  $L_{aa}^*$  is simply  $l_{aa}^*$ , the coupling coefficient between free cadmium ions, labelled and unlabelled. As complexing increases and concentrations of the species of the type  $(CdI_x)^{2-x}$  become significant, then additional terms, which allow for complex-to-complex interactions become increasingly important.

The binary coefficients  $L_{aa}^T$  of equation (4.1), discussed in chapter 3, are available from the experimental studies of Paterson, Anderson and Anderson<sup>46</sup> made in this laboratory. From these and the corresponding diffusion coefficients,  $D_{aa}$ , the isotope-isotope coupling term can be calculated, using equation (4.1). These coefficients are given in table (4.6).

Before discussing the results, a mention will be given to the units which have been used in these calculations. In normal practice the flow of a species,  $J_i$ , is defined as the molar flux through a one centimeter square area, normal to the direction of that flux, in unit time; dimensions,  $\text{mol.cm}^2 \text{s}^{-1}$ . The forces  $X_i$  have the dimensions  $\text{J mol}^{-1}\text{cm}^{-1}$  and are the gradients of electrochemical potential. Since the mobility coefficients are of the dimensions of  $J_i/X_i$ , the units for  $L_{ik}$  are  $\text{mol}^2 \text{cm}^{-1} \text{s}^{-1}\text{J}^{-1}$ . The diffusion coefficient  $D_{aa}$  therefore has the required dimensions ( $\text{cm}^2 \text{s}^{-1}$ ) if the concentration of the total cadmium,  $C_a^T$ , is expressed in  $\text{mol.cm}^{-3}$ .

In/

In Fig. 4.11, values of  $D_{aa}$  and  $RT L_{aa}^T / C_a^T$  are plotted against the square root of the molarity of cadmium iodide. From equation (4.1) the isotope-isotope coupling term  $-RT(L_{aa}^* / \rho \rho^*) / C_a^T$  is obtained by difference and is represented by the shaded area of the figure. In the experimental region ( $0.1-0.6 \text{ mol.l}^{-1}$ )  $L_{aa}^T / C_a^T$  exhibits a smooth decline with increasing concentration and so contributes a downward trend to  $D_{aa}$ . The variation in  $D_{aa}$  with increase in concentration (above  $0.1 \text{ mol.l}^{-1}$ ) is therefore due to the minimum and subsequent maximum observed in the coupling term  $-(L_{aa}^* / \rho \rho^*) / C_a^T$ , Figs. 4.11 and 4.12. It is therefore to this term that we must look for an interpretation of the anomalous variations in  $D_{aa}$ .

As mentioned above, in dilute solutions (below  $0.1 \text{ mol.l}^{-1}$ ) experimental values of  $D_{aa}$  are not available, due to the intrinsic limitations of the diaphragm cell method. In this region, however,  $L_{aa}^T / C_a^T$  has been shown to pass through a minimum, chapter 3. From equation (4.1), therefore, it is obvious that an initial increase in  $D_{aa}$  above the infinite dilution value can only be possible if the isotope-isotope coupling term  $-1/C_a^T (L_{aa}^* / \rho \rho^*)$  rises steeply from zero. As concentration is increased this coupling term passes through a maximum (at  $0.1 \text{ mol.l}^{-1}$ ), a minimum (at  $0.15 \text{ mol.l}^{-1}$ ) and a maximum once more at  $0.4 \text{ mol.l}^{-1}$ , Fig. 4.12, table (4.6).

The complex variations in  $L_{aa} / \rho \rho^*$  therefore determine the major trends in concentration dependence of/

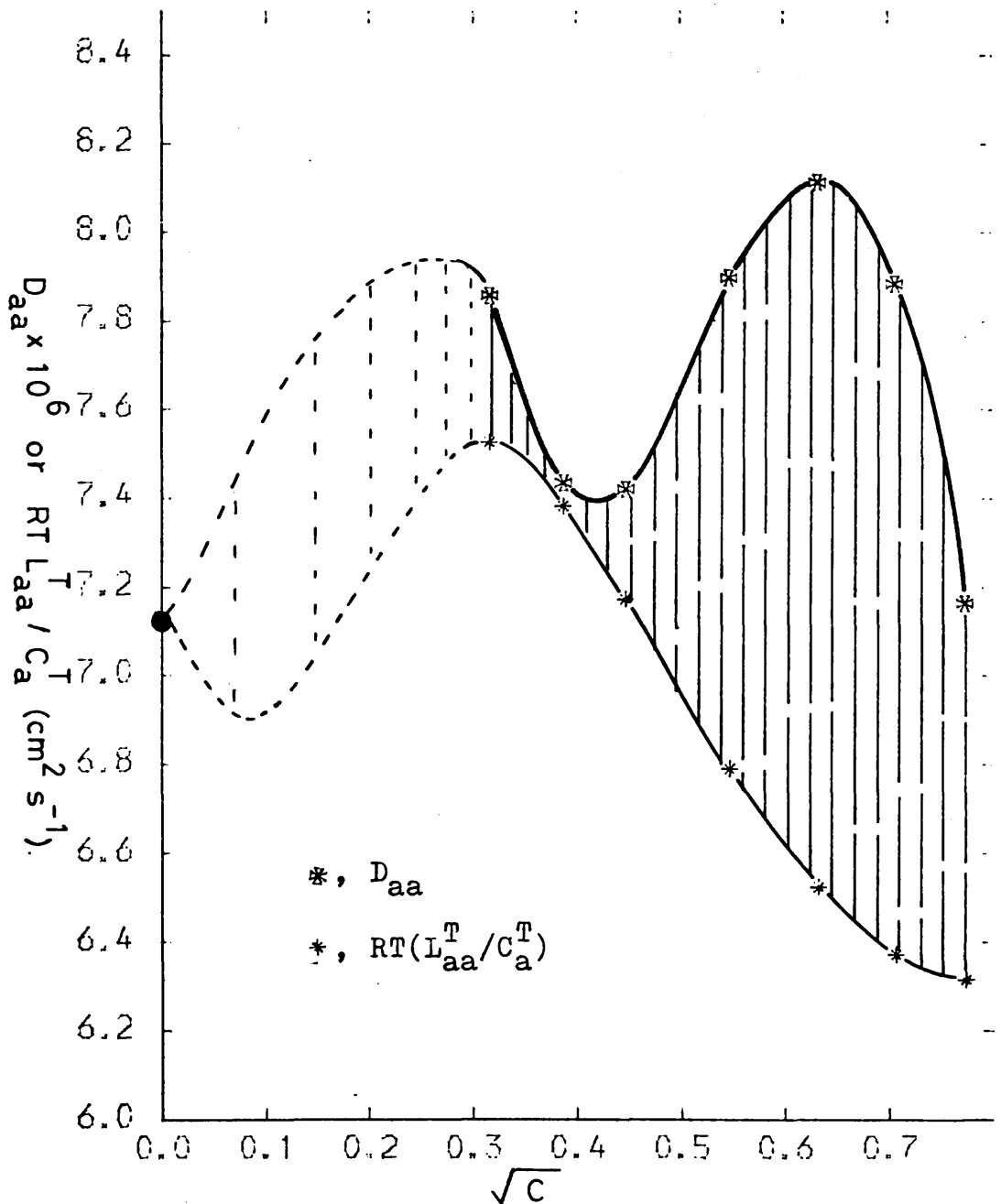


Fig. 4.11 - Cadmium iodide: Isotopic diffusion coefficients,  $D_{aa}$ , and the contribution of the thermodynamic terms,  $RT L_{aa}^T / C_a^T$ . The shaded area representing the difference between the two curves is a measure of the isotope-isotope coupling contribution  $-RT (L_{aa}^* / \rho \rho^*) / C_a^T$ .

of the experimental diffusion coefficients. Although there is little possibility of explaining the variations in this function in the higher concentration range (above  $0.1 \text{ mol.l}^{-1}$ ), experience of predictive calculations for the binary coefficients of this salt lead us to believe that theoretical predictions based upon the Onsager Limitin Laws (as expressed by Pikal) would prove interesting in dilute solutions.

#### 4.4.4 Prediction of the Isotope-Isotope Coupling Coefficients

In the theoretical section it was shown that the isotope-isotope coupling contribution, which has been evaluated from experimental data, can be expressed as a summation.

Comparing equations (4.1) and (4.35):

$$C_a^T L_{aa}^*/C_a^0 C_a^* = ((L_{aa}^*/\rho\rho^*)/C_a^T) = \sum_{k=a}^4 \sum_{i=a}^4 ((\ell_{ki}^*/\rho\rho^*)/C_a^T)$$

4.66

The  $\ell_{ki}^*$  coefficients define the coupling between species  $k$  (unlabelled) and species  $i^*$  (labelled). It has been shown above that the isotope-isotope coupling term largely determines the complex variation of the cadmium diffusion coefficient,  $D_{aa}$ , with concentration.

Pikal, in his analysis of coupling coefficients, has used the Limiting Laws equations of Fuoss and Onsager to obtain a general expression for such coefficients, equation (4.67).

$$10^{12} \ell_{ik}^*/$$

$$10^{12} \ell_{ik}^* / \sqrt{c_i^0 c_k^*} = A \sqrt{\mu_i^0 \mu_k^*} [B] I^{\frac{1}{2}} \quad 4.67$$

The units of  $\ell_{ik}^*$  are those used in this study ( $\text{mol}^2 \text{cm}^{-1} \text{s}^{-1} \text{J}^{-1}$ ) but concentrations are expressed in molar units.  $A$  is a constant (0.1074),  $[B]$  is a combination of relaxation and electrophoretic terms, discussed below and  $I$  is the true ionic strength of the solution, equation (4.68).

$$I = \frac{1}{2} \sum (c_j^0 + c_j^*) z_j^2 \quad (j=a,1,2,3,4,b) \quad 4.68$$

$\mu_j$  is defined by Pikal as the ionic strength fraction, equation (4.69).

$$\mu_j = c_j^0 z_j^2 / \sum (c_j^0 + c_j^*) z_j^2 = c_j z_j^2 / 2I \quad 4.69$$

Thus in equation (4.67)

$$\sqrt{\mu_i^0 \mu_k^*} = \sqrt{c_i^0 c_k^*} |z_i z_k| / 2I \quad 4.70$$

From equations (4.67), (4.70) and (4.5), equation (4.71) is obtained in the same mathematical form as equation (4.35).

$$10^{12} k_i^* / \rho \rho^* = A c_i c_k \frac{|z_i z_k|}{2I} [B] I^{\frac{1}{2}} \quad 4.71$$

The term  $[B]$  used in these equations is defined by Pikal, equation (4.72).

$$[B] = (x/y A_{ik}^* - (B_0/2) z_i z_k) \quad 4.72$$

Where terms in  $A_{ik}^*$  and  $B_0$  involve the relaxation and electrophoretic effects respectively.

In/



In equation (4.72),  $x = \lambda_i \lambda_k / |Z_i| Z_k^*$ , it is assumed from the postulated identical chemical characteristics of labelled and unlabelled species that  $\lambda_j = \lambda_j^*$  where  $\lambda_j$  is the equivalent conductance of the ion at infinite dilution, and  $y = \sum \mu_j \lambda_j / |Z_j|$ , where the summation is over all species, labelled and unlabelled, in the solution. From equations (4.69) and (4.4):

$$y = \left( \sum_{j=a}^b C_j |Z_j| \lambda_j \right) / 2I \quad 4.73$$

Pikal has shown that  $A_{ik}^* = a_{ik} |Z_i Z_k|$  where  $a_{ik}$  at 25°C is a constant, 0.22962. Similarly  $B_0$  is a constant, 60.495.

Thus equation (4.73) becomes:

$$[B] = \left[ \frac{2 \lambda_i \lambda_k I a_{ik}}{\sum_{j=a}^b C_j |Z_j| \lambda_j} - (B_0/2) Z_i Z_k \right] \quad 4.74$$

Combination of equations (4.67) and (4.74) gives:

$$10^{12} \ell_{ik}^* / \rho \rho^* = \left[ \frac{|Z_i C_i| |Z_k C_k| \lambda_i \lambda_k A a_{ik}}{\sum_{j=a}^b C_j |Z_j| \lambda_j} \right] I^{\frac{1}{2}}$$

(relaxation term)

$$+ \left[ - |Z_i C_i| |Z_k C_k| (Z_i Z_k) A B_0 / 4 \right] I^{-\frac{1}{2}}$$

(electrophoretic term)

4.75

The relaxation/

The relaxation contribution to  $l_{ik}^*$  increases while the electrophoretic term decreases with increasing ionic strength. Furthermore, although the relaxation term is always positive the sign of the electrophoretic contribution will depend upon that of the valency product  $Z_i Z_k$ . Pikal's analysis deals solely with interionic coupling and so ignores the coupling coefficients  $l_{2j}^*$  and  $l_{j2}^*$  of equation (4.76). Equally since it is based upon the Limiting Law it is precise only in very dilute solutions. With these two limitations however, it remains the most viable method for estimation of these coupling terms.

Expanding the summations of equation (4.66):

$$\sum_{k=a}^4 \sum_{i=a}^4 (l_{ki}^* / \rho \rho^*) / C_a^T = 1 / C_a^T \cdot 1 / \rho \rho^* \times$$

$$\begin{aligned} & ( l_{aa}^* + l_{a1}^* + l_{a2}^* + l_{a3}^* + l_{a4}^* \\ & + l_{1a}^* + l_{11}^* + l_{12}^* + l_{13}^* + l_{14}^* \\ & + l_{2a}^* + l_{21}^* + l_{22}^* + l_{23}^* + l_{24}^* \\ & + l_{3a}^* + l_{31}^* + l_{32}^* + l_{33}^* + l_{34}^* \\ & + l_{4a}^* + l_{41}^* + l_{42}^* + l_{43}^* + l_{44}^* ) \end{aligned}$$

4.76

These  $l_{ik}^*$  coefficients of equation (4.76) were evaluated using equation (4.75) and the optimised  $\lambda_i$  values, obtained in chapter 3. The results are given in table (4.7),/

in table (4.7), where the matrices of  $\ell_{ik}^*$  coefficients are displayed in the formate of equation (4.76).

The negative  $\ell_{ik}^*$  coefficients are seen to be seperated into two groups at the upper left and lower right quadrants of the matrix. These involve positive-to-positive ion and negative-to-negative ion interactions respectively. In dilute solutions, where higher complexes are not present in significant proportions, the negative contributions to  $1/C_a^T L_{aa}^*/\rho\rho^*$  are largely  $(\ell_{aa}^* + 2\ell_{a1}^* + \ell_{11}^*)$ . Only in the highest concentrations considered do the negative-negative ion interactions  $(\ell_{33}^* + 2\ell_{34}^* + \ell_{44}^*)$  contribute significantly.

The positive contributions are due solely to positive-to-negative ion coupling interactions  $2(\ell_{3a}^* + \ell_{31}^* + \ell_{4a}^* + \ell_{41}^*)$ . In the lower concentration range, below  $0.07 \text{ mol.l}^{-1}$  negative terms dominate, table (4.7).

As complexing becomes more significant the positive-to-negative coupling interactions increase disproportionately in magnitude and ultimately at concentration greater than  $0.07 \text{ mol.l}^{-1}$  the predicted value of  $1/C_a^T L_{aa}^*/\rho\rho^*$  become positive.

In Fig. 4.12 the predicted and experimental isotope-isotope coupling terms are compared. It is observed that in dilute solutions up to  $0.07 \text{ mol.l}^{-1}$  the calculation predicts a maximum in  $L_{aa}^*/\rho\rho^*$  which was expected and effectively interpolates the function between the lowest experimental value and infinite dilution.

As for/

Table 4.7

The component coefficients  $l_{ik}^*$ , displayed in the formate of equation (4.76), for individual concentrations, N.

N = 0.003

-7.40597E-04	-1.53919E-04	1.56066E-06	2.27328E-07
-1.53919E-04	-3.16554E-05	3.48424E-07	5.05351E-08
1.56066E-06	3.48424E-07	-1.55138E-09	-2.41624E-10
2.27328E-07	5.05351E-08	-2.41624E-10	-3.73335E-11

N = 0.005

-1.13392E-03	-3.38795E-04	7.82327E-06	1.81425E-06
-3.38795E-04	-1.00197E-04	2.50770E-06	5.79094E-07
7.82327E-06	2.50770E-06	-2.58272E-08	-6.39498E-09
1.81425E-06	5.79094E-07	-6.39498E-09	-1.57123E-09

N = 0.01

-1.87303E-03	-8.73612E-04	5.76232E-05	2.45372E-05
-8.73612E-04	-4.03415E-04	2.88000E-05	1.22126E-05
5.76232E-05	2.88000E-05	-8.59336E-07	-3.90197E-07
2.45372E-05	1.22126E-05	-3.90197E-07	-1.75845E-07

N = 0.02

-2.99609E-03	-1.98470E-03	3.23005E-04	2.37355E-04
-1.98470E-03	-1.30158E-03	2.29341E-04	1.67822E-04
3.23005E-04	2.29341E-04	-1.68330E-05	-1.31935E-05
2.37355E-04	1.67822E-04	-1.31935E-05	-1.02629E-05

N = 0.03

-4.05779E-03	-3.09545E-03	7.72356E-04	7.47019E-04
-3.09545E-03	-2.33711E-03	6.32372E-04	6.09037E-04
7.72356E-04	6.32372E-04	-7.00018E-05	-7.23252E-05
7.47019E-04	6.09037E-04	-7.23252E-05	-7.41438E-05

N = 0.04

-5.17990E-03	-4.22966E-03	1.36061E-03	1.56591E-03
-4.22966E-03	-3.41723E-03	1.19436E-03	1.36866E-03
1.36061E-03	1.19436E-03	-1.67194E-04	-2.05917E-04
1.56591E-03	1.36866E-03	-2.05917E-04	-2.51561E-04

(Continued)

Table 4.7 Continued

N = 0.05

-6.39945E-03	-5.40769E-03	2.06094E-03	2.68705E-03
-5.40769E-03	-4.51986E-03	1.87516E-03	2.43415E-03
2.06094E-03	1.87516E-03	-3.05085E-04	-4.26428E-04
2.68705E-03	2.43415E-03	-4.26428E-04	-5.91051E-04

N = 0.06

-7.72978E-03	-6.63969E-03	2.85876E-03	4.10317E-03
-6.63969E-03	-5.63948E-03	2.64794E-03	3.78374E-03
2.85876E-03	2.64794E-03	-4.78002E-04	-7.36748E-04
4.10317E-03	3.78374E-03	-7.36748E-04	-1.12575E-03

N = 0.07

-9.17709E-03	-7.93051E-03	3.74454E-03	5.81105E-03
-7.93050E-03	-6.77458E-03	3.49412E-03	5.39814E-03
3.74454E-03	3.49412E-03	-6.80283E-04	-1.13548E-03
5.81105E-03	5.39814E-03	-1.13548E-03	-1.87839E-03

N = 0.09

-1.24373E-02	-1.06978E-02	5.75554E-03	1.00795E-02
-1.06978E-02	-9.09126E-03	5.35842E-03	9.34112E-03
5.75554E-03	5.35842E-03	-1.15453E-03	-2.18070E-03
1.00795E-02	9.34112E-03	-2.18070E-03	-4.08039E-03

N = 0.1

-1.42531E-02	-1.21749E-02	6.87161E-03	1.26372E-02
-1.21749E-02	-1.02727E-02	6.35990E-03	1.16422E-02
6.87161E-03	6.35990E-03	-1.41932E-03	-2.81865E-03
1.26372E-02	1.16422E-02	-2.81865E-03	-5.54404E-03

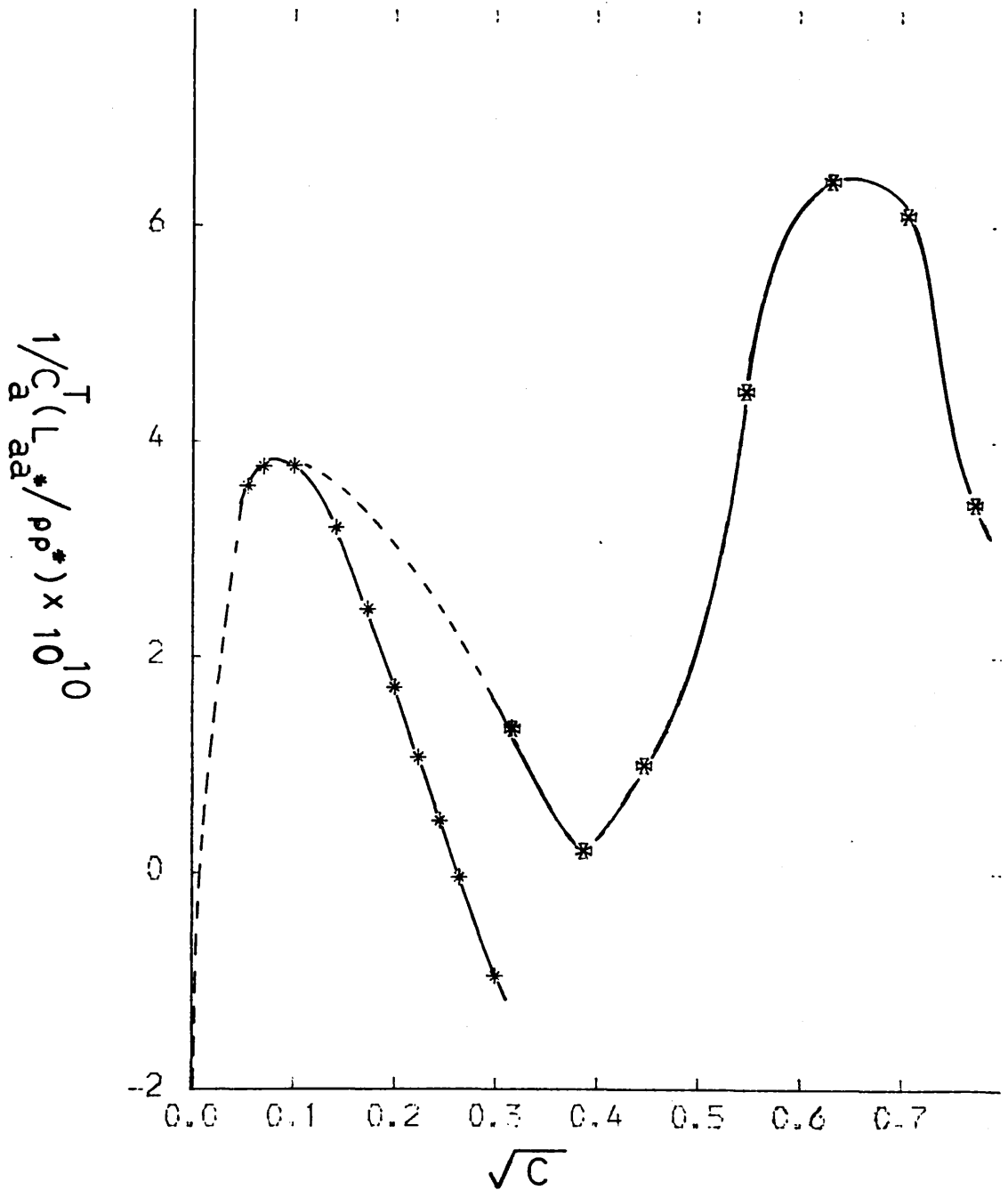


Fig. 4.12 — Isotope-isotope coupling coefficients,  $-(1/C_a^T)L_{aa}^*/\rho\rho^*$ , as a function of square root concentration, for cadmium iodide. \*, experimental values, obtained from equation (4.1); \*, calculated from equation (4.35). The optimised values of  ${}^0\lambda_i$ , obtained in chapter 3, were used to calculate both the intrinsic mobilities and the isotope-isotope coupling terms, using equation (4.67).

As for the prediction of binary  $L_{ik}$  coefficients, chapter 3, the agreement between the observed coefficients and those calculated become progressively poorer as the concentration increases above  $0.06 \text{ mol.l}^{-1}$ . ( Additional calculations in which  $\lambda_{\text{CdI}^+}$  was varied, as in chapter 3, showed no significant variations in the concentration dependence of  $L_{aa}^*/\rho\rho^*$ ).

The limiting Law predicts that the terms  $-L_{aa}^*/\rho\rho^*$  will become progressively more positive as concentrations increase above  $0.1 \text{ mol.l}^{-1}$ , while the experimental values are shown to remain positive and to pass through a maximum, Fig. 4.12.

#### 4.4.5 Prediction of Isotopic Diffusion, $D_{aa}$

With the validity of the calculation method justified, at least as regards dilute solutions, it was of interest to predict the isotopic diffusion coefficient,  $D_{aa}$ . These diffusion coefficients may be obtained by combining the calculated values of  $L_{aa}^T$  (denoted by  $L_{11}$  in chapter 3) and  $L_{aa}^*/\rho\rho^*$  obtained here. In each case the optimised values of  $\lambda_i$  were used in the Pikal evaluation of the component  $\ell_{ik}$  and  $\ell_{ik}^*$  coefficients.

The results of these calculations are given in table (4.8) and Fig. 4.13. The calculated diffusion coefficients are shown to increase initially as the concentration is increased from infinite dilution and to pass through a maximum value as inferred in the discussion/

Table 4.8

Predicted diffusion coefficients for isotopic cadmium in the dilute solutions range  $0.003-0.1 \text{ mol.l}^{-1}$  of cadmium iodide are given below.

The values of  $(1/C_a^T) L_{aa}^*/\rho\rho^*$  were obtained from equation (4.76), using optimised values of  ${}^0\lambda_i$  (Chapter 3, table (3.4).)

$C_a^T \times 10^3$ mol. $\text{cm}^3$	$(1/C_a^T) L_{aa}^*/\rho\rho^*$ $\times 10^{10}$	$L_{aa}^T/C_a^T$ $\times 10^9$	$D_{aa} \times 10^6$ (Predicted)
0.003	-3.5857	2.7382	7.677
0.005	-3.7726	2.7579	7.772
0.01	-3.7791	2.7903	7.854
0.02	-3.2027	2.8587	7.882
0.03	-2.4510	2.9328	7.878
0.04	-1.7270	2.9993	7.863
0.05	-1.0738	3.0551	7.840
0.06	-0.4898	3.1015	7.810
0.07	0.03619	3.1404	7.776
0.09	0.94986	3.2006	7.698
0.10	1.35455	3.2243	7.657

$L_{aa}^T/C_a^T$ , tabulated in the third column of this table, equals  $2 \times L_{11}/N \times 10^3$  obtained with optimised values of  ${}^0\lambda_i$  (Chapter 3, table (3.5).).



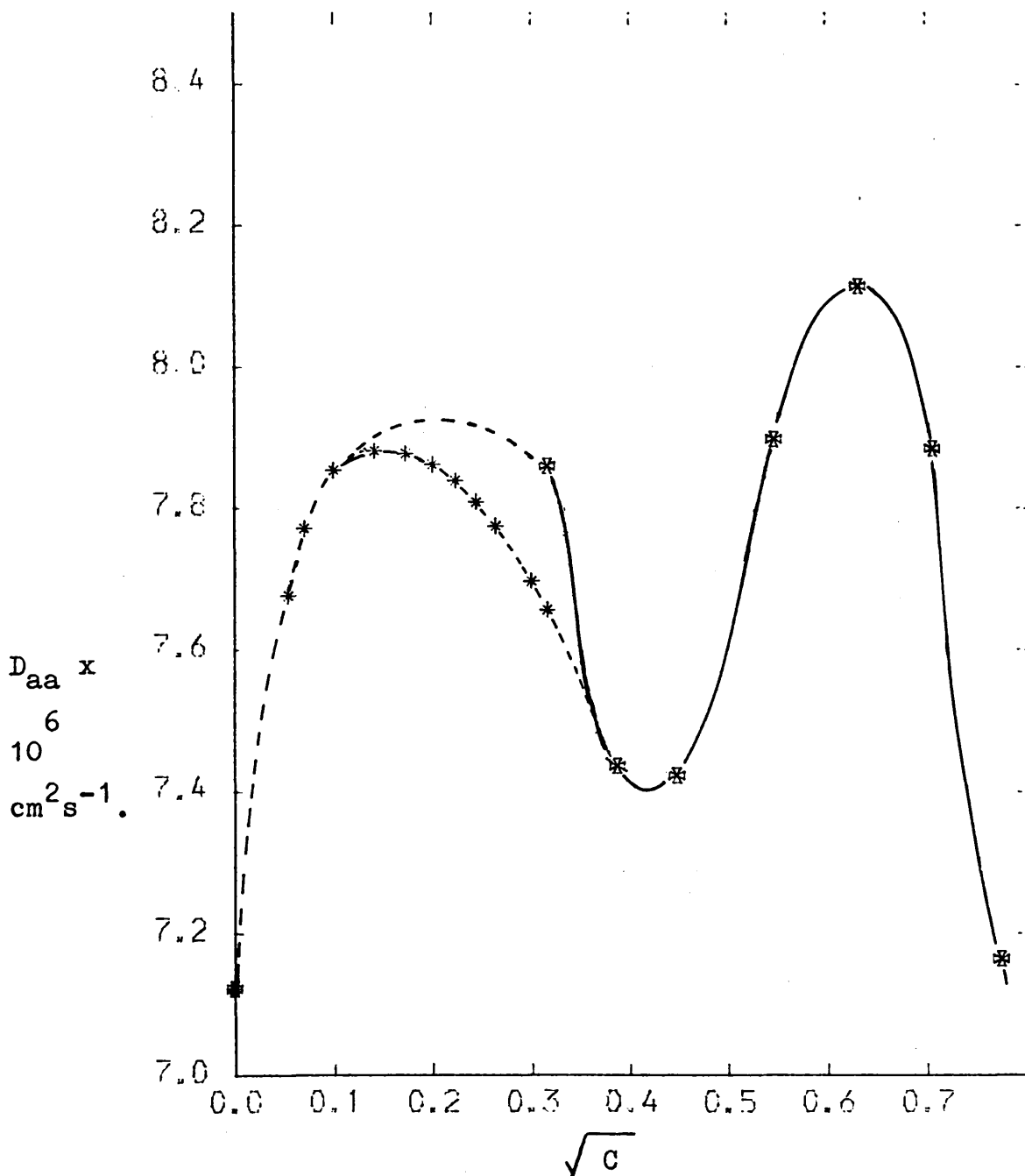


Fig. 4.13 - Isotopic diffusion coefficients,  $D_{aa}$ , for  $^{115}\text{Cd}^{2+}$  ions in aqueous cadmium iodide.

Observed and calculated diffusion coefficients are represented by \* and x respectively.

discussion of experimental data, given earlier (Section (4.4.2)). At  $0.1 \text{ mol.l}^{-1}$  the predicted diffusion coefficient is only 2.5% lower than that observed.

Thus, in the region below  $0.1 \text{ mol.l}^{-1}$ , it is seen that the predicted diffusion coefficient has the expected concentration dependence and is semi-quantitative.

This calculation, taken with those for the predictions of binary transport data for cadmium iodide, shows that the classical laws of transport in dilute solution may be applied with considerable success to the prediction of both isotopic diffusion and the binary solution transport parameters, conductance, transport number and salt diffusion coefficient.

Irreversible thermodynamics provides the theoretical bases of these calculations and the relationships between  $L_{ik}$  and  $\ell_{ik}$  coefficients are mathematical identities independent of any assumptions other than that of local equilibrium within the system.

Although the Onsager Limiting theory as expressed by Pikal's equations is truly valid only at or near infinite dilution, these irreversible thermodynamic methods allow semi-quantitative predictions of transport data for cadmium iodide up to  $0.06 \text{ mol.l}^{-1}$ . In addition to its predictive element the method also allows assessment of what are the most important factors in determining transport in such complexed systems.

References for Chapter 4

1. Anderson, J. and Paterson, R.,  
J. Chem. Soc., Farad. Trans. I, 1975, 71, 1335.
2. Kedem, O. and Essig, A.,  
J. Gen. Physiol., 1965, 48, 1047.
3. Evans, D.F. and Matesich, M.A.,  
'Techniques of Electrochemistry', Vol.2, Chapter 4,  
Wiley-Interscience, 1973.
4. Longsworth, L.G., Ann. N.Y. Acad. Sci., 1945, 46, 211.
5. Robinson, R.A. and Stokes, R.H.,  
'Electrolyte Solutions', 2nd Ed., Butterworths, London,  
1970.
6. Mills, R. and Woolf, L.A. 'The Diaphragm Cell',  
Diffusion Research Unit, The Australian National  
University, Canberra, A.C.T., Australia, 1968.
7. Gordon, A.R., Ann. N.Y. Acad. Sci., 1945, 46, 285.
8. Stokes, R.H., J. Amer. Chem. Soc., 1950, 72, 763.
9. Mills, R., Rev. Pure and Appl. Chem., 1961, 11, 78.
10. Goüy, G.L., Compt. rend., 1880, 90, 307.
11. Gosting, L.J. and Onsager, L.,  
J. Amer. Chem. Soc., 1952, 74, 6066.
12. Culson, C.A., Cox, J.T., Ogston, A.G. and Philpot,  
J.St.L., Proc. Roy. Soc.(London), 1948, 192A, 382.
13. Kegeles, G. and Gosting, L.J.,  
J. Amer. Chem. Soc., 1947, 69, 2516.
14. Longsworth, L.G., J. Amer. Chem. Soc., 1947, 69, 2510.

## References cont.

15. Philpot, J.St.L. and Cook, G.H.,  
Research, 1948, 1, 234.
16. Longsworth, L.G., Rev. Sci. Inst., 1950, 21, 524.
17. Harned, H.S. and French, D.M.,  
Ann. N.Y. Acad. Sci., 1945, 46, 267.
18. Harned, H.S. and Nuttall, R.L.,  
J. Amer. Chem. Soc., 1947, 69, 736.
19. Wall, F.T., Grieger, P.F. and Childers, C.W.,  
J. Amer. Chem. Soc., 1952, 74, 3562.
20. Nelson, F., J. Polym. Sci., 1959, 40, 563.
21. Marcinkowsky, A.E., Nelson, F. and Kraus, K.A.,  
J. Phys. Chem., 1965, 66, 1960.
22. Anderson, J.S. and Saddington, K.,  
J. Chem. Soc., 1949, S, 381.
23. Mills, R., J. Amer. Chem. Soc., 1955, 77, 6116.
24. Wang, J.H., J. Amer. Chem. Soc., 1951, 73, 510.
25. Mills, R. and Kennedy, J.W., *ibid.*, 1953, 75, 5696.
26. Mills, R. and Adamson, A.W., *ibid.*, 1955, 77, 3454.
27. Mills, R., *ibid.*, 1955, 77, 6116.
28. Wang, J.H., J. Amer. Chem. Soc., 1952, 74, 1182.
29. Berne, E. and Berggren, J.,  
Acta Chem. Scand., 1960, 14, 428.
30. Mills, R., Nature, 1957, 179, 187.
31. Thomas, H.C., Proc. Natl. Acad. Sci. U.S., 1956, 42, 428.
32. Northrup, J.H. and Anson, M.L.,  
J. Gen. Physiol., 1928, 12, 543.
33. Hartley, G.S. and Runnicles, D.F.,  
Proc. Roy. Sci., 1938, A168, 401.

## References cont.

34. Barnes, C., Physics, 1934, 5, 4.
35. Mills, R., Woolf, L.A. and Watts, R.O.,  
A. I. Chem. E. Journal, 1968, 14, 671.
36. Nielson, J.M., Adamson, A.W. and Cobble, J.W.,  
J. Amer. Chem. Soc., 1952, 74, 446.
37. Lewis, J.B., J. App. Chem., 1955, 5, 228.
38. Dullien, F.A.L. and Shemilt, L.W.,  
Can. J. Chem. Eng., 1961, 39, 242.
39. Janz, G.J. and Mayer, G.E., 'Diffusion of Electrolytes:  
Principles and Practice of the Diaphragm Cell  
Technique' O.S.W. Report, 1966.
40. Jalota, S.K. and Paterson, R., J. Chem. Soc.  
Farad. Trans. I, 1973, 69, 1510.
41. Albright, J.A. and Mills, R.,  
J. Phys. Chem., 1965, 69, 3120.
42. International Critical Tables, Volume III, pp. 28.
43. Vogel, A.I., 'Quantitative Inorganic Analysis',  
Longmans, London, 1961.
44. Matheson, R.A., J. Phys. Chem., 1962, 66, 439.
45. Olsztajn, M., Turq, P and Chemla, M.,  
J. Chim. Phys. Physicochem. Biol., 1970, 67, 217.
46. Paterson, R., Anderson, J. and Anderson, S.,  
J. Chem. Soc., Farad. Trans. I, in preparation.

APPENDICES

The computer programs reproduced here are written in FORTRAN IV language suitable for use with the 'NUMAC' I.B.M. 370/360 computing service. Extensive use of the NAG Subroutines have been made and slight modifications may be required before being used with ICL 1900 Series or other computing systems.

```

IMPLICIT REAL*8(A-H,O-Z)
DIMENSION XX(50),YY(50),X(50),Y(50),w(50),P(8),S1(8),

```

```

1 NAME (20)
  LOGICAL L
  L=.FALSE.
10 FORMAT(5I5)
11 FORMAT(3F10.0)
12 FORMAT(20A4)
  READ(5,10)NSETS
  KOUNT=0
  1 READ(5,10)M
  DO 900 I=1,M
900 READ(5,11)XX(I),YY(I),W(I)
  WRITE(6,56)
  WRITE(6,500)(XX(I),YY(I),I=1,M)
  NC=0
  READ(5,10)NCON
99 READ(5,10)K1,KX,NX,KY,NY
  READ(5,12)NAME
  WRITE(6,51)
  WRITE(6,55)NAME
  IF(KX.EQ.0)GO TO 7
  DO 80 I=1,M
  IF(NX)2,3,4
  2 X(I)=DLOG(XX(I))
  GO TO 80
  3 X(I)=DLOG10(XX(I))
  GO TO 80
  4 X(I)=DSQRT(XX(I))
80 CONTINUE
  GO TO 21
  7 CONTINUE
  DO 61 I=1,M
61 X(I)=XX(I)
21 CONTINUE
  IF(KY.EQ.0)GO TO 6
  DO 70 I=1,M
  IF(NY)8,9,13
  8 Y(I)=DLOG(YY(I))
  GO TO 70
  9 Y(I)=DLOG10(YY(I))
  GO TO 70
13 Y(I)=DSQRT(YY(I))
70 CONTINUE
  GO TO 22
  6 CONTINUE
  DO 62 I=1,M
62 Y(I)=YY(I)
22 CONTINUE

```

```

CALL E02ABF(M,X,Y,W,K1,N,S1,P,L)
WRITE(6,52)
DO 30 I=1,K1
30 WRITE(6,53)P(I),S1(I)
WRITE(6,54)N
WRITE(6,300)
SUMSQR=0.00
DO 40 I=1,N
AX=X(I)
AY=Y(I)
YCAL=0.00
DO 100 J=1,K1
IF(AX.EQ.0.00)GO TO 101
100 YCAL=YCAL+P(J)*AX**(J-1)
GO TO 102
101 YCAL=P(1)
102 DIF=YCAL-AY
SUMSQR=SUMSQR+DIF**2
PE=DABS(DIF/AY)*100.00
40 WRITE(6,200)AX,AY,YCAL,DIF,PE
STDEV=DSQRT(SUMSQR/(N-1))
WRITE(6,400)STDEV
NC=NC+1
IF(NC.NE.NCOM)GO TO 99
KOUNT=KOUNT+1
IF(KOUNT.NE.NSETS)GO TO 1
STOP
56 FORMAT(1H1)
51 FORMAT(/6X,'LEAST SQUARE FIT OF ')
52 FORMAT(/6X,'COEFFICIENTS          GOODNESS  '/')
53 FORMAT(2(1PD18.8))
54 FORMAT(/6X,'DEGREE OF BEST POLY',14)
55 FORMAT(/6X,20A4/)
200 FORMAT(4(1PD16.6),0PF10.3)
300 FORMAT(/5X,'      X              Y(OBS)          Y(CAL)',
1'      DIFF          P.DEV.')
```

```

400 FORMAT(/6X,'STANDARD DEVIATION',1PD12.4////)
500 FORMAT(/6X,'INPUT DATA (X-Y PAIRS)'/8(2X,F10.4))
END
```



## APPENDIX A.2

THIS PROGRAM CALCULATES THE STANDARD EMF (E0) FOR  
UNSYMMETRIC ELECTROLYTES BY GRONWALL LAMER AND  
SANDVED THEORY.

```

C
C
C
C
C
C
      IMPLICIT REAL*8(A-H,O-Z)
      EXTERNAL CURVFT,SOLVE
      DIMENSION X(50),X3Y3(50),X2Y2(50),XYSTAR(50),E0(50),
1E(50),NAME(20)
      COMMON/KHYBER/N3,N2,NS
      COMMON/PUSHTU/CO3(8),CO2(8),COS(8)
      C1=0.5691500
      C2=1.5363500
      C3=0.2174000
      C4=0.1538200
      C5=0.0887400
      C6=0.200700
10  FORMAT(2I5)
11  FORMAT(20A4)
12  FORMAT(4F10.0)
13  FORMAT(2F10.0)
      READ(5,10)M,N
      READ(5,12)(X(I),X3Y3(I),X2Y2(I),XYSTAR(I),I=1,M)
      WRITE(6,1400)
      CALL CURVFT(M,N,X,X3Y3,CO3,N3)
      WRITE(6,1500)
      CALL CURVFT(M,N,X,X2Y2,CO2,N2)
      WRITE(6,1600)
      CALL CURVFT(M,N,X,XYSTAR,COS,NS)
      KOUNT=0
      READ(5,10)NSETS
2  READ(5,11)NAME
      WRITE(6,1000)NAME
      READ(5,10)NOP
      READ(5,13)(X(I),E(I),I=1,NOP)
      READ(5,12)A0S,A0I,A0L
      A0=A0S
      WRITE(6,1700)A0
1  SUM=0.00
      DO 100 I=1,NOP
      XYSTAR(I)=C1*DSORT(X(I))
      SX=XYSTAR(I)*A0
      UX=1.00/(1.00+SX)
      P=1.00/A0
      SA=1.00/A0**2
      CALL SOLVE(SX,ALPHA,BETA,GAMA)
      X2Y2(I)=C2*UX+C3*R*ALPHA-3.00*C4*SA*BETA
1-9.00*C4*SA*GAMA
      X3Y3(I)=-2.00*XYSTAR(I)*X2Y2(I)
      E0(I)=E(I)+C5*(C6+DLOG10(X(I)))+C5*X3Y3(I)
100 SUM=SUM+E0(I)
      FLNOP=FLOAT(NOP)
      AVERG=SUM/FLNOP
      SUMSOR=0.00
      WRITE(6,1100)

```

```

DO 200 I=1,NOP
DIF=AVERG-E0(I)
SUMSQR=SUMSQR+DIF**2
ECAL=AVERG-C5*X3Y3(I)-C5*(C6+DLOG10(X(I)))
DIFC=ECAL-E(I)
200 WRITE(6,1200)X(I),E(I),XYSTAR(I),X2Y2(I),X3Y3(I),
1E0(I),DIF,ECAL,DIFC
SDEV=DSQRT(SUMSQR/(FLNOP-1))*1.D+03
WRITE(6,1300)AVERG,SDEV
A0=A0+A0I
IF(A0.LE.A0L)GO TO 1
KOUNT=KOUNT+1
IF(KOUNT.NE.NSETS)GO TO 2
STOP
1000 FORMAT(/ /5X,20A4/)
1100 FORMAT(/ /)
1200 FORMAT(5X,9(2X,F10.5))
1300 FORMAT(50X,'AVERAGE E0=',F10.5,' S. DEV.=',F6.2)
1400 FORMAT(/5X,'COEFFICIENTS OF 10**3(1/2X3-2Y3) VS X')
1500 FORMAT(/5X,'COEFFICIENTS OF 10**2(1/2X2-Y2) VS X')
1600 FORMAT(/5X,'COEFFICIENTS OF 10**3(1/2X3*-2Y3*) VS X')
1700 FORMAT(/5X,'A0=',F10.2)
END
SUBROUTINE CURVFT(M,N,X,Y,COE,K)
IMPLICIT REAL*8(A-H,O-Z)
DIMENSION X(M),Y(M),COE(N),W(40),S(8)
LOGICAL L
L=.FALSE.
DO 20 I=1,M
20 W(I)=1.D0
CALL E0ZABF(M,X,Y,W,N,KN,S,COE,L)
K=KN+1
DO 30 J=1,K
30 WRITE(6,100)COE(J)
WRITE(6,200)KN
WRITE(6,300)
SUM=0.D0
DO 40 I=1,M
YCAL=0.D0
DO 50 J=1,N
IF(X(I).EQ.0.D0)GO TO 1
50 YCAL=YCAL+COE(J)*X(I)**(J-1)
GO TO 2
1 YCAL=COE(1)
2 DIFF=Y(I)-YCAL
SUM=SUM+DIFF**2
40 WRITE(6,400)X(I),Y(I),YCAL,DIFF
SDEV=DSQRT(SUM/(FLOAT(M)-1))
100 FORMAT(5X,1PD14.7)
200 FORMAT(/5X,'DEGREE OF FIT FOUND=',I2)
300 FORMAT(/ /)
400 FORMAT(3X,4(1PD14.5))
500 FORMAT(/5X,'STANDARD DEVIATION=',1PD14.4)
RETURN
END
SUBROUTINE SOLVE(SX,ALPHA,BETA,GAMA)

```

```

      IMPLICIT REAL*8 (A-H,O-Z)
      COMMON/KHYBER/N3,N2,NS
      COMMON/PUSHTU/C03(8),C02(8),COS(8)
      ALPHA=0.00
      DO 20 J=1,N2
20    ALPHA=ALPHA+C02(J)*SX**(J-1)
      ALPHA=ALPHA/SX
      BETA=0.00
      DO 30 J=1,NS
30    BETA=BETA+COS(J)*SX**(J-1)
      BETA=BETA/SX
      GAMA=0.00
      DO 40 J=1,N3
40    GAMA=GAMA+C03(J)*SX**(J-1)
      GAMA=GAMA/SX
      RETURN
      END

```

## APPENDIX B.1

Computer program for optimisation  
of stability constants and the activity  
coefficient parameters by the method of  
Reilly and Stokes, as described in  
Chapter 2.

```

IMPLICIT REAL*8 (A-H,O-Z)
DIMENSION X(10),H(10),F(100),FP(100),IP(20),DX(10),AA(20,10),
1 DFDX(100,10),CH(10,10),SU(10),NAL(10),IZ(10),INM(30)
COMMON A1(100),A112(100),AE(100),ENew(100),YNew(100)
COMMON /RES/ SUSQ,NAGA(100),JT
COMMON/JKLM/BC(40),NVAR(40),E,EM1,EM2,EM112,CL,CD,CDCLB,CDCLC,
1 CDCLD,CDCLE,ALO,GA0,MAR
LOGICAL DER,FLAG,FIRST
NDIM=20
MDIM=100
IPRIN=1
READ(5,13) N,M,NOP,NM,ITM,MAR
13 FORMAT(16I5)
WRITE(6,36) N,M,NOP,NM,ITM,MAR
36 FORMAT(' PARAMS,READINGS, VALUES, CHOSEN STARTS, MAX ITERS, EMERG
1NCY PRINT',/,I6,2I8,3I11)
READ(5,12) (BC(I),I=1,NOP)
WRITE(6,66) (BC(I),I=1,NOP)
66 FORMAT(7H VALUES,/, (1P8G14.5),/)
READ(5,122) (A1(I),A112(I),AE(I),I=1,M)
WRITE(6,14) (A1(I),A112(I),AE(I),I=1,M)
122 FORMAT(3F10.0)
12 FORMAT(8F10.0)
14 FORMAT(//'      M1          2*M1+M2          E',/, (1P3G14.5))
NA=0
UB=1.D16
IWW=1
K=0
UU=0.D0
KK=1
DO 16 J=1,N
  READ(5,15) NVAL,NVAR(J),(AA(I,J),I=1,NVAL)
  WRITE(6,34) NVAL,NVAR(J),(AA(I,J),I=1,NVAL)
34 FORMAT(/,I5,24H GUESSES AT VALUE NUMBER,I5,/, (8F13.6))
15 FORMAT(2I5,/, (8F10.0))
  NAL(J)=NVAL
  IWW=IWW*NVAL
  IZ(J)=1
16 H(J)=AA(1,J)
  IF(IWW.GT.10000.OR.IWW.LE.0) STOP 2
  DO 1 IW=1,IWW
    IF(IW.EQ.1) GO TO 10
    DO 8 J=1,N
      IF(IZ(J).GE.NAL(J)) GO TO 28
      IZ(J)=IZ(J)+1
      IJ=IZ(J)
      H(J)=AA(IJ,J)
      GO TO 10
28 IZ(J)=1
8 H(J)=AA(1,J)
  STOP 3
10 CALL FUNCTN(H,F,M,N)
  S=0.D0
  DO 6 I=1,M
6 S=S+F(I)*F(I)
  IF(K.GE.NM) GO TO 7

```

```

      K=K+1
      DO 30 I=1,N
30    CH(I,K)=H(I)
      SU(K)=S
      IF(S.LE.UU) GO TO 11
      UU=S
      KK=K
      GO TO 1
7     IF(S.GE.UU) GO TO 11
      IK=KK
      SU(IK)=S
      DO 31 I=1,N
31    CH(I,IK)=H(I)
      UU=0.D0
      DO 32 I=1,NM
      IF(SU(I).LE.UU) GO TO 32
      KK=I
      UU=SU(I)
32    CONTINUE
11    CONTINUE
1     CONTINUE
      IF(NM.LE.0) GO TO 88
      DO 3 K=1,NM
      INM(K)=0
3     WRITE(6,5) SU(K),(CH(I,K),I=1,N)
5     FORMAT(/,,' STARTING POINT. SUM OF SQUARES =',1PE14.4,/,
1     ' PARAMS=',(8E14.4))
      WRITE(6,26)
26    FORMAT(1H1)
      DO 181 MJ=1,NM
      UU=1.D10
      DO 20 JM=1,NM
      IF(SU(JM).GE.UU.OR.INM(JM).EQ.1) GO TO 20
      IJK=JM
      UU=SU(JM)
20    CONTINUE
      INM(IJK)=1
      WRITE(6,5) SU(IJK),(CH(I,IJK),I=1,N)
      DO 35 KJI=1,N
      DX(KJI)=1.D10
      IF(NVAR(KJI).EQ.5) DX(KJI)=1.D-4
35    X(KJI)=CH(KJI,IJK)
      ITMAX=IPRIN
      NLP=(ITM+ITMAX-1)/ITMAX
      ITER=0
      FIRST=.TRUE.
      FLAG=.FALSE.
      DER=.FALSE.
      S=1.D30
      DO 27 IR=1,NLP
      IF(IR.EQ.NLP) ITMAX=ITM-ITER
      DO 39 KJI=1,N
      HKJ=DMIN1(1.D-3*DABS(X(KJI)+1.D0),DABS(DX(KJI))*0.1D0)
39    H(KJI)=DMAX1(HKJ,1.D-6)
      CALL TAYLOR(N,M,X,H,F,ITMAX,FIRST,1.D-6,1.D-2,DER,S,KENN
1     ,FLAG,MDIM,NDIM,AA,DFDX,FP,IP,DX,UB)

```

```

ITER=ITER+ITMAX
WRITE(6,17) FLAG,ITER,KENN,S,(X(J),J=1,N)
17  FORMAT(' FLAG=',L4,' ITER=',I4,' KENN=',I4,' SUM OF SQUARES=',
1    1PE14.4,/, ' PARAMS',(7E15.7))
WRITE(6,77)
77  FORMAT(/,' IONIC STRENGTH      E(CALC)-E(MEAS)      GA21
1GA11      GA0      GA12      STOICH')
THR=1.00/3.00
DO 78 J=1,M
AY=1.00/YNEW(J)
SQAY=DSQRT(AY)
SQT=-1.023000*SQAY
GA21=SQT/(1.00+BC(6)*SQAY)+AY*(BC(7)+AY*(BC(8)+AY*BC(9)))
GA21=10.00**GA21
GA11=SQT*.500/(1.00+BC(10)*SQAY)+AY*(BC(11)+AY*(BC(12)+AY*BC(13)))
GA11=10.00**GA11
GA0=10.00** (AY*(BC(14)+AY*(BC(15)+AY*BC(16))))
GA12=SQT/(1.00+BC(17)*SQAY)+AY*(BC(18)+AY*(BC(19)+AY*BC(20)))
GA12=10.00**GA12
AL0=10.00**((BC(5)-ENEW(J))/0.02957900)
STOICH=(AL0/(A1(J)*A112(J)*A112(J)))*THR
78  WRITE(6,79) AY,F(J),GA21,GA11,GA0,GA12,STOICH
79  FORMAT(2F15.7,5F15.5)
WRITE(6,818) (BC(J),J=1,20)
818  FORMAT(' BC',(1P5G14.5))
IF(FLAG.OR.KENN.NE.1) GO TO 18
WRITE(6,26 )
27  CONTINUE
18  MAT=MAR
IF(MAR.LT.1) MAR=1
CALL FUNCTN(X,F,M,N)
MAR=MAT
181  CONTINUE
88  CONTINUE
STOP
END
SUBROUTINE FUNCTN(X,F,M,N)
IMPLICIT REAL*8 (A-H,O-Z)
COMMON/JKLM/BC(40),NVAR(40),E,EM1,EM2,EM112,CL,CD,CDCLB,CDCLC,
1  CDCLD,CDCLE,AL0,GA0,MAR
COMMON /RES/ SUSQ,NAGA(100),JT
COMMON A1(100),A112(100),AE(100),ENEW(100),YNEW(100)
DIMENSION X(1),F(1)
COMMON /L/ AYL
EXTERNAL YA,AYD,YAYA
PRINT 87,(X(I),I=1,N)
87  FORMAT(7H PARAMS,(1P8E15.7))
DO 98 I=1,N
J=NVAR(I)
IF(J.LE.5.AND.X(I).LE.0.D0) GO TO 94
98  BC(J)=X(I)
TH=1.00/3.00
AY*I=0.00
RAT=0.00
SUSQ=0.00
JT=M

```

```

DO 19 JS=1,M
NJS=NAGA(JS)
NAGA(JS)=0
F(JS)=10.00
EM1=A1(JS)
EM112=A112(JS)
EM12=EM112-EM1
EM2=EM12-EM1
IF(NJS.NE.1) GO TO 76
E=ENEW(JS)
AYN=YNEW(JS)
CALL PARTS(AYN,IGDBD,8)
DE=E-AE(JS)
F(JS)=DE
AYNI=1.00/AYN
IF(MAR.GE.1) PRINT 60,IGDBD,AYNI,E,DE
IF(IGDBD.LT.0) GO TO 76
NAGA(JS)=1
JT=JT-1
ENEW(JS)=E
YNEW(JS)=AYN
GO TO 19
76 E=AE(JS)
ADEW=10.00
AL0=10.00*((BC(5)-E)/0.029579D0)
IF(MAR.GE.2) PRINT 27,EM1,EM2,EM112,E
27 FORMAT(/,5H DATA,1P8E14.4)
NK=1000
IF(EM1.GT.EM2.AND.EM1.GT.3.D-4) GO TO 17
ST=(EM112+EM1)*0.9999999D0
FAC=1.00-0.1*EM1
FINI=EM12*0.63D0
WIJ=5.00
GO TO 18
17 FINI=(EM112+EM1)*0.9999999D0
FAC=1.07D0
ST=EM12*0.63D0
18 CONTINUE
DO 7 J=1,NK
AYI=ST
IF(FAC.GT.1.00) GO TO 20
IF(MOD(J,20).EQ.0) FAC=FAC**WIJ
IF(AYI.LT.FINI) GO TO 19
GO TO 22
20 IF(AYI.GT.FINI) AYI=FINI
IF(AYWI.EQ.FINI) GO TO 19
22 ST=ST*FAC
AY=1.00/AYI
AYNEW=YA(AY)
DAY=AYNEW-AY
IS=DSIGN(1.00,DAY)
IF(J.EQ.1) GO TO 37
RAT=(AYOLD-AYW)/DAY
IF(IS.EQ.IW) GO TO 38
AYM=(AYW*AYNEW-AY*AYOLD)/(DAY-AYOLD+AYW)
IF(MAR.GE.2) PRINT 56,AYM

```



```

56  FORMAT(6H START,1P6E14.4)
    VAN=0.D0
    AYP=YA(AYM)
    YAP=(AYP-AYW)/(AY-AYW)
    IF(YAP.GE.0.D0.AND.YAP.LT.1.D0) GO TO 77
    DRELD=DMIN1(AYW,AY)
    DRAY=DMAX1(AYW,AY)
    CALL DRTMI(AYN,VAL,YAYA,DRELD,DRAY,1.D-7,40,IER)
    GO TO 78
77  CALL DRTWI(AYN,VAL,YA,AYM,1.D-7,40,IER)
78  AYL=0.D0
    IF(VAL.EQ.0.D0) IER=3
58  IF(MAR.GE.2) PRINT 48,IER,AYN,VAL,AYL,VAN
48  FORMAT(4H IER,I5,1P6E14.4)
    IF(IER.GE.2) GO TO 37
    DM1=CD+CDCLB+CDCLC+CDCLD+CDCLE-EM1
    DM2=CL+CDCLD+CDCLE+CDCLE-CD-CD-CDCLB-EM2
    IF(MAR.GE.2) PRINT 57, AYN,DM1,DM2
57  FORMAT(8H AT CONV,1P4E14.4)
    CALL PARTS(AYN,IGDBD,8)
    DE=E-AE(JS)
    AYN1=1.D0/AYN
    IF(MAR.GE.1) PRINT 60,IGDBD,AYN1,E,DE
60  FORMAT(/,6H N RAP,I4,1P3E16.6,/)
    IF(IGDBD.LT.0) E=AE(JS)
    IF(DABS(DE).GT.ADEW) GO TO 99
    ADEW=DABS(DE)
    F(JS)=DE
99  IF(IGDBD.LT.0) GO TO 37
    NAGA(JS)=1
    ENEW(JS)=E
    YNEW(JS)=AYN
    JT=JT-1
    GO TO 19
38  IF(J.LE.2) GO TO 37
    IF(RATW.LT.1.D0.OR.1.D0/RAT.LT.1.D0) GO TO 37
    IF(MAR.GE.2) PRINT 63,AYELD,AY
63  FORMAT(18H NEAR SOLN BETWEEN,1P2E14.4)
    DRELD=DMIN1(AYELD,AY)
    DRAY=DMAX1(AYELD,AY)
    CALL DRTMI(AYN,VAN,AYD,DRELD,DRAY,1.D-7,40,IER)
    IF(VAN.EQ.0.D0) IER=3
    VAL=AYN-AYL
    GO TO 58
37  IW=IS
    AYELD=AYW
    AYOLD=AYNEW
    AYW=AY
    AYWI=AYI
    RATW=RAT
7   CONTINUE
19  SUSQ=SUSQ+F(JS)**2
8   MMM=M-1
    IF(MAR.GE.1) MMM=1
    PRINT 49,JT,SUSQ,(F(I),I=1,M,MMM)
49  FORMAT(I4,' FAILURES, SUM OF SQS =',F15.8,', DELTA E',1P5E13.4,

```

```

1 /,(10E13.4))
  RETURN
94 DO 95 I=1,M
95 F(I)=1.010
  RETURN
  END
  SUBROUTINE DERIVE(X,F,DFDX,MD,M,N)
  IMPLICIT REAL*8 (A-H,O-Z)
  DIMENSION DFDX(MD,N),X(1),F(1)
  RETURN
  END
  SUBROUTINE TAYLOR(N,M,X,H,F,ITMAX,FIRST,EPS1,EPS2,DER,S,KENN,FLAG
1 MDIM,NDIM,AA,DFDX,FP,IP,DX,UB)
  DOUBLE PRECISION HS,HL,HF,HH,HZ,S,X,H,F,EPS1,EPS2,AA,DFDX,FP,DX,U
1 ,HT
  DIMENSION X(N),H(N),F(M),FP(M),DFDX(MDIM,N),AA(NDIM,N),IP(N),DX(N
  LOGICAL DER,FLAG,FIRST
  HS=S
  KENN=0
  IZ=0
  IF(.NOT.FIRST) GO TO 71
  FIRST=.FALSE.
1 L=0
  HL=1.00
3 L=L+1
4 CALL FUNCTN(X,F,M,N)
  HF=0.00
  DO 5 I=1,M
5 HF=HF+F(I)*F(I)
  IF(L.EQ.1) HT=HF
  IF(HF.LE.HS*(1.00-0.200*HL)) GO TO 7
  IF(L.GT.7) GO TO 72
  HL=HL/(L+1.00)
  HH=L*HL
  DO 6 K=1,N
6 X(K)=X(K)+HH*DX(K)
  GO TO 3
7 HS=HF
  IF(HS.LT.EPS1) GO TO 73
  IF(IZ.LT.ITMAX) GO TO 71
  KENN=1
73 S=HF
  ITMAX=IZ
  RETURN
72 KENN=-1
  IF(HT.LT.HS) HL=HL-1.00
  DO 74 K=1,N
74 X(K)=X(K)+HL*DX(K)
  GO TO 18
71 IZ=IZ+1
  IF(DER) GO TO 9
  DO 8 I=1,N
  HF=H(I)
  HH=X(I)
  X(I)=X(I)+HF
  CALL FUNCTN(X,FP,M,N)

```

```

      X(I)=HH
      HF=1.D0/HF
      DO 8 K=1,M
8     DFDX(K,I)=HF*(F(K)-F(K))
      GO TO 10
9     CALL DERIVE(X,F,DFDX,MDIM,M,N)
10    IF(M.EQ.N) GO TO 14
      DO 13 I=1,N
      HF=0.D0
      DO 11 K=1,M
11    HF=HF+DFDX(K,I)*F(K)
      DX(I)=HF
      DO 13 K=I,N
      HF=0.D0
      DO 12 J=1,M
12    HF=HF+DFDX(J,I)*DFDX(J,K)
      AA(I,K)=HF
13    AA(K,I)=HF
      CALL DECOMP(N,NDIM,AA,IP)
      IF(IP(N).EQ.0) GO TO 20
      CALL SOLVE(N,NDIM,AA,DX,IP)
      GO TO 16
14    CALL DECOMP(N,MDIM,DFDX,IP)
      IF(IP(N).EQ.0) GO TO 20
      CALL SOLVE(N,MDIM,DFDX,F,IP)
      DO 15 I=1,N
15    DX(I)=F(I)
16    HZ=0.D0
      HF=0.D0
      DO 17 I=1,N
      X(I)=X(I)-DX(I)
      HZ=HZ+DABS(X(I))
17    HF=HF+DABS(DX(I))
      IF(HZ.GT.UB) GO TO 21
      IF(HF.GE.EPS2*HZ) GO TO 1
      KENN=-2
      GO TO 18
21    KENN=-3
      DO 181 I=1,N
181   X(I)=X(I)+DX(I)
18    CALL FUNCTN(X,F,M,N)
      S=0.D0
      ITMAX=IZ
      DO 19 I=1,M
19    S=S+F(I)*F(I)
      RETURN
20    FLAG=.TRUE.
      ITMAX=IZ
      KENN=-4
      RETURN
      END
      SUBROUTINE DECOMP(N,NDIM,A,IP)
C     CACM ALGORITHM NO 423
      DOUBLE PRECISION A,T
      DIMENSION A(NDIM,N),IP(N)
      IP(N)=1

```

```

DO 6 K=1,N
IF (K.EQ.N) GO TO 5
KP1=K+1
M=K
DO 1 I=KP1,N
IF (DABS(A(I,K)).GT.DABS(A(M,K))) M=I
1 CONTINUE
IP(K)=M
IF (M.NE.K) IP(N)=~IP(N)
T=A(M,K)
A(M,K)=A(K,K)
A(K,K)=T
IF (T.EQ.0.D0) GO TO 5
DO 2 I=KP1,N
2 A(I,K)=-A(I,K)/T
DO 4 J=KP1,N
T=A(M,J)
A(M,J)=A(K,J)
A(K,J)=T
IF (T.EQ.0.D0) GO TO 4
DO 3 I=KP1,N
3 A(I,J)=A(I,J)+A(I,K)*T
4 CONTINUE
5 IF (A(K,K).EQ.0.D0) IP(N)=0
6 CONTINUE
RETURN
END
SUBROUTINE SOLVE(N,NDIM,A,B,IP)
C CACM ALGORITHM NO 423
DOUBLE PRECISION A,T,B
DIMENSION A(NDIM,N),IP(N),B(NDIM)
IF (N.EQ.1) GO TO 9
NM1=N-1
DO 7 K=1,NM1
KP1=K+1
M=IP(K)
T=B(M)
B(M)=B(K)
B(K)=T
DO 7 I=KP1,N
7 B(I)=B(I)+A(I,K)*T
DO 8 KB=1,NM1
KM1=N-KB
K=KM1+1
B(K)=B(K)/A(K,K)
T=-B(K)
DO 8 I=1,KM1
8 B(I)=B(I)+A(I,K)*T
9 B(1)=B(1)/A(1,1)
RETURN
END
FUNCTION YAYA(AY)
IMPLICIT REAL*8 (A-H,O-Z)
YAYA=YA(AY)-AY
RETURN
END

```

```

FUNCTION AYD(AY)
  IMPLICIT REAL*8 (A-H,O-Z)
  COMMON /L/ AYL
  IF(AY.LT.0.D0) GO TO 91
  SP=(AY+1.D0)*1.D-6
  AYK=YA(AY+SP)
  AYL=YA(AY)
  AYK=(AYK-AYL-SP)/SP
  AYD=AYK
  RETURN
91  AYD=0.D0
  AYL=AY
  RETURN
END
FUNCTION YA(AZ)
  IMPLICIT REAL*8 (A-H,O-Z)
  COMMON/JKLM/BC(40),NVAR(40),E,EM1,EM2,EM112,CL,CD,CDCLB,CDCLC,
1  CDCLD,CDCLE,ALO,GA0,MAR
  IF(AZ.LT.0.D0) GO TO 91
  AY=1.D0/AZ
  SQAY=DSQRT(AY)
  SQT=-1.0230D0*SQAY
  GA21=SQT/(1.D0+BC(6)*SQAY)
1  +AY*(BC(7)+AY*(BC(8)+AY*BC(9)))
  GA21=10.D0**GA21
  GA11=SQT*0.5D0/(1.D0+BC(10)*SQAY)
1  +AY*(BC(11)+AY*(BC(12)+AY*BC(13)))
  GA11=10.D0**GA11
  GA0=10.D0**((AY*(BC(14)+AY*(BC(15)+AY*BC(16))))
  GA12=SQT/(1.D0+BC(17)*SQAY)
1  +AY*(BC(18)+AY*(BC(19)+AY*BC(20)))
  GA12=10.D0**GA12
  GA12C=GA12**3
  GA21C=GA21**3
  GA11S=GA11*GA11
  GA11F=GA11S*GA11S
  ALO=10.D0**((BC(5)-E)/0.029579D0)
  VA=ALO/GA21C
  VB=ALO*BC(1)/GA11S
  VC=ALO*BC(2)/GA0
  VD=ALO*BC(3)
  VE=ALO*BC(4)*GA11F/GA12C
  C=3.D0*VB
  S=VB
  A=3.D0*VD-1.D0
  Q=2.D0+A
  R=VC+VC-EM112
  B=R+R+EM2+AY+AY
  P=4.D0*VE
  PDA=P/A
  BPDA=B*PDA
  CL=(A*S-C*(Q-BPDA))/(B*(Q-BPDA)-A*(R-C*PDA))
  CLS=CL*CL
  CD=VA/CLS
  CDCLB=VB/CL
  CDCLC=VC

```

```

CDCLD=VD*CL
CDCLE=VE*CLS
AYNEW=0.5D0*(4.D0*(CD+CDCLE)+CL+CDCLB+CDCLD+EM2)
YA=1.D0/AYNEW
RETURN
91 YA=AZ
RETURN
END
SUBROUTINE PARTS(AY,IGDBD,ITMA)
IMPLICIT REAL*8 (A-H,O-Z)
COMMON/JKLM/BC(40),NVAR(40),E,EM1,EM2,EM112,CL,CD,CDCLB,CDCLC,
1 CDCLD,CDCLE,ALO,GA0,MAR
TEST=1.D-2
DELT=0.D0
DALT=0.D0
IGDBD=0
N=0
7 Z1=YA(AY)-AY
W1=CD+CDCLB+CDCLC+CDCLD+CDCLE-EM1
Y1=CL+CDCLD+CDCLE+CDCLC-CD-CD-CDCLB-EM2
T1=Z1/(AY*(AY+1.D0))
U1=W1/(EM112+1.D0)
IF(N.GT.0.AND.T1*T1+U1*U1.LT.1.D-12) GO TO 9
IF(DABS(DELT).LT.TEST) GO TO 6
16 IGDBD=-1
GO TO 10
6 AYDD=AY*1.D-4*(-1)**(N/2+2)
AYP=AY+AYDD
Z2=YA(AYP)-AYP
W2=CD+CDCLB+CDCLC+CDCLD+CDCLE-EM1
EX=E
EDD=(E+1.D0)*1.D-6*(-1)**(N+1)
E=E+EDD
Z3=YA(AY)-AY
W3=CD+CDCLB+CDCLC+CDCLD+CDCLE-EM1
DEL=(Z2-Z1)*(W3-W1)-(Z3-Z1)*(W2-W1)
IF(DEL.EQ.0.D0) GO TO 14
DALT=AYDD*(Z3*W1-Z1*W3)/DEL
DELT=EDD*(Z1*W2-Z2*W1)/DEL
E=EX+DELT
AY=AY+DALT
N=N+1
IF(AY.LT.0.D0.OR.DABS(E-BC(5)).GT.0.5D0) GO TO 16
IF(N-ITMA) 7,10,10
14 PRINT 18
18 FORMAT(' ZERO DENOMINATOR IN SUBROUTINE PARTS')
E=EX
9 IGDBD=1
67 FORMAT(4H TRY,I4,1P7E14.4)
10 IF(MAR-1) 11,12,13
13 PRINT 67,N,AY,DALT,E,DELT,Z1,W1,Y1
12 PRINT 17,CL,CD,CDCLB,CDCLC,CDCLD,CDCLE
17 FORMAT(' CONCENTRATIONS',1P8E14.4)
11 RETURN
END

```

.....

SUBROUTINE DRTMI

PURPOSE

TO SOLVE GENERAL NONLINEAR EQUATIONS OF THE FORM  $FCT(X)=0$   
BY MEANS OF MUELLER-S ITERATION METHOD.

USAGE

CALL DRTMI (X,F,FCT,XLI,XRI,EPS,IEND,IER)  
PARAMETER FCT REQUIRES AN EXTERNAL STATEMENT.

DESCRIPTION OF PARAMETERS

X - DOUBLE PRECISION RESULTANT ROOT OF EQUATION  
 $FCT(X)=0$ .  
F - DOUBLE PRECISION RESULTANT FUNCTION VALUE  
AT ROOT X.  
FCT - NAME OF THE EXTERNAL DOUBLE PRECISION FUNCTION  
SUBPROGRAM USED.  
XLI - DOUBLE PRECISION INPUT VALUE WHICH SPECIFIES THE  
INITIAL LEFT BOUND OF THE ROOT X.  
XRI - DOUBLE PRECISION INPUT VALUE WHICH SPECIFIES THE  
INITIAL RIGHT BOUND OF THE ROOT X.  
EPS - SINGLE PRECISION INPUT VALUE WHICH SPECIFIES THE  
UPPER BOUND OF THE ERROR OF RESULT X.  
IEND - MAXIMUM NUMBER OF ITERATION STEPS SPECIFIED.  
IER - RESULTANT ERROR PARAMETER CODED AS FOLLOWS  
IER=0 - NO ERROR,  
IER=1 - NO CONVERGENCE AFTER IEND ITERATION STEPS  
FOLLOWED BY IEND SUCCESSIVE STEPS OF  
BISECTION,  
IER=2 - BASIC ASSUMPTION  $FCT(XLI)*FCT(XRI)$  LESS  
THAN OR EQUAL TO ZERO IS NOT SATISFIED.

REMARKS

THE PROCEDURE ASSUMES THAT FUNCTION VALUES AT INITIAL  
BOUNDS XLI AND XRI HAVE NOT THE SAME SIGN. IF THIS BASIC  
ASSUMPTION IS NOT SATISFIED BY INPUT VALUES XLI AND XRI, THE  
PROCEDURE IS BYPASSED AND GIVES THE ERROR MESSAGE IER=2.

SUBROUTINES AND FUNCTION SUBPROGRAMS REQUIRED

THE EXTERNAL DOUBLE PRECISION FUNCTION SUBPROGRAM FCT(X)  
MUST BE FURNISHED BY THE USER.

METHOD

SOLUTION OF EQUATION  $FCT(X)=0$  IS DONE BY MEANS OF MUELLER-S  
ITERATION METHOD OF SUCCESSIVE BISECTIONS AND INVERSE  
PARABOLIC INTERPOLATION, WHICH STARTS AT THE INITIAL BOUNDS  
XLI AND XRI. CONVERGENCE IS QUADRATIC IF THE DERIVATIVE OF  
 $FCT(X)$  AT ROOT X IS NOT EQUAL TO ZERO. ONE ITERATION STEP  
REQUIRES TWO EVALUATIONS OF  $FCT(X)$ . FOR TEST ON SATISFACTOR  
ACCURACY SEE FORMULAE (3.4) OF MATHEMATICAL DESCRIPTION.  
FOR REFERENCE, SEE G. K. KRISTIANSEN, ZERO OF ARBITRARY  
FUNCTION, BIT, VOL. 3 (1963), PP.205-206.

.....

```

C
C
SUBROUTINE DRTMI(X,F,FCT,XLI,XRI,EPS,IEND,IER)

```

```

C
C
DOUBLE PRECISION X,F,FCT,XLI,XRI,XL,XR,FL,FR,TOL,TOLF,A,DX,XM,FM

```

```

C
C
PREPARE ITERATION

```

```

IER=0

```

```

XL=XLI

```

```

XR=XRI

```

```

X=XL

```

```

TOL=X

```

```

F=FCT(TOL)

```

```

IF(F)1,16,1

```

```

1 FL=F

```

```

X=XR

```

```

TOL=X

```

```

F=FCT(TOL)

```

```

IF(F)2,16,2

```

```

2 FR=F

```

```

IF(DSIGN(1.D0,FL)+DSIGN(1.D0,FR))25,3,25

```

```

C
C
BASIC ASSUMPTION FL*FR LESS THAN 0 IS SATISFIED.

```

```

C
GENERATE TOLERANCE FOR FUNCTION VALUES.

```

```

3 I=0

```

```

TOLF=100.*EPS

```

```

C
C
START ITERATION LOOP

```

```

4 I=I+1

```

```

C
C
START BISECTION LOOP

```

```

DO 13 K=1,IEND

```

```

X=.5D0*(XL+XR)

```

```

TOL=X

```

```

F=FCT(TOL)

```

```

IF(F)5,16,5

```

```

5 IF(DSIGN(1.D0,F)+DSIGN(1.D0,FR))7,6,7

```

```

C
C
INTERCHANGE XL AND XR IN ORDER TO GET THE SAME SIGN IN F AND FR

```

```

6 TOL=XL

```

```

XL=XR

```

```

XR=TOL

```

```

TOL=FL

```

```

FL=FR

```

```

FR=TOL

```

```

7 TOL=F-FL

```

```

A=F*TOL

```

```

A=A+A

```

```

IF(A-FR*(FR-FL))8,9,9

```

```

8 IF(I-IEND)17,17,9

```

```

9 XR=X

```

```

FR=F

```

```

C
C
TEST ON SATISFACTORY ACCURACY IN BISECTION LOOP

```

```

TOL=EPS

```



```

      A=DABS(XR)
      IF (A-1.00) 11,11,10
10  TOL=TOL*A
11  IF (DABS(XR-XL)-TOL) 12,12,13
12  IF (DABS(FR-FL)-TOLF) 14,14,13
13  CONTINUE
C   END OF BISECTION LOOP
C
C   NO CONVERGENCE AFTER IEND ITERATION STEPS FOLLOWED BY IEND
C   SUCCESSIVE STEPS OF BISECTION OR STEADILY INCREASING FUNCTION
C   VALUES AT RIGHT BOUNDS. ERROR RETURN.
      IER=1
14  IF (DABS(FR)-DABS(FL)) 16,16,15
15  X=XL
      F=FL
16  RETURN
C
C   COMPUTATION OF ITERATED X-VALUE BY INVERSE PARABOLIC INTERPOLATIO
17  A=FR-F
      DX=(X-XL)*FL*(1.00+F*(A-TOL)/(A*(FR-FL)))/TOL
      XM=X
      FM=F
      X=XL-DX
      TOL=X
      F=FCT(TOL)
      IF (F) 18,16,18
C
C   TEST ON SATISFACTORY ACCURACY IN ITERATION LOOP
18  TOL=EPS
      A=DABS(X)
      IF (A-1.00) 20,20,19
19  TOL=TOL*A
20  IF (DABS(DX)-TOL) 21,21,22
21  IF (DABS(F)-TOLF) 16,16,22
C
C   PREPARATION OF NEXT BISECTION LOOP
22  IF (DSIGN(1.00,F)+DSIGN(1.00,FL)) 24,23,24
23  XR=X
      FR=F
      GO TO 4
24  XL=X
      FL=F
      XR=XM
      FR=FM
      GO TO 4
C   END OF ITERATION LOOP
C
C
C   ERROR RETURN IN CASE OF WRONG INPUT DATA
25  IER=2
      RETURN
      END

```

CENDSB

C  
 C  
 C  
 C

.....

## SUBROUTINE DRTWI

## PURPOSE

TO SOLVE GENERAL NONLINEAR EQUATIONS OF THE FORM  $X=FCT(X)$   
BY MEANS OF WEGSTEIN-S ITERATION METHOD.

## USAGE

CALL DRTWI (X,VAL,FCT,XST,EPS,IEND,IER)  
PARAMETER FCT REQUIRES AN EXTERNAL STATEMENT.

## DESCRIPTION OF PARAMETERS

X - DOUBLE PRECISION RESULTANT ROOT OF EQUATION  
 $X=FCT(X)$ .  
VAL - DOUBLE PRECISION RESULTANT VALUE OF  $X-FCT(X)$   
AT ROOT X.  
FCT - NAME OF THE EXTERNAL DOUBLE PRECISION FUNCTION  
SUBPROGRAM USED.  
XST - DOUBLE PRECISION INPUT VALUE WHICH SPECIFIES THE  
INITIAL GUESS OF THE ROOT X.  
EPS - SINGLE PRECISION INPUT VALUE WHICH SPECIFIES THE  
UPPER BOUND OF THE ERROR OF RESULT X.  
IEND - MAXIMUM NUMBER OF ITERATION STEPS SPECIFIED.  
IER - RESULTANT ERROR PARAMETER CODED AS FOLLOWS  
IER=0 - NO ERROR,  
IER=1 - NO CONVERGENCE AFTER IEND ITERATION STEPS  
IER=2 - AT ANY ITERATION STEP THE DENOMINATOR OF  
ITERATION FORMULA WAS EQUAL TO ZERO.

## REMARKS

THE PROCEDURE IS BYPASSED AND GIVES THE ERROR MESSAGE IER=2  
IF AT ANY ITERATION STEP THE DENOMINATOR OF ITERATION  
FORMULA WAS EQUAL TO ZERO. THAT MEANS THAT THERE IS AT  
LEAST ONE POINT IN THE RANGE IN WHICH ITERATION MOVES WITH  
DERIVATIVE OF  $FCT(X)$  EQUAL TO 1.

## SUBROUTINES AND FUNCTION SUBPROGRAMS REQUIRED

THE EXTERNAL DOUBLE PRECISION FUNCTION SUBPROGRAM  $FCT(X)$   
MUST BE FURNISHED BY THE USER.

## METHOD

SOLUTION OF EQUATION  $X=FCT(X)$  IS DONE BY MEANS OF  
WEGSTEIN-S ITERATION METHOD, WHICH STARTS AT THE INITIAL  
GUESS XST OF A ROOT X. ONE ITERATION STEP REQUIRES ONE  
EVALUATION OF  $FCT(X)$ . FOR TEST ON SATISFACTORY ACCURACY SEE  
FORMULAE (2) OF MATHEMATICAL DESCRIPTION.

FOR REFERENCE, SEE

- (1) G. N. LANCE, NUMERICAL METHODS FOR HIGH SPEED COMPUTERS,  
ILIFFE, LONDON, 1960, PP.134-138,
- (2) J. WEGSTEIN, ALGORITHM 2, CACM, VOL.3, ISS.2 (1960),  
PP.74,
- (3) H.C. THACHER, ALGORITHM 15, CACM, VOL.3, ISS.8 (1960),  
PP.475,
- (4) J.G. HERRIOT, ALGORITHM 26, CACM, VOL.3, ISS.11 (1960),  
PP.603.

```

C
C      SUBROUTINE DRTWI(X,VAL,FCT,XST,EPS,IEND,IER)
C
C      DOUBLE PRECISION X,VAL,FCT,XST,A,B,D,TOL
C
C      PREPARE ITERATION
      IER=0
      TOL=XST
      X=FCT(TOL)
      A=X-XST
      B=-A
      TOL=X
      VAL=X-FCT(TOL)
C
C
C      START ITERATION LOOP
      DO 6 I=1,IEND
      IF(VAL)1,7,1
C
C      EQUATION IS NOT SATISFIED BY X
      1 B=B/VAL-1.D0
      IF(B)2,8,2
C
C      ITERATION IS POSSIBLE
      2 A=A/B
      X=X+A
      B=VAL
      TOL=X
      VAL=X-FCT(TOL)
C
C      TEST ON SATISFACTORY ACCURACY
      TOL=EPS
      D=DABS(X)
      IF(D-1.D0)4,4,3
      3 TOL=TOL*D
      4 IF(DABS(A)-TOL)5,5,6
      5 IF(DABS(VAL)-1.D1*TOL)7,7,6
      6 CONTINUE
      END OF ITERATION LOOP
C
C
C      NO CONVERGENCE AFTER IEND ITERATION STEPS. ERROR RETURN.
      IER=1
      7 RETURN
C
C      ERROR RETURN IN CASE OF ZERO DIVISOR
      8 IER=2
      RETURN
      END
CENDSB

```

## APPENDIX B.2

```

C
C
C   THIS PROGRAM FINDS THE PARAMETERS
C   OF EXTENDED DEBY-HUCHEL EQUATION BY
C   NAG SUBROUTINE E04GAF
C
      IMPLICIT REAL*8(A-H,O-Z)
      EXTERNAL SAJAD,WASIM,RASHAD
      DIMENSION X(4),F(50),E(4),D(4),B(150),NAME(20)
      COMMON AZZ,B,GAMMA(50),STRION(50),AJAC(50,4)
10  FORMAT(4I5)
11  FORMAT(20A4)
12  FORMAT(2F10.0)
13  FORMAT(4F10.0)
      KOUNT=0
      READ(5,10) NSET
1  READ(5,11) NAME
      WRITE(6,1100) NAME
      READ(5,10) M,N,IPRINT,MAXITR
      WRITE(6,1200) M,N,IPRINT,MAXITR
      READ(5,12) AZZ,B
      WRITE(6,1300) AZZ,B
      READ(5,13) (X(I),I=1,N)
      WRITE(6,1400) (X(I),I=1,N)
      READ(5,12) (STRION(I),GAMMA(I),I=1,M)
      WRITE(6,1500) (STRION(I),GAMMA(I),I=1,M)
      DO 99 I=1,M
        STRION(I)=USORT(STRION(I))
99  GAMMA(I)=-DLOG10(GAMMA(I))
      DO 100 I=1,N
100 F(I)=1.D-07
        IFAIL=1
        IW=(N+4)*N+M
        CALL E04GAF(M,N,X,F,S,E,1,D,X,IW,SAJAD,WASIM,RASHAD,
/        IPRINT,MAXITR,IFAIL)
        WRITE(6,1600) IFAIL
        IF(N.EQ.2) WRITE(6,1800)
        IF(N.EQ.4) WRITE(6,1700)
        CALL RASHAD(M,N,X,F,S,E,-1)
        KOUNT=KOUNT+1
        IF(KOUNT.NE.NSET) GO TO 1
      STOP
1100 FORMAT(1H1,2X,20A4/)
1200 FORMAT(7X,'M      N      IPRINT  MAXITR'/4I8)
1300 FORMAT(2X,'A*/Z+Z-/='',F8.4,4X,'B='',F8.4)
1400 FORMAT(2X,'GUESSES ON PARAMETERS',4(2X,F10.6))
1500 FORMAT(2X,'IONIC STR. AND GAMMA+-'/10(F10.4))
1600 FORMAT(/2X,'IFAIL='',I2,3X,'(0) IS A SUCCESSFUL CALL')
1700 FORMAT(/2X,'D-H EQN FITTED  -LOG GAMMA=A*Z**Z-*SQRT(1)'/,
/        '(1+A0*B*SQRT(1))+C1*1+C2*1**2+C3*1**3'/)
1800 FORMAT(/2X,'D-H EQN FITTED  -LOG GAMMA+-=A*Z**Z-*SQRT(1)',
/        '/(1+A0*B*SQRT(1))+C1*1'/)
      END
      SUBROUTINE SAJAD(M,N,X,O,IFL)
      IMPLICIT REAL*8(A-H,O-Z)
      LOGICAL IFL

```

```

      DIMENSION X(N),O(M)
      COMMON AZZ,DF,GPM(50),SI(50),AJAC(50,4)
      DO 103 I=1,M
        SQI=SI(I)
        SI1=SQI*SQI
        SI2=SI1*SI1
        SI3=SI2*SI1
        O(I)=GPM(I)-AZZ*SQI/(1.00+X(1)*DF*SQI)
        /-X(2)*SI1-X(3)*SI2-X(4)*SI3
103  CONTINUE
      RETURN
      END
      SUBROUTINE WASIM (H,N,X,F,A,V)
      IMPLICIT REAL*8(A-H,O-Z)
      DIMENSION X(N),F(N),A(N,N),V(N)
      COMMON AZZ,DF,GPM(50),SI(50),AJAC(50,4)
      DO 104 J=1,M
        SSI=SI(J)*SI(J)
        SI2=SSI*SSI
        SI3=SI2*SSI
        AJAC(J,1)=AZZ*SSI/(1.00+X(1)*DF*SI(J))**2
        AJAC(J,2)=-SSI
        AJAC(J,3)=-SI2
        AJAC(J,4)=-SI3
104  CONTINUE
      DO 105 I=1,N
        SUM=0.00
        DO 106 K=1,M
106  SUM=SUM+AJAC(K,I)*F(K)
        V(I)=SUM
        DO 105 J=1,M
          SUM=0.00
          DO 108 K=1,M
108  SUM=SUM+AJAC(K,I)*AJAC(K,J)
          A(I,J)=SUM
105  CONTINUE
      RETURN
      END
      SUBROUTINE RASHAD(M,N,X,Q,S,T,IR)
      IMPLICIT REAL*8(A-H,O-Z)
      DIMENSION X(N),Q(M),T(N)
      IF(IR)10,11,11
11  WRITE(6,301)IR
10  WRITE(6,302)S
      WRITE(6,304)(X(I),I=1,M)
      IF(IP.LT.0)GO TO 310
      WRITE(6,305)(T(I),I=1,N)
      GO TO 311
310  WRITE(6,306)(Q(I),I=1,M)
311  RETURN
301  FORMAT(2X,'AFTER ',I4,' EVALUATIONS')
302  FORMAT(2X,'E04GAF SUM OF SQUARES ',1PD16.5)
304  FORMAT(2X,'ACT. COEFF. PARAM. ARE ',4(1PD16.5))
305  FORMAT(2X,'GRADIENT ',4(1PD16.5))
306  FORMAT(2X,'DEVIATIONS FROM THE EQUATION'/10(F10.4))
      END

```

## APPENDIX C

A COMPREHENSIVE PROGRAM FOR PERFORMING  
 A: CALCULATION OF CONCENTRATIONS OF INDIVIDUAL COMPLEX  
 SPECIES IN 2:1 ELECTROLYTES, FROM KNOWN STABILITY  
 CONSTANTS AND ACTIVITY COEFFICIENT PARAMETERS OF  
 EXTENDED D-H EQUATION, BY THE METHOD OF REILLY AND  
 STOKES.  
 B: OPTIMIZATION OF LAMBDA(0) VALUES OF INDIVIDUAL SPECIES  
 REQUIRED ARE THE VALUES OF MOLARITIES AND EQUIVALENT  
 CONDUCTANCE.  
 C: CALCULATION OF THE IRREVERSIBLE THERMODYNAMIC  
 PARAMETERS USING PIKAL'S THEORY.  
 THE NAG SUBROUTINES E04FAF AND C02AEF HAVE BEEN CALLED.

```

IMPLICIT REAL*8(A-H,O-Z)
EXTERNAL STEVE,PATHAN,LUTFI
DIMENSION FF(30),OPTLAM(6),CHANG(6),WW(900),NAME(20)
/ ,CMOLR(30),BETA(4),ACTEXP(15),CA(3),CB(3),GESLAM(6)
COMMON CNOLL(30),ACTCOE(8),NACOE
COMMON/RAB/SPECIS(30,6),STRION(30),CNORMY(30),ALAND(6)
1 ,EXPEQV(30),SCALNG(6)
COMMON/KHAN/MOLAM(6),NPRNT,ISWITCH,LAMFIX
DATA CA/1.00261100,0.06573900,0.007853400/
DATA CB/0.99773700,-0.06684800,0.002942800/
10 FORMAT(20A4)
11 FORMAT(7I5)
12 FORMAT(2D10.1)
13 FORMAT(8F10.5)
14 FORMAT(15,5X,3F10.5)
15 FORMAT(2F10.5)
  READ(5,11)NSET
  KOUNT=0
999 WRITE(5,112)
  READ(5,10)NAME
  WRITE(6,100)NAME
  READ(5,11)NOP,NTRIAL,IPRINT,MAXITR,LAMFIX,IOPIN
  WRITE(6,101)NOP,NTRIAL,IPRINT,MAXITR,LAMFIX,IOPIN
  IF(LAMFIX.EQ.0)GO TO 8
  READ(5,12)VEPS,VALF
  WRITE(6,102)VEPS,VALF
  READ(5,11)NACOE
  READ(5,13)(ACTCOE(I),I=1,NACOE)
  WRITE(6,123)(ACTCOE(I),I=1,NACOE)
  READ(5,13)(BETA(I),I=1,4)
  WRITE(6,121)(BETA(I),I=1,4)
  READ(5,13)(ACTEXP(I),I=1,15)
  WRITE(6,122)(ACTEXP(I),I=1,15)
  IF(LAMFIX.EQ.0)GO TO 16
  READ(5,15)(CMOLR(I),EXPEQV(I),I=1,NOP)
  WRITE(6,116)(CMOLR(I),EXPEQV(I),I=1,NOP)
  GO TO 17
16 READ(5,13)(CMOLR(I),I=1,NOP)
  WRITE(6,124)(CMOLR(I),I=1,NOP)
17 CONTINUE

```

```

DO 1100 I=1,NOP
CMR=CMOLR(I)
IF(CMR.GE..005D0)GO TO 4
CMOLL(I)=CMR*1.0029647D0
GO TO 1100
4 AMBYC=CA(1)+CA(2)*CMR+CA(3)*CMR**2
CMOLL(I)=AMBYC*CMR
1100 CONTINUE
CALL PATHAN(NOP,CMOLL,BETA,ACTEXP,SPECIS)
WRITE(6,117)
WRITE(6,104)
DO 7000 I=1,NOP
7000 WRITE(6,105)(SPECIS(I,N),N=1,6)
DO 2100 I=1,NOP
DO 2100 N=1,6
SP=SPECIS(I,N)
IF(SP.GE..005D0)GO TO 3
SPECIS(I,N)=SP/1.0029647D0
GO TO 2100
3 CBYM=CB(1)+CB(2)*SP+CB(3)*SP**2
SPECIS(I,N)=CBYM*SP
2100 CONTINUE
WRITE(6,118)
WRITE(6,119)
DO 2200 I=1,NOP
CNORMY(I)=CMOLP(I)*2.D0
STRION(I)=.5D0*(4.D0*SPECIS(I,1)+SPECIS(I,2)+SPECIS(I,4)+
/ 4.D0*SPECIS(I,5)+SPECIS(I,6))
2200 WRITE(6,120)(SPECIS(I,N),N=1,6),STRION(I),CMOLR(I)
IF(IOPTN.EQ.-1)GO TO 7
IF(LAMFIX.NE.0)GO TO 1
READ(5,11)LCOMB
LCC=0
6 WRITE(6,114)
READ(5,13)(ALAMD(I),I=1,6)
IF(IOPTN.EQ.0)NPRNT=0
ISATCH=0
CALL STEVE(NOP,NATTAK,OPTLAM,FF)
LCC=LCC+1
IF(LCC.NE.LCOMB)GO TO 6
GO TO 7
1 KTRY=0
5 READ(5,11)NATTAK
READ(5,13)(ALAMD(I),I=1,6)
WRITE(6,114)
WRITE(6,103)(ALAMD(I),I=1,6)
DO 2000 I=1,NATTAK
READ(5,14)NOLAM(I),GESLAM(I),CHANG(I),SCALNG(I)
2000 WRITE(6,107)NOLAM(I),GESLAM(I),CHANG(I),SCALNG(I)
WRITE(6,114)
ISATCH=1
NPRNT=1
DO 4000 I=1,NATTAK
4000 OPTLAM(I)=GESLAM(I)
EPS=VEPS
ALF=VALF

```

```

NA=NATTAK
IP=NA+3+NA/3
NW=2*NOP+4*NA+NOP*NA+(NA*NA+NA)/2+IP*(NOP+2+2*NA)
IFAIL=1
CALL E04FAF(NOP,NA,OPTLAM,FF,SUMSQR,EPS,ALF,CHANG,WW,
1 NW,STEVE,LUTFI,IPRINT,MAXITER,IFAIL)
WRITE(6,108)IFAIL,EPS
WRITE(6,110)SUMSQR
WRITE(6,109)(OPTLAM(I),I=1,NA)
DO 3000 I=1,NA
J=NOLAM(I)
3000 ALAMB(J)=OPTLAM(I)/SCALNG(I)
WRITE(6,109)(ALAMB(I),I=1,6)
IF(IUPTN.EQ.0)NPRINT=0
ISATCH=0
CALL STEVE(NOP,NA,OPTLAM,FF)
KTRY=KTRY+1
IF(KTRY.NE.NTRIAL)GO TO 5
7 KOUNT=KOUNT+1
IF(KOUNT.NE.NSET)GO TO 999
STOP
100 FORMAT(/5X,20A4/)
101 FORMAT(/5X,'CONTROL PARAMETERS',/,,'      NOP      TRIALS',
1 '      PRNT      ITER      LAMFIX      OPTION',/,5X,
2 I3,5I10)
102 FORMAT(/5X,'LIMIT ON SUM SQR ',1PD10.1,5X,'ACCURACY',D10.1)
103 FORMAT(/5X,'VALUES OF LAMBDA',S',/,6(3X,F10.3))
104 FORMAT(/10X,'M++      MA+      MA2',
1 '      MA3-      MA4--      A-')
105 FORMAT(2X,6(1PD15.6))
107 FORMAT(/5X,'LAMBDA NO. =',I2,3X,'GUESS VALUE =',
1 F10.2,3X,'CONSTRAINT =',F10.2,3X,'SCALING=',F10.2)
108 FORMAT(/5X,'IFAIL= ',I2,3X,'EPS= ',F5.1)
109 FORMAT(/5X,'OPTIMIZED LAMBDA'S ARE',6(3X,F12.4))
110 FORMAT(/5X,'SUM OF SQUARES ',1PD15.4)
112 FORMAT(1H1/)
114 FORMAT(/)
116 FORMAT(/5X,'MOLARITY      EQV.COND.',/,,(F12.6,F10.2))
117 FORMAT(/5X,'MOLALITY OF COMPLEX SPECIES')
118 FORMAT(/5X,'MOLARITY OF COMPLEX SPECIES')
119 FORMAT(/10X,'M++      MA+      MA2',
1 '      MA3-      MA42-      A-',
2 '      ION STRENGTH      MOLARITY')
120 FORMAT(2X,7(1PD15.6),0PF11.6)
121 FORMAT(/5X,'LOG BETA(1-4) ',4(3X,F10.5))
122 FORMAT(/5X,'VALUES OF THE ACT.COEFFICIENT PARAMETERS'/
1 5(1PD16.5))
123 FORMAT(/5X,'COEFFICIENTS OF DLN(GAMA)/DLN(M)',
1 7,7(1PD15.7))
124 FORMAT(/5X,'INPUT MOLARITIES',/,8(F10.5))
END
SUBROUTINE STEVE(NCONC,MATAK,ESTLAM,FUNCTN)
IMPLICIT REAL*8(A-H,O-Z)
EXTERNAL FURHAT
DIMENSION ESTLAM(MATAK),FUNCTN(NCONC),Z(6),ABZ(6),RMU(6),
1 CALEGV(30),DIFEGV(30),RLIJ(6,6),PERCNT(6,6)

```



```

COMMON/RAB/CONC(30,6),U(30),ANORM(30),ALAM(6),OBSEGV(30)
1  ,SCALNG(6)
COMMON/SUPPER/RL11(30),RL12(30),RL22(30)
COMMON/KFAN/NUMBER(6),NPR,KSW,LFA
DATA Z/2.00,1.00,0.00,-1.00,-2.00,-1.00/
DATA ABZ/2.00,1.00,0.00,1.00,2.00,1.00/
C1=.107400
C2=.23001500
C3=30.247500
IF(NPR.EQ.0.OR.KSW.EQ.0)GO TO 111
DO 1000 I=1,MATAK
J=NUMBER(I)
1000 ALAM(J)=ESTLAM(I)/SCALNG(I)
111 CONTINUE
WRITE(6,705)
DO 2000 I=1,NCONC
IF(NPR.NE.0)GO TO 55
WRITE(6,680)ANORM(I)
55 CONTINUE
ROOTU=LSORT(U(I))
SUM=0.00
DO 3000 N=1,6
IF(Z(N).EQ.0.00)GO TO 3000
RMU(N)=CONC(I,N)*Z(N)**2/(2.00*U(I))
SUM=SUM+RMU(N)*ALAM(N)/ABZ(N)
3000 CONTINUE
DO 1100 L=1,6
DO 1100 M=1,6
IF(Z(L).EQ.0.00.OR.Z(M).EQ.0.00)GO TO 10
IF(L.NE.M)GO TO 20
RLIJ(L,M)=(C1*ALAM(L)/ABZ(L))-C1*ROOTU*((ALAM(L)*ALAM(L)/
/ SUM*(1.00-RMU(L))*C2)+C3*Z(L)*Z(L)*RMU(L))
RLIJ(L,M)=RLIJ(L,M)*CONC(I,L)
GO TO 1100
20 SMU=DSQRT(RMU(L)*RMU(M))
PLIJ(L,M)=C1*SMU*ROOTU*((ALAM(L)*ALAM(M))/SUM*C2)-C3*
1 Z(L)*Z(M))
RLIJ(L,M)=RLIJ(L,M)*DSQRT(CONC(I,L)*CONC(I,M))
GO TO 1100
10 RLIJ(L,M)=0.00
1100 CONTINUE
IF(NPR.NE.0)GO TO 1120
WRITE(6,188)
DO 1150 L=1,6
1150 WRITE(6,704)(RLIJ(L,M),M=1,6)
1120 CONTINUE
RL11(I)=0.00
DO 1200 K=1,5
DO 1200 L=1,5
1200 RL11(I)=RL11(I)+RLIJ(K,L)
IF(NPR.NE.0)GO TO 1
DO 30 K=1,5
30 WRITE(6,620)(RLIJ(K,L),L=1,5)
WRITE(6,707)
DO 988 K=1,5
DO 977 L=1,5

```

```

977 PERCNT(K,L)=RLIJ(K,L)/RL11(I)*100.00
988 WRITE(6,706) (PERCNT(K,L),L=1,5)
    WRITE(6,650) PL11(I)
    1 PL12(I)=0.00
    DO 1300 K=1,5
    DO 1300 L=3,5
1300 PLIJ(K,L)=(L-1)*RLIJ(K,L)
    IF(NPR.NE.0)GO TO 299
    WRITE(6,186)
    DO 199 K=1,6
199 WRITE(6,704) (RLIJ(K,L),L=1,6)
299 CONTINUE
    DO 1400 K=1,5
    DO 1400 L=2,6
1400 PL12(I)=RL12(I)+RLIJ(K,L)
    IF(NPR.NE.0)GO TO 2
    DO 31 K=1,5
    31 WRITE(6,620) (RLIJ(K,L),L=2,6)
    WRITE(6,707)
    DO 966 K=1,5
    DO 955 L=2,6
955 PERCNT(K,L)=RLIJ(K,L)/PL12(I)*100.00
966 WRITE(6,706) (PERCNT(K,L),L=2,6)
    WRITE(6,660) PL12(I)
    2 PL22(I)=0.00
    IF(NPR.NE.0)GO TO 399
    WRITE(6,186)
    DO 499 K=1,6
499 WRITE(6,704) (RLIJ(K,L),L=1,6)
399 CONTINUE
    DO 1500 K=3,5
    DO 1500 L=2,6
1500 PLIJ(K,L)=(K-1)*RLIJ(K,L)
    DO 1600 K=2,6
    DO 1600 L=2,6
1600 PL22(I)=PL22(I)+PLIJ(K,L)
    IF(NPR.NE.0)GO TO 3
    DO 32 K=2,6
    32 WRITE(6,620) (PLIJ(K,L),L=2,6)
    WRITE(6,707)
    DO 944 K=2,6
    DO 933 L=2,6
933 PERCNT(K,L)=PLIJ(K,L)/PL22(I)*100.00
944 WRITE(6,706) (PERCNT(K,L),L=2,6)
    WRITE(6,670) PL22(I)
    3 PL11(I)=RL11(I)/ANORM(I)
    PL12(I)=RL12(I)/ANORM(I)
    PL22(I)=PL22(I)/ANORM(I)
    CALERQV(I)=9.310900*(4.00*RL11(I)+PL22(I)-4.00*PL12(I))
    DIFERQV(I)=OBSEQV(I)-CALERQV(I)
    FUNCTN(I)=DIFERQV(I)
2000 CONTINUE
    IF(KSW.NE.0)GO TO 4
    WRITE(6,100)
    IF(LFX.EQ.0)GO TO 5
    WRITE(6,702)

```

```

      DO 5000 I=1,NCONC
5000  WRITE(6,703) ANORM(I), OBSERV(I), CALEQV(I), DIFEQV(I)
      5  CONTINUE
      CALL FURHAT(NCONC,ANORM)
      4  CONTINUE
100  FORMAT(///)
620  FORMAT(1X,B(1P014.4))
650  FORMAT(1X,'*** L11 =',F13.6)
660  FORMAT(1X,'*** L12 =',F13.6)
670  FORMAT(1X,'*** L22 =',F13.6)
680  FORMAT(1X,'FORMAL NORMALITY =',F12.5)
690  FORMAT(1X,'VALUES OF LAMBDA'S USED ',/,6(3X,F12.4))
702  FORMAT(1X,'NORMALITY EQ.COND(OBS) EQ.COND(CAL)',
      1' DIFFERENCE')
703  FORMAT(4(3X,F10.4))
704  FORMAT(5X,B(1P014.4))
705  FORMAT(1H1/)
706  FORMAT(5X,5F10.3)
707  FORMAT(1X,'PERCENT CONTRIBUTION OF EACH COEFFICIENT')
188  FORMAT(1X,'***** CURRENT VALUES OF 6 X 6 MATRIX')
      RETURN
      END
      SUBROUTINE PATHAN(NOP,C,BETA,P,SPS)
      IMPLICIT REAL*8(A-H,O-Z)
      DIMENSION C(30),BETA(4),P(15),SPS(30,6),RA(6),AI(6),COE(6)
      F=2.30258509300
      Z11=-0.511500
      Z21=-1.02300
      D=0.329100
      DO 20 I=1,4
      BETA(I)=DEXP(BETA(I)*F)
20  CONTINUE
      DO 30 I=1,NOP
      CM1=C(I)
      CM2=C(I)*2.00
      U=CM2*CM1
      NC=0
1  SU=DSQRT(U)
      US=U*U
      UC=US*U
      A21=Z21*SU
      A11=Z11*SU
      DSU=0*SU
      G21=A21/(1.00+P(1)*DSU)+P(2)*U+P(3)*US+P(4)*UC
      G11=A11/(1.00+P(5)*DSU)+P(6)*U+P(7)*US+P(8)*UC
      G0=P(9)*U+P(10)*US+P(11)*UC
      G12=A21/(1.00+P(12)*DSU)+P(13)*U+P(14)*US+P(15)*UC
      G21=DEXP(G21*F)
      G11=DEXP(G11*F)
      G0=DEXP(G0*F)
      G12=DEXP(G12*F)
      G21C=G21**3
      G11S=G11*G11
      G11F=G11S*G11S
      G12C=G12**3
      R1=BETA(I)*G21C/G11S

```

```

P2=BETA(2)*G21C/G0
B3=BETA(3)*G21C
R4=BETA(4)*G21C*G11F/G12C
COE(1)=B4
COE(2)=B3+B4*(4.00*CM1-CM2)
COE(3)=B2+B3*(3.00*CM1-CM2)
COE(4)=B1+B2*(2.00*CM1-CM2)
COE(5)=1.00+B1*(CM1-CM2)
COE(6)=-CM2
N=6
IFAIL=1
TOL=16.0**(-13)
CALL C02AEF(COE,N,RA,AI,TOL,IFAIL)
IF(IFAIL.NE.0)WRITE(6,9)IFAIL
8  FORMAT(/5X,'FAILED IN C02AEF  IFAIL=',I3)
DO 40 J=1,5
  A=RA(J)
  IF(A.GT.0.00.AND.A.LE.CM2)GO TO 4
40 CONTINUE
  IF(A.LE.0.00.OR.A.GT.CM2)WRITE(6,105)A,CM2
105 FORMAT(/5X,'WARNING A= ',F10.6,' TOTAL MOLALITY ',F10.6)
  4  AS=A*A
  AC=AS*A
  AF=AS*AS
  DENOM=1.00+B1*A+B2*AS+B3*AC+B4*AF
  CM=CM1/DENOM
  CMA=B1*CM*A
  CMA2=B2*CM*AS
  CMA3=B3*CM*AC
  CMA4=B4*CM*AF
  UN=.500*(4.00*(CM+CMA4)+CMA+CMA3+A)
  PE=DABS((UN-U)/UN)*100.00
  IF(PE.LE..0100)GO TO 3
  NC=NC+1
  IF(PE.GT..01.AND.NC.EQ.1000)GO TO 2
  U=UN
  GO TO 1
  2  WRITE(6,109)CM,NC,PE
109 FORMAT(' **** FAILURE N ',F13.6,' ITER ',I10,
1  ' P.ERROR ',F6.2)
  3  SPS(I,1)=CM
  SPS(I,2)=CMA
  SPS(I,3)=CMA2
  SPS(I,4)=CMA3
  SPS(I,5)=CMA4
  SPS(I,6)=A
30 CONTINUE
RETURN
END
SUBROUTINE FURHAT(N,BNORM)
IMPLICIT REAL*8(A-H,O-Z)
DIMENSION BNORM(30),R11(30),R12(30),R22(30),X(30),
1  WR13(30),WR23(30),WR33(30),R13(30),R23(30),R33(30)
COMMON CMOLL(30),COE(8),NCOE
COMMON/SUPPER/PL11(30),BL12(30),BL22(30)
CONST1=9.310900

```

```

CONST2=1.4873400
CONST3=1.0-12
WRITE(6,600)
DO 20 I=1,N
  CMOLR=BNORM(I)/2.00
  ALPHA=4.00*BL11(I)+BL22(I)-4.00*BL12(I)
  PLN=BL06(CMOLL(I))
  FACTOR=0.00
  DO 30 J=1,NCOE
    IF(PLN.EQ.0.00)GO TO 31
30  FACTOR=FACTOR+COE(J)*PLN**(J-1)
    GO TO 2
31  FACTOR=COE(1)
    2  ACTERM=1.00+FACTOR
    BIGLAM=CONST1*ALPHA
    TPLUS=(4.00*BL11(I)-2.00*BL12(I))/ALPHA
    DIFFV=(CONST2*(BL11(I)*BL22(I)-BL12(I)**2)/ALPHA)*ACTERM
    PL11(I)=BL11(I)*CONST3
    PL12(I)=BL12(I)*CONST3
    PL22(I)=BL22(I)*CONST3
    X(I)=BL11(I)*BL22(I)-BL12(I)**2
    R11(I)=BL22(I)/X(I)
    R12(I)=-BL12(I)/X(I)
    R22(I)=BL11(I)/X(I)
    X(I)=1000.00*CMOLR/(15.0154*CMOLL(I))
    WR13(I)=-0.500*(R11(I)+2.00*R12(I))
    WR23(I)=-0.500*(R12(I)+2.00*R22(I))
    R13(I)=WR13(I)/X(I)
    R23(I)=WR23(I)/X(I)
    WR33(I)=-0.500*(R13(I)+2.00*R23(I))
    R33(I)=WR33(I)/X(I)
20  WRITE(6,610)CMOLR,CMOLL(I),BNORM(I),BIGLAM,TPLUS,DIFFV,
    1  ACTERM
    WRITE(6,620)
    DO 100 I=1,N
100  WRITE(6,660)BL11(I),BL12(I),BL22(I),R11(I),R12(I),R22(I)
    1  ,BNORM(I)
    WRITE(6,650)
    DO 200 I=1,N
200  WRITE(6,660)WR13(I),WR23(I),WR33(I),R13(I),R23(I),
    1  R33(I),X(I)
600  FORMAT(/5X,'MOLARITY    MOLALITY    NORMALITY    LAMBDA',
    1  '    TPLUS    D(V)    ACT.TERM')
610  FORMAT(5X,7F10.4)
620  FORMAT(/5X,'L11/N      L12/N      L22/N',
    1  '      R**R11      N*R12      N*R22')
630  FORMAT(1X,6D15.5)
650  FORMAT(/5X,'C3*R13      C3*R23      C3*R33',
    1  '      R13      R23      R33',
    2  '      C-WATER(C3)')
660  FORMAT(1X,6D15.5,F10.4)
    RETURN
    END
    SUBROUTINE LUTFI(NPOINT,LATAK,VLAMDA,SMOQR,ITER,SIN,LIM)
    IMPLICIT REAL*8(A-H,O-Z)
    LOGICAL SIN,LIM

```

```

DIMENSION VLAMDA(LATAK)
WRITE(6,100)ITER,SMSQR,(VLAMDA(I),I=1,LATAK)
IF(SIN)WRITE(6,300)
IF(LIN)WRITE(6,400)
RETURN
100 FORMAT(4X,'***ITER',I3,'  SMSQR',1PD12.3,'  LAMBDAS'
/ ,6(2X,0PF8.2))
300 FORMAT(5X,'GUESS FAILED NEW VALUE GENERATED')
400 FORMAT(5X,'VALUES CONSTRAINED BY SUPPLIED LIMITS')
END

```

## APPENDIX D.1

THIS PROGRAM PERFORMS THE ITERATIONS FOR CALCULATION OF  
THE CONCENTRATIONS AND COMPUTES THE CELL CONSTANT FOR A  
DIAPHRAGM CELL WITH KCL CALIBRATION DIFFUSION RUN

```

DIMENSION A(5),B(5),NAME(20)
REAL KSPB,KSPT
10 FORMAT(3I5)
11 FORMAT(20A4)
12 FORMAT(8F10.0)
READ(5,10)N,NA,NB
READ(5,12)(A(I),I=1,NA)
WRITE(6,88)
WRITE(6,1000)(A(I),I=1,NA)
READ(5,12)(B(I),I=1,NB)
WRITE(6,1100)(B(I),I=1,NB)
NC=0
1 READ(5,11)NAME
READ(5,12)T,KSPT,KSPB,V,EST
READ(5,12)W1T,WT,W1B,WB
WRITE(6,99)
WRITE(6,1400)NAME
WRITE(6,2000)T
WRITE(6,2200)KSPT
WRITE(6,2300)KSPB
WRITE(6,2400)V
WRITE(6,2500)EST
WRITE(6,2600)W1T
WRITE(6,2700)WT
WRITE(6,2800)W1B
WRITE(6,2900)WB
C2=0.0
CALL CONC(A,B,NA,NB,KSPT,W1T,WT,EST,C4)
CALL CONC(A,B,NA,NB,KSPB,W1B,WB,EST,C3)
C1=C3+(C4-C2)*V
CMA=(C1+C3)/2.0
CALL DOBAR(D0CMA,CMA)
CMB=(C2+C4)/2.0
CALL DOBAR(D0CMB,CMB)
RC=CMA/CMB
DBAR=(D0CMA*CMA-D0CMB*CMB)/(CMA-CMB)
RCS=(C1-C2)/(C3-C4)
DBETA=1.0/T*ALOG(RCS)*10.0**5
BETA=DBETA/DBAR
WRITE(6,99)
WRITE(6,19)C1
WRITE(6,18)C2
WRITE(6,17)C3
WRITE(6,16)C4
WRITE(6,15)CMA

```

```

WRITE(6,14)CMB
WRITE(6,13)RCS
WRITE(6,22)DBETA
WRITE(6,21)DBAR
WRITE(6,20)BETA
NC=NC+1
IF(NC.NE.N)GO TO 1
STOP
88 FORMAT(1H1)
99 FORMAT(/)
13 FORMAT(5X,'(C1-C2)/(C3-C4) =',F10.6)
14 FORMAT(5X,'(C2+C4)/2 (CMB) =',F10.6)
15 FORMAT(5X,'(C1+C3)/2 (CMA) =',F10.6)
16 FORMAT(5X,'FINAL CONC. OF UPPER HALF (C4) =',F10.6)
17 FORMAT(5X,'FINAL CONC. OF LOWER HALF (C3) =',F10.6)
18 FORMAT(5X,'INITIAL CONC. OF UPPER HALF (C2) =',F10.6)
19 FORMAT(5X,'INITIAL CONC. OF LOWER HALF (C1) =',F10.6)
20 FORMAT(5X,'CELL CONSTANT (BETA) =',F10.6)
21 FORMAT(5X,'D BAR =',F10.6)
22 FORMAT(5X,'D * BETA =',F10.6)
1000 FORMAT(5X,'COEFFICIENTS OF C/P VS LAMBDA*P/1000'
1/6(1PD16.5))
1100 FORMAT(5X,'COEFFICIENTS OF C/M VS M'/6(1PD16.5))
1400 FORMAT(/5X,20A4/)
2000 FORMAT(5X,'TIME OF DIFFUSION RUN (SECS.) =',F10.1)
2200 FORMAT(5X,'SPECIFIC COND. OF UPPER SOLUTION =',F12.7)
2300 FORMAT(5X,'SPECIFIC COND. OF LOWER SOLUTION =',F12.7)
2400 FORMAT(5X,'V=(V2+V3/2)/(V1+V3/2) =',F8.3)
2500 FORMAT(5X,'GUESS VALUE OF CONC. =',F8.3)
2600 FORMAT(5X,'WEIGHT OF SOL. FROM UPPER HALF =',F10.4)
2700 FORMAT(5X,'WEIGHT AFTER DILUTION =',F10.4)
2800 FORMAT(5X,'WEIGHT OF SOL. FROM LOWER HALF =',F10.4)
2900 FORMAT(5X,'WEIGHT AFTER DILUTION =',F10.4)
END
SUBROUTINE CONC(C,P,N,M,SKSP,W1,W,E,CN)
DIMENSION C(5),P(5)
3 CRPL=0.
DO 1 I=1,N
1 CRPL=CRPL+C(I)*ALOG(E)**(I-1)
EN=SKSP/EXP(CRPL)
R=ABS((EN-E)/EN)*100.
IF(R.LE..02)GO TO 2
E=EN
GO TO 3
2 CRP=EN*W/W1
PP=0.
DO 4 I=1,M
4 PP=PP+P(I)*CRP**(I-1)
CN=CRP*PP
RETURN
END
SUBROUTINE DOBAR(D0,C)
CS=C*C
CC=CS*C
IF(C.GT..01)GO TO 2
D0=1.9834-10.4036*C+978.602*CS-39220.0*CC

```



```
GO TO 8
2 IF (C.GT..1)GO TO 3
  D0=1.959-2.4101*C+27.3377*CS-118.482*CC
  GO TO 8
3 IF (C.GT..5)GO TO 4
  D0=1.90175-0.36375*C+0.825*CS-0.625*CC
  GO TO 8
4 D0=1.84273+.000360167*C+.0186942*CS-.0021745*CC
8 RETURN
END
```

## APPENDIX D.2

C  
C  
C  
C  
C  
C

THIS PROGRAM CALCULATES THE ISOTOPE-ISOTOPE  
COUPLING COEFFICIENTS FOR COMPLEXED SYSTEM  
CADMIUM AND CADMIUM IODIDE

```

REAL IONSTR(50),LAMBDA(5),MOLAR(50),LIJ(5,5)
DIMENSION SPECIS(50,5),Z(5),ABZ(5),NAME(20)
DATA Z/2.,1.,-1.,-2.,-1./
DATA ABZ/2.,1.,1.,2.,1./
CONSTA=.1074
CONSTX=.22961
CONSTC=30.2475
10 FORMAT(15)
11 FORMAT(20A4)
12 FORMAT(7F10.0)
READ(5,10)NSETS
KOUNT=0
1 READ(5,10)NOP
WRITE(6,1700)
WRITE(6,1600)
DO 20 I=1,NOP
READ(5,12) (MOLAR(I),IONSTR(I),(SPECIS(I,J),J=1,5))
20 WRITE(6,1300) (MOLAR(I),IONSTR(I),(SPECIS(I,J),J=1,5))
READ(5,11)NAME
WRITE(6,1000)NAME
READ(5,12) (LAMBDA(I),I=1,5)
WRITE(6,1500) (LAMBDA(I),I=1,5)
DO 100 I=1,NOP
SQT1=SQRT(IONSTR(I))
DO 30 J=1,5
30 SPECIS(I,J)=SPECIS(I,J)*ABZ(J)
B=0.
DO 40 J=1,5
40 B=B+SPECIS(I,J)*LAMBDA(J)
DO 50 K=1,4
DO 50 L=1,4
FACTOR=SPECIS(I,K)*SPECIS(I,L)*CONSTA
50 LIJ(K,L)=FACTOR*LAMBDA(K)*LAMBDA(L)*CONSTX/B*SQT1
1 -(FACTOR*CONSTC*Z(K)*Z(L)/(2.*SQT1))
WRITE(6,1100)MOLAR(I)
WRITE(6,1101)
DO 70 K=1,4
70 WRITE(6,1200) (LIJ(K,L),L=1,4)
X=LIJ(1,1)+LIJ(2,2)+LIJ(3,3)+2.*LIJ(1,2)+2.*LIJ(3,4)
1 +LIJ(4,4)
Y=2.*LIJ(1,3)+2.*LIJ(1,4)+2.*LIJ(2,3)+2.*LIJ(2,4)
X=X/MOLAR(I)
Y=Y/MOLAR(I)
FUN=X+Y
WRITE(6,1400)X,Y,FUN
100 CONTINUE
KOUNT=KOUNT+1
IF(KOUNT.NE.NSETS)GO TO 1
STOP
1000 FORMAT(/5X,20A4/)

```

```
1100 FORMAT(/5X,'MOLARITY=',F10.6)
1101 FORMAT(/5X,'L-COEFFICIENTS')
1200 FORMAT(4(1PE16.5))
1300 FORMAT(7(1PE16.5))
1400 FORMAT(/5X,'NEGATIVE TERM',1PE15.5,' POSITIVE TERM',
1F15.5,' TOTAL',E15.5)
1500 FORMAT(/5X,'VALUES OF LAMBDA(0) 1-4'/5(F10.2))
1600 FORMAT(/5X,'INPUT MOLARITY, ION. STR., M++, MA+, MA3--, MA4--, A-')
1700 FORMAT(1H1)
      END
```